USDA Forest Service
U.S. DEPARTMENT OF AGRICULTURE

Southern Research Station General Technical Report SRS-266 May 2022

Forest Health Monitoring: National Status, Trends, and Analysis 2021

EDITORS: Kevin M. Potter and Barbara L. Conkling

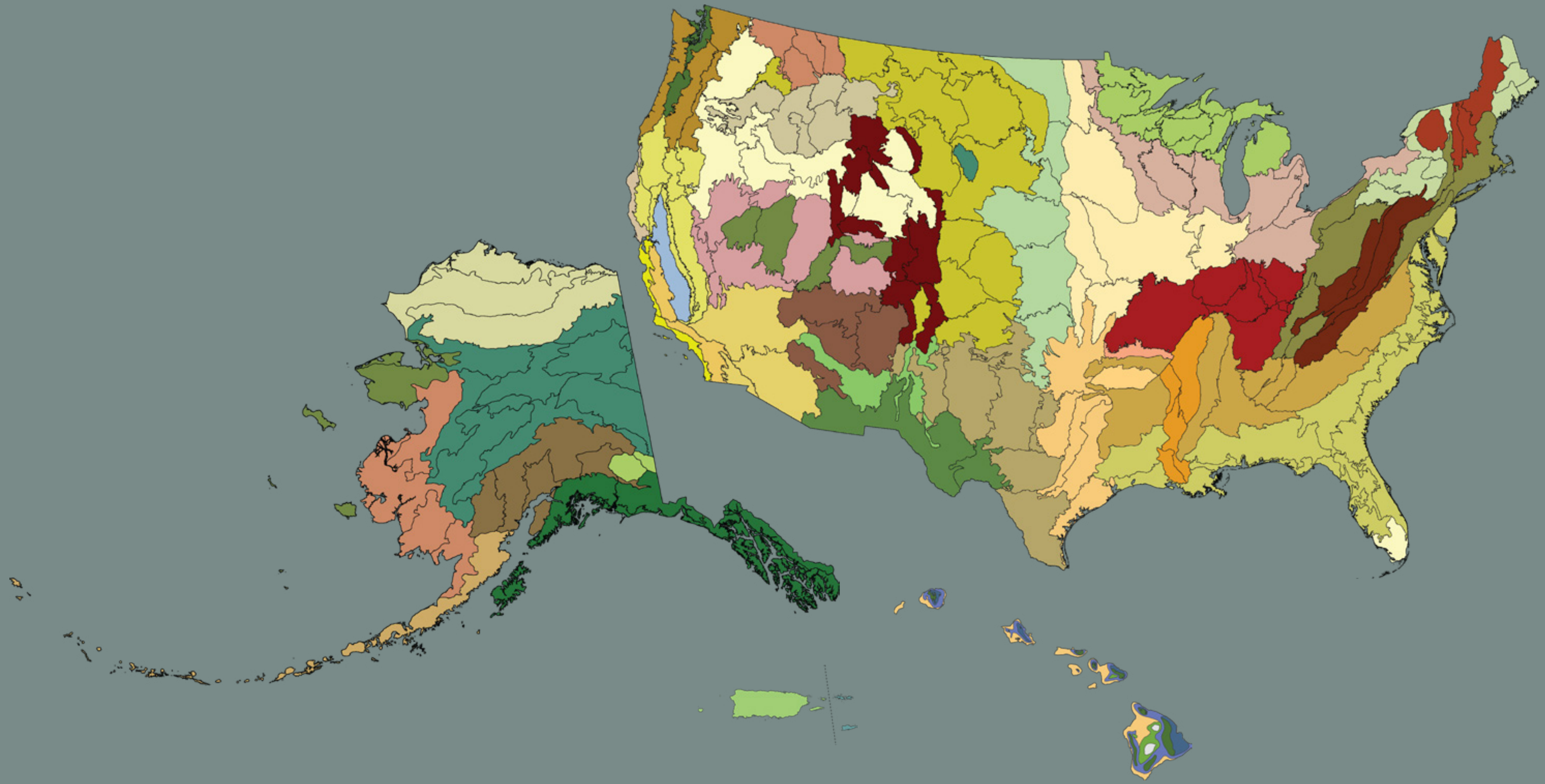

FRONT COVER MAP: Ecoregion provinces and ecoregion sections for the conterminous United States (Cleland and others 2007) and for Alaska (Spencer and others 2002), and ecoregions within the islands of Hawaii, along with Puerto Rico and the U.S. Virgin Islands, for which no corresponding ecoregion treatments exist.

BACK COVER MAPS: Tree canopy cover (green) for the conterminous 48 States, Hawaii, Puerto Rico, and the U.S. Virgin Islands based on data from a cooperative project between the Multi-Resolution Land Characteristics Consortium and the U.S. Department of Agriculture Forest Service, Geospatial Technology and Applications Center (GTAC) using the 2011 National Land Cover Database. Forest and shrubland cover for Alaska derived from the 2011 National Land Cover Database.

PESTICIDE PRECAUTIONARY STATEMENT: This publication reports research involving pesticides. It does not contain recommendations for their use, nor does it imply that the uses discussed here have been registered. All uses of pesticides must be registered by appropriate State and/or Federal agencies before they can be recommended.

May 2022
https://doi.org/10.2737/SRS-GTR-266

Forest Service
Research & Development
Southern Research Station
General Technical Report SRS-266

Southern Research Station
200 W.T. Weaver Blvd.
Asheville, NC 28804
www.srs.fs.usda.gov

Forest Health Monitoring: National Status, Trends, and Analysis 2021

EDITORS:

Kevin M. Potter, Research Professor, North Carolina State University,
Department of Forestry and Environmental Resources, Raleigh, NC 27695

Barbara L. Conkling, Research Assistant Professor, North Carolina State University,
Department of Forestry and Environmental Resources, Raleigh, NC 27695

ABSTRACT

The annual national report of the Forest Health Monitoring (FHM) program of the Forest Service, U.S. Department of Agriculture, presents forest health status and trends from a national or multistate regional perspective using a variety of sources, introduces new techniques for analyzing forest health data, and summarizes results of recently completed Evaluation Monitoring projects funded through the FHM national program. In this 21st edition in a series of annual reports, national survey data are used to identify recent geographic patterns of insect and disease activity. Satellite data are employed to detect geographic patterns of forest fire occurrence. Recent drought and moisture surplus conditions are compared across the conterminous United States. Data collected by the Forest Inventory and Analysis (FIA) program are employed to detect regional differences in tree mortality. Fine-scale change in Normalized Difference Vegetation Index (NDVI) was used to detect broad patterns of forest disturbance across the conterminous United States. Seven recently completed Evaluation Monitoring projects are summarized, addressing forest health concerns at smaller scales.

Keywords—Change detection, disturbance, drought, fire, forest health, forest insects and disease, tree canopy, tree mortality.

CONTENTS

CHAPTER 1

SECTION 1

CHAPTER 2

CHAPTER 3

CONTENTS

CHAPTER 4

CHAPTER 5

SECTION 2

CHAPTER 6

CONTENTS

SECTION 3

CHAPTER 7

CHAPTER 8

CHAPTER 9

CHAPTER 10

CONTENTS

CHAPTER 11

CHAPTER 12

CHAPTER 13

LIST OF FIGURES

LIST OF FIGURES

LIST OF FIGURES

LIST OF FIGURES

LIST OF FIGURES

LIST OF FIGURES

LIST OF FIGURES

LIST OF TABLES

LIST OF TABLES

EXECUTIVE SUMMARY

Healthy ecosystems are those that are stable and sustainable, able to maintain their organization and autonomy over time while remaining resilient to stress (Costanza 1992). Healthy forests are vital to our future (Edmonds and others 2011), and consistent, large-scale, and long-term monitoring of key indicators of forest health status, change, and trends is necessary to identify forest resources deteriorating across large regions (Riitters and Tkacz 2004). The Forest Health Monitoring (FHM) program of the Forest Service, U.S. Department of Agriculture, with cooperating researchers within and outside the Forest Service and with State partners, quantifies status and trends in the health of U.S. forests (ch. 1). The analyses and results outlined in sections 1 and 2 of this FHM annual national report offer a snapshot of the current condition of U.S. forests from a national or multistate regional perspective, incorporating baseline investigations of forest ecosystem health, examinations of change over time in forest health metrics, and assessments of developing threats to forest stability and sustainability. For datasets collected on an annual basis, analyses are presented from 2020 data. For datasets collected over several years, analyses are presented at a longer temporal scale. Finally, section 3 of this report presents seven summaries of results from recently completed Evaluation Monitoring (EM) projects that have been funded through the FHM national program to determine the extent, severity, and/or causes of specific forest health problems (FHM 2018).

Monitoring the occurrence of forest pest and pathogen outbreaks is important at regional scales because of the potential forest health impacts of insects and disease across landscapes (ch. 2). In 2020, the global COVID-19 pandemic required forest health specialists to quickly adapt new methods to monitor insect and disease damage, in addition to the traditional aerial surveys. National Insect and Disease Survey data identified 45 mortality-causing agents and complexes on approximately 1.17 million ha and 59 defoliating agents and complexes on approximately 1.54 million ha in the conterminous United States. Emerald ash borer (*Agrilus planipennis*) was the most widespread agent of tree mortality nationally and in the East. Fir engraver (*Scolytus ventralis*) was the most damaging mortality agent in the West. Spruce budworm (*Choristoneura fumiferana*) was the most commonly detected defoliator in the East, while western spruce budworm (*C. freemani*) was its counterpart in the West. Meanwhile, in Alaska, the most widespread mortality agent was spruce beetle (*Dendroctonus rufipennis*), while hemlock sawfly (*Neodiprion tsugae*) was the second most common mortality agent and the most common defoliation agent. Finally, surveyors in Hawaii identified approximately 32 000 ha of mortality, much of which may have been caused by rapid ʻōhiʻa death.

Forest fire occurrence outside the historic range of frequency and intensity can result in extensive economic and ecological impacts. The detection of regional patterns of fire occurrence density can allow for the identification of areas at greatest risk of significant impact and for the selection of locations for more intensive analysis (ch. 3). The number of satellite-detected forest fire occurrences recorded for the conterminous States in 2020 was the third highest in 20 full years of data collection, and the most since 2014. This was a 202-percent increase from a relatively low-activity fire year in 2019 and was 75 percent above the mean of the previous 19 years. Several ecoregion sections in California, Washington, and Oregon, as well as four in northwestern Colorado and northeastern Utah, had many more fire occurrences in 2020 than normal, compared to the previous 19-year mean and accounting for variability over time. Meanwhile, Alaska experienced a dramatic drop in fire occurrences from 2019, which was a year of extremely high fire activity in that State. Hawaii also had a generally low-activity fire year, with two ecoregions on the island of Maui having more fire occurrences than expected. Finally, none of the U.S. Caribbean islands were outside the range of near-normal fire occurrence density in 2020.

Droughts can significantly impact forests, particularly when they co-occur with heat waves. Prolonged drought stress can lead to the failure of a tree's hydraulic system, causing the death of its crown and potentially killing the tree itself. A standardized drought and moisture surplus indexing approach was applied to monthly climate data from 2020 and prior years to map drought conditions and surplus moisture availability across the conterminous United States at a fine scale (ch. 4). Moderate to extreme drought conditions were common across much of the Western United States in 2020, while moderate to extreme surplus conditions were widespread throughout the Southeast and Mid-Atlantic regions. Analyses of longer term (3-year and 5-year) conditions depict disparity between the western and eastern halves of the conterminous United States. Most concerning are the large areas of long-term severe to extreme drought in the Southwest and near the Pacific Coast, indicating the persistence of these conditions and minimal improvement in drought status in recent years. Meanwhile, only a few isolated locations in the East had moderate or worse long-term drought conditions, while areas of prolonged moisture surplus were far more common, extensive, and spatially contiguous.

Mortality is a natural process in all forested ecosystems, but high levels of mortality at large scales may be an indicator of forest health problems. Phase 2 data collected by the Forest Inventory and Analysis (FIA) program of the Forest Service provide tree mortality information on a relatively intense spatial basis of approximately one plot per 6,000 acres, and mortality analysis is possible for areas where data are available from repeated plot measurements using consistent sampling protocols (ch. 5). Due to the COVID-19 pandemic, FIA data collection was slowed during 2020, so no new data were available from many Eastern States. An ecoregion section in eastern Texas had high mortality relative to live volume, which was attributed to drought and disease. Preliminary analyses of FIA data from the Western States indicated especially high mortality as a percentage of live volume in southern California (fire, insects and disease, and drought), the Great Basin (fire and insects), the northern Rocky Mountains (insects and fire), and the central Rocky Mountains (insects). These mortality-causing agents are related in that drought stresses trees, making them more susceptible to insect attack, while both drought and insect-killed trees create conditions favorable for wildfires.

The rise of cloud computing, the availability of free satellite data archives, and the launch of satellites with higher-than-ever sensor resolution has recently allowed for the integration of satellite-based remote sensing with field and aircraft monitoring of forest disturbances (ch. 6). Imagery from the European Space Community's Sentinel-2 satellites in particular have nine times more spatial detail than Landsat and about 600 times more detail than Moderate Resolution Imaging Spectroradiometer (MODIS) imagery. Mapping forest change at this more precise resolution gives insights into the pattern and texture of disturbances that are helpful for accurate mapping and interpretation. Sentinel-2 satellite imagery was accessed using Google Earth Engine to produce 10-m national maps of the Normalized Difference Vegetation Index (NDVI) for summer 2019 and 2020. One-year absolute change in summer NDVI (dNDVI) was determined by comparing the 2019 and 2020 maps, with forest-only change below a threshold of -0.1 NDVI summarized nationally using hexagons of 834 km^2. Despite the technological advances, causal attribution can still be challenging. Local expertise is, therefore, a critical part of monitoring, and advances in remote sensing are best used in support of an integrated monitoring program.

Finally, seven recently completed Evaluation Monitoring (EM) projects address a wide variety of forest health concerns at a scale smaller than the national or multistate regional analyses included in the first sections of the report. These EM projects (funded by the FHM program):

- Identified eastern white pine (*Pinus strobus*) stands in the Northeast with white pine needle damage, determined the disease complexes associated with general decline and reduced regeneration, and developed management practices to lessen future mortality (ch. 7)
- Examined how invasion by the shade-tolerant, C4 grass *Microstegium vimineum* (Nepalese browntop, or stiltgrass) interacts with prescribed fire to affect the regeneration of naturally established tree seedlings and saplings of varying sizes in southern Illinois, and evaluated the potential long-term effects of prescribed fire and *M. vimineum* invasion on stand development using a forest growth and yield simulation model (ch. 8)
- Monitored the long-term growth and mortality of trees in the Beidler Forest in South Carolina following a severe ice storm in 2014, as part of a rapid-response study aimed at characterizing and modeling species-specific damage and mortality by assessing the immediate responses of different species (ch. 9)
- Summarized findings from ongoing research aimed at (1) describing patterns of sugarberry (*Celtis laevigata*) dieback and mortality at a single site in South Carolina, (2) determining the spatial extent and spread of the mortality in the Southeastern United States, and (3) investigating what role, if any, insects are playing in the deaths of trees (ch. 10)
- Determined the causes and rates of tree mortality during and after mountain pine beetle (*Dendroctonus ponderosae*) outbreaks based on

a network of plots in five States (Colorado, Idaho, Montana, Utah, and Wyoming), and described changes in forest conditions from 2004–2019 (ch. 11)

- Assessed site and stand characteristics that describe limber pine (*Pinus flexilis*) along Montana's Rocky Mountain Front, determined the status and health of limber pine trees and regeneration, characterized the major damage agents on limber pine trees and regeneration, and determined the occurrence, incidence, and severity of white pine blister rust (*Cronartium ribicola*) on limber pine (ch. 12)
- Addressed questions about the management of balsam woolly adelgid (*Adelges piceae*) in Utah, Montana, and Idaho through long-term monitoring of tree decline and death at BWA-infested fir (*Abies* spp.) stands, and explored the complexities of climate influences on the pest-host relationship under differing stand conditions (ch. 13)

The FHM program, in cooperation with forest health specialists and researchers inside and outside the Forest Service, continues to investigate a broad range of issues relating to forest health using a wide variety of data and techniques. This report presents some of the latest results from ongoing national-scale detection monitoring and smaller scale environmental monitoring efforts by FHM and its cooperators. For more information about efforts to determine the status, changes, and trends in indicators of the condition of U.S. forests, please visit the FHM website at https://www.fs.fed.us/foresthealth/protecting-forest/forest-health-monitoring.

LITERATURE CITED

Costanza, R. 1992. Toward an operational definition of ecosystem health. In: Costanza, R.; Norton, B.G.; Haskell, B.D., eds. Ecosystem health: new goals for environmental management. Washington, DC: Island Press: 239–256.

Edmonds, R.L.; Agee, J.K.; Gara, R.I. 2011. Forest health and protection. Long Grove, IL: Waveland Press, Inc. 667 p.

Forest Health Monitoring (FHM). 2018. Program description. Forest Health Monitoring fact sheet series. https://www.fhm.fs.fed.us/fact/. [Date accessed: September 20, 2018].

Riitters, K.H.; Tkacz, B. 2004. The U.S. Forest Health Monitoring program. In: Wiersma, G.B., ed. Environmental monitoring. Boca Raton, FL: CRC Press: 669–683.

CHAPTER 1

Introduction

Kevin M. Potter

Forests and woodlands cover an extensive area of the United States, 333 million ha or approximately 36 percent of the Nation's land area (Oswalt and others 2019). These forests provide a broad range of goods and services for current and future generations, safeguard biological diversity, and contribute to the resilience of ecosystems, societies, and economies (USDA Forest Service 2011). Their ecological roles include supplying large and consistent quantities of clean water, preventing soil erosion, and providing habitat for a broad diversity of plant and animal species. Their socioeconomic benefits include wood products, nontimber goods, recreational opportunities, and natural beauty. At the same time, both the ecological integrity and the continued capacity of these forests to provide ecological and economic goods and services are of concern in the face of a long list of threats, including insect and disease infestation, drought, fragmentation and forest conversion to other land uses, catastrophic fire, invasive species, and the effects of climate change.

Natural and anthropogenic stresses vary among biophysical regions and local environments; they also change over time and interact with each other. These and other factors make it challenging to establish baselines of forest health and to detect important departures from normal forest ecosystem functioning (Riitters and Tkacz 2004). Monitoring the health of forests is a critically important task, however, reflected within the Criteria and Indicators for the Conservation and Sustainable Management of Temperate and Boreal Forests (Montréal Process Working Group 1995), which the Forest Service, U.S. Department of Agriculture, uses as a forest sustainability assessment framework (USDA Forest Service 2004, 2011). The primary objective of such monitoring is to identify ecological resources whose condition is deteriorating in subtle ways over large regions in response to cumulative stresses, a goal that requires consistent, large-scale, and long-term monitoring of key indicators of forest health status, change, and trends (Riitters and Tkacz 2004). Given the magnitude of this task, it is best accomplished through the participation of multiple Federal, State, academic, and private partners.

The concept of a healthy forest has universal appeal, but forest ecologists and managers have struggled with how exactly to define forest health (Teale and Castello 2011). There is no universally accepted definition. Most definitions of forest health can be categorized as representing either an ecological or a utilitarian perspective (Kolb and others 1994). From an ecological perspective, the current understanding of ecosystem dynamics suggests that healthy ecosystems are those that maintain their organization and autonomy over time while remaining resilient to stress (Costanza 1992), and that evaluations of forest health should emphasize factors that affect the inherent processes and resilience of forests (Edmonds and others 2011, Kolb and others 1994, Raffa and others 2009). On the other hand, the utilitarian perspective holds that a forest is healthy if management objectives are met, and that a forest is unhealthy if these objectives are not met (Kolb and others 1994). Although this definition may be appropriate when a single, unambiguous management objective exists, such as the

How to cite this chapter:

Potter, Kevin M. 2022. Introduction. In: Potter, Kevin M.; Conkling, Barbara L., eds. Forest health monitoring: national status, trends, and analysis 2021. Gen. Tech. Rep. SRS-266. Asheville, NC: U.S. Department of Agriculture Forest Service, Southern Research Station: 5–21. https://doi.org/10.2737/SRS-GTR-266-Chap1.

production of wood fiber or the maintenance of wilderness attributes, it can be too narrow when multiple management objectives are required (Edmonds and others 2011, Teale and Castello 2011). Teale and Castello (2011) incorporate both ecological and utilitarian perspectives into their two-component definition of forest health: first, a healthy forest must be sustainable with respect to its size structure, including a correspondence between baseline and observed mortality; second, a healthy forest must meet the landowner's objectives, provided that these objectives do not conflict with sustainability.

This national report, the 21st in an annual series sponsored by the Forest Health Monitoring (FHM) program of the Forest Service, attempts to quantify the status of, changes to, and trends in a wide variety of broadly defined indicators of forest health. The indicators described in this report encompass forest insect and disease activity, wildland fire occurrence, drought, tree mortality, and general forest disturbance, among others. The previous reports in this series are Ambrose and Conkling (2007, 2009), Conkling (2011), Conkling and others (2005), Coulston and others (2005a, 2005b, 2005c), and Potter and Conkling (2012a, 2012b, 2013a, 2013b, 2014, 2015a, 2015b, 2016, 2017, 2018, 2019, 2020, 2021). Visit https://www.fs.fed.us/foresthealth/publications/fhm/fhm-annual-national-reports.shtml for links to each of these reports in their entirety and for searchable lists of links to chapters included in the reports.

This report has three specific objectives. The first is to present information about forest health from a national perspective, or from a multistate regional perspective when appropriate, using data collected by the Forest Health Protection (FHP) and Forest Inventory and Analysis (FIA) programs of the Forest Service, as well as from other sources available at a wide extent. The chapters that present analyses at a national scale, or multistate regional scale, are divided between section 1 and section 2 of the report. Section 1 presents analyses of forest health data that are available on an annual basis. Such repeated analyses of regularly collected indicator measurements allow for the detection of trends over time and help establish a baseline for future comparisons (Riitters and Tkacz 2004). Section 2 presents longer term forest health trends, in addition to describing new techniques for analyzing forest health data at national or regional scales (the second objective of the report). While in-depth interpretation and analysis of specific geographic or ecological regions are beyond the scope of these parts of the report, the chapters in sections 1 and 2 present information that can be used to identify areas that may require investigation at a finer scale.

The second objective of the report is to present new techniques for analyzing forest health data as well as new applications of established techniques, often applied to longer timescales, presented in section 2. The example in this report is chapter 6, which presents the results of a national assessment of forest disturbance, defined by change from 2019 to 2020 in 10-m maps of summer Normalized Difference Vegetation Index (NDVI), generated using imagery from the European Space Community's Sentinel-2 satellites.

The third objective of the report is to present results of recently completed Evaluation Monitoring (EM) projects funded through the FHM national program. These project summaries, presented in section 3, determine the extent, severity, and/or cause of forest health problems (FHM 2019), generally at a finer scale than that addressed by the analyses in sections 1 and 2. Each of the seven chapters in section 3 contains an overview of an EM project, key results, and contacts for more information.

When appropriate throughout this report, authors use the Forest Service revised ecoregions for the conterminous United States and Alaska (Cleland and others 2007, Spencer and others 2002) as a common ecologically based spatial framework for their forest health assessments (fig. 1.1). Specifically, when the spatial scale of the data and the expectation of an identifiable pattern in the data are appropriate, authors use ecoregion sections, larger scale provinces, or smaller scale subsections as assessment units for their analyses. Bailey's hierarchical system bases the two broadest ecoregion scales, domains and divisions, on large ecological climate zones, while each division is broken into provinces based on vegetation macro features (Bailey 1995). Provinces are further divided into sections, which may be thousands of km^2 in area and are expected to encompass regions similar in their geology, climate, soils, potential natural vegetation, and potential natural communities (Cleland and others 1997). Subsections are nested within sections as the smallest level in the hierarchy. This hierarchical system does not address either Hawaii or Puerto Rico beyond including each in a unique, single ecoregion province (Bailey 1995). A set of Hawaii ecoregions based on moisture and elevational characteristics was developed for use in FHM national reports (Potter 2020) because a finer scale and ecologically oriented spatial assessment framework was needed to estimate the impacts of a destructive forest disease (ch. 2) and of forest fire occurrences (ch. 3) (fig. 1.2, table 1.1).

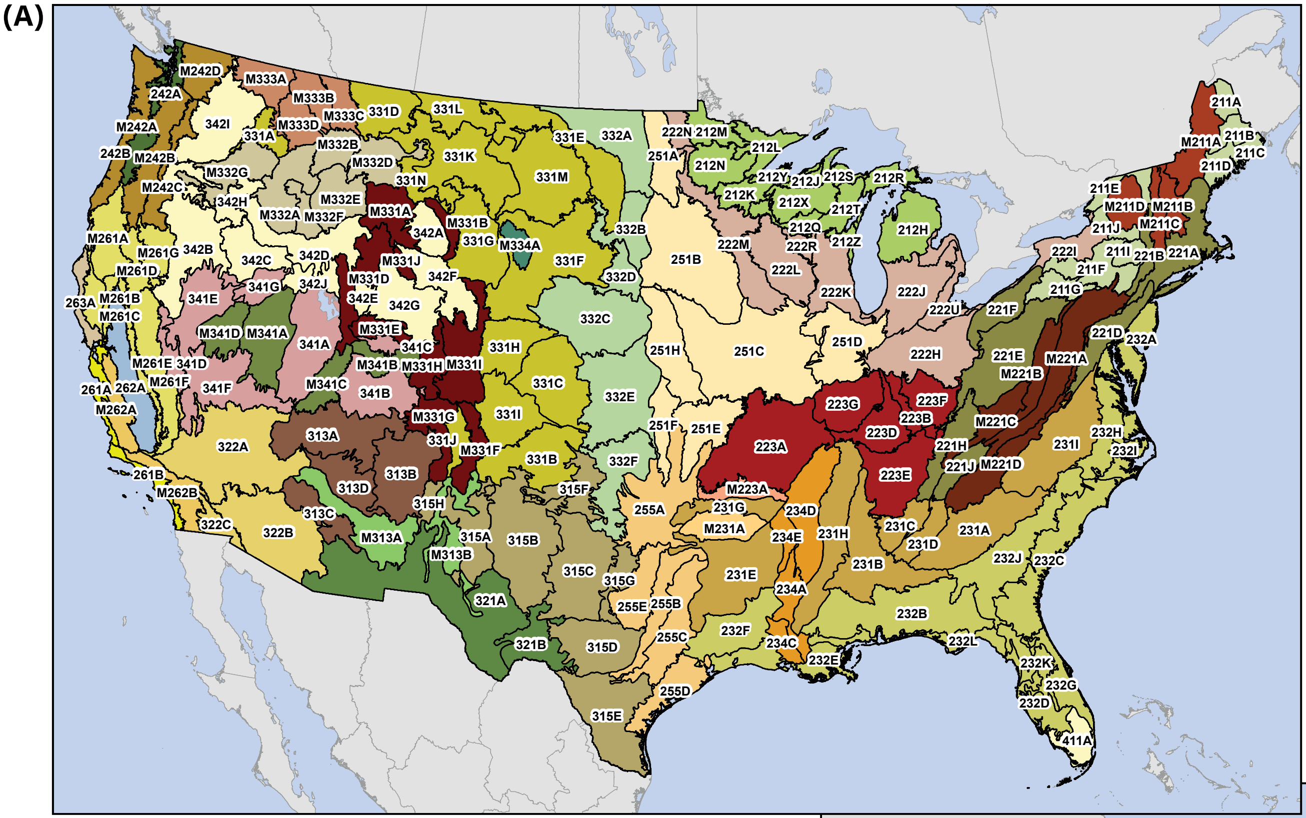

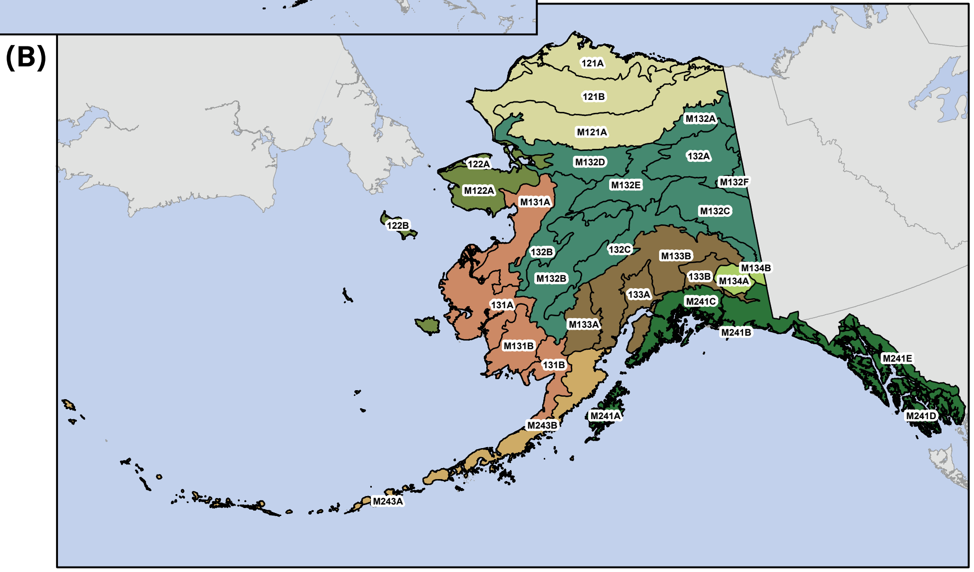

Figure 1.1—Ecoregion provinces and sections for (A) the conterminous United States (Cleland and others 2007) and (B) Alaska (Spencer and others 2002). Ecoregion sections within each ecoregion province are shown in the same color.

Conterminous States ecoregion provinces

- 🟩 211: Northeastern Mixed Forest
- 🟥 M211: Adirondack-New England Mixed Forest—Coniferous Forest—Alpine Meadow
- 🟩 212: Laurentian Mixed Forest
- 🟩 221: Eastern Broadleaf Forest
- 🟫 M221: Central Appalachian Broadleaf Forest—Coniferous Forest—Meadow
- 🟫 222: Midwest Broadleaf Forest
- 🟥 223: Central Interior Broadleaf Forest
- 🟧 M223: Ozark Broadleaf Forest
- 🟨 231: Southeastern Mixed Forest
- 🟨 M231: Ouachita Mixed Forest—Meadow
- 🟨 232: Outer Coastal Plain Mixed Forest
- 🟧 234: Lower Mississippi Riverine Forest
- 🟩 242: Pacific Lowland Mixed Forest
- 🟨 251: Prairie Parkland (Temperate)
- 🟧 255: Prairie Parkland (Subtropical)
- 🟫 M242: Cascade Mixed Forest—Coniferous Forest—Alpine Meadow
- 🟨 261: California Coastal Chaparral Forest and Shrub
- 🟨 M261: Sierran Steppe—Mixed Forest—Coniferous Forest—Alpine Meadow
- 🟦 262: California Dry Steppe
- 🟨 M262: California Coastal Range Open Woodland—Shrub—Coniferous Forest—Meadow
- 🟫 263: California Coastal Steppe—Mixed Forest—Redwood Forest
- 🟫 313: Colorado Plateau Semi-Desert
- 🟩 M313: Arizona-New Mexico Mountains Semi-Desert—Open Woodland—Coniferous Forest—Alpine Meadow
- 🟫 315: Southwest Plateau and Plains Dry Steppe and Shrub
- 🟩 321: Chihuahuan Semi-Desert
- 🟨 322: American Semi-Desert and Desert
- 🟨 331: Great Plains—Palouse Dry Steppe
- 🟥 M331: Southern Rocky Mountain Steppe—Open Woodland—Coniferous Forest—Alpine Meadow
- 🟩 332: Great Plains Steppe
- 🟫 M332: Middle Rocky Mountain Steppe—Coniferous Forest—Alpine Meadow
- 🟧 M333: Northern Rocky Mountain Forest-Steppe—Coniferous Forest—Alpine Meadow
- 🟩 M334: Black Hills Coniferous Forest
- 🟥 341: Intermountain Semi-Desert and Desert
- 🟩 M341: Nevada-Utah Mountains Semi-Desert—Coniferous Forest—Alpine Meadow
- 🟨 342: Intermountain Semi-Desert
- 🟨 411: Everglades

Alaska ecoregion provinces

- 🟨 121: Arctic Tundra
- 🟩 M122: Bering Tundra
- 🟧 M131: Bering Taiga
- 🟩 M132: Intermontane Boreal
- 🟫 133: Alaska Range Transition
- 🟩 M134: Coastal Mountains Transition
- 🟩 M241: Coastal Rainforest
- 🟫 M243: Aleutian Meadows

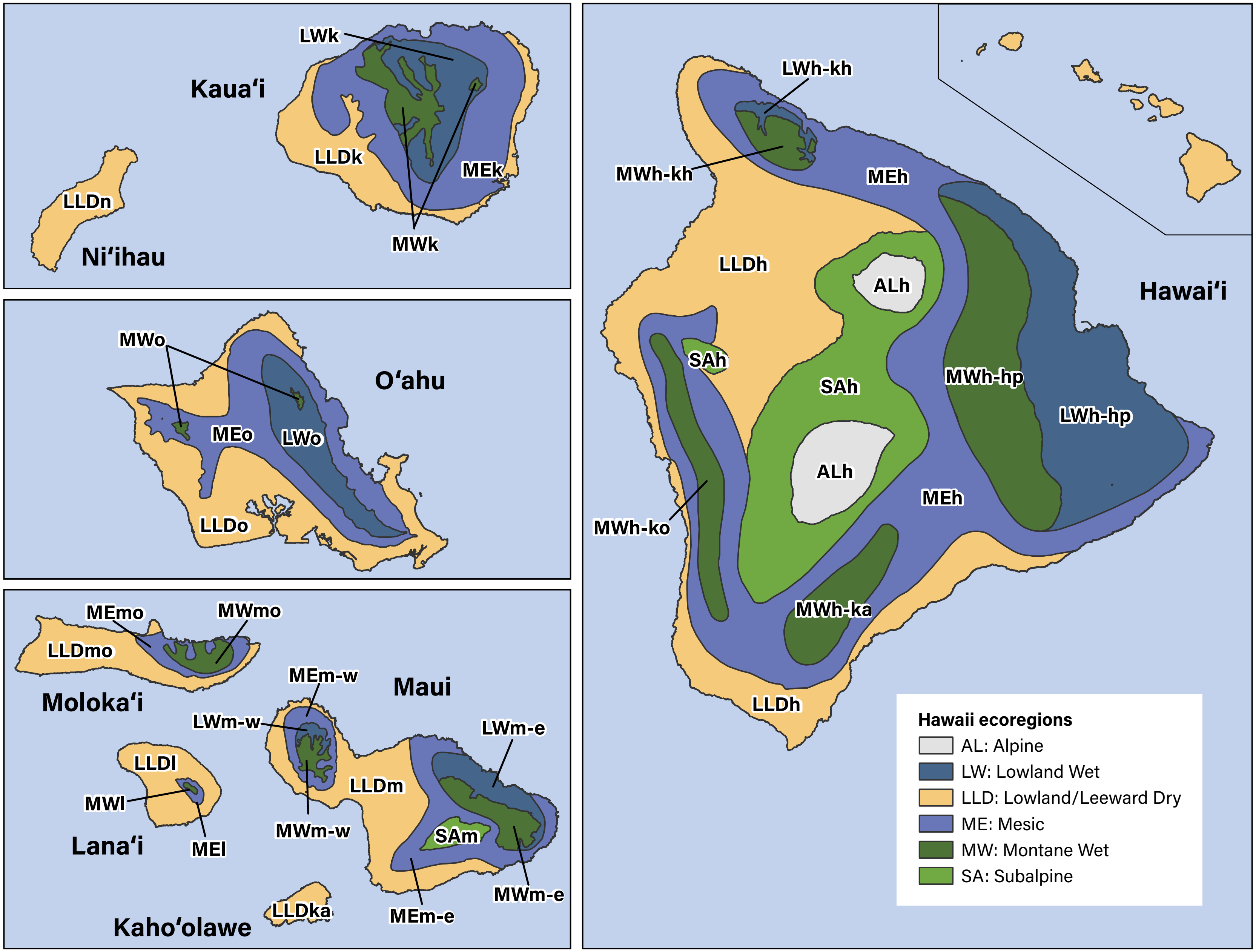

Figure 1.2—Ecoregions, and ecoregion subunits, for Hawaii, developed based on moisture zones and elevation (see box 1.1). Ecoregion subunits are shown in the same color by ecoregion. See table 1.1 for the names of the ecoregion subunits listed on the map.

Table 1.1—The six ecoregions and 34 ecoregion subunits for the State of Hawaii

Ecoregion	Subunit
AL: Alpine	Alh: Alpine-Hawai‘i
LW: Lowland Wet	LWh-hp: Lowland Wet-Hawai‘i-Hilo-Puna
	LWh-kh: Lowland Wet-Hawai‘i-Kohala-Hāmākua
	LWk: Lowland Wet-Kaua‘i
	LWm-e: Lowland Wet-Maui-East
	LWm-w: Lowland Wet-Maui-West
	LWo: Lowland Wet-O‘ahu
LLD: Lowland/ Leeward Dry	LLDh: Lowland/Leeward Dry-Hawai‘i
	LLDka: Lowland/Leeward Dry-Kaho‘olawe
	LLDk: Lowland/Leeward Dry-Kaua‘i
	LLDl: Lowland/Leeward Dry-Lāna‘i
	LLDm: Lowland/Leeward Dry-Maui
	LLDmo: Lowland/Leeward Dry-Moloka‘i
	LLDn: Lowland/Leeward Dry-Ni‘ihau
	LLDo: Lowland/Leeward Dry-O‘ahu
ME: Mesic	MEh: Mesic-Hawai‘i
	MEk: Mesic-Kaua‘i
	MEl: Mesic-Lāna‘i
	MEm-e: Mesic-Maui-East
	MEm-w: Mesic-Maui-West
	MEmo: Mesic-Moloka‘i
	MEo: Mesic-O‘ahu
MW: Montane Wet	MWh-hp: Montane Wet-Hawai‘i-Hilo-Puna
	MWh-ka: Montane Wet-Hawai‘i-Ka‘ū
	MWh-kh: Montane Wet-Hawai‘i-Kohala-Hāmākua
	MWh-ko: Montane Wet-Hawai‘i-Kona
	MWk: Montane Wet-Kaua‘i
	MWl: Montane Wet-Lāna‘i
	MWm-e: Montane Wet-Maui-East
	MWm-w: Montane Wet-Maui-West
	MWmo: Montane Wet-Moloka‘i
	MWo: Montane Wet-O‘ahu
SA: Subalpine	SAh: Subalpine-Hawai‘i
	SAm: Subalpine-Maui

THE FOREST HEALTH MONITORING PROGRAM

The national FHM program is designed to determine the status, changes, and trends in indicators of forest condition on an annual basis and covers all forested lands through a partnership encompassing the Forest Service, State foresters, and other State and Federal agencies and academic groups (FHM 2019). The FHM program utilizes data from a wide variety of data sources, both inside and outside the Forest Service, and develops analytical approaches for addressing forest health issues that affect the sustainability of forest ecosystems. The FHM program has four major components (fig. 1.3):

- **Detection Monitoring**—nationally standardized aerial and ground surveys to evaluate status and change in condition of forest ecosystems (sections 1 and 2 of this report)
- **Evaluation Monitoring**—projects to determine the extent, severity, and causes of undesirable changes in forest health identified through Detection Monitoring (section 3 of this report)
- **Research on Monitoring Techniques**—work to develop or improve indicators, monitoring systems, and analytical techniques, such as urban and riparian forest health monitoring, early detection of invasive species, multivariate analyses of forest health indicators, and spatial scan statistics (section 2 of this report)

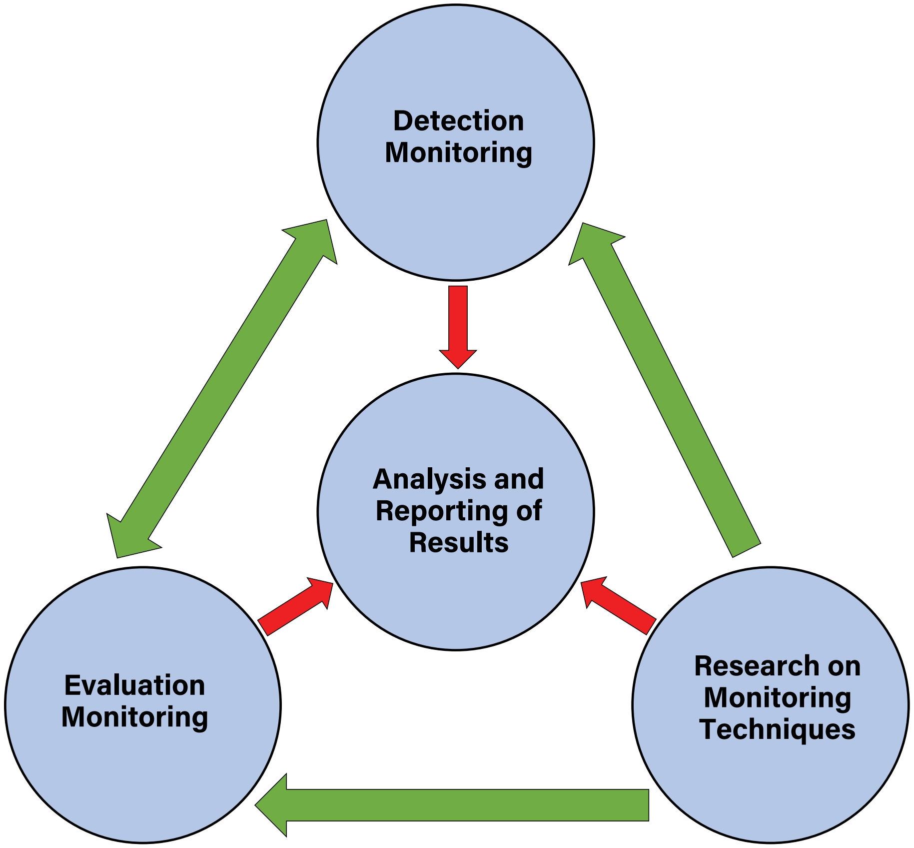

Figure 1.3—The design of the Forest Health Monitoring program (FHM 2003).

- **Analysis and Reporting**—synthesis of information from various data sources within and external to the Forest Service to produce issue-driven reports on status and change in forest health at national, regional, and State levels (sections 1, 2, and 3 of this report)

The FHM program, in addition to national reporting, generates regional and State reports, often in cooperation with FHM partners, both within the Forest Service and in State forestry and agricultural departments. For example, the FHM regions cooperate with their respective State partners to produce the annual Forest Health Highlights report series available on the FHM website at https://www.fs.fed.us/foresthealth/protecting-forest/forest-health-monitoring/monitoring-forest-highlights.shtml. Other examples include Steinman (2004) and Harris and others (2011).

The FHM program and its partners also produce peer-reviewed reports and journal articles on monitoring techniques and analytical methods (see https://www.fs.fed.us/foresthealth/publications/fhm/fhm-publications.shtml). The emphases of these publications include forest health data (Potter and others 2016, Siry and others 2018, Smith and Conkling 2004); soils as an indicator of forest health (O'Neill and others 2005); urban forest health monitoring (Bigsby and others 2014; Cumming and others 2006, 2007; Lake and others 2006); remote sensing of forest disturbances (Chastain and others 2015, Rebbeck and others 2015); health conditions in national forests (Morin and others 2006); crown conditions (Morin and others 2015; Randolph 2010a, 2010b, 2013; Randolph and Moser 2009; Schomaker and others 2007); indicators of regeneration (McWilliams and others 2015); vegetation diversity and structure (Schulz and Gray 2013, Schulz and others 2009, Simkin and others 2016); forest lichen communities (Jovan and others 2012, Root and others 2014); down woody materials in forests (Woodall and others 2012, 2013); drought (Vose and others 2016); ozone monitoring (Rose and Coulston 2009); patterns of nonnative invasive plant occurrence (Guo and others 2015, 2017; Iannone and others 2015, 2016a, 2016b, 2018; Jo and others 2018; Oswalt and others 2015; Riitters and others 2018a, 2018b); assessments of forest risk or tree species vulnerability to exotic invasive forest insects and diseases (Koch and others 2011, 2014; Krist and others 2014; Potter and others 2019a, 2019b; Vogt and Koch 2016; Yemshanov and others 2014); spatial patterns of land cover and forest fragmentation (Guo and others 2018; Riitters 2011; Riitters and Costanza 2019; Riitters and Wickham 2012; Riitters and others 2012, 2016, 2017); impacts of deer browse on forest structure (Russell and others 2017); broad-scale assessments of forest biodiversity (Guo and others 2019; Potter 2018; Potter and Koch 2014; Potter and Woodall 2012, 2014); predictions and indicators of climate change effects on forests and forest tree species (Anderson and others 2021, Fei and others 2017, Heath and others 2015, Potter and Hargrove 2013); legal, institutional, and economic indicators of forest conservation and sustainable management (McGinley and Cubbage 2020); and the overall forest health indicator program (Woodall and others 2010).

For more information about the FHM program, visit the FHM website at https://www.fs.fed.us/foresthealth/protecting-forest/forest-health-monitoring/. Among other resources, this website includes links to all past national forest health reports (https://www.fs.fed.us/foresthealth/publications/fhm/fhm-annual-national-reports.

shtml) and annual State Forest Health Highlights reports (https://www.fs.fed.us/foresthealth/protecting-forest/forest-health-monitoring/monitoring-forest-highlights.shtml).

DATA SOURCES

Forest Service data sources in this edition of the FHM national report include FIA annualized Phase 2 survey data (Bechtold and Patterson 2005, Burrill and others 2018, Woodall and others 2010); FHP national Insect and Disease Survey forest mortality and defoliation data for 2020 (FHP 2021); Moderate Resolution Imaging Spectroradiometer (MODIS) Active Fire Detections for the United States data for 2020 (USDA Forest Service 2021); tree canopy cover data generated from the 2011 National Land Cover Database (NLCD) (Homer and others 2015) through a cooperative project between the Multi-Resolution Land Characteristics Consortium and Forest Service Geospatial Technology and Applications Center (GTAC) (Coulston and others 2012); and FIA's publicly available Environmental Monitoring and Assessment Program (EMAP) hexagons (Brand and others 2000). Other sources of data include Parameter-elevation Regressions on Independent Slopes Model (PRISM) climate mapping system data (PRISM Climate Group 2021), imagery from the European Space Community's Sentinel-2 satellites used to produce national maps of the Normalized Difference Vegetation Index (NDVI) for summer 2019 and 2020, and Alaskan forest and shrub cover derived from the 2011 NLCD. For more information about the FIA program, which is a major source of data for several FHM analyses, see box 1.1.

FHM REPORT PRODUCTION

This FHM national report, the 21st in a series of such annual documents, is produced by forest health monitoring researchers at the Eastern Forest Environmental Threat Assessment Center (EFETAC) in collaboration with North Carolina State University cooperators in the Forest Health Monitoring Research Group (https://go.ncsu.edu/foresthealth). A unit of the Southern Research Station of the Forest Service, EFETAC was established under the Healthy Forests Restoration Act of 2003 to generate the knowledge and tools needed to anticipate and respond to environmental threats. For more information about the research team and about threats to U.S. forests, please visit https://www.forestthreats.org/about.

BOX 1.1

The Forest Inventory and Analysis (FIA) program collects forest inventory information across all forest land ownerships in the United States and maintains a network of more than 140,000 permanent forested ground plots across the conterminous United States, southeastern Alaska, Hawaii, and the Caribbean and Pacific territories with a sampling intensity of approximately one plot/2428 ha (one plot per 6,000 acres). Forest Inventory and Analysis Phase 2 encompasses the annualized inventory measured on plots at regular intervals, with each plot surveyed every 5 to 7 years in most Eastern States but with plots in the Rocky Mountain and Pacific Northwest regions surveyed once every 10 years (Reams and others 2005). The standard 0.067-ha plot (see figure) consists of four 7.315-m (24-foot) radius subplots (approximately 168.6 m^2 or 1/24th acre), on which field crews measure trees at least 12.7 cm (5 inches) in diameter. Within each of these subplots is nested a 2.073-m (6.8-foot) radius microplot (approximately 13.48 m^2 or 1/300th acre), on which crews measure trees smaller than 12.7 cm (5 inches) in diameter. A core-optional variant of the standard design includes four "macroplots," each with a radius of 17.953 m or 58.9 feet (approximately 0.1012 ha or 1/4 acre) that originates at the center of each subplot (Burrill and others 2018).

Forest Inventory and Analysis Phase 3 plots previously represented a subset of these Phase 2 plots, with one Phase 3 plot for every 16 standard FIA Phase 2 plots. In addition to traditional forest inventory measurements, data for a variety of important ecological indicators were collected from Phase 3 plots, including tree crown condition, lichen communities, down woody material, soil condition, and vegetation structure and diversity, whereas data on ozone bioindicator plants were collected on a separate grid of plots (Woodall and others 2010, 2011). Most of these additional forest health indicators were measured as part of the Forest Health Monitoring Detection Monitoring ground plot system prior to 2000[1](Palmer and others 1991). The FIA program recently updated its sampling techniques with flexible spatial and temporal intensities for some of these ecosystem health indicators (including down woody material, vegetation diversity and structure, and crown conditions) to improve field operation efficiency, address emerging user demands, and adjust to evolving forest health science (Castillo and Alvarez 2020). This "Phase 2 Plus Program/ Ecosystem Indicator Program" (P2+) sampling scheme facilitates the collection of a national core set of indicator information on more plots for less cost than the original indicator protocols, with sampling based on a systematic subsample that can change in response to budgetary fluctuations without compromising long-term analytical capabilities. The enhanced indicator protocols collect less-detailed information on each sampled plot than on the previous Phase 3 plots, but substantially more plots are sampled, increasing the statistical power of forest health analyses and improving the reliability of estimates in important national assessments (Castillo and Alvarez 2020).

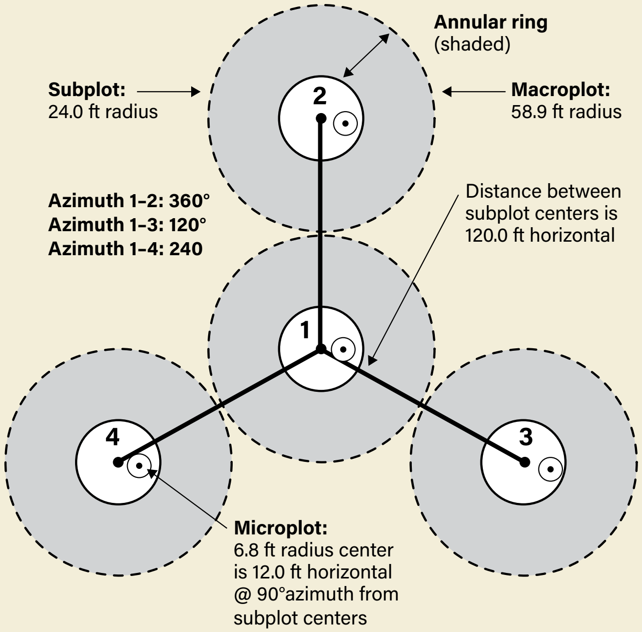

Box 1.1 figure—The Forest Inventory and Analysis mapped plot design. Subplot 1 is the center of the cluster with subplots 2, 3, and 4 located 120 feet away at azimuths of 360°, 120°, and 240°, respectively (Burrill and others 2018).

---

[1] *U.S. Department of Agriculture Forest Service. 1998. Forest Health Monitoring 1998 field methods guide. Research Triangle Park, NC: U.S. Department of Agriculture Forest Service, Forest Health Monitoring program. 473 p. On file with: Forest Health Monitoring program, 3041 Cornwallis Rd., Research Triangle Park, NC 27709.*

LITERATURE CITED

Ambrose, M.J.; Conkling, B.L., eds. 2007. Forest Health Monitoring 2005 national technical report. Gen. Tech. Rep. SRS-104. Asheville, NC: U.S. Department of Agriculture Forest Service, Southern Research Station. 76 p. https://doi.org/10.2737/SRS-GTR-104.

Ambrose, M.J.; Conkling, B.L., eds. 2009. Forest Health Monitoring 2006 national technical report. Gen. Tech. Rep. SRS-117. Asheville, NC: U.S. Department of Agriculture Forest Service, Southern Research Station. 118 p. https://doi.org/10.2737/SRS-GTR-117.

Anderson, S.M.; Heath, L.S.; Emery, M.R. [and others]. 2021. Developing a set of indicators to identify, monitor, and track impacts and change in the forests of the United States. Climatic Change.165: 13. https://doi.org/10.1007/s10584-021-02993-6.

Bailey, R.G. 1995. Descriptions of the ecoregions of the United States. 2d ed. Misc. Publ. No. 1391. Washington, DC: U.S. Department of Agriculture Forest Service. Map; presentation scale 1:7,500,000. 108 p.

Bechtold, W.A.; Patterson, P.L., eds. 2005. The enhanced Forest Inventory and Analysis program—national sampling design and estimation procedures. Gen. Tech. Rep. SRS-80. Asheville, NC: U.S. Department of Agriculture Forest Service, Southern Research Station. 85 p.

Bigsby, K.M.; Ambrose, M.J.; Tobin, P.C.; Sills, E.O. 2014. The cost of gypsy moth sex in the city. Urban Forestry & Urban Greening. 13(3): 459–468. https://doi.org/10.1016/j.ufug.2014.05.003.

Brand, G.J.; Nelson, M.D.; Wendt, D.G.; Nimerfro, K.K. 2000. The hexagon/panel system for selecting FIA plots under an annual inventory. In: McRoberts, R.E.; Reams, G.A.; Van Deusen, P.C., eds. Proceedings of the first annual Forest Inventory and Analysis symposium. Gen. Tech. Rep. NC-213. St. Paul, MN: U.S. Department of Agriculture Forest Service, North Central Research Station: 8–13.

Burrill, E.A.; Wilson, A.M.; Turner, J.A. [and others]. 2018. The Forest Inventory and Analysis Database: database description and user guide for Phase 2 (version 8.0). Washington, DC: U.S. Department of Agriculture Forest Service. 946 p. http://www.fia.fs.fed.us/library/database-documentation/. [Date accessed: August 23, 2019].

Castillo, P.S.B.; Alvarez, M. 2020. Forest Inventory and Analysis: fiscal year 2018 business report. FS-1153. Washington, DC: U.S. Department of Agriculture Forest Service. 71 p. https://www.fia.fs.fed.us/library/bus-org-documents/docs/17973%20FS%20FIA%20Fiscal%20Year%202018%20Business%20Reportv3%20508.pdf. [Date accessed: September 15, 2020].

Chastain, R.A.; Fisk, H.; Ellenwood, J.R. [and others]. 2015. Near-real time delivery of MODIS-based information on forest disturbances. In: Lippitt, C.D.; Stow, D.A.; Coulter, L.L., eds. Time-sensitive remote sensing. New York, NY: Springer: 147–164. https://doi.org/10.1007/978-1-4939-2602-2_10.

Cleland, D.T.; Avers, P.E.; McNab, W.H. [and others]. 1997. National hierarchical framework of ecological units. In: Boyce, M.S.; Haney, A., eds. Ecosystem management applications for sustainable forest and wildlife resources. New Haven, CT: Yale University Press: 181–200.

Cleland, D.T.; Freeouf, J.A.; Keys, J.E. [and others]. 2007. Ecological subregions: sections and subsections for the conterminous United States. Gen. Tech. Rep. WO-76D. Washington, DC: U.S. Department of Agriculture Forest Service. Map; Sloan, A.M., cartographer; presentation scale 1:3,500,000; colored. https://doi.org/10.2737/WO-GTR-76D.

Conkling, B.L., ed. 2011. Forest Health Monitoring 2007 national technical report. Gen. Tech. Rep. SRS-147. Asheville, NC: U.S. Department of Agriculture Forest Service, Southern Research Station. 159 p. https://doi.org/10.2737/SRS-GTR-147.

Conkling, B.L.; Coulston, J.W.; Ambrose, M.J., eds. 2005. Forest Health Monitoring 2001 national technical report. Gen. Tech. Rep. SRS-81. Asheville, NC: U.S. Department of Agriculture Forest Service, Southern Research Station. 204 p. https://doi.org/10.2737/SRS-GTR-81.

Costanza, R. 1992. Toward an operational definition of ecosystem health. In: Costanza, R.; Norton, B.G.; Haskell, B.D., eds. Ecosystem health: new goals for environmental management. Washington, DC: Island Press: 239–256.

Coulston, J.W.; Riitters, K.H.; Conkling, B.L., eds. 2005a. Forest Health Monitoring 2002 national technical report. Gen. Tech. Rep. SRS-84. Asheville, NC: U.S. Department of Agriculture Forest Service, Southern Research Station. 97 p. https://doi.org/10.2737/SRS-GTR-84.

Coulston, J.W.; Ambrose, M.J.; Riitters, K.H. [and others], eds. 2005b. Forest Health Monitoring 2003 national technical report. Gen. Tech. Rep. SRS-85. Asheville, NC: U.S. Department of Agriculture Forest Service, Southern Research Station. 97 p. https://doi.org/10.2737/SRS-GTR-85.

Coulston, J.W.; Ambrose, M.J.; Riitters, K.H.; Conkling, B.L., eds. 2005c. Forest Health Monitoring 2004 national technical report. Gen. Tech. Rep. SRS-90. Asheville, NC: U.S. Department of Agriculture Forest Service, Southern Research Station. 81 p. https://doi.org/10.2737/SRS-GTR-90.

Coulston, J.W.; Moisen, G.G.; Wilson, B.T. [and others]. 2012. Modeling percent tree canopy cover: a pilot study. Photogrammetric Engineering and Remote Sensing. 78(7): 715–727. https://doi.org/10.14358/PERS.78.7.715.

Cumming, A.B.; Nowak, D.J.; Twardus, D.B. [and others]. 2007. Urban forests of Wisconsin: pilot monitoring project 2002. NA-FR-05-07. Newtown Square, PA: U.S. Department of Agriculture Forest Service, Northeastern Area State and Private Forestry. 33 p.
Low resolution: http://www.na.fs.fed.us/pubs/fhm/pilot/pilot_study_wisconsin_02_lr.pdf.
High resolution: http://www.na.fs.fed.us/pubs/fhm/pilot/pilot_study_wisconsin2_02_hr.pdf.
[Date accessed: October 19, 2007].

Cumming, A.B.; Twardus, D.B.; Smith, W.D. 2006. National Forest Health Monitoring program, Maryland and Massachusetts street tree monitoring pilot projects. NA-FR-01-06. Newtown Square, PA: U.S. Department of Agriculture Forest Service, Northeastern Area State and Private Forestry. 23 p.

Edmonds, R.L.; Agee, J.K.; Gara, R.I. 2011. Forest health and protection. Long Grove, IL: Waveland Press, Inc. 667 p.

Fei, S.; Desprez, J.M.; Potter, K.M. [and others]. 2017. Divergence of species responses to climate change. Science Advances. 3(5): e1603055. https://doi.org/10.1126/sciadv.1603055.

Forest Health Monitoring (FHM). 2003. Forest Health Monitoring: a national strategic plan. 7 p. https://www.fs.fed.us/foresthealth/fhm/annc/strategic_plan03.pdf. [Date accessed: September 15, 2020].

Forest Health Monitoring (FHM). 2019. Program description. Forest Health Monitoring fact sheet series. https://www.fs.fed.us/foresthealth/protecting-forest/forest-health-monitoring/. [Date accessed: August 23, 2019].

Forest Health Protection (FHP). 2021. Insect and Disease Detection Survey (IDS) data downloads. Fort Collins, CO: U.S. Department of Agriculture Forest Service, Forest Health Technology Enterprise Team. https://www.fs.fed.us/foresthealth/applied-sciences/mapping-reporting/detection-surveys.shtml. [Date accessed: June 1, 2021].

Guo, Q.; Fei, S.; Dukes, J.S. [and others]. 2015. A unified approach to quantify invasibility and degree of invasion. Ecology. 95(10): 2613–2621. https://doi.org/10.1890/14-2172.1.

Guo, Q.; Fei, S.; Potter, K.M. [and others]. 2019. Tree diversity regulates forest pest invasion. Proceedings of the National Academy of Sciences. 116(15): 7382–7386. https://doi.org/10.1073/pnas.1821039116.

Guo, Q.; Iannone, B.V.; Nunez-Mir, G.C. [and others]. 2017. Species pool, human population, and global vs. regional invasion patterns. Landscape Ecology. 32(2): 229–238. https://doi.org/10.1007/s10980-016-0475-6.

Guo, Q.; Riitters, K.H.; Potter, K.M. [and others]. 2018. A subcontinental analysis of forest fragmentation and pest invasion. Forests. 9(12): 744. https://doi.org/10.3390/f9120744.

Harris, J.L., comp.; Region 2 Forest Health Protection staff. 2011. Forest health conditions, 2009–2010: Rocky Mountain Region (R2). R2-11-RO-31. Golden, CO: U.S. Department of Agriculture Forest Service, Renewable Resources, Forest Health Protection, Rocky Mountain Region. 108 p.

Heath, L.S.; Anderson, S.; Emery, M.R. [and others]. 2015. Indicators for climate change impacts for forests: National Climate Assessment indicators. Gen. Tech. Rep. NRS-155. Newtown Square, PA: U.S. Department of Agriculture Forest Service, Northern Research Station. 143 p.

Homer, C.G.; Dewitz, J.A.; Yang, L. [and others]. 2015. Completion of the 2011 National Land Cover Database for the conterminous United States: representing a decade of land cover change information. Photogrammetric Engineering and Remote Sensing. 81(5): 345–354.

Iannone, B.V.; Oswalt, C.M.; Liebhold, A.M. [and others]. 2015. Region-specific patterns and drivers of macroscale forest plant invasions. Diversity and Distributions. 21: 1181–1192. https://doi.org/10.1111/ddi.12354.

Iannone, B.V.; Potter, K.M.; Guo, Q. [and others]. 2016a. Biological invasion hotspots: a trait-based perspective reveals new sub-continental patterns. Ecography. 39: 961–969. https://doi.org/10.1111/ecog.01973.

Iannone, B.V.; Potter, K.M.; Guo, Q. [and others]. 2018. Environmental harshness drives spatial heterogeneity in biotic resistance. NeoBiota. 40: 87–105. https://doi.org/10.3897/neobiota.40.28558.

Iannone, B.V.; Potter, K.M.; Hamil, K.-A.D. [and others]. 2016b. Evidence of biotic resistance to invasions in forests of the Eastern USA. Landscape Ecology. 31: 85–99. https://doi.org/10.1007/s10980-015-0280-7.

Jo, I.; Potter, K.M.; Domke, G.; Fei, S. 2018. Dominant forest tree mycorrhizal type mediates understory plant invasions. Ecology Letters. 21: 217–224. https://doi.org/10.1111/ele.12884.

Jovan, S.; Riddell, J.; Padgett, P.E.; Nash, T.H., III. 2012. Eutrophic lichens respond to multiple forms of N: implications for critical levels and critical loads research. Ecological Applications. 22(7): 1910–1922. https://doi.org/10.1890/11-2075.1.

Koch, F.H.; Yemshanov, D.; Colunga-Garcia, M. [and others]. 2011. Potential establishment of alien-invasive forest insect species in the United States: where and how many? Biological Invasions. 13: 969–985. https://doi.org/10.1007/s10530-010-9883-8.

Koch, F.H.; Yemshanov, D.; Haack, R.A.; Magarey, R.D. 2014. Using a network model to assess risk of forest pest spread via recreational travel. PLOS ONE. 9(7): e102105. https://doi.org/10.1371/journal.pone.0102105.

Kolb, T.E.; Wagner, M.R.; Covington, W.W. 1994. Concepts of forest health: utilitarian and ecosystem perspectives. Journal of Forestry. 92: 10–15.

Krist, F.J., Jr.; Ellenwood, J.R.; Woods, M.E. [and others]. 2014. 2012–2027 national insect and disease forest risk assessment. FHTET-14-01. U.S. Department of Agriculture Forest Service, Forest Health Technology Enterprise Team. 199 p. http://www.fs.fed.us/foresthealth/technology/pdfs/2012_RiskMap_Report_web.pdf. [Date accessed: July 24, 2014].

Lake, M.; Marshall, P.; Mielke, M. [and others]. 2006. National Forest Health Monitoring program monitoring urban forests in Indiana: pilot study 2002, part 1. Analysis of field methods and data collection. NA-FR-06-06. Newtown Square, PA: U.S. Department of Agriculture Forest Service, Northeastern Area State and Private Forestry. http://www.fhm.fs.fed.us/pubs/ufhm/indianaforests02/indianaforests02.html. [Date accessed: November 6, 2007].

McGinley, K.A.; Cubbage, F.W., tech. eds. 2020. Legal, institutional, and economic indicators of forest conservation and sustainable management in the United States: analyzing criterion 7 of the Montréal Process criteria and indicators framework. Gen. Tech. Rep. IITF-GTR-52. Río Piedras, PR: U.S. Department of Agriculture Forest Service, International Institute of Tropical Forestry. 174 p.

McWilliams, W.H.; Westfall, J.A.; Brose, P.H. [and others]. 2015. A regeneration indicator for Forest Inventory and Analysis: history, sampling, estimation, analytics, and potential use in the Midwest and Northeast United States. Gen. Tech. Rep. NRS-148. Newtown Square, PA: U.S. Department of Agriculture Forest Service, Northern Research Station. 74 p. https://doi.org/10.2737/NRS-GTR-148.

Montréal Process Working Group. 1995. Criteria and indicators for the conservation and sustainable management of temperate and boreal forests. http://www.montrealprocess.org/. [Date accessed: March 4, 2015].

Morin, R.S.; Liebhold, A.M.; Gottschalk, K.W. [and others]. 2006. Analysis of Forest Health Monitoring surveys on the Allegheny National Forest (1998–2001). Gen. Tech. Rep. NE-339. Newtown Square, PA: U.S. Department of Agriculture Forest Service, Northeastern Research Station. 102 p. https://doi.org/10.2737/NE-GTR-339.

Morin, R.S.; Randolph, K.C.; Steinman, J. 2015. Mortality rates associated with crown health for eastern forest tree species. Environmental Monitoring and Assessment. 187(3): 87. https://doi.org/10.1007/s10661-015-4332-x.

O'Neill, K.P.; Amacher, M.C.; Perry, C.H. 2005. Soils as an indicator of forest health: a guide to the collection, analysis, and interpretation of soil indicator data in the Forest Inventory and Analysis program. Gen. Tech. Rep. NC-258. St. Paul, MN: U.S. Department of Agriculture Forest Service, North Central Research Station. 53 p. https://doi.org/10.2737/NC-GTR-258.

Oswalt, C.M.; Fei, S.; Guo, Q. [and others]. 2015. A subcontinental view of forest plant invasions. NeoBiota. 24: 49–54. https://doi.org/10.3897/neobiota.24.4526.

Oswalt, S.N.; Smith, W.B.; Miles, P.D.; Pugh, S.A., coords. 2019. Forest resources of the United States, 2017: a technical document supporting the Forest Service 2020 RPA Assessment. Gen. Tech. Rep. WO-97. Washington, DC: U.S. Department of Agriculture Forest Service, Washington Office. 223 p. https://doi.org/10.2737/WO-GTR-97.

Palmer, C.J.; Riitters, K.H.; Strickland, T. [and others]. 1991. Monitoring and research strategy for forests—Environmental Monitoring and Assessment Program (EMAP). EPA/600/4-91/012. Washington, DC: U.S. Environmental Protection Agency. 189 p.

Potter, K.M. 2018. Do United States protected areas effectively conserve forest tree rarity and evolutionary distinctiveness? Biological Conservation. 224: 34–46. https://doi.org/10.1016/j.biocon.2018.05.007.

Potter, K.M. 2020. Introduction. In: Potter, K.M.; Conkling, B.L., eds. Forest Health Monitoring: national status, trends, and analysis 2019. Gen. Tech. Rep. SRS-250. Asheville, NC: U.S. Department of Agriculture Forest Service, Southern Research Station: 5–24.

Potter, K.M.; Conkling, B.L., eds. 2012a. Forest Health Monitoring 2008 national technical report. Gen. Tech. Rep. SRS-158. Asheville, NC: U.S. Department of Agriculture Forest Service, Southern Research Station. 179 p. https://doi.org/10.2737/SRS-GTR-158.

Potter, K.M.; Conkling, B.L., eds. 2012b. Forest Health Monitoring 2009 national technical report. Gen. Tech. Rep. SRS-167. Asheville, NC: U.S. Department of Agriculture Forest Service, Southern Research Station. 252 p. https://doi.org/10.2737/SRS-GTR-167.

Potter, K.M.; Conkling, B.L., eds. 2013a. Forest Health Monitoring: national status, trends, and analysis 2010. Gen. Tech. Rep. SRS-176. Asheville, NC: U.S. Department of Agriculture Forest Service, Southern Research Station. 162 p. https://doi.org/10.2737/SRS-GTR-176.

Potter, K.M.; Conkling, B.L., eds. 2013b. Forest Health Monitoring: national status, trends, and analysis 2011. Gen. Tech. Rep. SRS-185. Asheville, NC: U.S. Department of Agriculture Forest Service, Southern Research Station. 149 p. https://doi.org/10.2737/SRS-GTR-185.

Potter, K.M.; Conkling, B.L., eds. 2014. Forest Health Monitoring: national status, trends, and analysis 2012. Gen. Tech. Rep. SRS-198. Asheville, NC: U.S. Department of Agriculture Forest Service, Southern Research Station. 192 p. https://doi.org/10.2737/SRS-GTR-198.

Potter, K.M.; Conkling, B.L., eds. 2015a. Forest Health Monitoring: national status, trends, and analysis 2013. Gen. Tech. Rep. SRS-207. Asheville, NC: U.S. Department of Agriculture Forest Service, Southern Research Station. 199 p. https://doi.org/10.2737/SRS-GTR-207.

Potter, K.M.; Conkling, B.L., eds. 2015b. Forest Health Monitoring: national status, trends, and analysis 2014. Gen. Tech. Rep. SRS-209. Asheville, NC: U.S. Department of Agriculture Forest Service, Southern Research Station. 190 p. https://doi.org/10.2737/SRS-GTR-209.

Potter, K.M.; Conkling, B.L., eds. 2016. Forest Health Monitoring: national status, trends, and analysis 2015. Gen. Tech. Rep. SRS-213. Asheville, NC: U.S. Department of Agriculture Forest Service, Southern Research Station. 199 p. https://doi.org/10.2737/SRS-GTR-213.

Potter, K.M.; Conkling, B.L., eds. 2017. Forest Health Monitoring: national status, trends, and analysis 2016. Gen. Tech. Rep. SRS-222. Asheville, NC: U.S. Department of Agriculture Forest Service, Southern Research Station. 195 p. https://doi.org/10.2737/SRS-GTR-222.

Potter, K.M.; Conkling, B.L., eds. 2018. Forest Health Monitoring: national status, trends, and analysis 2017. Gen. Tech. Rep. SRS-233. Asheville, NC: U.S. Department of Agriculture Forest Service, Southern Research Station. 190 p. https://doi.org/10.2737/SRS-GTR-233.

Potter, K.M.; Conkling, B.L., eds. 2019. Forest Health Monitoring: national status, trends, and analysis 2018. Gen. Tech. Rep. SRS-239. Asheville, NC: U.S. Department of Agriculture Forest Service, Southern Research Station. 168 p. https://doi.org/10.2737/SRS-GTR-239.

Potter, K.M.; Conkling, B.L., eds. 2020. Forest Health Monitoring: national status, trends, and analysis 2019. Gen. Tech. Rep. SRS-250. Asheville, NC: U.S. Department of Agriculture Forest Service, Southern Research Station. 189 p. https://doi.org/10.2737/SRS-GTR-250.

Potter, K.M.; Conkling, B.L., eds. 2021. Forest Health Monitoring: national status, trends, and analysis, 2020. Gen. Tech. Rep. SRS-261. Asheville, NC: U.S. Department of Agriculture Forest Service, Southern Research Station. 211 p. https://doi.org/10.2737/SRS-GTR-261.

Potter, K.M.; Escanferla, M.E.; Jetton, R.M.; Man, G. 2019a. Important insect and disease threats to United States tree species and geographic patterns of their potential impacts. Forests. 10(4): 304. https://doi.org/10.3390/f10040304.

Potter, K.M.; Escanferla, M.E.; Jetton, R.M. [and others]. 2019b. Prioritizing the conservation needs of United States tree species: evaluating vulnerability to forest insect and disease threats. Global Ecology and Conservation. 18: e00622. https://doi.org/10.1016/j.gecco.2019.e00622.

Potter, K.M.; Hargrove, W.W. 2013. Quantitative metrics for assessing predicted climate change pressure on North American tree species. Mathematical and Computational Forestry and Natural Resources Sciences. 5(2): 151–169.

Potter, K.M.; Koch, F.H. 2014. Phylogenetic community structure of forests across the conterminous United States: regional ecological patterns and forest health implications. Forest Science. 60(5): 851–861. https://doi.org/10.5849/forsci.13-115.

Potter, K.M.; Koch, F.H.; Oswalt, C.M.; Iannone, B.V. 2016. Data, data everywhere: detecting spatial patterns in fine-scale ecological information collected across a continent. Landscape Ecology. 31: 67–84. https://doi.org/10.1007/s10980-015-0295-0.

Potter, K.M.; Woodall, C.W. 2012. Trends over time in tree and seedling phylogenetic diversity indicate regional differences in forest biodiversity change. Ecological Applications. 22(2): 517–531. https://doi.org/10.1890/10-2137.1.

Potter, K.M.; Woodall, C.W. 2014. Does biodiversity make a difference? Relationships between species richness, evolutionary diversity, and aboveground live tree biomass across U.S. forests. Forest Ecology and Management. 321: 117–129. https://doi.org/10.1016/j.foreco.2013.06.026.

PRISM Climate Group. 2021. 2.5-arcmin (4 km) gridded monthly climate data. https://prism.oregonstate.edu. [Date accessed: August 20, 2021].

Raffa, K.F.; Aukema, B.; Bentz, B.J. [and others]. 2009. A literal use of "forest health" safeguards against misuse and misapplication. Journal of Forestry. 107: 276–277.

Randolph, K.C. 2010a. Equations relating compacted and uncompacted live crown ratio for common tree species in the South. Southern Journal of Applied Forestry. 34(3): 118–123. https://doi.org/10.1093/sjaf/34.3.118.

Randolph, K.C. 2010b. Comparison of the arithmetic and geometric means in estimating crown diameter and crown cross-sectional area. Southern Journal of Applied Forestry. 34(4): 186–189. https://doi.org/10.1093/sjaf/34.4.186.

Randolph, K.C. 2013. Development history and bibliography of the U.S. Forest Service crown-condition indicator for forest health monitoring. Environmental Monitoring and Assessment. 185(6): 4977–4993. https://doi.org/10.1007/s10661-012-2919-z.

Randolph, K.C.; Moser, W.K. 2009. Tree crown condition in Missouri, 2000–2003. Gen. Tech. Rep. SRS-113. Asheville, NC: U.S. Department of Agriculture Forest Service, Southern Research Station. 11 p. https://doi.org/10.2737/SRS-GTR-113.

Reams, G.A.; Smith, W.D.; Hansen, M.H. [and others]. 2005. The Forest Inventory and Analysis sampling frame. In: Bechtold, W.A.; Patterson, P.L., eds. The enhanced Forest Inventory and Analysis program—national sampling design and estimation procedures. Gen. Tech. Rep. SRS-80. Asheville, NC: U.S. Department of Agriculture Forest Service, Southern Research Station: 11–26.

Rebbeck, J.; Kloss, A.; Bowden, M. [and others]. 2015. Aerial detection of seed-bearing female *Ailanthus altissima*: a cost-effective method to map an invasive tree in forested landscapes. Forest Science. 61: 1068–1078. https://doi.org/10.5849/forsci.14-223.

Riitters, K.H. 2011. Spatial patterns of land cover in the United States: a technical document supporting the Forest Service 2010 RPA assessment. Gen. Tech. Rep. SRS-136. Asheville, NC: U.S. Department of Agriculture Forest Service, Southern Research Station. 64 p. https://doi.org/10.2737/SRS-GTR-136.

Riitters, K.; Costanza, J. 2019. The landscape context of family forests in the United States: anthropogenic interfaces and forest fragmentation from 2001 to 2011. Landscape and Urban Planning. 188: 64–71. https://doi.org/10.1016/j.landurbplan.2018.04.001.

Riitters, K.H.; Costanza, J.K.; Buma, B. 2017. Interpreting multiscale domains of tree cover disturbance patterns in North America. Ecological Indicators. 80: 147–152. https://doi.org/10.1016/j.ecolind.2017.05.022.

Riitters, K.H.; Coulston, J.W.; Wickham, J.D. 2012. Fragmentation of forest communities in the Eastern United States. Forest Ecology and Management. 263: 85–93. https://doi.org/10.1016/j.foreco.2011.09.022.

Riitters, K.; Potter, K.M.; Iannone, B.V. [and others]. 2018a. Exposure of protected forest to plant invasions in the Eastern United States. Forests. 9(11): 723. https://doi.org/10.3390/f9110723.

Riitters, K.; Potter, K.M.; Iannone, B.V. [and others]. 2018b. Landscape correlates of forest plant invasions: a high-resolution analysis across the Eastern United States. Diversity and Distributions. 24: 274–284. https://doi.org/10.1111/ddi.12680.

Riitters, K.H.; Tkacz, B. 2004. The U.S. Forest Health Monitoring program. In: Wiersma, G.B., ed. Environmental monitoring. Boca Raton, FL: CRC Press: 669–683. https://doi.org/10.1201/9780203495476.ch30.

Riitters, K.H.; Wickham, J.D. 2012. Decline of forest interior conditions in the conterminous United States. Scientific Reports. 2: 653. https://doi.org/10.1038/srep00653.

Riitters, K.H.; Wickham, J.D.; Costanza, J.K.; Vogt, P. 2016. A global evaluation of forest interior area dynamics using tree cover data from 2000 to 2012. Landscape Ecology. 31: 137–148. https://doi.org/10.1007/s10980-015-0270-9.

Root, H.T.; McCune, B.; Jovan, S. 2014. Lichen communities and species indicate climate thresholds in southeast and south-central Alaska, USA. The Bryologist. 117(3): 241–252. https://doi.org/10.1639/0007-2745-117.3.241.

Rose, A.K.; Coulston, J.W. 2009. Ozone injury across the Southern United States, 2002–06. Gen. Tech. Rep. SRS-118. Asheville, NC: U.S. Department of Agriculture Forest Service, Southern Research Station. 25 p. https://doi.org/10.2737/SRS-GTR-118.

Russell, M.B.; Woodall, C.W.; Potter, K.M. [and others]. 2017. Interactions between white-tailed deer density and the composition of forest understories in the Northern United States. Forest Ecology and Management. 384: 26–33. https://doi.org/10.1016/j.foreco.2016.10.038.

Schomaker, M.E.; Zarnoch, S.J.; Bechtold, W.A. [and others]. 2007. Crown-condition classification: a guide to data collection and analysis. Gen. Tech. Rep. SRS-102. Asheville, NC: U.S. Department of Agriculture Forest Service, Southern Research Station. 78 p. https://doi.org/10.2737/SRS-GTR-102.

Schulz, B.K.; Bechtold, W.A.; Zarnoch, S.J. 2009. Sampling and estimation procedures for the vegetation diversity and structure indicator. Gen. Tech. Rep. PNW-781. Portland, OR: U.S. Department of Agriculture Forest Service, Pacific Northwest Research Station. 53 p. https://doi.org/10.2737/PNW-GTR-781.

Schulz, B.K.; Gray, A.N. 2013. The new flora of Northeastern USA: quantifying introduced plant species occupancy in forest ecosystems. Environmental Monitoring and Assessment. 185: 3931–3957. https://doi.org/10.1007/s10661-012-2841-4.

Simkin, S.M.; Allen, E.B.; Bowman, W.D. [and others]. 2016. Conditional vulnerability of plant diversity to atmospheric nitrogen deposition across the United States. Proceedings of the National Academy of Sciences. 113: 4086–4091. https://doi.org/10.1073/pnas.1515241113.

Siry, J.; Cubbage, F.W.; Potter, K.M.; McGinley, K. 2018. Current perspectives on sustainable forest management: North America. Current Forestry Reports. 4(3): 138–149. https://doi.org/10.1007/s40725-018-0079-2.

Smith, W.D.; Conkling, B.L. 2004. Analyzing forest health data. Gen. Tech. Rep. SRS-077. Asheville, NC: U.S. Department of Agriculture Forest Service, Southern Research Station. 33 p. https://doi.org/10.2737/SRS-GTR-77.

Spencer, P.; Nowacki, G.; Fleming, M. [and others]. 2002. Home is where the habitat is: an ecosystem foundation for wildlife distribution and behavior. Arctic Research of the United States. 16: 6–17.

Steinman, J. 2004. Forest Health Monitoring in the Northeastern United States: disturbances and conditions during 1993–2002. NA-TP-01-04. Newtown Square, PA: U.S. Department of Agriculture Forest Service, Northeastern Area State and Private Forestry. 46 p. http://fhm.fs.fed.us/pubs/tp/dist_cond/dc.shtml. [Date accessed: December 8, 2009].

Teale, S.A.; Castello, J.D. 2011. The past as key to the future: a new perspective on forest health. In: Castello, J.D.; Teale, S.A., eds. Forest health: an integrated perspective. New York: Cambridge University Press: 3–16. https://doi.org/10.1017/CBO9780511974977.002.

U.S. Department of Agriculture (USDA) Forest Service. 2004. National report on sustainable forests—2003. FS-766. Washington, DC: U.S. Department of Agriculture Forest Service. 139 p.

U.S. Department of Agriculture (USDA) Forest Service. 2011. National report on sustainable forests—2010. FS-979. Washington, DC: U.S. Department of Agriculture Forest Service. 134 p.

U.S. Department of Agriculture (USDA) Forest Service. 2021. Fire detection GIS data. https://fsapps.nwcg.gov/afm/gisdata.php. [Date accessed: June 23, 2021].

Vogt, J.T.; Koch, F.H. 2016. The evolving role of Forest Inventory and Analysis data in invasive insect research. American Entomologist. 62(1): 46–58. https://doi.org/10.1093/ae/tmv072.

Vose, J.M.; Clark, J.S.; Luce, C.H.; Patel-Weynand, T., eds. 2016. Effects of drought on forests and rangelands in the United States: a comprehensive science synthesis. Gen. Tech. Rep. WO-93b. Washington, DC: U.S. Department of Agriculture Forest Service, Washington Office. 289 p. https://doi.org/10.2737/WO-GTR-93b.

Woodall, C.W.; Amacher, M.C.; Bechtold, W.A. [and others]. 2011. Status and future of the forest health indicators program of the USA. Environmental Monitoring and Assessment. 177: 419–436. https://doi.org/10.1007/s10661-010-1644-8.

Woodall, C.W.; Conkling, B.L.; Amacher, M.C. [and others]. 2010. The Forest Inventory and Analysis Database version 4.0: database description and users manual for Phase 3. Gen. Tech. Rep. NRS-61. Newtown Square, PA: U.S. Department of Agriculture Forest Service, Northern Research Station. 180 p. https://doi.org/10.2737/NRS-GTR-61.

Woodall, C.W.; Walters, B.F.; Oswalt, S.N. [and others]. 2013. Biomass and carbon attributes of downed woody materials in forests of the United States. Forest Ecology and Management. 305: 48–59. https://doi.org/10.1016/j.foreco.2013.05.030.

Woodall, C.W.; Walters, B.F.; Westfall, J.A. 2012. Tracking downed dead wood in forests over time: development of a piece matching algorithm for line intercept sampling. Forest Ecology and Management. 277: 196–204. https://doi.org/10.1016/j.foreco.2012.04.031.

Yemshanov, D.; Koch, F.H.; Lu, B. [and others]. 2014. There is no silver bullet: the value of diversification in planning invasive species surveillance. Ecological Economics. 104: 61–72. https://doi.org/10.1016/j.ecolecon.2014.04.024.

SECTION 1

Analyses of Short-Term Forest Health Data

CHAPTER 2

Broad-Scale Patterns of Insect and Disease Activity across the 50 United States from the National Insect and Disease Survey, 2020

Kevin M. Potter
Jeanine L. Paschke

INTRODUCTION

Forest insects and diseases have widespread ecological and economic impacts on the forests of the United States and may represent the most serious threats to the Nation’s forests (Logan and others 2003, Lovett and others 2016, Tobin 2015). U.S. law therefore authorizes the Forest Service, U.S. Department of Agriculture, to “conduct surveys to detect and appraise insect infestations and disease conditions and man-made stresses affecting trees and establish a monitoring system throughout the forests of the United States to determine detrimental changes or improvements that occur over time, and report annually concerning such surveys and monitoring” (FHP 2021). Insects and diseases cause changes in forest structure and function, species succession, and biodiversity, which may be considered negative or positive depending on management objectives (Edmonds and others 2011). Nearly all native tree species of the United States are affected by at least one injury-causing insect or disease agent, with exotic agents on average considerably more severe than native ones (Potter and others 2019a). Additionally, the genetic integrity of several native tree species is highly vulnerable to exotic diseases and insects (Potter and others 2019b).

An important task for forest managers, pathologists, and entomologists is recognizing and distinguishing between natural and excessive mortality, a task that relates to ecologically based or commodity-based management objectives (Teale and Castello 2011). The impacts of insects and diseases on forests vary from natural thinning to disruption of valued ecosystem processes as a result of tree mortality, but insects and diseases are not necessarily enemies of the forest because they kill trees (Teale and Castello 2011). If disturbances, including insects and diseases, are viewed in their full ecological context, then some amount can be considered “healthy” to sustain the structure of the forest (Manion 2003, Zhang and others 2011) by facilitating a sanitation role, that is, causing tree mortality that culls weak competitors and releases resources that are needed to support the growth of surviving trees (Teale and Castello 2011).

Analyzing patterns of forest insect infestations, disease occurrences, forest declines, and related biotic stress factors is necessary to monitor the health of forested ecosystems and their potential impacts on forest structure, composition, biodiversity, and species distributions (Castello and others 1995). In particular, introduced insects and diseases can extensively damage the biodiversity, ecology, and economy of affected areas (Brockerhoff and others 2006, Mack and others 2000). Few forests remain unaffected by invasive species, and their devastating impacts in forests are undeniable, including, in some cases, wholesale changes to the structure and function of an ecosystem (Parry and Teale 2011).

Examining insect pest occurrences and related stress factors from a landscape-scale perspective is useful, given the regional extent of many infestations and the large-scale complexity of interactions between host distribution, stress factors, and the development of outbreaks (Holdenrieder and others 2004, Liebhold and

How to cite this chapter:

Potter, Kevin M.; Paschke, Jeanine L. 2022. Broad-scale patterns of insect and disease activity across the 50 United States from the National Insect and Disease Survey, 2020. In: Potter, Kevin M.; Conkling, Barbara L., eds. Forest Health Monitoring: national status, trends, and analysis 2021. Gen. Tech. Rep. SRS-266. Asheville, NC: U.S. Department of Agriculture Forest Service, Southern Research Station: 25–49. https://doi.org/10.2737/SRS-GTR-266-Chap2.

others 2013). One such landscape-scale approach is detecting geographic patterns of disturbance, which allows for the identification of areas at greater risk of significant ecological and economic impacts and for the selection of locations for more intensive monitoring and analysis. National Insect and Disease Survey (IDS) data (FHP 2021), coordinated by the Forest Health Protection (FHP) program of the Forest Service, provide an important source of information about forest disturbances and their causal agents across broad regions. Recent long-term analyses of these data underscored that insects have been much more widespread agents of mortality than diseases, with bark beetles consistently the most important mortality agents across regions and over time (Potter and others 2020a). Additionally, the tree canopy area affected by nonnative invasive agents of mortality and defoliation has remained relatively consistent over time (with a larger relative impact on forests in the North), and tree canopy area affected by defoliation agents has usually exceeded or equaled the area affected by mortality agents (Potter and others 2020a).

Efforts to monitor the extent of insect and disease mortality and defoliation damage in U.S. forests continued in 2020 despite the challenges posed by the global COVID-19 pandemic. Because aerial survey flights were curtailed or not possible in many States, forest health specialists in those States quickly adopted other approaches, relying heavily on other sources of remotely sensed data.

METHODS

Data

In a typical year, IDS data (FHP 2021) consist of information from low-altitude aerial survey and ground survey efforts by FHP and partners in State agencies. These data can be used to summarize insect and disease activity by regions in the conterminous States (CONUS), Alaska, and Hawaii (Potter 2012, 2013; Potter and Koch 2012; Potter and Paschke 2013, 2014, 2015a, 2015b, 2016, 2017; Potter and others 2018, 2019c, 2020b, 2021). The global COVID-19 pandemic in 2020, however, precluded the ability of many State and regional Forest Service personnel to conduct aerial survey flights because of the risks posed by spending extended periods of time in the confined space of an aircraft. Instead, a group of forest health specialists had to work together to generate new workflows, training materials, and help sessions to address this challenge (Hanavan and others 2021). Specifically, many forest health specialists used a method called "pan and sketch" to outline damage polygons and points directly on base imagery, mostly from the National Agriculture Imagery Program (NAIP) 2020 or WorldView (FHP 2020). Some users collected features using the Digital Mobile Sketch Mapping (DMSM) tablet application, which allowed them to use common shortcut Quick Keys to capture the standard attributes. Others used the DMSM Desktop Tools Add-In to ArcMap® to capture features and attribute them.

The IDS data identify areas with mortality and defoliation caused by insect and disease activity, although some important forest insects (such as emerald ash borer [*Agrilus planipennis*] and hemlock woolly adelgid [*Adelges tsugae*]), diseases (such as laurel wilt [*Raffaelea lauricola*], Dutch elm disease [*Ophiostoma novo-ulmi*], white pine blister rust [*Cronartium ribicola*], and thousand cankers disease [*Geosmithia morbida*]), and mortality complexes (such as oak decline) are not easily detected or thoroughly quantified through aerial detection and other remote sensing methods. Such pests may attack hosts that are widely dispersed throughout forests with high tree species diversity or may cause mortality or defoliation that is otherwise difficult to detect. A pathogen or insect might be considered a mortality-causing agent in one location and a defoliation-causing agent in another, depending on the level of damage to the forest in an area and the convergence of other stress factors such as drought. In some cases, the identified agents of mortality or defoliation are actually complexes of multiple agents summarized under an impact label related to a specific host tree species (e.g., "beech bark disease complex" or "yellow-cedar decline"). Additionally, differences in data collection, attribute recognition, and coding procedures among States and regions can complicate data analysis and interpretation of the results. A comparison of aerial survey data with ground presence/absence observations found that the accuracy of the aerial survey data exceeded 70 percent, and that damage type observations for tree mortality and defoliation had high levels of accuracy, but that accuracy declined for severity estimates and as the specificity for observations went from genera to species level for tree species and damage agents (Coleman and others 2018).

In 2020, IDS surveys of the CONUS covered about 98.34 million ha of both forested and unforested area (fig. 2.1), of which approximately 68.34 million ha was forested, or about 21.6 percent of the 315.99-million-ha tree canopy area of the CONUS. This was less than half the percentage of tree-canopied area surveyed in 2018 (46.6 percent) and 2019 (49.2 percent) (Potter and others 2020b, 2021). Meanwhile, about 2.8 percent (2.18 million ha) of Alaska's 77.78 million ha of forest or shrubland was surveyed in 2020, out of a total of 2.70 million ha surveyed across land cover types. This compares to 12.7 percent in 2018 and 10.8 percent in 2019. Meanwhile, Hawaiian surveyors covered about 710 000 ha of that State during 2020. Approximately 520 000 ha of that area had tree canopy cover, or about 60.3 percent of the 861 000 ha total, compared to 69.4 percent in 2018 and 63.9 percent in 2019.

Digital Mobile Sketch Mapping includes tablet hardware, software, and data support processes that allow trained aerial surveyors in light aircraft, as well as ground observers and those using other remote sensing data, to record forest disturbances and their causal agents. Digital Mobile Sketch Mapping enhances the quality and quantity of forest health data while having the potential to improve safety by integrating with programs such as operational remote sensing (ORS), which uses satellite imagery to monitor disturbances in areas of higher aviation risk (FHP 2019). Geospatial data collected with DMSM are stored in the national IDS database. In an important change from the legacy Digital Aerial Sketch Mapping (DASM) approach, the DMSM platform allows surveyors to both define the extent of

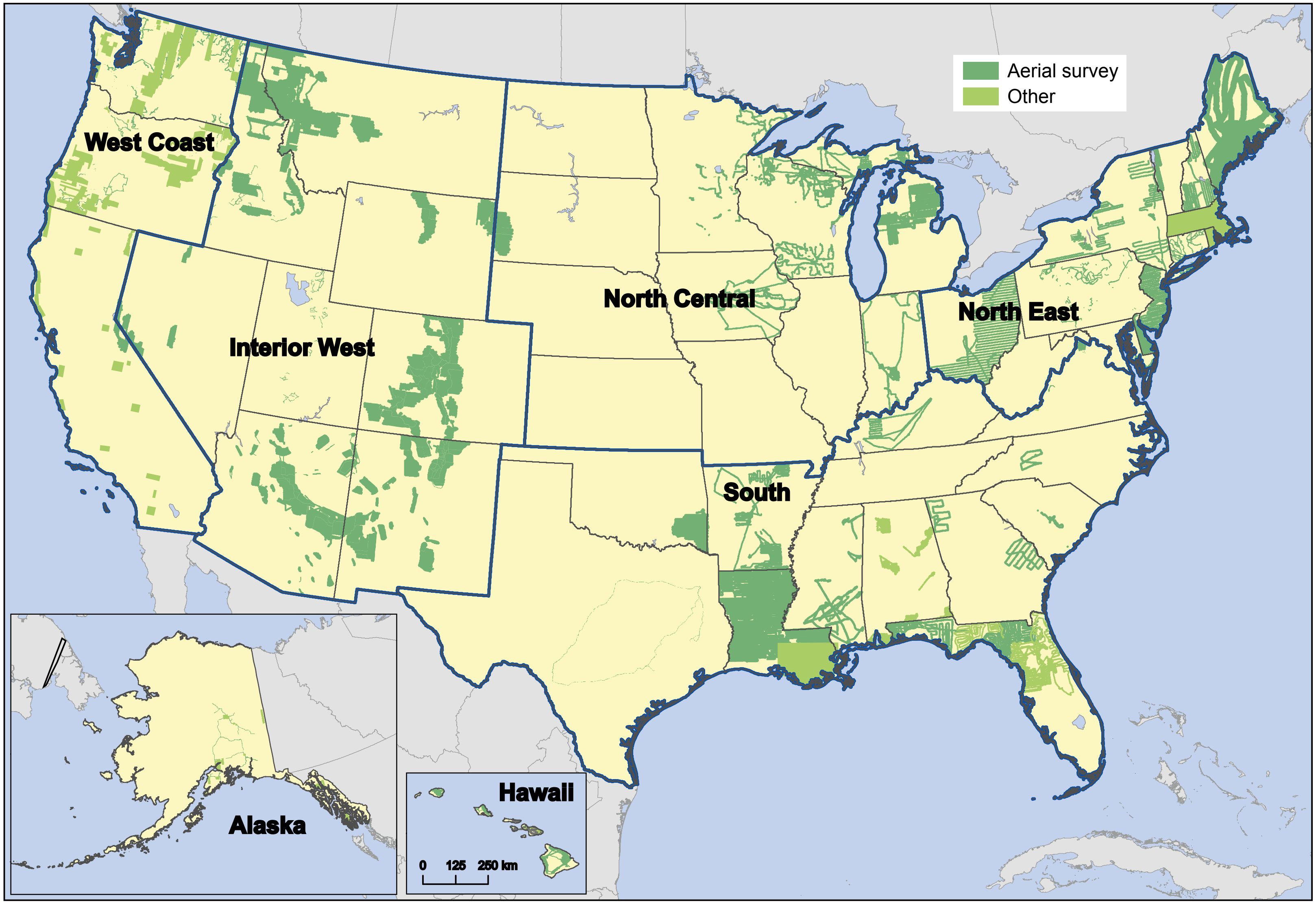

Figure 2.1—The extent of surveys for insect and disease activity conducted in the conterminous United States (CONUS), Alaska, and Hawaii in 2020. The blue lines delineate Forest Health Monitoring regions. Note: Alaska and Hawaii are not shown to scale with map of the CONUS. (Data source: U.S. Department of Agriculture Forest Service, Forest Health Protection)

an area experiencing damage and to estimate percent range of the area within the polygon that is affected (Berryman and McMahan 2019). While additional validation will be required for this new metric, it is expected to increase the accuracy of derived damage metrics because it potentially corrects for previous overestimation caused by "lassoing" areas of undamaged trees into large areas of damage (Coleman and others 2018, Slaton and others 2021). For this reason, FHM reports before 2019 did not incorporate any derived damage estimates beyond the areal footprint damage with mortality or defoliation polygon boundaries, but these are now possible because of the inclusion of damage percentage estimates within polygons (see "Analyses" below).

Digital Mobile Sketch Mapping includes both polygon geometry, used for damage areas where boundaries are discrete and obvious, and point geometry, used for small clusters of damage where the size and shape of the damage are less important than recording the location of damage, such as for sudden oak death (caused by the pathogen *Phytophthora ramorum*), southern pine beetle (*Dendroctonus frontalis*), and some types of bark beetle damage in the West. For the 2020 data, these points were assigned an area of 0.8 ha (about 2 acres). Additionally, DMSM allows for the use of grid cells (240-, 480-, 960-, or 1920-m resolution) to estimate the percentage of trees affected by damages that may be widespread and diffuse, such as those associated with spongy moth (*Lymantria dispar dispar*, formerly known as European gypsy moth) and emerald ash borer. When calculating the total areas affected by each damage agent, we used the entire areas of these grid cells (e.g., 240-m cell = 5.76 ha).

Analyses

To estimate the extent of damaging insect and disease agents in 2020, we conducted two types of analyses. In the first, we reported the most widely detected mortality and defoliation agents in a series of tables. Specifically, the 2020 mortality and defoliation polygons were used to identify the select mortality and defoliation agents and complexes causing damage on >5000 ha of forest in the CONUS in that year. Similarly, we listed the five most widely reported mortality and defoliation agents and complexes within each of five FHM regions within the CONUS (West Coast, Interior West, North Central, North East, and South), as well as for Alaska and Hawaii where data were available.

Because of the insect and disease aerial sketch-mapping process (i.e., digitization of polygons by a human interpreter aboard aircraft or by a forest health specialist applying the "pan and sketch" approach with remotely sensed data), all quantities are approximate "footprint" areas for each agent or complex, delineating areas of visible damage within which the agent or complex is present. Unaffected trees may exist within the footprint, and the amount of damage within the footprint is not reflected in the estimates of forest area affected. The sum of areas affected by all agents and complexes is not equal to the total affected area as a result of overlapping polygons and the reporting of multiple agents per polygon in some situations.

In our second set of analyses, we used the IDS data for 2020 to more directly estimate the impacts of insect- and disease-related mortality and defoliation on U.S. forests. These results are reported in a set of figures describing the percentage of surveyed tree canopy cover area with insect- and disease-related mortality or defoliation within ecoregions across the United States. As an indicator of the extent of damaging insect and disease agents, we summarized the percentage of surveyed tree canopy cover area experiencing mortality or defoliation for ecoregions within the CONUS and Hawaii, and for surveyed forest and shrubland in Alaska ecoregions. This is a change from FHM reports before 2019, in which we reported on the percentage of regions *exposed to* mortality and defoliating agents based only on the footprint with mortality or defoliation polygon boundaries (masked by forest cover) because information on the percentage of damage within polygons was not yet completely available. As noted above, DMSM now allows surveyors to both define the extent of an area experiencing damage and to estimate percent range of the area within the polygon that is affected (specifically, 1–3 percent, 4–10 percent, 11–29 percent, 30–50 percent, and >50 percent). By multiplying the area of damage within each polygon (after masking by tree canopy cover) by the midpoint of the estimated percent-affected range, it is possible to generate an adjusted estimate of the area affected by each mortality or defoliation agent detection (Berryman and McMahan 2019). These individual estimates can be summed for all the polygons within an ecoregion (intersected and dissolved) and divided by the total surveyed tree canopy cover area within the ecoregion to generate an estimate of the percentage of its canopy cover area affected by defoliating or mortality-causing agents. (Digital Mobile Sketch Mapping point data are also included in this estimate. Surveyors have the option to estimate the number of trees affected at a point and are required to assign an area value associated with each point, which is assumed to be 100 percent affected by its mortality or defoliation agent. For simplicity, we transformed each point into a 2-acre [0.809-ha] polygon. These areas for all the points in an ecoregion were then added to the polygon-adjusted affected area estimates for the ecoregion.)

For the CONUS, percentage of surveyed tree canopy area with mortality or defoliation was calculated within each of 190 ecoregion sections (Cleland and others 2007). Similarly, the mortality and defoliation data were summarized for each of the 32 ecoregion sections in Alaska (Spencer and others 2002). In Hawaii, the percentage of surveyed tree canopy area affected by mortality and defoliation agents was calculated by 34 ecoregion subunits on each of the major islands of the archipelago (Potter 2020). Statistics were not calculated for analysis regions in the CONUS with ≤2.5 percent of the tree canopy cover area surveyed (which is less than the ≤5 percent in a typical year because of the reduced extent of survey area resulting from the global COVID-19 pandemic), nor in Alaska with ≤1 percent of the forest and shrubland area surveyed (≤2.5 percent in a typical year), nor Hawaii with ≤5 percent of the tree canopy cover area surveyed (as in a typical year).

The tree canopy data used for the CONUS and Hawaii were resampled to 240 m from a 30-m raster dataset that estimates percentage of tree canopy cover (0–100 percent) for each grid cell; this dataset was generated from the 2011 National Land Cover Database (NLCD)

(Homer and others 2015) through a cooperative project between the Multi-Resolution Land Characteristics Consortium and the Forest Service Geospatial Technology and Applications Center (GTAC) (Coulston and others 2012). For our purposes, we treated any cell with >0-percent tree canopy cover as forest. Comparable tree canopy cover data were not available for Alaska, so we instead created a 240-m-resolution layer of forest and shrub cover from the 2011 NLCD.

In previous years, we used the Spatial Association of Scalable Hexagons (SASH) analytical approach to identify statistically significant geographic hot spots of mortality or defoliation in the CONUS (Potter and others 2016). This method consists of dividing an analysis area into scalable equal-area hexagonal cells within which data are aggregated, followed by identifying statistically significant geographic clusters of hexagonal cells within which mean values are greater or less than those expected by chance. To identify these clusters, we employ a Getis-Ord (G_i^*) hot spot analysis (Getis and Ord 1992) in ArcMap® 10.3 (ESRI 2017). The low density of survey data in 2020 from both the CONUS and Alaska, as well as the small spatial extent of Hawaii (fig. 2.1), precluded the use of Getis-Ord G_i^* hot spot analyses, so we were not able to include these analyses in this report.

RESULTS AND DISCUSSION

Conterminous United States Mortality

The national IDS data in 2020 identified 45 mortality-causing agents and complexes across the CONUS on approximately 1.17 million ha, an area slightly less than the land area of Connecticut. In comparison, forests cover approximately 257 million ha of the CONUS (Oswalt and others 2019). Thirteen of the agents were detected on >5000 ha. All these numbers were lower than in a typical year (e.g., Potter and others 2020b), in large part because of the challenge of collecting insect and disease damage data during the COVID-19 pandemic. About 211 000 ha with mortality were detected using remotely sensed data other than from aerial surveys, or 18 percent of the total for the CONUS.

In 2020, the most widely detected mortality agent was emerald ash borer, identified on approximately 716 000 ha (table 2.1), or about 61 percent of the total mortality area in the CONUS. The next most widespread agent was fir engraver (*Scolytus ventralis*), detected on 150 000 ha; this mortality agent was the most widespread in 2018 and 2019 (Potter and others 2020b). No other mortality agents or complexes were detected on >100 000 ha. Mortality from the western bark beetle group, including 15 different agents in the IDS data (table 2.2), encompassed about 31 percent of all the 2020 mortality area across the CONUS, much less than during a typical year.

The North Central FHM region in 2020 had the largest area on which mortality agents and complexes were detected, about 702 000 ha (table 2.3). All but 700 ha of this was attributed to emerald ash borer. Another nine agents totaled about 0.1 percent of the mortality area. The North Central ecoregion sections with the highest mortality of surveyed tree canopy cover were 251C–Central Dissected Till Plains of southern Iowa (10.93 percent) and 251B–North

Table 2.1—Mortality agents and complexes affecting >5000 ha in the conterminous United States during 2020, including area and percentage of area surveyed by remote sensing methods other than aerial surveys

Agents/complexes causing mortality, 2020	Total area	Remotely sensed area	
	ha	*ha*	*percent*
Emerald ash borer	715 518	0	0.0
Fir engraver	149 776	100 197	66.9
Unknown	81 057	54 189	66.9
Douglas-fir beetle	52 042	16 786	32.3
Spruce beetle	38 844	0	0.0
Mountain pine beetle	31 379	16 349	52.1
Unknown bark beetle[a]	30 508	0	0.0
Western pine beetle	26 954	14 494	53.8
Balsam woolly adelgid	10 685	0	0.0
Ips engraver beetles	9309	0	0.0
Western balsam bark beetle	9053	0	0.0
Pinyon ips	6571	0	0.0
Flatheaded fir borer	5167	0	0.0
Other (32)	21 544	0	0.0
Total, all mortality agents	**1 166 528**	**211 110**	**18.1**

Note: All values are “footprint” areas for each agent or complex. The sum of the individual agents is not equal to the total for all agents due to the reporting of multiple agents per polygon.

[a] In the Interior West, this is primarily damage on ponderosa pines. The group of bark beetles is known and varied but not distinguishable from the air. Regions have characterized it as "Southwest bark beetle complex" consisting mainly of damage caused by roundheaded pine beetle, western pine beetle, and ips beetles.

Table 2.2—Beetle taxa included in the “western bark beetle” group

Western bark beetle mortality agents	
Cedar and cypress bark beetles	*Phloeosinus* spp.
Douglas-fir beetle	*Dendroctonus pseudotsugae*
Fir engraver	*Scolytus ventralis*
Flatheaded borer	Buprestidae
Ips engraver beetles	*Ips* spp.
Jeffrey pine beetle	*Dendroctonus jeffreyi*
Mountain pine beetle	*Dendroctonus ponderosae*
Pine engraver	*Ips pini*
Pinyon ips	*Ips confusus*
Roundheaded pine beetle	*Dendroctonus adjunctus*
Silver fir beetle	*Pseudohylesinus sericeus*
Spruce beetle	*Dendroctonus rufipennis*
Unknown bark beetle	—
Western balsam bark beetle	*Dryocoetes confusus*
Western pine beetle	*Dendroctonus brevicomis*

Table 2.3—The top five mortality agents or complexes for each Forest Health Monitoring region and for Alaska and Hawaii in 2020, including area and percentage of area surveyed by remote sensing methods other than aerial surveys

Mortality agents and complexes, 2020	Total area	Remotely sensed area	
	ha	*ha*	*percent*
Interior West			
Spruce beetle	38 774	0	0.0
Unknown bark beetle[a]	30 457	12	0.0
Douglas-fir beetle	26 002	262	1.0
Fir engraver	12 265	4	0.0
Mountain pine beetle	9699	0	0.0
Other mortality agents (10)	28 423	31	0.1
Total, all mortality agents and complexes	**144 341**	309	0.2
North Central			
Emerald ash borer	701 656	0	0.0
Spruce budworm	326	0	0.0
Oak decline	229	0	0.0
Unknown	36	0	0.0
Dutch elm disease	25	0	0.0
Other mortality agents (5)	52	0	0.0
Total, all mortality agents and complexes	**702 310**	0	0.0
North East			
Emerald ash borer	8407	0	0.0
Southern pine beetle	3843	0	0.0
Unknown	1236	0	0.0
Black turpentine beetle	1218	0	0.0
White pine needle damage	315	0	0.0
Other mortality agents (10)	583	0	0.0
Total, all mortality agents and complexes	**15 585**	0	0.0

Mortality agents and complexes, 2020	Total area	Remotely sensed area	
	ha	*ha*	*percent*
South			
Emerald ash borer	5455	0	0.0
Unknown	2036	0	0.0
Laurel wilt	1774	0	0.0
Ips engraver beetles	1054	0	0.0
Southern pine beetle	19	0	0.0
Other mortality agents (2)	1	0	0.0
Total, all mortality agents and complexes	**10 339**	0	0.0
West Coast			
Fir engraver	137 511	100 193	72.9
Unknown	75 132	54 165	72.1
Western pine beetle	26 565	14 493	54.6
Douglas-fir beetle	26 040	16 525	63.5
Mountain pine beetle	21 680	16 349	75.4
Other mortality agents (20)	27 593	12 396	44.9
Total, all mortality agents and complexes	**293 952**	210 801	71.7
Alaska			
Spruce beetle	45 826	43 408	94.7
Hemlock sawfly	32 202	32 201	100.0
Yellow-cedar decline	4177	4067	97.4
Brown crumbly rot (red belt fungus)	1	0	0.0
Unknown canker, diffuse	1	0	0.0
Other mortality agents (7)	1	0	0.0
Total, all mortality agents and complexes	**82 204**	79 673	96.9
Hawaii			
Unknown[b]	32 297	0	0.0
Total, all mortality agents and complexes	**32 297**	0	0.0

Note: The total area affected by other agents is listed at the end of each section. All values are "footprint" areas for each agent or complex. The sum of the individual agents is not equal to the total for all agents due to the reporting of multiple agents per polygon.

[a] In the Interior West, this is primarily damage on ponderosa pines. The group of bark beetles is known and varied but not distinguishable from the air. Regions have characterized it as "Southwest bark beetle complex" consisting mainly of damage caused by roundheaded pine beetle, western pine beetle, and ips beetles.

[b] Most of the mortality recorded in Hawaii is coded as "unknown" mortality on ʻōhiʻa lehua. Damage is likely attributed to rapid ʻōhiʻa death but has not been confirmed in all cases.

Central Glaciated Plains of northwestern Iowa and southwestern Minnesota (6.02 percent), where emerald ash borer was detected killing white, green, and black ash (*Fraxinus americana*, *F. pennsylvanica*, and *F. nigra*) (fig. 2.2). Two adjacent ecoregions also experienced extensive mortality associated with emerald ash borer: 222M–Minnesota and Northeast Iowa Morainal-Oak Savannah (4.36 percent) and 222L–North Central U.S. Driftless and Escarpment of southwestern Wisconsin, northeastern Iowa, and southeastern Minnesota (3.99 percent).

In 2020, the West Coast FHM region had the second-largest area on which mortality agents and complexes were detected, about 294 000 ha (table 2.3). A little less than half of this area (138 000 ha) was associated with fir engraver mortality. The next most commonly detected and known mortality agents were western pine beetle (*D. brevicomis*) on 27 000 ha (9.0 percent of the mortality area), Douglas-fir beetle (*D. pseudotsugae*) on 26 000 ha (8.9 percent), and mountain pine beetle (*D. ponderosae*) on 22 000 ha (7.4 percent). Another 20 mortality-causing agents and complexes accounted for 9.4 percent of the mortality area in the West Coast region.

Most of the sufficiently surveyed ecoregions in the West Coast region had at least a moderate amount of mortality in their surveyed area (>0.25 percent) (fig. 2.2). For example, the M261A–Klamath Mountains ecoregion section in northwestern California and southwestern Oregon had 1.35-percent mortality in surveyed canopy area, the result of fir engraver mortality in Pacific silver fir (*Abies amabilis*), grand fir (*A. grandis*), California red fir (*A. magnifica* var. *shastensis*), and noble fir (*A. procera*) forests, and of flatheaded fir borer (*Phaenops drummondi*) in Douglas-fir (*Pseudotsuga menziesii*) forests. In 261A–Central California Coast (1.20-percent mortality in surveyed areas), an unknown agent was causing mortality in California live oak (*Quercus agrifolia*) stands. Western pine beetle in stands of ponderosa pine (*Pinus ponderosa*) and fir engraver in stands of white fir (*A. concolor*) were issues in M261D–Southern Cascades (0.89-percent mortality of surveyed areas), while a long list of agents caused mortality in M333A–Okanogan Highland (0.92 percent), including ips engraver beetles and western pine beetle in ponderosa pine; Douglas-fir beetle in Douglas-fir; fir engraver and balsam woolly adelgid (*Adelges piceae*) in Pacific silver fir, noble fir, and grand fir; and mountain pine beetle in lodgepole pine (*P. contorta*). Similarly, several agents caused mortality in the M262B–Southern California Mountain and Valley ecoregion section (0.63 percent): fir engraver in white fir stands; Jeffrey pine beetle (*D. jeffreyi*) in Jeffrey pine (*P. jeffreyi*) stands; western pine beetle in ponderosa pine stands; and goldspotted oak borer (*A. auroguttatus*) in valley oak (*Q. lobata*), interior live oak (*Q. wislizeni*), canyon live oak (*Q. chrysolepis*), Engelmann oak (*Q. engelmannii*), and California black oak (*Q. kelloggii*). Finally, the M332G–Blue Mountains ecoregion section of northeastern Oregon had 0.58-percent mortality of surveyed areas due to mountain pine beetle-caused mortality in lodgepole pine, western pine beetle in ponderosa pine, and fir engraver in various firs.

In the Interior West FHM region, damage from 15 mortality agents and complexes was identified across 144 000 ha (table 2.3). As in 2018, spruce beetle (*D. rufipennis*) was the most

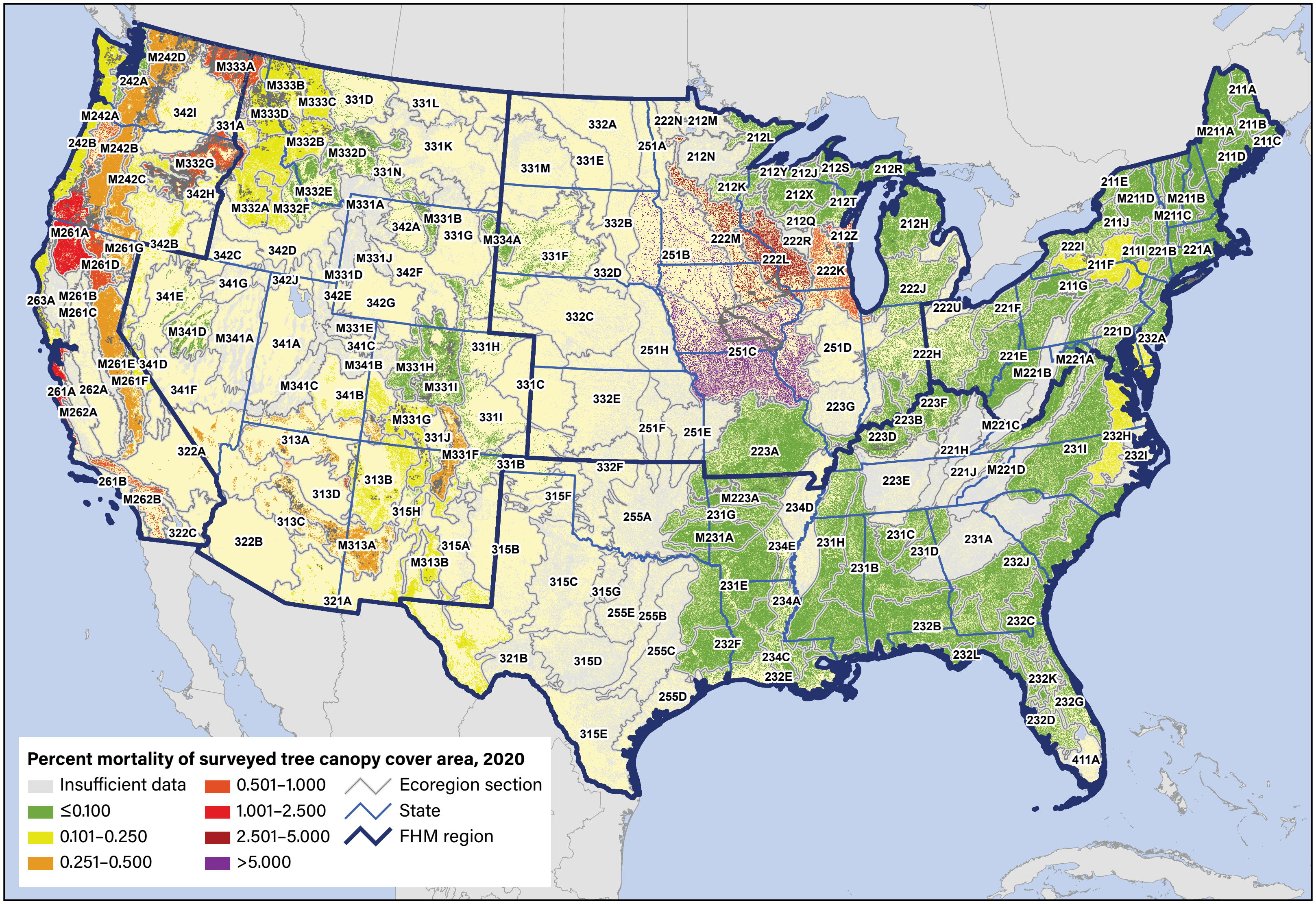

Figure 2.2—The percentage of surveyed tree canopy cover area with insect and disease mortality, by ecoregion section within the conterminous United States, for 2020. The gray lines delineate ecoregion sections (Cleland and others 2007). The 240-m tree canopy cover is based on data from a cooperative project between the Multi-Resolution Land Characteristics Consortium (Coulston and others 2012) and the Forest Service Geospatial Technology and Applications Center using the 2011 National Land Cover Database. (Data source: U.S. Department of Agriculture Forest Service, Forest Health Protection)

widely detected agent, recorded on about 39 000 ha, or 26.9 percent of the total mortality area. Next, unknown bark beetles affected 21.1 percent of the total mortality area, or 30 000 ha. This was primarily damage in ponderosa pine forests by a group of known and varied bark beetles that are not possible to distinguish using remotely sensed data. This also has been characterized as "Southwest bark beetle complex" consisting mainly of damage caused by roundheaded pine beetle (*D. adjunctus*), western pine beetle, and ips beetles. Other widespread mortality agents in the region were Douglas-fir beetle detected on 26 000 ha (18.0 percent), fir engraver beetle on 12 000 ha (8.5 percent), and mountain pine beetle on 10 000 ha (6.7 percent) (table 2.3).

Interior West mortality was highest in the Four Corners States (fig. 2.2). The 313D–Painted Desert ecoregion section had the highest percentage of surveyed tree canopy area mortality (0.67) in the region, mostly the result of pinyon ips in two-needle pinyon (*P. edulis*) stands, as well as some mortality caused by cedar and cypress bark beetles in stands of Arizona cypress (*Cupressus arizonica*) and various junipers (*Juniperus* spp.) In the M331F–Southern Parks and Rocky Mountain Range ecoregion section, 0.43 percent of surveyed canopy area had mortality, the result of Engelmann spruce (*Picea engelmannii*) mortality by spruce beetle in the northern half of the ecoregion, and of Douglas-fir beetle in Douglas-fir stands and Southwest bark beetle complex in ponderosa pine stands (described above) in the southern half. Three other ecoregion sections, 313A–Grand Canyon (0.32 percent mortality), M313A–White Mountains-San Francisco Peaks-Mogollon Rim (0.31 percent), and 313C–Tonto Transition (0.28 percent), also experienced mortality from Southwest bark beetle complex in ponderosa pine. This was in addition to roundheaded pine beetle in ponderosa pine and pinyon ips in two-needle pinyon in 313A–Grand Canyon, as well as to spruce beetle in Engelmann spruce, Douglas-fir beetle in Douglas-fir, and western balsam bark beetle in corkbark fir (*Abies lasiocarpa* var. *arizonica*) in M313A–White Mountains-San Francisco Peaks-Mogollon Rim.

Approximately 16 000 ha in the North East FHM region had recorded damage from 15 mortality agents and complexes in 2020 (table 2.3). The most commonly detected was emerald ash borer, on 8000 ha (53.9 percent of the total mortality area in the region). Less commonly identified agents were southern pine beetle (4000 ha, 24.7 percent) and black turpentine beetle (*Dryocoetes terebrans*) (1000 ha, 7.8 percent). Two ecoregion sections had mortality exceeding 0.1 percent of the surveyed tree canopy area (fig. 2.2): 211F–Northern Glaciated Allegheny Plateau (0.12 percent) as a result of emerald ash borer and 232H–Middle Atlantic Coastal Plains and Flatwoods (also 0.12 percent) as a result of an unknown conifer mortality agent.

Finally, in the South FHM region, surveyors identified seven agents causing 10 000 ha with mortality (table 2.3). As with the North Central and North East regions, emerald ash borer was the most common mortality category (5000 ha, 52.8 percent), followed by "unknown" (2000 ha, 19.7 percent), laurel wilt (2000 ha, 17.2 percent), and ips engraver beetles (1000 ha, 10.2 percent).

Conterminous United States Defoliation

The national IDS in 2020 identified 59 defoliation agents and complexes affecting approximately 1.54 million ha across the CONUS (table 2.4), which is somewhat larger than the combined land area of Connecticut and Rhode Island. The most widespread defoliation agent was spruce budworm (*Choristoneura fumiferana*), detected on 496 000 ha, or approximately 32 percent of the total area with defoliation. In 2018 and 2019 (Potter and others 2020b, 2021), the most widespread defoliation agent was western spruce budworm (*C. freemani*), which was the third-most common in 2020, found on 220 000 ha or 14 percent of the total. Four additional agents were each detected on >100 000 ha: spongy moth on 388 000 ha, forest tent caterpillar (*Malacosoma disstria*) on 195 000 ha, and baldcypress leafroller (*Archips goyerana)* on 136 000 ha. About 14.5 percent of the total CONUS defoliation (223 000 ha) was detected

Table 2.4—Defoliation agents and complexes affecting >5000 ha in the conterminous United States in 2020, including area and percentage of area surveyed by remote sensing methods other than aerial surveys

Agents/complexes causing defoliation, 2020	Total area	Remotely sensed area	
	ha	*ha*	*percent*
Spruce budworm	496 493	0	0.0
Spongy moth	388 480	0	0.0
Western spruce budworm	219 735	0	0.0
Forest tent caterpillar	195 382	195 364	100.0
Baldcypress leafroller	135 709	135 709	100.0
Unknown defoliator	33 629	0	0.0
Douglas-fir tussock moth	31 958	0	0.0
Unknown	31 665	0	0.0
Gelechiid moths/needleminers	19 842	0	0.0
Browntail moth	17 943	0	0.0
Agromyzid fly	17 491	0	0.0
Fall webworm	14 839	0	0.0
Fall cankerworm	10 406	10 336	99.3
Maple leafcutter	8026	0	0.0
Pinyon needle scale	7350	0	0.0
Other (44)	38 141	5494	14.4
Total, all defoliation agents	**1 535 291**	**222 690**	**14.5**

Note: All values are "footprint" areas for each agent or complex. The sum of the individual agents is not equal to the total for all agents due to the reporting of multiple agents per polygon.

through remotely sensed methods other than the standard aerial surveys.

The North Central FHM region had the largest area on which defoliation was detected in 2020 (table 2.5). Surveyors identified 16 defoliation agents on approximately 924 000 ha, with slightly more than half of the defoliation area attributed to spruce budworm (496 000 ha). Spongy moth also caused widespread damage (385 000 ha, 41.6 percent).

Two ecoregion sections in the Great Lakes area exceed 5-percent defoliation of surveyed canopy cover (fig. 2.3): 212L–Northern Superior Uplands in northeastern Minnesota and 212H–Northern Lower Peninsula. In the former, the defoliation was by spruce budworm in spruce and fir forests, while it was by spongy moth in oak forests and spruce budworm in the latter. Other areas of extensive defoliation included 222J–South Central Great Lakes in southern Michigan (spongy moth), 251B–North Central Glaciated Plains of northwestern Iowa and southwestern Minnesota (Japanese beetle [*Popillia japonica*] and oak skeletonizer [*Bucculatrix ainsliella*]), and 223B–Interior Low Plateau-Transition Hills of south-central Indiana (unknown hardwood defoliator).

In the Interior West FHM region, 306 000 ha of damage was associated with 17 defoliators (table 2.5). Most of this area (71.7 percent) was affected by western spruce budworm (220 000 ha), as in recent years (Potter and others 2020b, 2021). Other widespread and known defoliators were Douglas-fir tussock moth (*Orgyia pseudotsugata*) which affected 30 000 ha (9.7 percent), Gelechiid moths/needleminers (*Coleotechnites* spp.) identified on 20 000 ha (6.5 percent), and pinyon needle scale (*Matsucoccus acalyptus*) detected on 7000 ha (2.4 percent).

Western spruce budworm caused extensive defoliation in areas of both the southern and northern Rockies, which was highest in M331F–Southern Parks and Rocky Mountain Range (4.99-percent defoliation of surveyed area) and M331G–South-Central Highlands (3.76 percent), both in south-central Colorado and north-central New Mexico (fig. 2.3). Western spruce budworm was also an issue in three adjacent ecoregion sections, M331I–Northern Parks and Ranges (0.78 percent) and M331H–North-Central Highlands and Rocky Mountains (0.61 percent) in north-central Colorado, and 313A–Grand Canyon (0.73 percent) in the Four Corners area. Meanwhile, it was also widespread in several ecoregion sections in northern Idaho, western Montana, and north-central Wyoming: M332B–Northern Rockies and Bitterroot Valley (0.85 percent), M333D–Bitterroot Mountains (0.73 percent), M332D–Belt Mountains (0.57 percent), and M331B–Bighorn Mountains (0.77 percent). Throughout the Interior West FHM region, western spruce budworm infested a variety of spruce (*Picea*) and fir (*Abies*) species, as well as Douglas-fir.

Additional defoliators were active in these ecoregion sections, usually to a lesser extent than western spruce beetle where it was present. For example, Douglas-fir tussock moth defoliated grand and subalpine fir (*A. lasiocarpa*) in M333D–Bitterroot Mountains and M332B–Northern Rockies and Bitterroot Valley. Quaking aspen

Table 2.5—The top five defoliation agents or complexes for each Forest Health Monitoring region and for Alaska and Hawaii in 2020, including area and percentage of area surveyed by remote sensing methods other than aerial surveys

Defoliation agents and complexes, 2020	Total area	Remotely sensed area	
	ha	*ha*	*percent*
Interior West			
Western spruce budworm	219 631	285	0.1
Unknown defoliator	32 868	98	0.3
Douglas-fir tussock moth	29 713	0	0.0
Gelechiid moths/needleminers	19 842	0	0.0
Pinyon needle scale	7350	0	0.0
Other defoliation agents (12)	4318	156	3.6
Total, all defoliation agents and complexes	**306 188**	540	0.2
North Central			
Spruce budworm	496 493	0	0.0
Spongy moth	384 605	0	0.0
Unknown	31 072	0	0.0
Japanese beetle	4478	0	0.0
Oak skeletonizer	2212	0	0.0
Other defoliation agents (11)	4698	0	0.0
Total, all defoliation agents and complexes	**923 557**	0	0.0
North East			
Browntail moth	17 943	0	0.0
Agromyzid fly	17 491	0	0.0
Fall webworm	14 839	0	0.0
Maple leafcutter	8026	0	0.0
Spongy moth	3875	31	0.8
Other defoliation agents (13)	11 246	2549	22.7
Total, all defoliation agents and complexes	**73 419**	2580	3.5

Defoliation agents and complexes, 2020	Total area	Remotely sensed area	
	ha	*ha*	*percent*
South			
Forest tent caterpillar	195 208	195 208	100.0
Baldcypress leafroller	135 709	135 709	100.0
Fall cankerworm	7787	7787	100.0
Sawflies	409	0	0.0
Unknown	7	0	0.0
Other defoliation agents (1)	<1	0	0.0
Total, all defoliation agents and complexes	**214 907**	214 491	99.8
West Coast			
Balsam woolly adelgid	3229	1855	57.5
Pandora moth	2929	0	0.0
Larch casebearer	2567	168	6.5
Lophodermium needle cast of pines	2343	0	0.0
Douglas-fir tussock moth	2245	2110	94.0
Other defoliation agents (15)	3957	947	23.9
Total, all defoliation agents and complexes	**17 219**	5079	29.5
Alaska			
Hemlock sawfly	49 407	42 492	86.0
Aspen leafminer	15 670	14 527	92.7
Unknown defoliator	1184	600	50.7
Birch leafminer	1152	0	0.0
Willow leaf blotchminer	169	122	72.4
Other defoliation agents (41)	108	0	0.0
Total, all defoliation agents and complexes	**67 683**	57 741	85.3
Hawaii			
'Ōhi'a / guava rust	5	0	0.0
Total, all defoliation agents and complexes	**5**	0	0.0

Note: The total area affected by other agents is listed at the end of each section. All values are "footprint" areas for each agent or complex. The sum of the individual agents is not equal to the total for all agents due to the reporting of multiple agents per polygon.

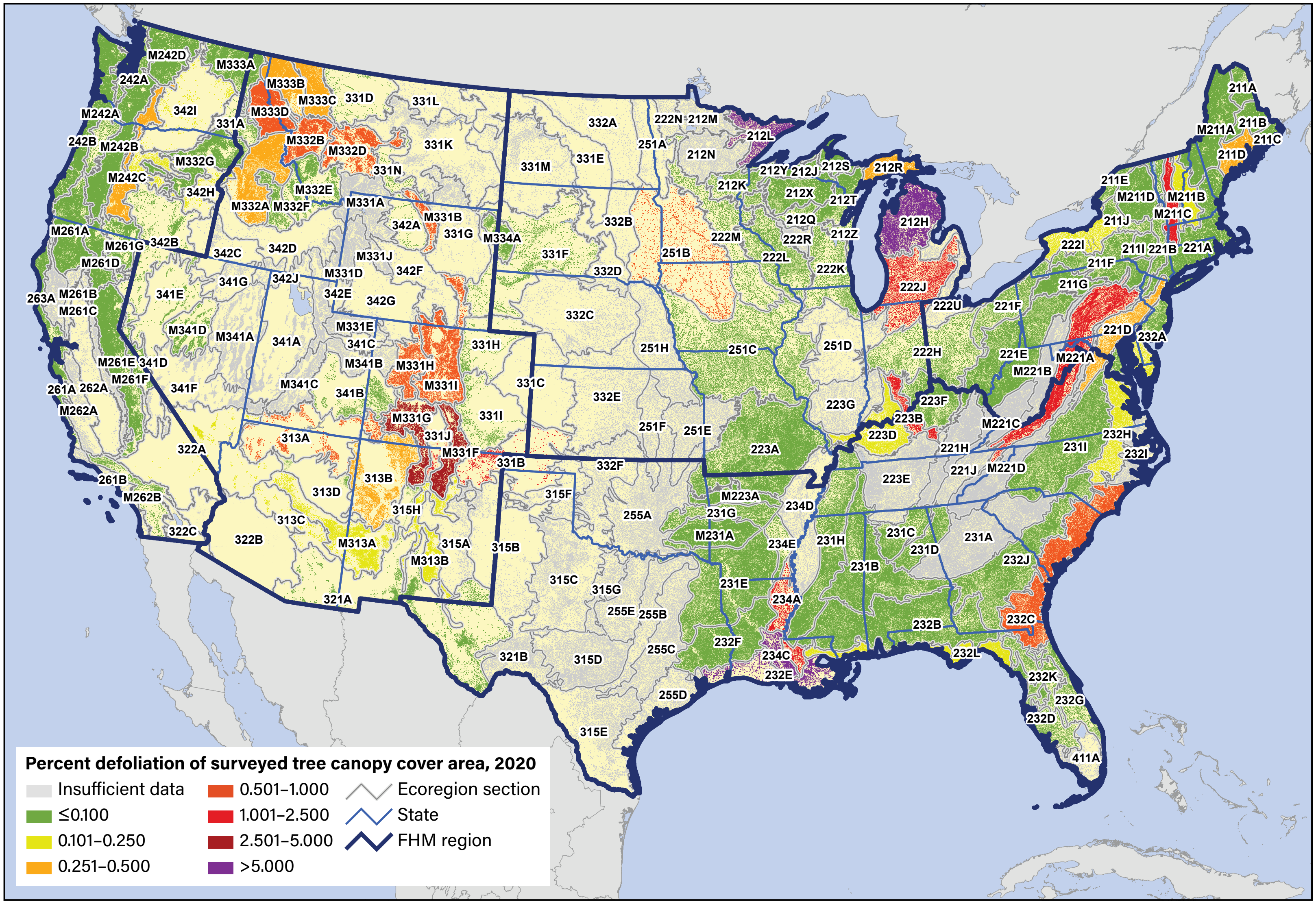

Figure 2.3—The percentage of surveyed tree canopy cover area with insect and disease defoliation, by ecoregion section within the conterminous United States, for 2020. The gray lines delineate ecoregion sections (Cleland and others 2007). The 240-m tree canopy cover is based on data from a cooperative project between the Multi-Resolution Land Characteristics Consortium (Coulston and others 2012) and the Forest Service Geospatial Technology and Applications Center using the 2011 National Land Cover Database. (Data source: U.S. Department of Agriculture Forest Service, Forest Health Protection)

(*Populus tremuloides*) was defoliated by Marssonina blight in M331G–South-Central Highlands and by unknown defoliators there and in M331F–Southern Parks and Rocky Mountain Range (where Gelechiid moths/needleminers also defoliated ponderosa pine), M331I–Northern Parks and Ranges, and 313A–Grand Canyon (where pinyon needle scale also defoliated two-needle pinyon).

In the South FHM region, two of six agents were the most widely identified: forest tent caterpillar on about 195 000 ha (90.8 percent of the regional total) and baldcypress leafroller on about 136 000 ha (63.1 percent). The two co-occurred on large areas of surveyed tree canopy cover. Fall cankerworm (*Alsophila pometaria*) defoliation was detected on an additional 8000 ha (3.6 percent).

The combination of forest tent caterpillar (in a variety of southern hardwoods) and baldcypress leafroller (in baldcypress [*Taxodium distichum*]) resulted in high levels of defoliation in southern and eastern Louisiana: 232E–Louisiana Coastal Prairie and Marshes (8.83 percent defoliation of surveyed canopy area) and 234C–Atchafalaya and Red River Alluvial Plains (2.27 percent) (fig. 2.3). The 232C–Atlantic Coastal Flatwoods ecoregion section, which stretches along the Atlantic Coast from North Carolina to northern Florida, also had relatively high defoliation (0.51 percent) as a result of forest tent caterpillar.

Surveyors in 2020 documented about 73 000 ha with defoliation in the North East FHM region (table 2.5), with browntail moth (*Euproctis chrysorrhoea*) detected on about 18 000 ha (24.4 percent of the area with defoliation), agromyzid fly (*Agromyza viridula*) on about 17 000 ha (23.8 percent), and fall webworm (*Hyphantria cunea*) on about 15 000 ha (20.2 percent). Among the other 15 defoliating agents detected in the region, maple leafcutter (*Paraclemensia acerifoliella*) and spongy moth were recorded on an additional 8000 ha and 4000 ha, respectively.

The North East ecoregion section with the highest proportion of defoliation was M221A–Northern Ridge and Valley in east-central Pennsylvania (2.12 percent), where locust leafminer (*Odontota dorsalis*) infested black locust (*Robinia pseudoacacia*) and where fall webworm impacted various hardwoods (fig. 2.3). A relatively high proportion of defoliated surveyed canopy area (1.26 percent) was caused in M211C–Green-Taconic-Berkshire Mountains in Vermont and Massachusetts by maple leafcutter in stands of sugar maple (*Acer saccharum*) and red maple (*A. rubrum*). Meanwhile, fall webworm was an issue in the 221D–Northern Appalachian Piedmont of southeastern Pennsylvania and northern New Jersey (0.33-percent defoliation), and browntail moth was an issue in northern red oak (*Quercus rubra*) stands in 211D–Central Maine Coastal and Embayment (0.31 percent).

Finally, 20 defoliating agents were recorded in the West Coast FHM region on 17 000 ha (table 2.5), with no single agent responsible for a majority of the defoliation. Five agents each represent between 13 and 19 percent of defoliation: balsam woolly adelgid (3000 ha), pandora moth (*Coloradia pandora*) (3000 ha), larch casebearer (*Coleophora laricella*) (2600 ha), Lophodermium needle cast of pines (*Lophodermium* spp.) (2000 ha), and Douglas-fir tussock moth (2000 ha).

One West Coast ecoregion section, M242C–Eastern Cascades of south-central Washington and central Oregon, had a moderate proportion of defoliation (0.31 percent of surveyed canopy area) (fig. 2.3). This was the result of a suite of defoliating agents: pandora moth in ponderosa and lodgepole pines; lodgepole pine sawfly (*Neodiprion nanulus contortae*) in lodgepole stands; balsam woolly adelgid in Pacific silver, subalpine, and grand fir stands; and larch needle cast (*Rhabdocline laricis*) in western larch (*Larix occidentalis*).

Alaska and Hawaii

In 2020, surveyors detected 82 000 ha with mortality in Alaska, attributed to 12 agents (table 2.3), an increase from 2019. As in previous years, spruce beetle was the most widely detected mortality agent, encompassing 46 000 ha and 55.7 percent of total area with mortality. Other widespread mortality agents were hemlock sawfly (*Neodiprion tsugae*), identified on 32 000 ha (39.2 percent of the total) and yellow-cedar (*Chamaecyparis nootkatensis*) decline, on 4000 ha or 5.1 percent of the total.

Also as in recent years, spruce beetle mortality was concentrated in south-central Alaska (fig. 2.4). The 133A–Cook Inlet Basin ecoregion section had the highest mortality of surveyed forest and shrubland in the State (2.89 percent). Two neighboring ecoregion sections also had relatively high mortality: M241C–Chugach-St. Elias Mountains (0.47) and M133B–Alaska Range (0.38 percent). Additionally, mortality from hemlock sawfly in western hemlock (*Tsuga heterophylla*) stands resulted in 0.78-percent mortality of the surveyed forest and shrubland of M241D–Alexander Archipelago in the Alaska panhandle.

Meanwhile, 46 agents resulted in 68 000 ha of Alaskan defoliation detected in 2020 (table 2.5). Hemlock sawfly encompassed 73.0 percent of the total defoliation area (49 000 ha). Aspen leafminer (*Phyllocnistis populiella*) was detected on an additional 16 000 ha (23.2 percent of the total).

The highest levels of defoliation occurred in east-central Alaska and in the panhandle (fig. 2.5). The 2.03-percent defoliation of surveyed forest and shrubland in M241D–Alexander Archipelago, in the Alaska panhandle, was attributed to hemlock sawfly, which also generated a relatively high level of mortality in the area (see above). Farther north, aspen leafminer was the primary cause of defoliation in M132C–Yukon-Tanana Uplands (1.93 percent of surveyed forest and shrubland), M132F–North Ogilvie Mountains (1.06 percent), and 132C–Tanana-Kuskokwim Lowlands (0.53 percent).

In the pandemic year of 2020, >85 percent of Alaska mortality (table 2.3) and defoliation (table 2.5) were detected using alternative methods to the standard aerial detection surveys.

Finally, about 32 000 ha with mortality were detected in Hawaii during 2020 using standard aerial survey methods (table 2.3), compared to

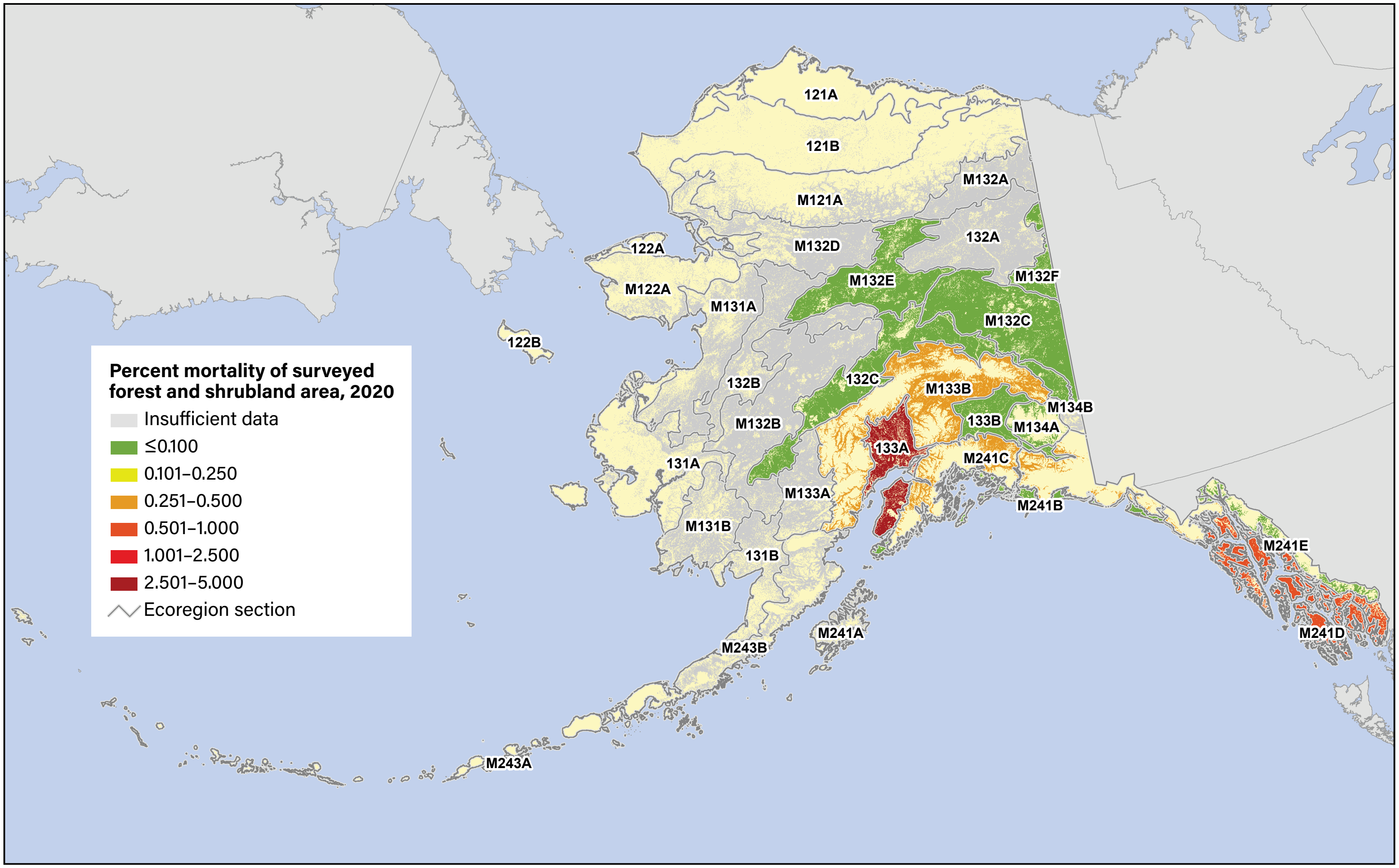

Figure 2.4—Percentage of 2020 surveyed Alaska forest and shrubland area within ecoregions with mortality caused by insects and diseases. The gray lines delineate ecoregion sections (Spencer and others 2002). Forest and shrub cover is derived from the 2011 National Land Cover Database. (Data source: U.S. Department of Agriculture Forest Service, Forest Health Protection)

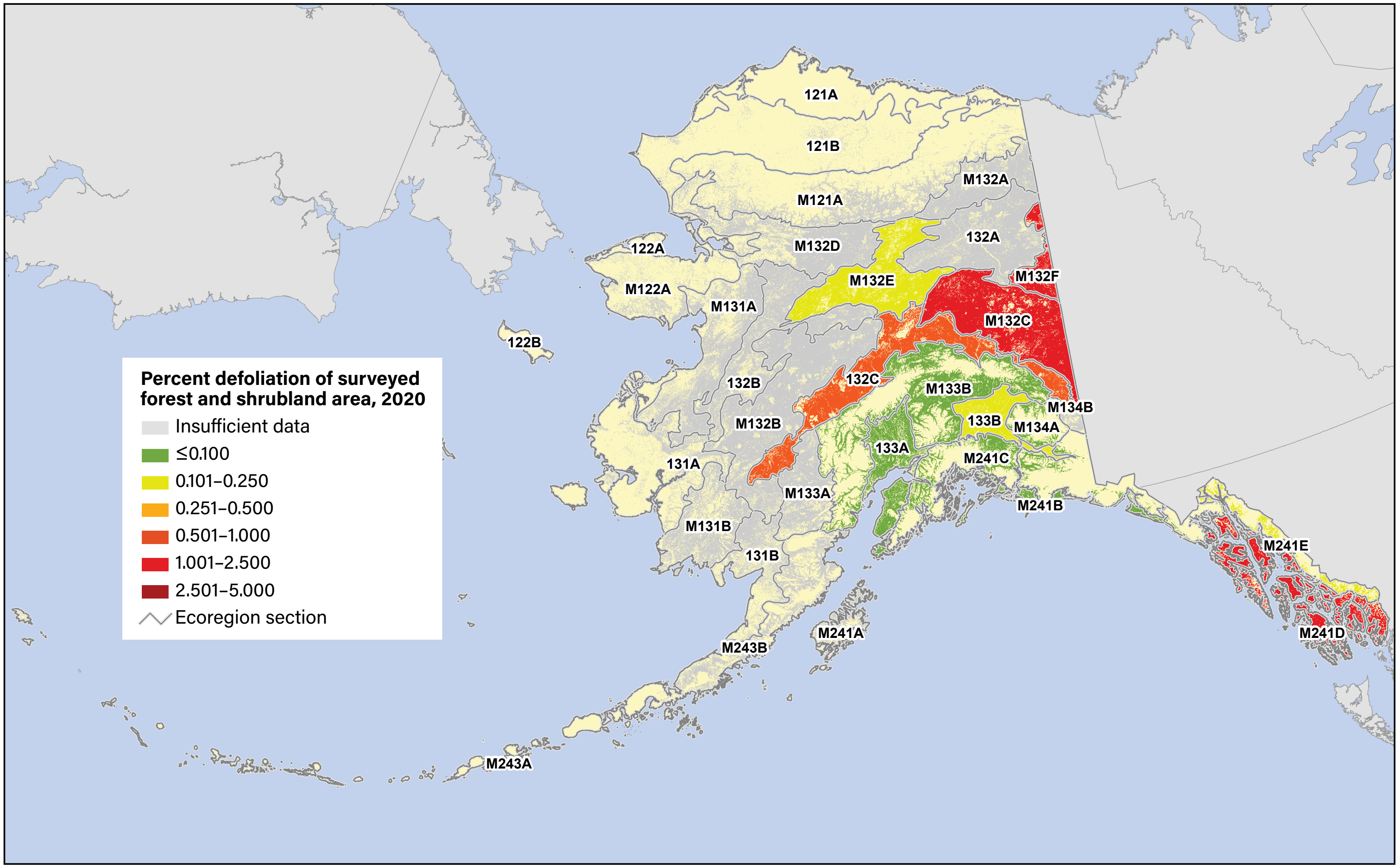

Figure 2.5—Percentage of 2020 surveyed Alaska forest and shrubland area within ecoregions with defoliation caused by insects and diseases. The gray lines delineate ecoregion sections (Spencer and others 2002). Forest and shrub cover is derived from the 2011 National Land Cover Database. (Data source: U.S. Department of Agriculture Forest Service, Forest Health Protection)

27 000 ha in 2019 (Potter and others 2021). While all of this was coded as having an “unknown” mortality agent, at least some of the damage was likely caused by rapid ʻōhiʻa death, a wilt disease that affects ʻōhiʻa lehua (*Metrosideros polymorpha*). This endemic species is the most abundant native tree in Hawaii, where it is deeply woven into Hawaiian culture (University of Hawaiʻi 2021). Two fungal pathogens cause rapid ʻōhiʻa death, the more aggressive *Ceratocystis lukuohia* and the less aggressive *C. huliohia*, though both can kill ʻōhiʻa (Barnes and others 2018). Both pathogens have been confirmed on the islands of Hawaiʻi (the Big Island), where 90 percent of detections are of the more aggressive *C. lukuohia*, and Kauaʻi; meanwhile, in 2019 a small number of trees infected with *C. huliohia* were detected on Oʻahu and Maui (University of Hawaiʻi 2021).

All the montane wet ecoregions on the Island of Hawaiʻi had high levels of detected mortality in 2020 (fig. 2.6). The highest was Montane Wet-Hawaiʻi-Kona (MWh-ko) with 3.81-percent mortality of the surveyed tree canopy area, followed by Montane Wet-Hawaiʻi-Hilo-Puna (MWh-hp) with 1.72 percent, Montane Wet-Hawaiʻi-Kaʻū (MWh-ka) with 1.22 percent, and Montane Wet-Hawaiʻi-Kohala-Hāmākua (MWh-kh) with 0.90 percent.

CONCLUSIONS

Forest health specialists needed to quickly adapt new methods to monitor insect and disease damage in U.S. forests during 2020 as a result of the global COVID-19 pandemic. They were successful in surveying large areas of forest across the country, if not as much as in a typical year, despite the challenging circumstances. Caution is warranted, however, in comparing 2020 mortality and defoliation results to previous years because of the differences in the survey methods employed and in the proportion of forest surveyed.

Continued monitoring of insect and disease outbreaks across the United States will be necessary for determining appropriate followup investigation and management activities. Due to the limitations of survey efforts to detect certain important forest insects and diseases, the pests and pathogens discussed in this chapter do not include all the biotic forest health threats that should be considered when making management decisions and budget allocations. However, large-scale assessments of mortality and defoliation severity offer a useful approach for identifying geographic areas where the concentration of monitoring and management activities might be most effective.

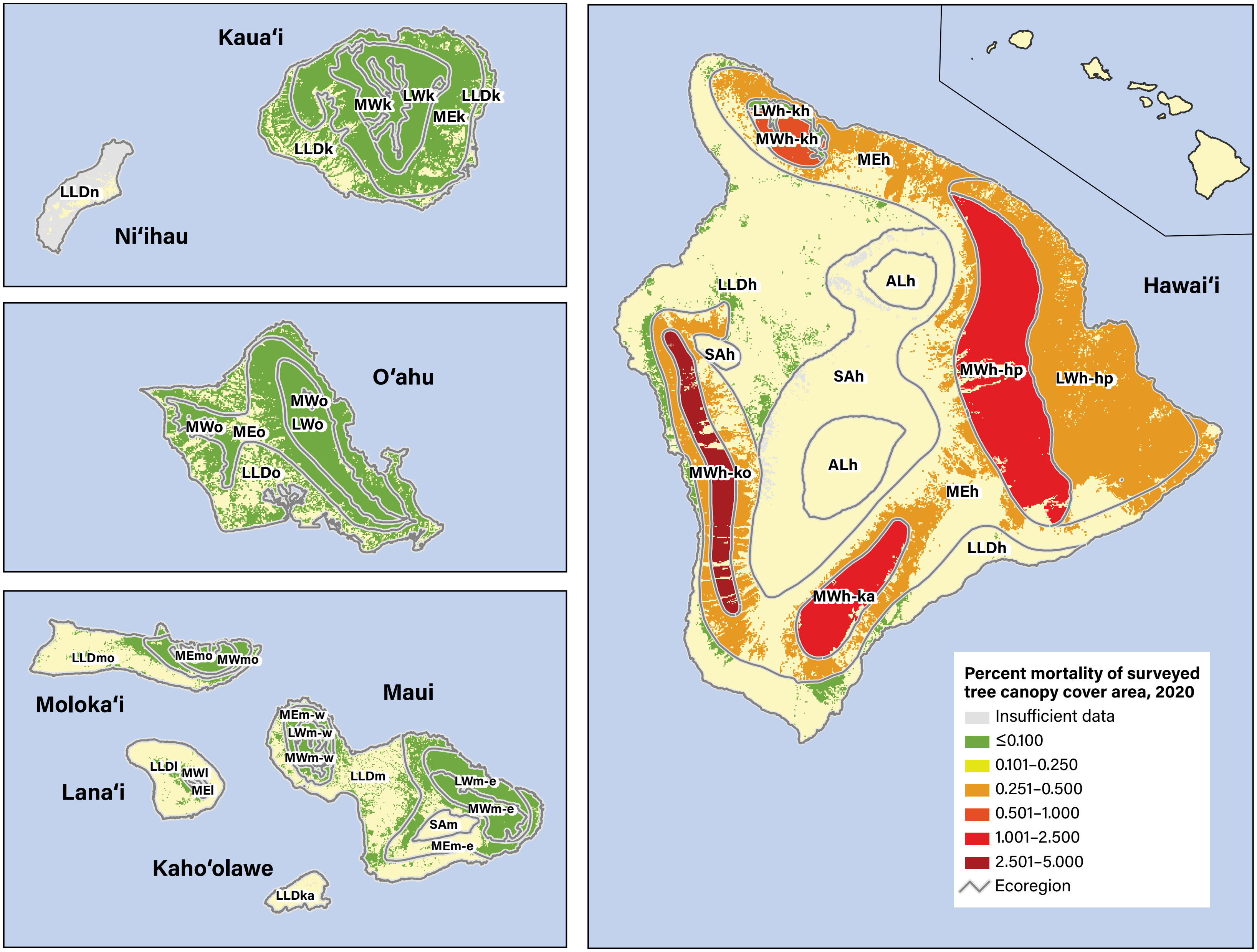

Figure 2.6—Percentage of 2020 surveyed Hawaii tree canopy area within island/ecoregion combinations with mortality caused by insects and diseases. Tree canopy cover is based on data from a cooperative project between the Multi-Resolution Land Characteristics Consortium (Coulston and others 2012) and the Forest Service Geospatial Technology and Applications Center using the 2011 National Land Cover Database. See table 1.1 for ecoregion identification. (Data source: U.S. Department of Agriculture Forest Service, Forest Health Protection)

LITERATURE CITED

Barnes, I.; Fourie, A.; Wingfield, M.J. [and others]. 2018. New *Ceratocystis* species associated with rapid death of *Metrosideros polymorpha* in Hawaii. Persoonia-Molecular Phylogeny and Evolution of Fungi. 40(1): 154–181. https://doi.org/10.3767/persoonia.2018.40.07.

Berryman, E.; McMahan, A. 2019. Using tree canopy cover data to help estimate acres of damage. In: Potter, K.M.; Conkling, B.L., eds. Forest Health Monitoring: national status, trends, and analysis 2018. Gen. Tech. Rep. SRS-239. Asheville, NC: U.S. Department of Agriculture Forest Service, Southern Research Station: 125–141.

Brockerhoff, E.G.; Liebhold, A.M.; Jactel, H. 2006. The ecology of forest insect invasions and advances in their management. Canadian Journal of Forest Research. 36(2): 263–268. https://doi.org/10.1139/x06-013.

Castello, J.D.; Leopold, D.J.; Smallidge, P.J. 1995. Pathogens, patterns, and processes in forest ecosystems. BioScience. 45(1): 16–24. https://doi.org/10.2307/1312531.

Cleland, D.T.; Freeouf, J.A.; Keys, J.E. [and others]. 2007. Ecological subregions: sections and subsections for the conterminous United States. Gen. Tech. Rep. WO-76D. Washington, DC: U.S. Department of Agriculture Forest Service. Map; Sloan, A.M., cartographer; presentation scale 1:3,500,000; colored. https://doi.org/10.2737/WO-GTR-76D.

Coleman, T.W.; Graves, A.D.; Heath, Z. [and others]. 2018. Accuracy of aerial detection surveys for mapping insect and disease disturbances in the United States. Forest Ecology and Management. 430: 321–336. https://doi.org/10.1016/j.foreco.2018.08.020.

Coulston, J.W.; Moisen, G.G.; Wilson, B.T. [and others]. 2012. Modeling percent tree canopy cover: a pilot study. Photogrammetric Engineering and Remote Sensing. 78(7): 715–727. https://doi.org/10.14358/PERS.78.7.715.

Edmonds, R.L.; Agee, J.K.; Gara, R.I. 2011. Forest health and protection. Long Grove, IL: Waveland Press, Inc. 667 p.

ESRI. 2017. ArcMap® 10.5.1. Redlands, CA: Environmental Systems Research Institute.

Forest Health Protection (FHP). 2019. Digital Mobile Sketch Mapping user's manual 2.1. Fort Collins, CO: U.S. Department of Agriculture Forest Service, Forest Health Assessment and Applied Sciences Team. https://www.fs.fed.us/foresthealth/technology/docs/DMSM_Tutorial/story_content/external_files/DMSM_User_Guide.pdf. [Date accessed: July 10, 2020].

Forest Health Protection (FHP). 2020. Metadata codes for the DMSM geodatabase notes section. Fort Collins, CO: U.S. Department of Agriculture Forest Service, Forest Health Technology Enterprise Team.

Forest Health Protection (FHP). 2021. Insect and Disease Detection Survey (IDS) data downloads. Fort Collins, CO: U.S. Department of Agriculture Forest Service, Forest Health Technology Enterprise Team. https://www.fs.fed.us/foresthealth/applied-sciences/mapping-reporting/detection-surveys.shtml. [Date accessed: June 1, 2021].

Getis, A.; Ord, J.K. 1992. The analysis of spatial association by use of distance statistics. Geographical Analysis. 24(3): 189–206. https://doi.org/10.1111/j.1538-4632.1992.tb00261.x.

Hanavan, R.P.; Kamoske, A.G.; Schaaf, A.N. [and others]. 2021. Supplementing the Forest Health National Aerial Survey Program with remote sensing during the COVID-19 pandemic: lessons learned from a collaborative approach. Journal of Forestry. 2021: 1–8. https://doi.org/10.1093/jofore/fvab056.

Holdenrieder, O.; Pautasso, M.; Weisberg, P.J.; Lonsdale, D. 2004. Tree diseases and landscape processes: the challenge of landscape pathology. Trends in Ecology & Evolution. 19(8): 446–452. https://doi.org/10.1016/j.tree.2004.06.003.

Homer, C.G.; Dewitz, J.A.; Yang, L. [and others]. 2015. Completion of the 2011 National Land Cover Database for the conterminous United States: representing a decade of land cover change information. Photogrammetric Engineering and Remote Sensing. 81(5): 345–354.

Liebhold, A.M.; McCullough, D.G.; Blackburn, L.M. [and others]. 2013. A highly aggregated geographical distribution of forest pest invasions in the USA. Diversity and Distributions. 19: 1208–1216. https://doi.org/10.1111/ddi.12112.

Logan, J.A.; Regniere, J.; Powell, J.A. 2003. Assessing the impacts of global warming on forest pest dynamics. Frontiers in Ecology and the Envionment. 1: 130–137. https://doi.org/10.1890/1540-9295(2003)001[0130:ATIOGW]2.0.CO;2.

Lovett, G.M.; Weiss, M.; Liebhold, A.M. [and others]. 2016. Nonnative forest insects and pathogens in the United States: impacts and policy options. Ecological Applications. 26: 1437–1455. https://doi.org/10.1890/15-1176.

Mack, R.N.; Simberloff, D.; Lonsdale, W.M. [and others]. 2000. Biotic invasions: causes, epidemiology, global consequences, and control. Ecological Applications. 10(3): 689–710. https://doi.org/10.1890/1051-0761(2000)010[0689:BICEGC]2.0.CO;2.

Manion, P.D. 2003. Evolution of concepts in forest pathology. Phytopathology. 93: 1052–1055. https://doi.org/10.1094/PHYTO.2003.93.8.1052.

Oswalt, S.N.; Smith, W.B.; Miles, P.D.; Pugh, S.A., coords. 2019. Forest resources of the United States, 2017: a technical document supporting the Forest Service 2020 RPA Assessment. Gen. Tech. Rep. WO-97. Washington, DC: U.S. Department of Agriculture Forest Service. 223 p. https://doi.org/10.2737/WO-GTR-97.

Parry, D.; Teale, S.A. 2011. Alien invasions: the effects of introduced species on forest structure and function. In: Castello, J.D.; Teale, S.A., eds. Forest health: an integrated perspective. New York: Cambridge University Press: 115–162. https://doi.org/10.1017/CBO9780511974977.006.

Potter, K.M. 2012. Large-scale patterns of insect and disease activity in the conterminous United States and Alaska from the national Insect and Disease Detection Survey database, 2007 and 2008. In: Potter, K.M.; Conkling, B.L., eds. Forest Health Monitoring 2009 national technical report. Gen. Tech. Rep. SRS-167. Asheville, NC: U.S. Department of Agriculture Forest Service, Southern Research Station: 63–78.

Potter, K.M. 2013. Large-scale patterns of insect and disease activity in the conterminous United States and Alaska from the national Insect and Disease Detection Survey, 2009. In: Potter, K.M.; Conkling, B.L., eds. Forest Health Monitoring: national status, trends, and analysis 2010. Gen. Tech. Rep. SRS-176. Asheville, NC: U.S. Department of Agriculture Forest Service, Southern Research Station: 15–29.

Potter, K.M. 2020. Introduction. In: Potter, K.M.; Conkling, B.L., eds. Forest Health Monitoring: national status, trends, and analysis 2019. Gen. Tech. Rep. SRS-250. Asheville, NC: U.S. Department of Agriculture Forest Service, Southern Research Station: 5–24.

Potter, K.M., Canavin, J.C.; Koch, F.H. 2020a. A forest health retrospective: national and regional results from 20 years of Insect and Disease Survey data. In: Potter, K.M.; Conkling, B.L., eds. Forest Health Monitoring: national status, trends, and analysis 2019. Gen. Tech. Rep. SRS-250. Asheville, NC: U.S. Department of Agriculture Forest Service, Southern Research Station: 125–149.

Potter, K.M.; Escanferla, M.E.; Jetton, R.M.; Man, G. 2019a. Important insect and disease threats to United States tree species and geographic patterns of their potential impacts. Forests. 10(4): 304. https://doi.org/10.3390/f10040304.

Potter, K.M.; Escanferla, M.E.; Jetton, R.M. [and others]. 2019b. Prioritizing the conservation needs of United States tree species: evaluating vulnerability to forest insect and disease threats. Global Ecology and Conservation. 18: e00622. https://doi.org/10.1016/j.gecco.2019.e00622.

Potter, K.M.; Koch, F.H. 2012. Large-scale patterns of insect and disease activity in the conterminous United States and Alaska, 2006. In: Potter, K.M.; Conkling, B.L., eds. Forest Health Monitoring 2008 national technical report. Gen. Tech. Rep. SRS-158. Asheville, NC: U.S. Department of Agriculture Forest Service, Southern Research Station: 63–72.

Potter, K.M.; Koch, F.H.; Oswalt, C.M.; Iannone, B.V. 2016. Data, data everywhere: detecting spatial patterns in fine-scale ecological information collected across a continent. Landscape Ecology. 31: 67–84. https://doi.org/10.1007/s10980-015-0295-0.

Potter, K.M.; Paschke, J.L. 2013. Large-scale patterns of insect and disease activity in the conterminous United States and Alaska from the national Insect and Disease Detection Survey database, 2010. In: Potter, K.M.; Conkling, B.L., eds. Forest Health Monitoring: national status, trends, and analysis 2011. Gen. Tech. Rep. SRS-185. Asheville, NC: U.S. Department of Agriculture Forest Service, Southern Research Station: 15–28.

Potter, K.M.; Paschke, J.L. 2014. Large-scale patterns of insect and disease activity in the conterminous United States and Alaska from the national Insect and Disease Survey database, 2011. In: Potter, K.M.; Conkling, B.L., eds. Forest Health Monitoring: national status, trends, and analysis 2012. Gen. Tech. Rep. SRS-198. Asheville, NC: U.S. Department of Agriculture Forest Service, Southern Research Station: 19–34.

Potter, K.M.; Paschke, J.L. 2015a. Large-scale patterns of insect and disease activity in the conterminous United States and Alaska from the national Insect and Disease Survey, 2012. In: Potter, K.M.; Conkling, B.L., eds. Forest Health Monitoring: national status, trends, and analysis 2013. Gen. Tech. Rep. SRS-207. Asheville, NC: U.S. Department of Agriculture Forest Service, Southern Research Station: 19–36.

Potter, K.M.; Paschke, J.L. 2015b. Large-scale patterns of insect and disease activity in the conterminous United States, Alaska, and Hawaii from the national Insect and Disease Survey, 2013. In: Potter, K.M.; Conkling, B.L., eds. Forest Health Monitoring: national status, trends, and analysis 2014. Gen. Tech. Rep. SRS-209. Asheville, NC: U.S. Department of Agriculture Forest Service, Southern Research Station: 19–38.

Potter, K.M.; Paschke, J.L. 2016. Large-scale patterns of insect and disease activity in the conterminous United States and Alaska from the national Insect and Disease Survey, 2014. In: Potter, K.M.; Conkling, B.L., eds. Forest Health Monitoring: national status, trends, and analysis 2015. Gen. Tech. Rep. SRS-213. Asheville, NC: U.S. Department of Agriculture Forest Service, Southern Research Station: 21–40.

Potter, K.M.; Paschke, J.L. 2017. Large-scale patterns of insect and disease activity in the conterminous United States and Alaska from the national Insect and Disease Survey, 2015. In: Potter, K.M.; Conkling, B.L., eds. Forest Health Monitoring: national status, trends, and analysis 2016. Gen. Tech. Rep. SRS-222. Asheville, NC: U.S. Department of Agriculture Forest Service, Southern Research Station: 21–42.

Potter, K.M., Paschke, J.L.; Koch, F.H.; Berryman, E.M. 2020b. Large-scale patterns of insect and disease activity in the conterminous United States, Alaska, and Hawaii from the national Insect and Disease Survey, 2018. In: Potter, K.M.; Conkling, B.L., eds. Forest Health Monitoring: national status, trends, and analysis 2019. Gen. Tech. Rep. SRS-250. Asheville, NC: U.S. Department of Agriculture Forest Service, Southern Research Station: 27–55.

Potter, K.M.; Paschke, J.L.; Koch, F.H.; Zweifler, M. 2019c. Large-scale patterns of insect and disease activity in the conterminous United States, Alaska, and Hawaii from the national Insect and Disease Survey, 2017. In: Potter, K.M.; Conkling, B.L., eds. Forest Health Monitoring: national status, trends, and analysis 2018. Gen. Tech. Rep. SRS-239. Asheville, NC: U.S. Department of Agriculture Forest Service, Southern Research Station: 21–49.

Potter, K.M., Paschke, J.L.; Berryman, E.M. 2021. Large-scale patterns of insect and disease activity in the conterminous United States, Alaska, and Hawaii from the national Insect and Disease Survey, 2019. In: Potter, K.M.; Conkling, B.L., eds. Forest Health Monitoring: national status, trends, and analysis 2020. Gen. Tech. Rep. SRS-261. Asheville, NC: U.S. Department of Agriculture Forest Service, Southern Research Station: 27–57.

Potter, K.M.; Paschke, J.L.; Zweifler, M. 2018. Large-scale patterns of insect and disease activity in the conterminous United States, Alaska, and Hawaii from the national Insect and Disease Survey, 2016. In: Potter, K.M.; Conkling, B.L., eds. Forest Health Monitoring: national status, trends, and analysis 2017. Gen. Tech. Rep. SRS-233. Asheville, NC: U.S. Department of Agriculture Forest Service, Southern Research Station: 23–44.

Slaton, M.R.; Warren, K.; Koltunov, A.; Smith, S. 2021. Accuracy assessment of Insect and Disease Survey and eDART for monitoring forest health. In: Potter, K.M.; Conkling, B.L., eds. Forest Health Monitoring: national status, trends, and analysis 2020. Gen. Tech. Rep. SRS-261. Asheville, NC: U.S. Department of Agriculture Forest Service, Southern Research Station: 187–195.

Spencer, P.; Nowacki, G.; Fleming, M. [and others]. 2002. Home is where the habitat is: an ecosystem foundation for wildlife distribution and behavior. Arctic Research of the United States. 16: 6–17.

Teale, S.A.; Castello, J.D. 2011. Regulators and terminators: the importance of biotic factors to a healthy forest. In: Castello, J.D.; Teale, S.A., eds. Forest health: an integrated perspective. New York: Cambridge University Press: 81–114. https://doi.org/10.1017/CBO9780511974977.005.

Tobin, P.C. 2015. Ecological consequences of pathogen and insect invasions. Current Forestry Reports. 1: 25–32. https://doi.org/10.1007/s40725-015-0008-6.

University of Hawaiʻi, College of Tropical Agriculture and Human Resources. 2021. Rapid ʻōhiʻa death. http://rapidohiadeath.org. [Date accessed: August 8, 2021].

Zhang, L.; Rubin, B.D.; Manion, P.D. 2011. Mortality: the essence of a healthy forest. In: Castello, J.D.; Teale, S.A., eds. Forest health: an integrated perspective. New York: Cambridge University Press: 17–49. https://doi.org/10.1017/CBO9780511974977.003.

CHAPTER 3

Broad-Scale Patterns of Forest Fire Occurrence across the 50 United States and the Caribbean Territories, 2020

Kevin M. Potter

INTRODUCTION

Wildland fire is a pervasive disturbance agent in many forest ecosystems across the United States, causing widespread tree damage and mortality and acting as a key abiotic factor affecting forest health both positively and negatively (Agee 1998, Thom and Seidl 2016, Wade and others 2000). Wildland fire is an important ecological mechanism that shapes the distributions of species, maintains the structure and function of fire-prone communities, and acts as a significant evolutionary force (Bond and Keeley 2005, Pausas and Keeley 2019). In some ecosystems, wildland fires have been essential for regulating processes that maintain forest health (Lundquist and others 2011), and some forest types and tree species are adapted to fire under certain intensities and return intervals (Hanberry and others 2018, Jeronimo and others 2019). At the same time, wildland fires have created forest health (i.e., sustainability) problems in some ecosystems (Edmonds and others 2011).

Current fire regimes on more than half of the forested area in the conterminous United States have been moderately or significantly altered from historical regimes (Barbour and others 1999), potentially altering key ecosystem components such as species composition, structural stage, stand age, canopy closure, and fuel loadings (Schmidt and others 2002, Stephens and others 2018). Evidence, in fact, suggests that few entirely natural fire regimes remain in North America (Parisien and others 2016). Fires in some regions and ecosystems have become larger, more intense, and more damaging because of the accumulation of fuels as a result of prolonged fire suppression (Pyne 2010). In some regions, plant communities have experienced or are undergoing rapid compositional and structural changes as a result of fire suppression (Coop and others 2020, Nowacki and Abrams 2008). Additionally, changes in fire intensity and recurrence could result in decreased forest resilience and persistence (Lundquist and others 2011), and fire regimes altered by global climate change could cause large-scale shifts in vegetation spatial patterns (McKenzie and others 1996). Robust research indicates that climate change, via more common drought conditions and higher temperatures, has already resulted in increased wildfire activity (Abatzoglou and Williams 2016, Higuera and Abatzoglou 2020).

At the same time, large wildland fires also can have long-lasting social and economic consequences, which include the loss of human life and property, smoke-related human health impacts, and the economic cost and dangers of fighting the fires themselves (Gill and others 2013, Richardson and others 2012). These impacts are particularly intense within the wildland-urban interface, the zone in which human development mixes with forest (Calkin and others 2015, Radeloff and others 2018). Additionally, some evidence exists that exposure to wildfire smoke may have increased SARS-CoV-2 positivity rates among the public and thereby exacerbated the COVID-19 pandemic (Kiser and others 2021), while inhalation of wildfire smoke may expose firefighters to increased likelihood of SARS-CoV-2 infection and increased COVID-19 disease severity (Navarro and others 2021).

How to cite this chapter:

Potter, Kevin M. 2022. Broad-scale patterns of forest fire occurrence across the 50 United States and the Caribbean territories, 2020. In: Potter, Kevin M.; Conkling, Barbara L., eds. Forest Health Monitoring: national status, trends, and analysis 2021. Gen. Tech. Rep. SRS-266. Asheville, NC: U.S. Department of Agriculture Forest Service, Southern Research Station: 51–78. https://doi.org/10.2737/SRS-GTR-266-Chap3.

This chapter presents analyses of daily satellite-based fire occurrence data that map and quantify the locations and intensities of fire occurrences spatially across the conterminous United States, Alaska, Hawaii, and the Caribbean territories in 2020. It also compares 2020 fire occurrences, within a geographic context, to all the recent years for which such data are available. Quantifying and monitoring such large-scale patterns of fire occurrence across the United States, as described in this chapter, can help improve our understanding of the ecological and economic impacts of fire as well as the appropriate management and prescribed use of fire. Specifically, large-scale assessments of fire occurrence can help identify areas where specific management activities may be needed, or where research into the ecological and socioeconomic impacts of fires may be required. Additionally, given the potential for climate change and shifting species distributions to alter historic fire regimes, quantifying the location and frequency of forest fire occurrences across the United States can help us to better understand emerging spatiotemporal patterns of fire occurrence.

METHODS

Data

Annual monitoring and reporting of active wildland fire events using the Moderate Resolution Imaging Spectroradiometer (MODIS) Active Fire Detections for the United States database (USDA Forest Service 2021) allow analysts to spatially display and summarize fire occurrences across broad geographic regions (Coulston and others 2005; Potter 2012a, 2012b, 2013a, 2013b, 2014, 2015a, 2015b, 2016, 2017, 2018, 2019, 2020a, 2021). A fire occurrence is defined as one daily satellite detection of wildland fire in a 1-km pixel, with multiple fire occurrences possible on a pixel across multiple days resulting from a single wildland fire that lasts more than 1 day. The data are derived using the MODIS Rapid Response System (Justice and others 2002, 2011) to extract fire location and intensity information from the thermal infrared bands of imagery collected daily by two satellites at a resolution of 1 km, with the center of a pixel recorded as a fire occurrence (USDA Forest Service 2021). The Terra and Aqua satellites' MODIS sensors identify the presence of a fire at the time of image collection, with Terra observations collected in the morning and Aqua observations collected in the afternoon. The resulting fire occurrence data represent only whether a fire was active because the MODIS data bands may not differentiate between a hot fire in a relatively small area (0.01 km^2, for example) and a cooler fire over a larger area (1 km^2, for example) if the foreground-to-background temperature contrast is not sufficiently high. The MODIS Active Fire database does well at capturing large fires during cloud-free conditions but may underrepresent rapidly burning, small, and low-intensity fires, as well as fires in areas with frequent cloud cover (Hawbaker and others 2008). For large-scale assessments, the dataset represents a good alternative to the use of information on ignition points, which may be preferable but can be difficult to obtain or may not exist (Tonini and others 2009). More information about the performance of this product is provided by Justice and others (2011). The fire occurrence data additionally do not differentiate fires intentionally set for management purposes (controlled burns), which are common in some parts of the United States, particularly in the South, where many prescribed fires are not detected by satellite sensors (Nowell and others 2018).

It is important to underscore that estimates of burned area (e.g., Monitoring Trends in Burn Severity data [Eidenshink and others 2007, Picotte and others 2020]) and calculations of MODIS-detected fire occurrences are two different metrics for quantifying fire activity within a given year. Most importantly, the MODIS data contain both spatial and temporal components because persistent fire will be detected repeatedly over several days on a given 1-km pixel. In other words, a location can be counted as having a fire occurrence multiple times, once for each day a fire is detected at the location. Analyses of the MODIS-detected fire occurrences, therefore, measure the total number of daily 1-km pixels with fire during a year, as opposed to quantifying only the area on which fire occurred at some point during the course of the year. A fire detected on a single pixel for every day in the month of July, for example, would be equivalent to 31 fire occurrences.

The Terra and Aqua satellites, which carry the MODIS sensors, were launched in 1999 and 2002, respectively, and eventually will be decommissioned. An alternative fire occurrence data source is the Visible Infrared Imaging Radiometer Suite (VIIRS) sensor on board the Suomi National Polar-orbiting Partnership (Suomi NPP) weather satellite. The transition to this new data source will require a comparison of fire occurrence detections between it and MODIS. This is because VIIRS data are available from 2014 onward (USDA Forest Service 2021), but it will be important for assessments of fire occurrence trends to be able to analyze as long a window of time as possible (i.e., from the beginning of MODIS data availability).

Analyses

These MODIS products for 2020, and for the 19 preceding full years of data, were processed in ArcMap® (ESRI 2017) to determine forest fire occurrence density (that is, the number of fire occurrences/100 km^2 [10 000 ha] of tree canopy cover area) for each ecoregion section in the conterminous United States (Cleland and others 2007), for ecoregions on each of the major islands of Hawaii (Potter 2020b), and for the islands of the Caribbean territories of Puerto Rico and the U.S. Virgin Islands. For the current analyses, the forest fire occurrence density metrics for the conterminous 48 States, Hawaii, and the Caribbean territories (the number of fire occurrences/100 km^2 of tree canopy cover area) were calculated after screening out wildland fires that did not intersect with tree canopy data. The tree canopy data had been resampled to 240 m from a 30-m raster dataset that estimates percentage of tree canopy cover (from 0 to 100 percent) for each grid cell; this dataset was generated from the 2011 National Land Cover Database (NLCD) (Homer and others 2015) through a cooperative project between the Multi-Resolution Land Characteristics Consortium and the U.S. Department of Agriculture Forest Service, Geospatial Technology and Applications

Center (GTAC) (Coulston and others 2012). For our purposes, we treated any cell with >0-percent tree canopy cover as forest. Comparable tree canopy cover data were not available for Alaska, so we instead created a 240-m-resolution layer of forest and shrub cover from the 2011 NLCD. The MODIS fire occurrence detection data were then intersected with this layer and with ecoregion sections for the State (Spencer and others 2002) to calculate the number of fire occurrences/100 km^2 of forest and shrub cover within each ecoregion section in Alaska. In Forest Health Monitoring national reports before 2019, the number of fire occurrences/100 km^2 of forest was determined for the conterminous States, Alaska, and Hawaii using a forest cover mask derived from MODIS imagery by the Forest Service GTAC (USDA Forest Service 2008).

The total numbers of forest fire occurrences were also determined separately for the conterminous States, Alaska, Hawaii, and the Caribbean territories after clipping the MODIS fire occurrences by the canopy cover or tree and shrub cover data.

The fire occurrence density value for each of the ecoregions of the States and for the Caribbean islands in 2020 was then compared with the mean fire density values for the first 19 full years of MODIS Active Fire data collection (2001–2019). Specifically, the difference of the 2020 value and the previous 19-year mean for an ecoregion was divided by the standard deviation across the previous 19-year period, assuming a normal distribution of fire density over time in the ecoregion. The result for each ecoregion was a standardized z-score, which is a dimensionless quantity describing the degree to which the fire occurrence density in the ecoregion in 2020 was higher, lower, or the same relative to all the previous years for which data have been collected, accounting for the variability in the previous years. The z-score is the number of standard deviations between the observation and the mean of the historic observations in the previous years. Approximately 68 percent of observations would be expected within one standard deviation of the mean, and 95 percent within two standard deviations. Near-normal conditions are classified as those within a single standard deviation of the mean, although such a threshold is somewhat arbitrary. Conditions between about one and two standard deviations of the mean are moderately different from mean conditions but are not significantly different statistically. Those outside about two standard deviations would be considered statistically greater than or less than the long-term mean (at $p < 0.025$ at each tail of the distribution).

Additionally, we used the Spatial Association of Scalable Hexagons (SASH) analytical approach to identify forested areas in the conterminous United States with higher-than-expected fire occurrence density in 2020. This method identifies locations where ecological phenomena occur at greater or lower occurrences than expected by random chance and is based on a sampling frame optimized for spatial neighborhood analysis, adjustable to the appropriate spatial resolution, and applicable to multiple data types (Potter and others 2016). Specifically, it consists of dividing an analysis area into scalable equal-area hexagonal cells within which data are aggregated, followed by identifying statistically significant geographic clusters of hexagonal cells within which mean values are greater or less than those expected by chance. To identify these clusters, we employed a Getis-Ord G_i^* hot spot analysis (Getis and Ord 1992) in ArcMap® 10.5.1 (ESRI 2017).

The spatial units of analysis were 9,810 hexagonal cells, each approximately 834 km^2 in area, generated in a lattice across the conterminous United States using intensification of the Environmental Monitoring and Assessment Program (EMAP) North American hexagon coordinates (White and others 1992). These coordinates are the foundation of a sampling frame in which a hexagonal lattice was projected onto the conterminous United States by centering a large base hexagon over the region (Reams and others 2005, White and others 1992). The hexagons are compact and uniform in their distance to the centroids of neighboring hexagons, meaning that a hexagonal lattice has a higher degree of isotropy (uniformity in all directions) than does a square grid (Shima and others 2010). These are convenient and highly useful attributes for spatial neighborhood analyses. These scalable hexagons also are independent of geopolitical and ecological boundaries, avoiding the possibility of different sample units (such as counties, States, or watersheds) encompassing vastly different areas (Potter and others 2016). We selected hexagons 834 km^2 in area because this is a manageable size for making monitoring and management decisions in analyses across the conterminous United States (Potter and others 2016).

Fire occurrence density values for each hexagon were quantified as the number of forest fire occurrences/100 km^2 of tree canopy cover area within the hexagon. The Getis-Ord G_i^* statistic was used to identify clusters of hexagonal cells with fire occurrence density values higher than expected by chance. This statistic allows for the decomposition of a global measure of spatial association into its contributing factors, by location, and is therefore particularly suitable for detecting outlier assemblages of similar conditions in a dataset, such as when spatial clustering is concentrated in one subregion of the data (Anselin 1992).

Briefly, G_i^* sums the differences between the mean values in a local sample, determined in this case by a moving window of each hexagon and its 18 first- and second-order neighbors (the 6 adjacent hexagons and the 12 additional hexagons contiguous to those 6) and the global mean of the 9,644 hexagonal cells with tree canopy cover (of the total 9,810) in the conterminous United States. As described in Laffan (2006), it is calculated as:

$$G_i{}^*(\boldsymbol{d}) = \frac{\sum_j w_{ij}\,(\boldsymbol{d})x_j - W_i^*\bar{x}^*}{s^*\sqrt{\frac{(ns_{1i}^*) - {W_i^*}^2}{n-1}}}$$

where

G_i^* = the local clustering statistic (in this case, for the target hexagon)

i = the center of local neighborhood (the target hexagon)

d = the width of local sample window (the target hexagon and its first- and second-order neighbors)

x_j = the value of neighbor j

w_{ij} = the weight of neighbor j from location i (all the neighboring hexagons in the moving window were given an equal weight of 1)

n = number of samples in the dataset (the 9,644 hexagons containing tree cover)

W^*_i = the sum of the weights

s^*_{1i} = the number of samples within d of the central location (19: the focal hexagon and its 18 first- and second-order neighbors)

$\bar{x}^*$ = the mean of whole dataset (in this case, for all 9,644 hexagons containing tree cover)

s^* = the standard deviation of whole dataset (for all 9,644 hexagons containing tree cover)

G_i^* is standardized as a z-score with a mean of 0 and a standard deviation of 1, with values >1.96 representing significant local clustering of higher fire occurrence densities ($p < 0.025$) and values < -1.96 representing significant clustering of lower fire occurrence densities ($p < 0.025$), because 95 percent of the observations under a normal distribution should be within approximately two standard deviations of the mean (Laffan 2006). Values between -1.96 and 1.96 have no statistically significant concentration of high or low values; a hexagon and its 18 neighbors, in other words, have a normal range of both high and low numbers of fire occurrences/100 km^2 of tree canopy cover area. It is worth noting that the threshold values are not exact because the correlation of spatial data violates the assumption of independence required for statistical significance (Laffan 2006). In addition, the Getis-Ord approach does not require that the input data be normally distributed, because the local G_i^* values are computed under a randomization assumption, with G_i^* equating to a standardized z-score that asymptotically tends to a normal distribution (Anselin 1992). The z-scores are considered to be reliable, even with skewed data, as long as the local neighborhood encompasses several observations (ESRI 2017), in this case, via the target hexagon and its 18 first- and second-order neighbors.

RESULTS AND DISCUSSION

Trends in Forest Fire Occurrence Detections for 2020

The MODIS Active Fire database recorded 122,938 forest fire occurrences across the conterminous United States in 2020, the third highest in 20 full years of data collection and the most since 2014 (fig. 3.1). Only 2012 and 2014 saw more fire occurrences. This was a 202-percent increase from a relatively low-activity fire year in 2019, which had the fewest fire occurrences (40,657) since 2005. It was also 75 percent above the mean of the previous 19 years of data. Meanwhile, Alaska had a 98-percent drop in fire occurrences between 2019 (26,493) and 2020 (474), the fewest there since 2011. Hawaii had 22 fire occurrences in 2020, 92 percent below the 2001–2019 average and a 39-percent reduction from 2019. Finally, only four fire occurrences were detected in Puerto Rico, a decrease from 18 in 2019 and 57 percent below the average of about nine per year.

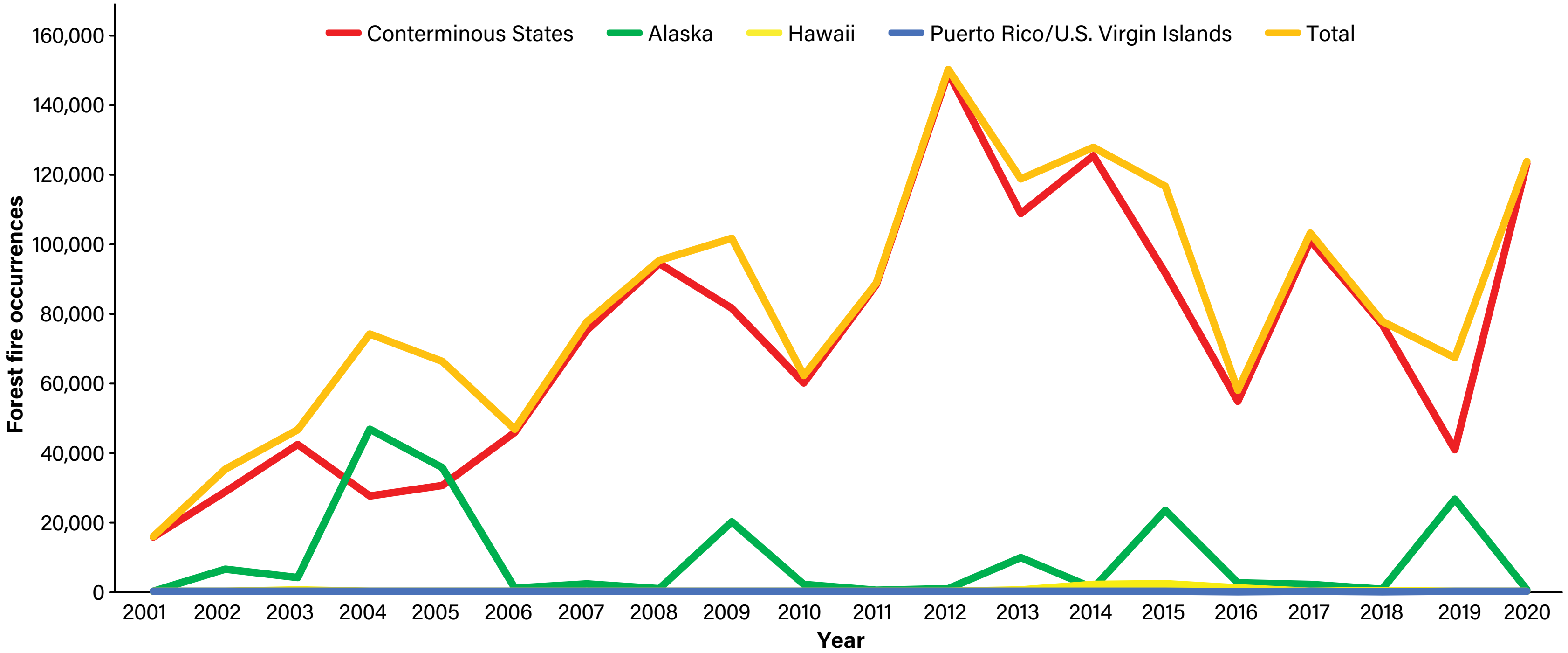

Figure 3.1—Forest fire occurrences detected by Moderate Resolution Imaging Spectroradiometer (MODIS) from 2001 through 2020 for the conterminous United States, Alaska, and Hawaii, and Puerto Rico/U.S. Virgin Islands, and for the entire Nation combined. (Data source: U.S. Department of Agriculture Forest Service, Geospatial Technology and Applications Center, in conjunction with the NASA MODIS Rapid Response group)

The dramatic increase in fire occurrences in the conterminous United States, along with the precipitous drop in Alaska fire occurrences, is consistent with official national wildland fire statistics, which track area burned and the numbers of wildfires reported (National Interagency Coordination Center 2021). These statistics indicate that the area burned more than doubled from 1 887 601 ha in 2019 to >4 046 856 ha (10 million acres) in 2020 (National Interagency Coordination Center 2020, 2021). California accounted for 38 percent of the 2020 burned area. At the same time, the number of reported wildfires increased from 50,477 in 2019 to 58,950. Beyond these general statistics, the 2020 fire season was marked by several notable and alarming superlatives (CALFIRE 2021, National Interagency Coordination Center 2021):

- The first reported fire incident exceeding 404 686 ha (1 million acres), the August Complex in northern California
- Six of the seven largest wildfire events ever recorded in California
- The three largest wildfires in Colorado history (Cameron Peak, East Troublesome, Pine Gulch)
- The first-ever tornado warning issued by the National Weather Service resulting from a wildfire, for pyrotornadoes generated by the Loyalton Fire in northeastern California

In 2020, the number of wildland fires and fire complexes exceeding 16 187 ha (40,000 acres, a benchmark threshold for the National Interagency Coordination Center) was 50, compared to 27 in 2019 and 49 in 2018 (National Interagency Coordination Center 2019, 2020, 2021). As noted in the Methods section above, estimates of burned area and numbers of reported fires are different metrics for quantifying fire activity than calculations of MODIS-detected fire occurrences, though they are often correlated.

The areas with the highest (extremely high) fire occurrence densities in 2020 were in California (the Sierra Nevada, the northwestern part of the State, and along the central and southern coast), and in north-central Colorado and south-central Wyoming (fig. 3.2). Areas with very high fire occurrence densities included the Cascade Mountains of Washington and Oregon, southwestern Oregon and northwestern California, northeastern Utah, and south-central Idaho/northeastern Nevada/northwestern Utah. A handful of ecoregion sections in the Pacific Coast States, in the Four Corners States, in the Midwest, and in the Southeast had high fire occurrence densities.

The three specific ecoregion sections with the highest fire occurrence density in 2020 (and seven of the top eight) were in California: M261B–Northern California Coast Ranges (125.9 fire occurrences/100 km^2 of tree canopy cover), M261E–Sierra Nevada (50.9 fire occurrences), and M262B–Southern California Mountain and Valley (35.0 fire occurrences) (table 3.1). The fourth ecoregion on the list was M331I–Northern Parks and Ranges in Colorado and Wyoming (28.4 fire occurrences). In the previous year, the ecoregion section with the highest fire occurrence

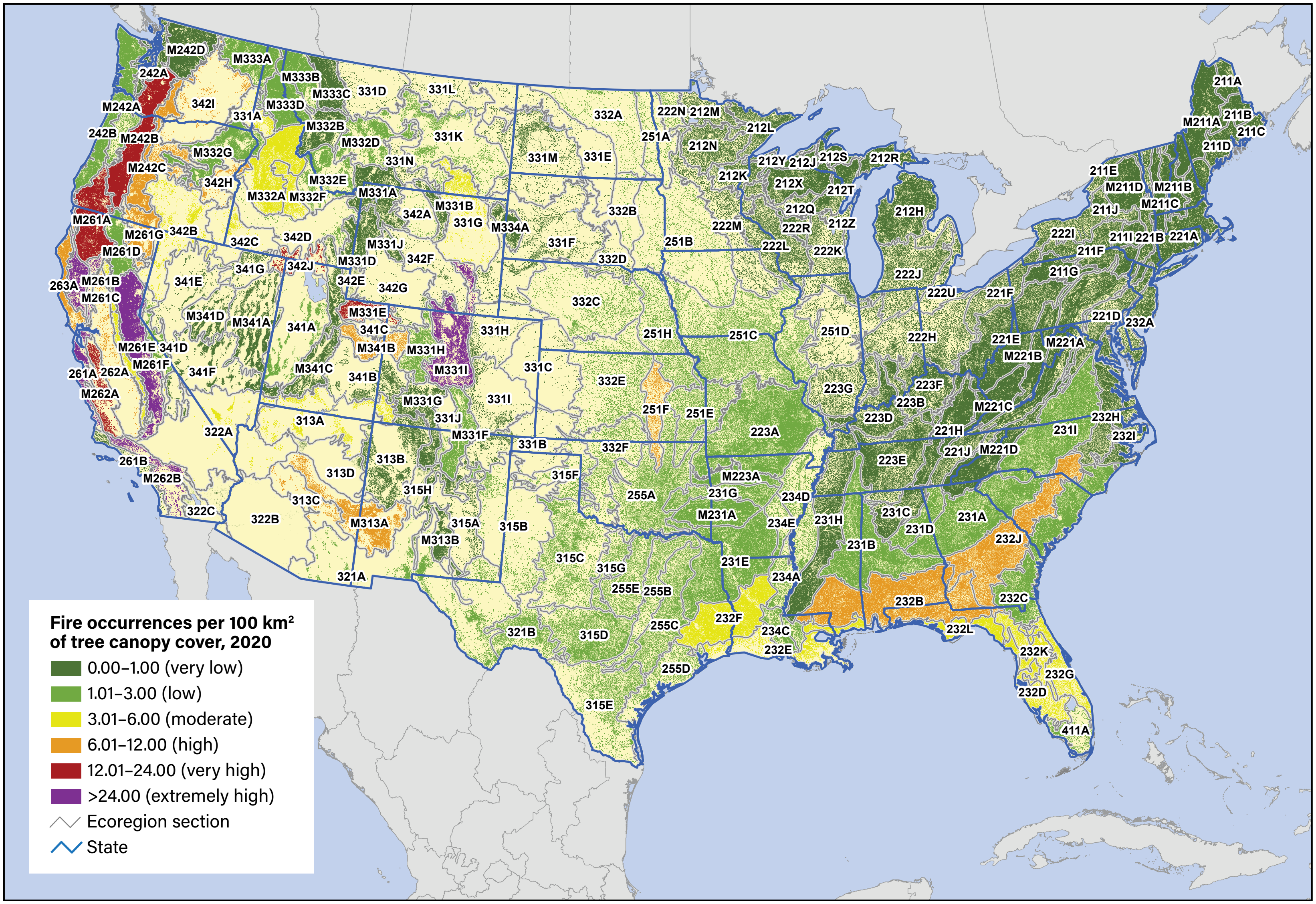

Figure 3.2—The number of forest fire occurrences, per 100 km² (10 000 ha) of tree canopy coverage area, by ecoregion section within the conterminous United States, for 2020. The gray lines delineate ecoregion sections (Cleland and others 2007). Tree canopy cover is based on data from a cooperative project between the Multi-Resolution Land Characteristics Consortium (Coulston and others 2012) and the Forest Service Geospatial Technology and Applications Center using the 2011 National Land Cover Database. See figure 1.1A for ecoregion identification. (Source of fire data: U.S. Department of Agriculture Forest Service, Geospatial Technology and Applications Center, in conjunction with the NASA MODIS Rapid Response group)

Table 3.1—The 15 ecoregion sections in the conterminous United States with the highest fire occurrence densities in 2020

Section	Name	Tree canopy area	Fire occurrences	Density[a]
		km²	*number*	
M261B	Northern California Coast Ranges	114.1	14,362	125.9
M261E	Sierra Nevada	427.8	21,757	50.9
M262B	Southern California Mountain and Valley	58.1	2,032	35.0
M331I	Northern Parks and Ranges	302.7	8,591	28.4
M261C	Northern California Interior Coast Ranges	18.2	476	26.1
261A	Central California Coast	66.8	1,725	25.8
M262A	Central California Coast Ranges	78.9	1,846	23.4
M261A	Klamath Mountains	338.5	7,796	23.0
M242B	Western Cascades	427.9	9,704	22.7
M331E	Uinta Mountains	85.3	1,380	16.2
342J	Eastern Basin and Range	37.5	501	13.4
342H	Blue Mountain Foothills	108.6	1,302	12.0
M261G	Modoc Plateau	128.7	1,296	10.1
262A	Great Valley	19.4	183	9.4
M341B	Tavaputs Plateau	92.0	744	8.1

[a] Density = fire occurrences/100 km^2 of tree canopy coverage area.

density (342C–Owyhee Uplands) experienced only 8.8 fire occurrences/100 km^2 of tree canopy cover (Potter 2021). In 2020, 14 of the top 15 ecoregion sections on the list of highest fire occurrence densities exceeded this number (table 3.1). The relatively high fire occurrence densities across the West in 2020 were attributable to long-term severe drought and periodic heat waves across many areas of the West that led to dry fuels that were ignited by lightning events and spread by strong wind events (Higuera and Abatzoglou 2020, National Interagency Coordination Center 2021).

Meanwhile, Alaska contributed little to the total burned area nationally in 2020 following a winter of near- or above-average snowpack (National Interagency Coordination Center 2021). As a result, fire occurrence densities across the entire State were very low (fig. 3.3), with only one ecoregion section exceeding 0.3 fire occurrences/100 km^2 of forest and shrub cover. This was M123E–Ray Mountains in the central interior part of the State, with 0.32 fire occurrences/100 km^2.

In 4 previous years, Alaska had MODIS-detected fire occurrence peaks: 2004/2005, 2009, and 2015 (fig. 3.1). Each was followed by a steep drop in Alaskan fire occurrences, and with an increase in fire occurrences in the conterminous States. That was the pattern again in 2019 and 2020: A year of many fire occurrences in Alaska was followed by a peak in the conterminous States. Such broad-scale North American patterns of wildfire result from the interaction between climate and vegetation development across a range of spatial and temporal scales with climate influencing fine fuel moisture, ignition frequency, and rates of wildfire spread at annual to interannual timescales (Gedalof 2011). Intermediate-term patterns in wildfire occurrence in North America, meanwhile, are driven by interannual to multidecadal variability in sea surface temperatures, associated with the El Niño-Southern Oscillation (ENSO), Pacific Decadal Oscillation (PDO), and Atlantic Multidecadal Oscillation (AMO) (Kitzberger and others 2007).

Meanwhile, Hawaii had generally low fire occurrence density in 2020, with three ecoregions exceeding a fire occurrence density of 1/100 km^2 of tree canopy cover (fig. 3.4), Lowland/Leeward Dry-Maui (LLDm) (2.3), Mesic-Maui-West (MEm-w) (1.6), and Lowland/Leeward Dry-O‘ahu (LLDo) (1.4). There were no Big Island volcanic eruptions in 2020 that burned forests and buildings, as in 2018 (Potter 2021).

Finally, 2020 fire occurrence densities were ≤1/100 km^2 of tree canopy cover for all the islands of the U.S. Caribbean territories (Puerto Rico and the U.S. Virgin Islands) (fig. 3.5).

Comparison to Longer Term Trends

Because the MODIS Active Fire data have been collected in a consistent fashion for 2 decades, it is possible to use the data to contrast short-term (2020) forest fire occurrence densities with longer term trends (2001–2019) for ecoregions in the conterminous States, Alaska, and Hawaii, and for Caribbean islands. The highest mean annual fire occurrences (>6 fire occurrences/100 km^2 of tree canopy cover annually) across that period in the conterminous States were located in ecoregions

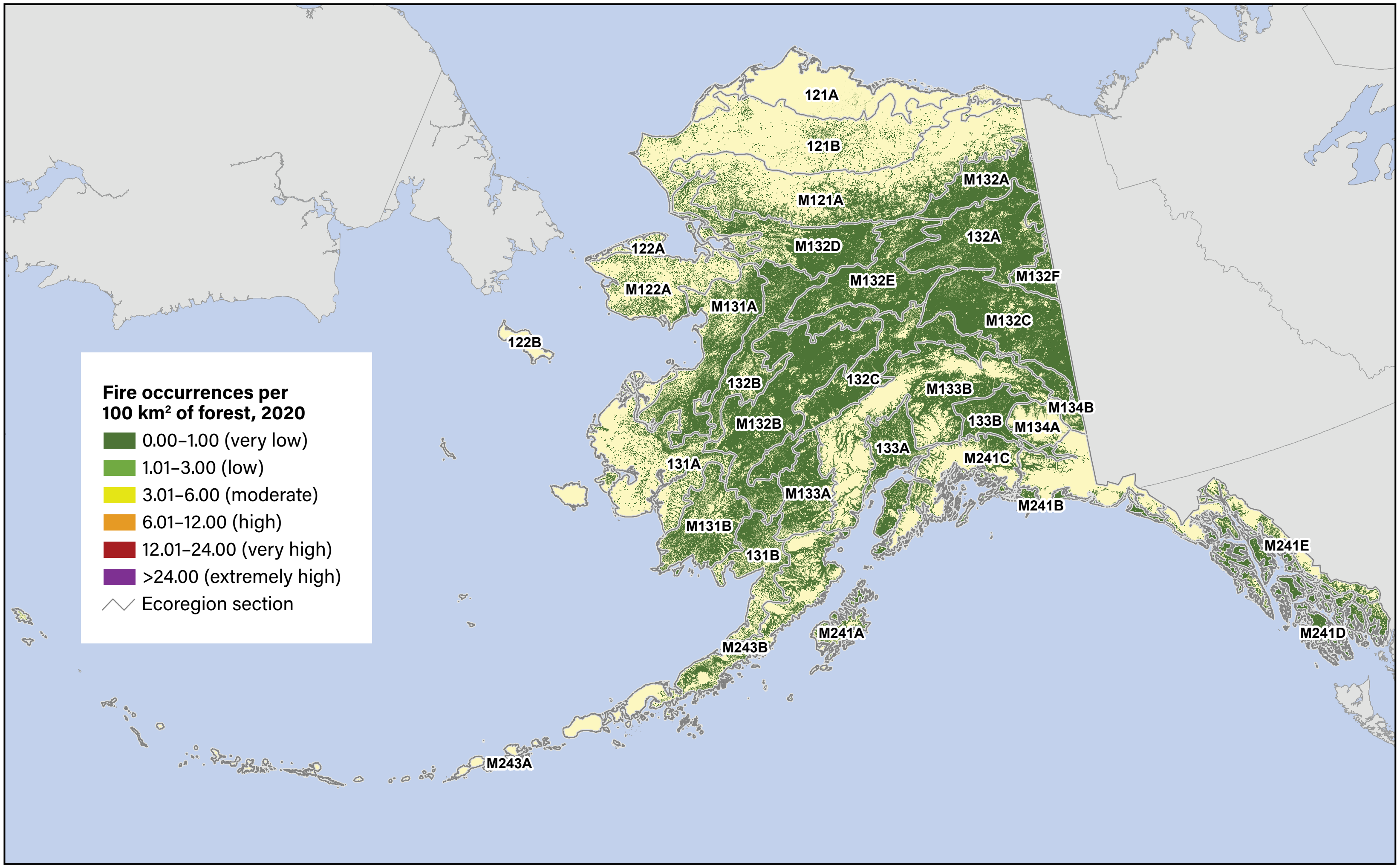

Figure 3.3—The number of forest fire occurrences, per 100 km² (10 000 ha) of forest and shrub cover, by ecoregion section within Alaska, for 2020. The gray lines delineate ecoregion sections (Spencer and others 2002). Forest and shrub cover are derived from the 2011 National Land Cover Database. See figure 1.1B for ecoregion identification. (Source of fire data: U.S. Department of Agriculture Forest Service, Geospatial Technology and Applications Center, in conjunction with the NASA MODIS Rapid Response group)

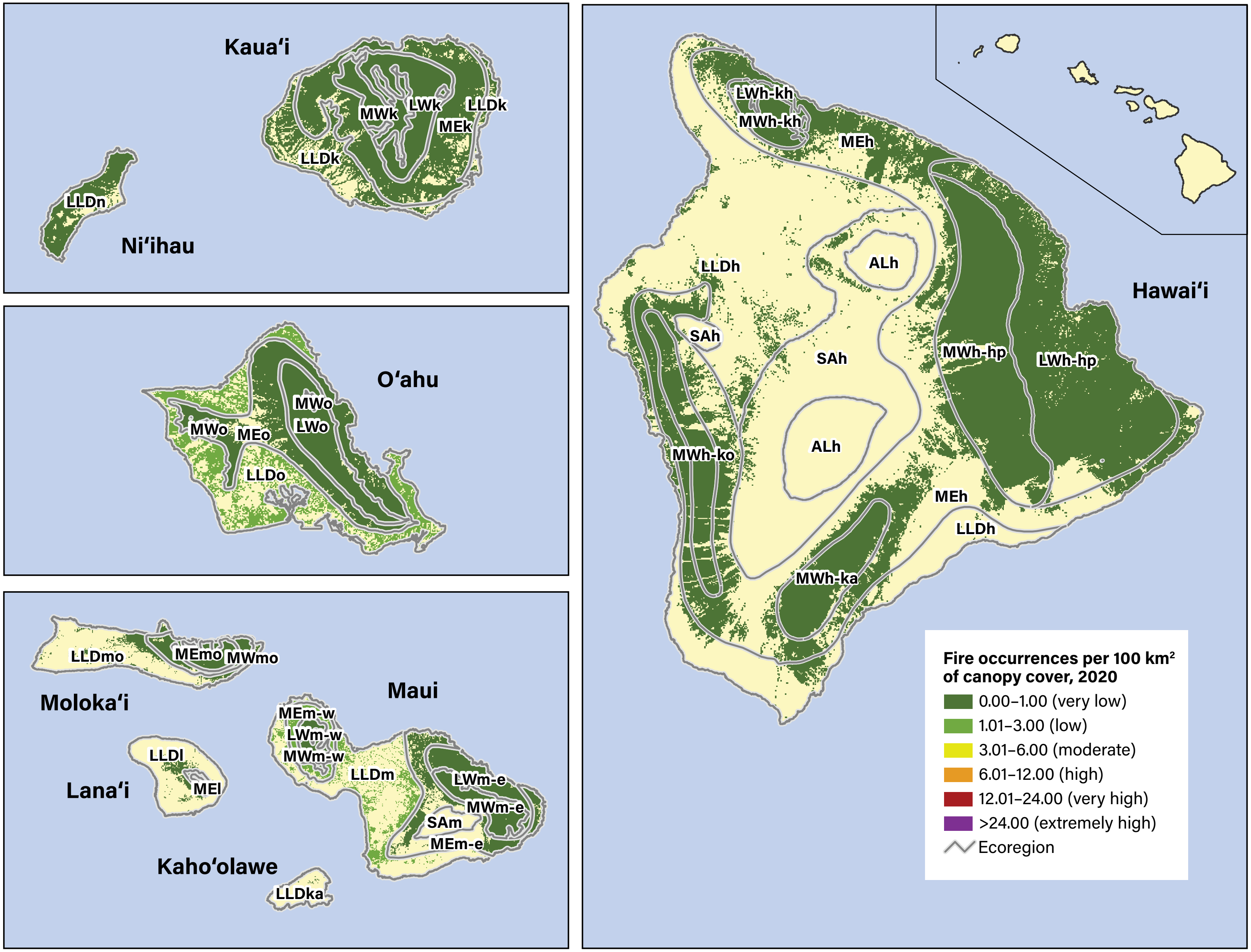

Figure 3.4—The number of forest fire occurrences, per 100 km² (10 000 ha) of tree canopy coverage area, by island/ecoregion combination in Hawaii, for 2020. Tree canopy cover is based on data from a cooperative project between the Multi-Resolution Land Characteristics Consortium (Coulston and others 2012) and the Forest Service Geospatial Technology and Applications Center using the 2011 National Land Cover Database. See table 1.1 for ecoregion identification. (Source of fire data: U.S. Department of Agriculture Forest Service, Geospatial Technology and Applications Center, in conjunction with the NASA MODIS Rapid Response group)

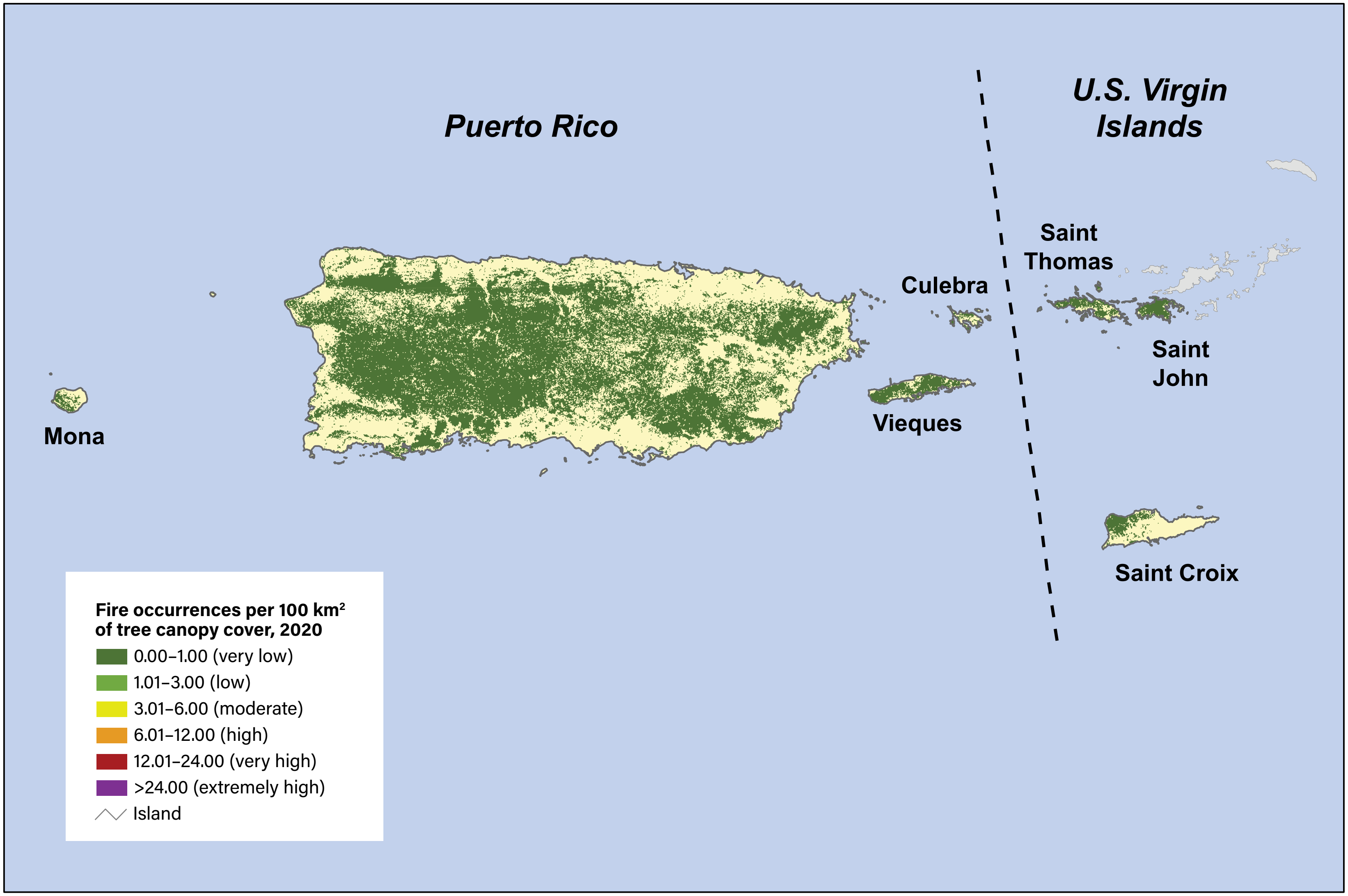

Figure 3.5—The number of forest fire occurrences, per 100 km² (10 000 ha) of tree canopy coverage area, by island in Puerto Rico and the U.S. Virgin Islands, for 2020. Tree canopy cover is based on data from a cooperative project between the Multi-Resolution Land Characteristics Consortium (Coulston and others 2012) and the Forest Service Geospatial Technology and Applications Center using the 2011 National Land Cover Database. (Source of fire data: U.S. Department of Agriculture Forest Service, Geospatial Technology and Applications Center, in conjunction with the NASA MODIS Rapid Response group)

along the Gulf Coast in the Southeast; in coastal, northern, and central areas of California; in north-central Washington; in central Arizona and west-central New Mexico; in the northern Rocky Mountains; and in central Kansas and northeastern Oklahoma (fig. 3.6A). Elsewhere outside of the West and the Southeast, ecoregions experienced ≤3 fire occurrences/100 km^2 of tree canopy cover annually, with much of the Midwest and all the Northeast experiencing ≤1. The ecoregion section with the highest fire occurrence density on average was M332A–Idaho Batholith in central Idaho (12.8), followed by M261A–Klamath Mountains of northwestern California and southeastern Oregon (10.7), and M262B–Southern California Mountain and Valley near the southern California coast (8.9) (table 3.2). The M332A–Idaho Batholith ecoregion was also the one with the greatest annual variation in fire occurrence densities from 2001 to 2019 (fig. 3.6B). More moderate variation was apparent in California, southern Oregon, northeastern Washington and northwestern Idaho, western and southeastern Montana, west-central Wyoming, and central Arizona and west-central New Mexico. Meanwhile, the interannual variation was the lowest in the Midwest and Northeast and in coastal areas of Oregon and Washington (standard deviation <1), with slightly higher variation (standard deviation 1–5) across the Southeast, the central Rocky Mountains, the Great Basin, and central Oregon and Washington.

Several ecoregions in California, Washington, and Oregon, as well as four in northwestern Colorado and northeastern Utah, had many more fire occurrences in 2020 than normal, compared to the previous 19-year mean and accounting for variability over time (fig. 3.6C). Several of these are ecoregions that both had a high fire occurrence density in 2020 and a relatively high mean for the previous years. The ecoregion section with the highest z-score in 2020, however, was M331E–Uinta Mountains in northeast Utah, an area with typically very few fire occurrences. A handful of ecoregions in the Northeast also had moderately or much higher fire occurrence density than normal, though these are areas that tend to have few fires in a typical year, so they don't require many fire occurrences to be classified as having more than normal.

A few ecoregion sections, mostly in the eastern half of the United States, had 2020 fire occurrence densities that were lower than expected, as determined by z-scores that were ≤-1. Four of these were in the Great Lakes States: 212H–Northern Lower Peninsula and 212R–Eastern Upper Peninsula in Michigan, 212X–Northern Highlands in Wisconsin, and 212K–Western Superior Uplands in Minnesota and Wisconsin. Three were in the South: M231A–Ouachita Mountains in southeast Oklahoma and west-central Arkansas, 221H–Northern Cumberland Plateau in eastern Tennessee and Kentucky, and 411A–Everglades in southern Florida. One was in the West: 341B–Northern Canyonlands in eastern Utah and western Colorado. Most of these are ecoregion sections that have low annual fire occurrence densities on average, but two were exceptions that have moderately high mean fire occurrence densities (M231A–Ouachita Mountains and 411A–Everglades).

In Alaska, meanwhile, mean annual fire occurrence densities for 2001–2019 were relatively low except for in M132E–Ray Mountains and

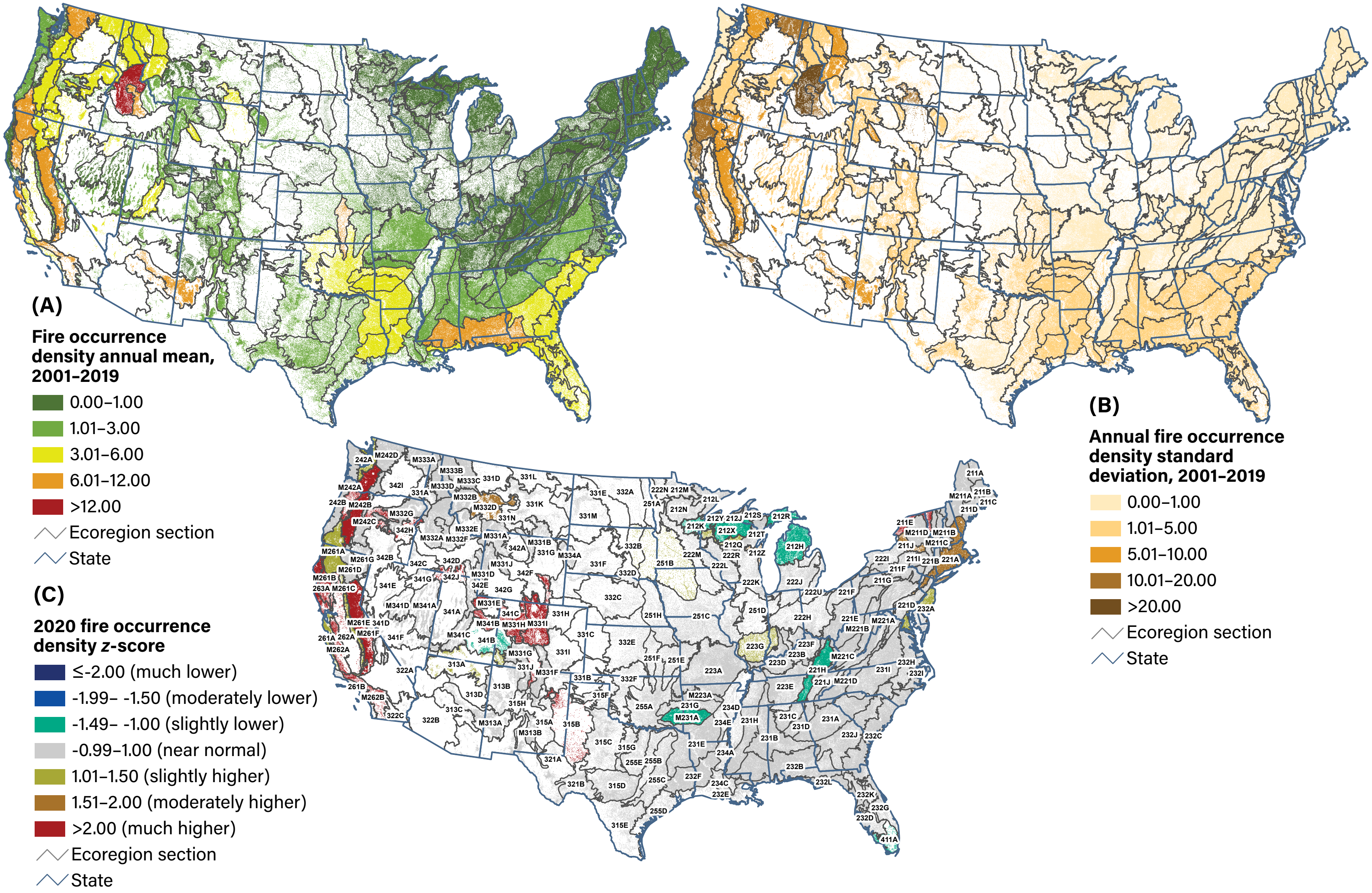

Figure 3.6—(A) Mean number and (B) standard deviation of forest fire occurrences per 100 km^2 (10 000 ha) of tree canopy coverage area from 2001 through 2019, by ecoregion section within the conterminous United States. (C) Degree of 2020 fire occurrence density excess or deficiency by ecoregion relative to 2001–2019 and accounting for variation over that time period. The gray lines delineate ecoregion sections (Cleland and others 2007). Tree canopy cover is based on data from a cooperative project between the Multi-Resolution Land Characteristics Consortium (Coulston and others 2012) and the Forest Service Geospatial Technology and Applications Center using the 2011 National Land Cover Database. (Source of fire data: U.S. Department of Agriculture Forest Service, Geospatial Technology and Applications Center, in conjunction with the NASA MODIS Rapid Response group)

Table 3.2—The 15 ecoregion sections in the conterminous United States with the highest mean annual fire occurrence densities from 2001 to 2019

Section	Name	Tree canopy area	Mean annual fire occurrence density[a]
		km²	
M332A	Idaho Batholith	338.9	12.8
M261A	Klamath Mountains	338.5	10.7
M262B	Southern California Mountain and Valley	58.1	8.9
M261E	Sierra Nevada	427.8	8.1
M313A	White Mountains-San Francisco Peaks-Mogollon Rim	202.5	7.9
313C	Tonto Transition	17.5	7.6
251F	Flint Hills	57.8	7.3
M261B	Northern California Coast Ranges	114.1	6.9
M242D	Northern Cascades	251.1	6.7
232B	Gulf Coastal Plains and Flatwoods	888.7	6.4
261A	Central California Coast	66.8	6.3
M332F	Challis Volcanics	72.2	6.1
331A	Palouse Prairie	33.4	6.0
M333C	Northern Rockies	176.3	6.0
M332B	Northern Rockies and Bitterroot Valley	154.9	5.8

[a] Mean annual fire occurrence density = fire occurrences/100 km^2 of tree canopy coverage area.

132A–Yukon-Old Crow Basin in the central and east-central parts of the State (fig. 3.7A). Along with the neighboring M132C–Yukon-Tanana Uplands and M132F–North Ogilvie Mountains, these ecoregion sections exhibited the most variability over the 19-year period preceding 2020 (fig. 3.7B). All Alaska ecoregions in 2020 had fire occurrence densities that were near normal compared to the previous 19 years and accounting for variability (fig. 3.7C).

In Hawaii, the area exhibiting the highest annual fire occurrence density mean (fig. 3.8A) and variability (fig. 3.8B) from 2001–2019 was the Lowland Wet-Hilo-Puna ecoregion (LWh-hp) on the eastern side of the Big Island (19.6 fire occurrences/100 km^2 of tree canopy cover, standard deviation 42.0). This ecoregion contains recently active portions of the lower east rift zone of Kīlauea volcano, where lava flows have incinerated some forested areas. For all other ecoregions in the State, the annual mean was ≤1 fire occurrence/100 km^2 of tree cover, with the exception of the Mesic region on the Big Island (MEh), where it was 2.3. In 2020, two ecoregions on Maui had fire occurrence densities higher than expected, controlling for variability over the previous 19 years (z-score >1): the Mesic-Maui-West ecoregion (MEm-w) and the Maui Lowland/Leeward Dry ecoregion (LLDm) (fig. 3.8C).

Finally, all the islands of the Caribbean territories of Puerto Rico and the U.S. Virgin Islands had fire occurrence means and standard deviations ≤1 for the 2001–2019 period (figs. 3.9A and 3.9B). None of the islands was outside the range of near-normal fire occurrence density (z-score ≤-1 or >1) in 2020 (fig. 3.9C).

Geographic Hot Spots of Fire Occurrence Density

Geographic hot spot analyses, conducted across the conterminous United States using analysis units smaller than ecoregions (the main unit of analysis thus far), can offer additional insights into where, statistically, fire occurrences are more concentrated than expected by chance. Even in a year marked by high fire activity for much of the conterminous United States, this analysis identifies areas that have higher-than-expected fire occurrence densities compared to the entire study region. For 2020, the SASH method detected two geographic hot spots of extremely high fire occurrence density (G_i^* >24), both in California, and several of very high fire occurrence density (G_i^* >12 and ≤24) throughout the West (fig. 3.10).

One of the hot spots of extremely high fire occurrence density was centered in M261B–Northern California Coast Ranges in the northwestern part of the State. This was the location of the August Complex of fires, which burned from August 17 to November 11 across 417 898 ha (the largest in the United States in 2020), costing approximately $116 million to contain (National Interagency Coordination Center 2021). It was the largest recorded fire complex in California history (CALFIRE 2021), encompassing 1 percent of the State—an area larger than Rhode Island. The second extremely high fire density hot spot was in the central part of M261E–Sierra Nevada, caused by the 153 738-ha Creek Fire. Ignited on September 4

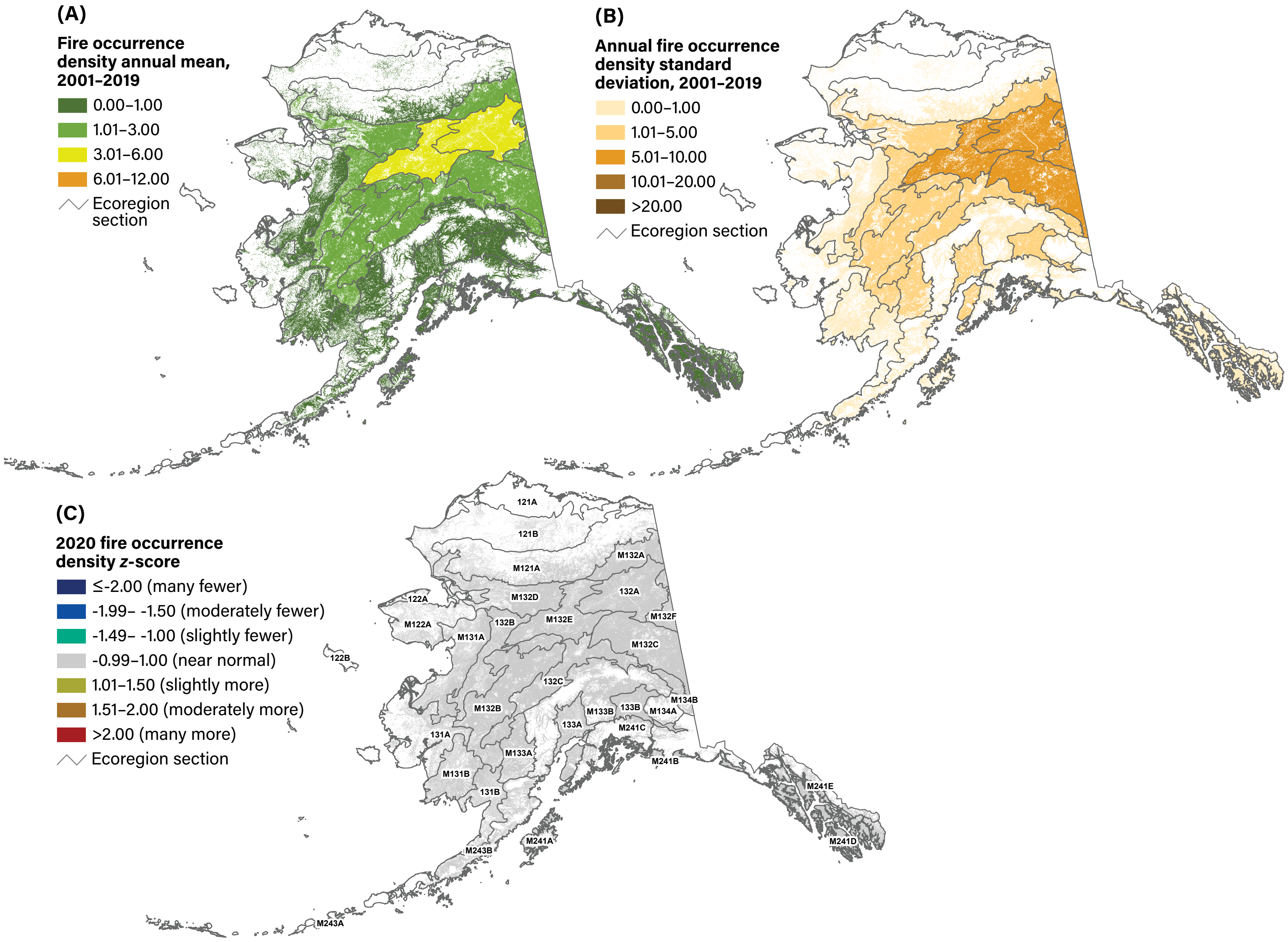

Figure 3.7—(A) Mean number and (B) standard deviation of forest fire occurrences per 100 km^2 (10 000 ha) of forest and shrub cover from 2001 through 2019, by ecoregion section in Alaska. (C) Degree of 2020 fire occurrence density excess or deficiency by ecoregion relative to 2001–2019 and accounting for variation over that time period. The gray lines delineate ecoregion sections (Spencer and others 2002). Forest and shrub cover are derived from the 2011 National Land Cover Database. (Source of fire data: U.S. Department of Agriculture Forest Service, Geospatial Technology and Applications Center, in conjunction with the NASA MODIS Rapid Response group)

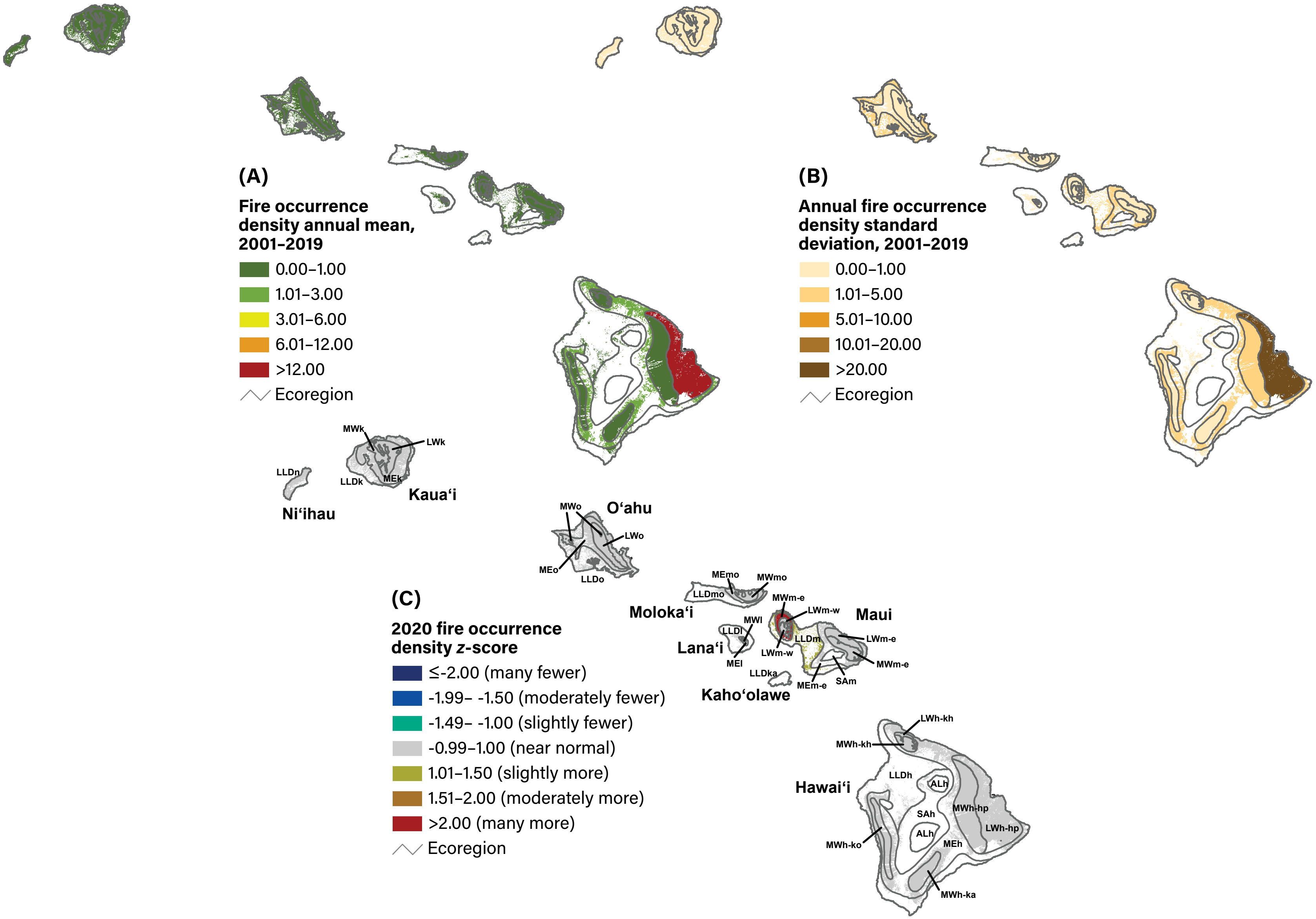

Figure 3.8—(A) Mean number and (B) standard deviation of forest fire occurrences per 100 km^2 (10 000 ha) of tree canopy coverage area from 2001 through 2019, by island/ecoregion combination in Hawaii. (C) Degree of 2020 fire occurrence density excess or deficiency by ecoregion relative to 2001–2019 and accounting for variation over that time period. Tree canopy cover is based on data from a cooperative project between the Multi-Resolution Land Characteristics Consortium (Coulston and others 2012) and the Forest Service Geospatial Technology and Applications Center using the 2011 National Land Cover Database. (Source of fire data: U.S. Department of Agriculture Forest Service, Geospatial Technology and Applications Center, in conjunction with the NASA MODIS Rapid Response group)

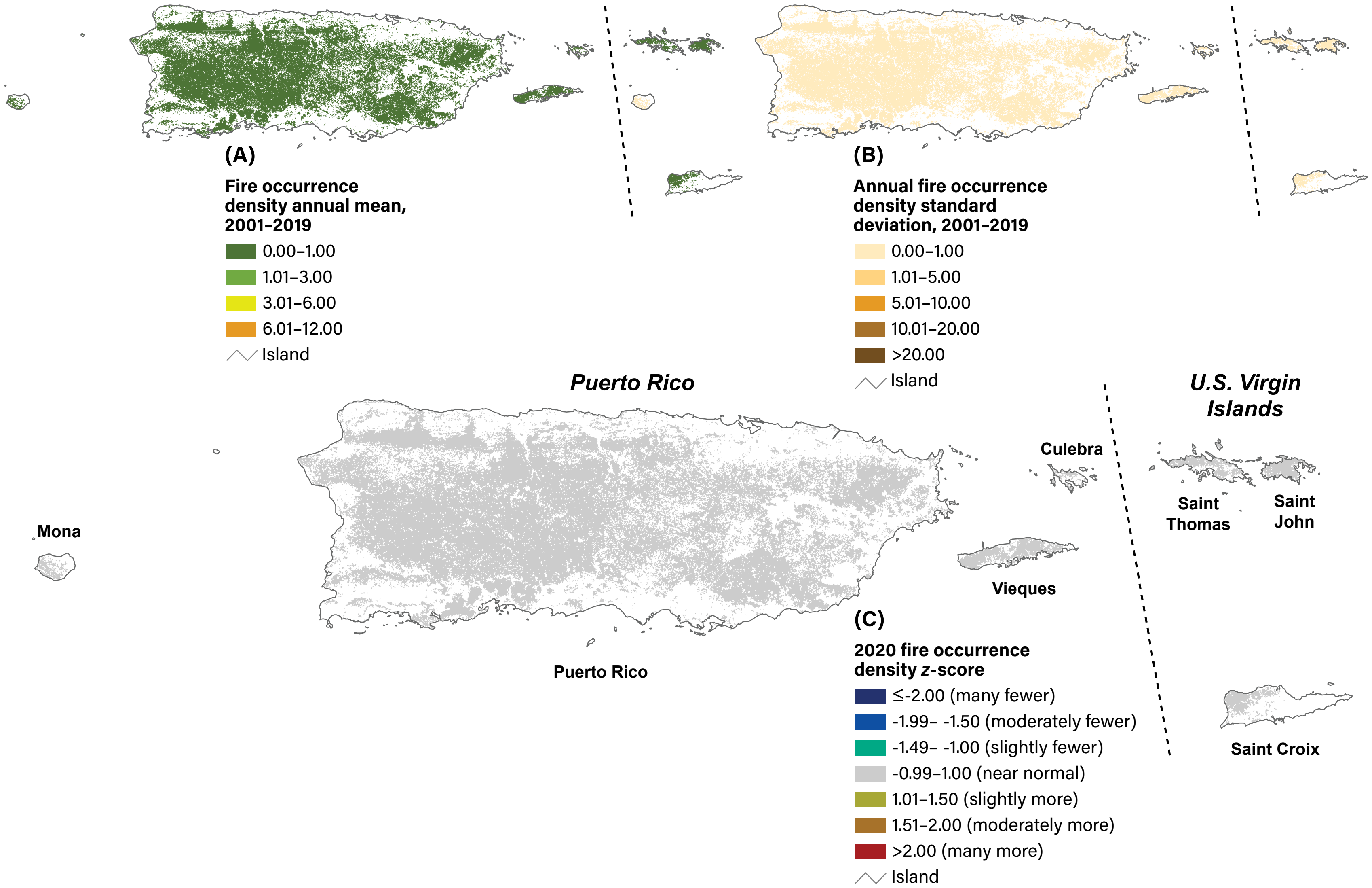

Figure 3.9—(A) Mean number and (B) standard deviation of forest fire occurrences per 100 km^2 (10 000 ha) of forested area from 2001 through 2019, by island in Puerto Rico and the U.S. Virgin Islands. (C) Degree of 2020 fire occurrence density excess or deficiency by ecoregion relative to 2001–2019 and accounting for variation over that time period. Tree canopy cover is based on data from a cooperative project between the Multi-Resolution Land Characteristics Consortium (Coulston and others 2012) and the U.S. Department of Agriculture Forest Service, Geospatial Technology and Applications Center using the 2011 National Land Cover Database. (Source of fire data: U.S. Department of Agriculture Forest Service, Geospatial Technology and Applications Center, in conjunction with the NASA MODIS Rapid Response group)

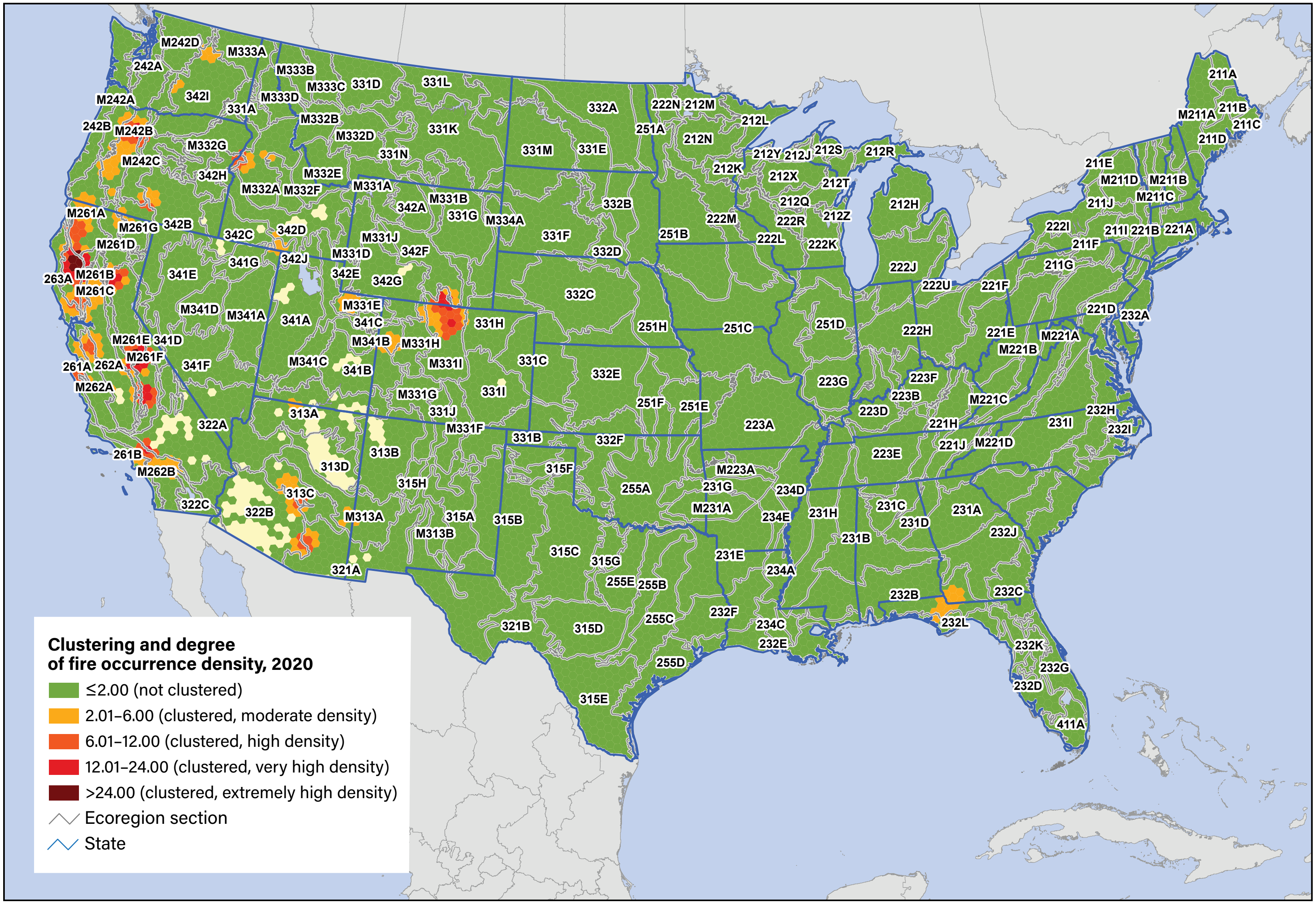

Figure 3.10—Hot spots of fire occurrence across the conterminous United States for 2020. Values are Getis-Ord G_i^* *scores, with values >2 representing significant clustering of high fire occurrence densities. (No areas of significant clustering of lower fire occurrence densities, <-2, were detected). The gray lines delineate ecoregion sections (Cleland and others 2007). (Source of fire data: U.S. Department of Agriculture Forest Service, Geospatial Technology and Applications Center, in conjunction with the NASA MODIS Rapid Response group)*

and reported as contained on December 17, it cost in the neighborhood of $193 million to contain (National Interagency Coordination Center 2021) and was the largest single fire (i.e., not a complex) in California history, destroying 853 structures (CALFIRE 2021).

The five hot spots of very high fire occurrence density in 2020 (fig. 3.10) were also each associated with megafires:

- In the northern part of M261E–Sierra Nevada in California, where the North Complex fire burned 129 068 ha between August 17 and December 2, killing 15 people, destroying 2,352 structures, and costing approximately $113 million to contain (CALFIRE 2021, National Interagency Coordination Center 2021)
- In the southern part of M261E–Sierra Nevada in California, location of the SQF Complex fire, which burned 70 487 ha between August 24 and December 24, destroying 228 structures (CALFIRE 2021, National Interagency Coordination Center 2021)
- In the M262B–Southern California Mountain and Valley in the southwestern part of the State, where the Bobcat Fire cost approximately $100 million to contain between September 6 and November 27, burning 46 942 ha (National Interagency Coordination Center 2021)
- In the M242B–Western Cascades in northwestern Oregon, location of the 82 746-ha Lionshead Fire; the 78 336-ha Beachie Creek Fire, and the 55 868-ha Riverside Fire, ignited between mid-August and early September and contained by late-November at a combined cost of about $115 million (National Interagency Coordination Center 2021). The Beachie Creek Fire killed five people and destroyed 500 homes (Templeton 2020).
- In M331I–Northern Parks and Ranges in north-central Colorado and south-central Wyoming, where three fires burned across large areas in the autumn: Cameron Peak (84 544 ha) and East Troublesome (78 433 ha) in Colorado, and Mullen (71 580 ha) in Wyoming and Colorado. Together, they cost roughly $191 million to contain (National Interagency Coordination Center 2021). Cameron Peak and East Troublesome were the largest fires in recorded Colorado history, and the East Troublesome Fire grew by 48 562 ha in a single day, by far the most rapid fire expansion ever seen in the State, and then jumped the Continental Divide despite a lack of fuels above treeline (Brasch 2021).

Additionally, hot spots of high fire density in 2020 (G_i^* >6 and ≤12) were identified in scattered locations throughout much of the West, including California, Oregon, and Arizona (fig. 3.10). Unusually, a single 2020 hot spot occurred in the Eastern United States, and it was of only moderate fire density (G_i^* >2 and ≤6), in the panhandle of Florida and the southeastern corner of Georgia (232B–Gulf Coastal Plains and Flatwoods and 232L–Gulf Coastal Lowlands).

CONCLUSIONS

During a year marked by several worrying wildfire superlatives, the number of MODIS satellite-detected forest fire occurrences recorded for the conterminous States in 2020 was among the highest in 20 full years of data collection. Only 2012 and 2014 had more fire occurrences. The year included the first-ever fire incident that exceeded 404 686 ha (1 million acres), six of the seven largest wildfire events in California history, and the three largest wildfires ever recorded in Colorado. Areas with the highest forest fire occurrence densities were almost entirely limited to the West, attributable to long-term severe drought and periodic heat waves across much of the region.

In particular, ecoregions in California, Colorado, Oregon, Washington, and Utah had the highest forest fire occurrence densities (fire occurrences/100 km^2 tree canopy cover area) in 2020. Geographic hot spots of extremely high fire occurrence density were detected in California and Colorado, while areas of very high forest fire occurrence density were identified in California, Oregon, and Arizona. Not surprisingly, these areas experienced much higher than normal fire occurrence densities in 2020 compared to the previous 19-year mean and accounting for variability over time. At the same time, a few ecoregions scattered across the East had significantly lower fire occurrence densities than normal.

Alaska, meanwhile, experienced a quiet fire season compared to 2019 and to the conterminous States, with the fewest fire occurrences since 2011. Similarly, most Hawaiian forests had low fire occurrence densities in 2020, although two ecoregions on the island of Maui had fire occurrence densities that were higher than expected, controlling for variability over the previous 19 years. All the U.S. islands in the Caribbean had near-normal fire occurrence densities.

The results of these geographic analyses are intended to offer insights into where fire occurrences have been concentrated spatially in a given year and compared to previous years but are not intended to quantify the severity of a given fire season. Given the limits of MODIS active fire detection using 1-km-resolution data, these products also may underrepresent the number of fire occurrences in some ecosystems where small and low-intensity fires are common, and where high cloud frequency can interfere with fire detection. These products can also have commission errors. However, these high-temporal-fidelity products currently offer the best means for daily monitoring of forest fire occurrences.

Ecological and forest health impacts relating to fire and other abiotic disturbances are scale-dependent properties, which in turn are affected by management objectives (Lundquist and others 2011). Information about the concentration of fire occurrences may help pinpoint areas of concern for aiding management activities and for investigations into the ecological and socioeconomic impacts of forest fire potentially outside the range of historic frequency.

LITERATURE CITED

Abatzoglou, J.T.; Williams, A.P. 2016. Impact of anthropogenic climate change on wildfire across Western US forests. Proceedings of the National Academy of Sciences. 113(42): 11770–11775. https://doi.org/10.1073/pnas.1607171113.

Agee, J.K. 1998. The landscape ecology of western forest fire regimes. Northwest Science. 72: 24–34.

Anselin, L. 1992. Spatial data analysis with GIS: an introduction to application in the social sciences. Tech. Rep. 92-10. Santa Barbara, CA: University of California, National Center for Geographic Information and Analysis. 53 p.

Barbour, M.G.; Burk, J.H.; Pitts, W.D. [and others]. 1999. Terrestrial plant ecology. Menlo Park, CA: Addison Wesley Longman, Inc. 649 p.

Bond, W.J.; Keeley, J.E. 2005. Fire as a global "herbivore": the ecology and evolution of flammable ecosystems. Trends in Ecology & Evolution. 20(7): 387–394. https://doi.org/10.1016/j.tree.2005.04.025.

Brasch, S. 2021. Colorado's East Troublesome wildfire may signal a new era of big fire blow-ups. Colorado Public Radio. https://www.cpr.org/2021/01/25/colorados-east-troublesome-wildfire-may-signal-a-new-era-of-big-fire-blow-ups/. [Date accessed: June 22, 2021].

CALFIRE. 2021. Top 20 largest California wildfires. https://www.fire.ca.gov/media/4jandlhh/top20_acres.pdf/. [Date accessed: June 22, 2021].

Calkin, D.E.; Thompson, M.P.; Finney, M.A. 2015. Negative consequences of positive feedbacks in US wildfire management. Forest Ecosystems. 2: 9. https://doi.org/10.1186/s40663-015-0033-8.

Cleland, D.T.; Freeouf, J.A.; Keys, J.E. [and others]. 2007. Ecological subregions: sections and subsections for the conterminous United States. Gen. Tech. Rep. WO-76D. Washington, DC: U.S. Department of Agriculture Forest Service. Map; Sloan, A.M., cartographer; presentation scale 1:3,500,000; colored. https://doi.org/10.2737/WO-GTR-76D.

Coop, J.D.; Parks, S.A.; Stevens-Rumann, C.S. [and others]. 2020. Wildfire-driven forest conversion in western North American landscapes. BioScience. 70(8): 659–673. https://doi.org/10.1093/biosci/biaa061.

Coulston, J.W.; Ambrose, M.J.; Riitters, K.H.; Conkling, B.L. 2005. Forest Health Monitoring 2004 national technical report. Gen. Tech. Rep. SRS-90. Asheville, NC: U.S. Department of Agriculture Forest Service, Southern Research Station. 81 p. https://doi.org/10.2737/SRS-GTR-90.

Coulston, J.W.; Moisen, G.G.; Wilson, B.T. [and others]. 2012. Modeling percent tree canopy cover: a pilot study. Photogrammetric Engineering and Remote Sensing. 78(7): 715–727. https://doi.org/10.14358/PERS.78.7.715.

Edmonds, R.L.; Agee, J.K.; Gara, R.I. 2011. Forest health and protection. Long Grove, IL: Waveland Press, Inc. 667 p.

Eidenshink, J.; Schwind, B.; Brewer, K. [and others]. 2007. A project for monitoring trends in burn severity. Fire Ecology. 3(1): 3–21. https://doi.org/10.4996/fireecology.0301003.

ESRI. 2017. ArcMap® 10.5.1. Redlands, CA: Environmental Systems Research Institute.

Gedalof, Z. 2011. Climate and spatial patterns of wildfire in North America. In: McKenzie, D.; Miller, C.; Falk, D.A., eds. The landscape ecology of fire. Dordrecht: Springer Netherlands: 89–115. https://doi.org/10.1007/978-94-007-0301-8_4.

Getis, A.; Ord, J.K. 1992. The analysis of spatial association by use of distance statistics. Geographical Analysis. 24(3): 189–206. https://doi.org/10.1111/j.1538-4632.1992.tb00261.x.

Gill, A.M.; Stephens, S.L.; Cary, G.J. 2013. The worldwide "wildfire" problem. Ecological Applications. 23(2): 438–454. https://doi.org/10.1890/10-2213.1.

Hanberry, B.B.; Bragg, D.C.; Hutchinson, T.F. 2018. A reconceptualization of open oak and pine ecosystems of eastern North America using a forest structure spectrum. Ecosphere. 9(10): e02431. https://doi.org/10.1002/ecs2.2431.

Hawbaker, T.J.; Radeloff, V.C.; Syphard, A.D. [and others]. 2008. Detection rates of the MODIS active fire product. Remote Sensing of Environment. 112: 2656–2664. https://doi.org/10.1016/j.rse.2007.12.008.

Higuera, P.E.; Abatzoglou, J.T. 2020. Record-setting climate enabled the extraordinary 2020 fire season in the Western United States. Global Change Biology. 27(1): 1–2. https://doi.org/10.1111/gcb.15388.

Homer, C.G.; Dewitz, J.A.; Yang, L. [and others]. 2015. Completion of the 2011 National Land Cover Database for the conterminous United States: representing a decade of land cover change information. Photogrammetric Engineering and Remote Sensing. 81(5): 345–354.

Jeronimo, S.M.; Kane, V.R.; Churchill, D.J. [and others]. 2019. Forest structure and pattern vary by climate and landform across active-fire landscapes in the montane Sierra Nevada. Forest Ecology and Management. 437: 70–86. https://doi.org/10.1016/j.foreco.2019.01.033.

Justice, C.O.; Giglio, L.; Korontzi, S. [and others]. 2002. The MODIS fire products. Remote Sensing of Environment. 83(1–2): 244–262. https://doi.org/10.1016/S0034-4257(02)00076-7.

Justice, C.O.; Giglio, L.; Roy, D. [and others]. 2011. MODIS-derived global fire products. In: Ramachandran, B.; Justice, C.O.; Abrams, M.J., eds. Land remote sensing and global environmental change: NASA's earth observing system and the science of ASTER and MODIS. New York: Springer: 661–679. https://doi.org/10.1007/978-1-4419-6749-7_29.

Kiser, D.; Elhanan, G.; Metcalf, W.J. [and others]. 2021. SARS-CoV-2 test positivity rate in Reno, Nevada: association with PM2.5 during the 2020 wildfire smoke events in the Western United States. Journal of Exposure Science and Environmental Epidemiology. 31: 797–803. https://doi.org/10.1038/s41370-021-00366-w.

Kitzberger, T.; Brown, P.M.; Heyerdahl, E.K. [and others]. 2007. Contingent Pacific-Atlantic Ocean influence on multicentury wildfire synchrony over western North America. Proceedings of the National Academy of Sciences. 104(2): 543–548. https://doi.org/10.1073/pnas.0606078104.

Laffan, S.W. 2006. Assessing regional scale weed distributions, with an Australian example using *Nassella trichotoma*. Weed Research. 46(3): 194–206. https://doi.org/10.1111/j.1365-3180.2006.00491.x.

Lundquist, J.E.; Camp, A.E.; Tyrrell, M.L. [and others]. 2011. Earth, wind and fire: abiotic factors and the impacts of global environmental change on forest health. In: Castello, J.D.; Teale, S.A., eds. Forest health: an integrated perspective. New York: Cambridge University Press: 195–243. https://doi.org/10.1017/CBO9780511974977.008.

McKenzie, D.; Peterson, D.L.; Alvarado, E. 1996. Predicting the effect of fire on large-scale vegetation patterns in North America. Res. Pap. PNW-489. Portland, OR: U.S. Department of Agriculture Forest Service, Pacific Northwest Research Station. 38 p. https://doi.org/10.5962/bhl.title.87888.

National Interagency Coordination Center. 2019. Wildland fire summary and statistics annual report: 2018. https://www.predictiveservices.nifc.gov/intelligence/2018_statssumm/intro_summary18.pdf. [Date accessed: June 27, 2019].

National Interagency Coordination Center. 2020. Wildland fire summary and statistics annual report: 2019. https://www.predictiveservices.nifc.gov/intelligence/2019_statssumm/intro_summary19.pdf. [Date accessed: April 3, 2020].

National Interagency Coordination Center. 2021. Wildland fire summary and statistics annual report: 2020. https://www.predictiveservices.nifc.gov/intelligence/2020_statssumm/intro_summary20.pdf. [Date accessed: May 20, 2021].

Navarro, K.M.; Clark, K.A.; Hardt, D.J. [and others]. 2021. Wildland firefighter exposure to smoke and COVID-19: a new risk on the fire line. Science of the Total Environment. 760: 144296. https://doi.org/10.1016/j.scitotenv.2020.144296.

Nowacki, G.J.; Abrams, M.D. 2008. The demise of fire and "mesophication" of forests in the Eastern United States. BioScience. 58(2): 123–138. https://doi.org/10.1641/B580207.

Nowell, H.K.; Holmes, C.D.; Robertson, K. [and others]. 2018. A new picture of fire extent, variability, and drought interaction in prescribed fire landscapes: insights from Florida government records. Geophysical Research Letters. 45(15): 7874–7884. https://doi.org/10.1029/2018GL078679.

Parisien, M.A.; Miller, C.; Parks, S.A. [and others]. 2016. The spatially varying influence of humans on fire probability in North America. Environmental Research Letters. 11(7): 1–18. https://doi.org/10.1088/1748-9326/11/7/075005.

Pausas, J.G.; Keeley, J.E. 2019. Wildfires as an ecosystem service. Frontiers in Ecology and the Environment. 17(5): 289–295. https://doi.org/10.1002/fee.2044.

Picotte, J.J.; Bhattarai, K.; Howard, D. [and others]. 2020. Changes to the Monitoring Trends in Burn Severity program mapping production procedures and data products. Fire Ecology. 16: 16. https://doi.org/10.1186/s42408-020-00076-y.

Potter, K.M. 2012a. Large-scale patterns of forest fire occurrence in the conterminous United States and Alaska, 2005–07. In: Potter, K.M.; Conkling, B.L., eds. Forest Health Monitoring 2008 national technical report. Gen. Tech. Rep. SRS-158. Asheville, NC: U.S. Department of Agriculture Forest Service, Southern Research Station: 73–83.

Potter, K.M. 2012b. Large-scale patterns of forest fire occurrence in the conterminous United States and Alaska, 2001–08. In: Potter, K.M.; Conkling, B.L., eds. Forest Health Monitoring 2009 national technical report. Gen. Tech. Rep. SRS-167. Asheville, NC: U.S. Department of Agriculture Forest Service, Southern Research Station: 151–161.

Potter, K.M. 2013a. Large-scale patterns of forest fire occurrence in the conterminous United States and Alaska, 2009. In: Potter, K.M.; Conkling, B.L., eds. Forest Health Monitoring: national status, trends, and analysis 2010. Gen. Tech. Rep. SRS-176. Asheville, NC: U.S. Department of Agriculture Forest Service, Southern Research Station: 31–39.

Potter, K.M. 2013b. Large-scale patterns of forest fire occurrence in the conterminous United States and Alaska, 2010. In: Potter, K.M.; Conkling, B.L., eds. Forest Health Monitoring: national status, trends, and analysis 2011. Gen. Tech. Rep. SRS-185. Asheville, NC: U.S. Department of Agriculture Forest Service, Southern Research Station: 29–40.

Potter, K.M. 2014. Large-scale patterns of forest fire occurrence in the conterminous United States and Alaska, 2011. In: Potter, K.M.; Conkling, B.L., eds. Forest Health Monitoring: national status, trends, and analysis 2012. Gen. Tech. Rep. SRS-198. Asheville, NC: U.S. Department of Agriculture Forest Service, Southern Research Station: 35–48.

Potter, K.M. 2015a. Large-scale patterns of forest fire occurrence in the conterminous United States and Alaska, 2012. In: Potter, K.M.; Conkling, B.L., eds. Forest Health Monitoring: national status, trends, and analysis 2013. Gen. Tech. Rep. SRS-207. Asheville, NC: U.S. Department of Agriculture Forest Service, Southern Research Station: 37–53.

Potter, K.M. 2015b. Large-scale patterns of forest fire occurrence in the conterminous United States and Alaska, 2013. In: Potter, K.M.; Conkling, B.L., eds. Forest Health Monitoring: national status, trends, and analysis 2014. Gen. Tech. Rep. SRS-209. Asheville, NC: U.S. Department of Agriculture Forest Service, Southern Research Station: 39–55.

Potter, K.M. 2016. Large-scale patterns of forest fire occurrence in the conterminous United States, Alaska, and Hawaii, 2014. In: Potter, K.M.; Conkling, B.L., eds. Forest Health Monitoring: national status, trends, and analysis 2015. Gen. Tech. Rep. SRS-213. Asheville, NC: U.S. Department of Agriculture Forest Service, Southern Research Station: 41–60.

Potter, K.M. 2017. Large-scale patterns of forest fire occurrence in the conterminous United States, Alaska, and Hawaii, 2015. In: Potter, K.M.; Conkling, B.L., eds. Forest Health Monitoring: national status, trends, and analysis 2016. Gen. Tech. Rep. SRS-222. Asheville, NC: U.S. Department of Agriculture Forest Service, Southern Research Station: 43–62.

Potter, K.M. 2018. Large-scale patterns of forest fire occurrence in the conterminous United States, Alaska, and Hawaii, 2016. In: Potter, K.M.; Conkling, B.L., eds. Forest Health Monitoring: national status, trends, and analysis 2017. Gen. Tech. Rep. SRS-233. Asheville, NC: U.S. Department of Agriculture Forest Service, Southern Research Station: 45–64.

Potter, K.M. 2019. Large-scale patterns of forest fire occurrence across the 50 United States and the Caribbean territories, 2017. In: Potter, K.M.; Conkling, B.L., eds. Forest Health Monitoring: national status, trends, and analysis 2018. Gen. Tech. Rep. SRS-239. Asheville, NC: U.S. Department of Agriculture Forest Service, Southern Research Station: 51–76.

Potter, K.M. 2020a. Large-scale patterns of forest fire occurrence across the 50 United States and the Caribbean territories, 2018. In: Potter, K.M.; Conkling, B.L., eds. Forest Health Monitoring: national status, trends, and analysis 2019. Gen. Tech. Rep. SRS-250. Asheville, NC: U.S. Department of Agriculture Forest Service, Southern Research Station: 57–82.

Potter, K.M. 2020b. Introduction. In: Potter, K.M.; Conkling, B.L., eds. Forest Health Monitoring: national status, trends, and analysis 2019. Gen. Tech. Rep. SRS-250. Asheville, NC: U.S. Department of Agriculture Forest Service, Southern Research Station: 5–24.

Potter, K.M. 2021. Broad-scale patterns of forest fire occurrence across the 50 United States and the Caribbean territories, 2019. In: Potter, K.M.; Conkling, B.L., eds. Forest Health Monitoring: national status, trends, and analysis 2020. Gen. Tech. Rep. SRS-261. Asheville, NC: U.S. Department of Agriculture Forest Service, Southern Research Station: 59-84.

Potter, K.M.; Koch, F.H.; Oswalt, C.M.; Iannone, B.V. 2016. Data, data everywhere: detecting spatial patterns in fine-scale ecological information collected across a continent. Landscape Ecology. 31: 67–84. https://doi.org/10.1007/s10980-015-0295-0.

Pyne, S.J. 2010. America's fires: a historical context for policy and practice. Durham, NC: Forest History Society. 91 p.

Radeloff, V.C.; Helmers, D.P.; Anu Kramer, H. [and others]. 2018. Rapid growth of the US wildland-urban interface raises wildfire risk. Proceedings of the National Academy of Sciences. 115(13): 3314–3319. https://doi.org/10.1073/pnas.1718850115.

Reams, G.A.; Smith, W.D.; Hansen, M.H. [and others]. 2005. The Forest Inventory and Analysis sampling frame. In: Bechtold, W.A.; Patterson, P.L., eds. The enhanced Forest Inventory and Analysis program—national sampling design and estimation procedures. Gen. Tech. Rep. SRS-80. Asheville, NC: U.S. Department of Agriculture Forest Service, Southern Research Station: 11–26.

Richardson, L.A.; Champ, P.A.; Loomis, J.B. 2012. The hidden cost of wildfires: economic valuation of health effects of wildfire smoke exposure in southern California. Journal of Forest Economics. 18(1): 14–35. https://doi.org/10.1016/j.jfe.2011.05.002.

Schmidt, K.M.; Menakis, J.P.; Hardy, C.C. [and others]. 2002. Development of coarse-scale spatial data for wildland fire and fuel management. Gen. Tech. Rep. RMRS-87. Fort Collins, CO: U.S. Department of Agriculture Forest Service, Rocky Mountain Research Station. 41 p. https://doi.org/10.2737/RMRS-GTR-87.

Shima, T.; Sugimoto, S.; Okutomi, M. 2010. Comparison of image alignment on hexagonal and square lattices. In: 2010 IEEE international conference on image processing. [Place of publication unknown]: Institute of Electrical and Electronics Engineers, Inc.: 141–144. https://doi.org/10.1109/ICIP.2010.5654351.

Spencer, P.; Nowacki, G.; Fleming, M. [and others]. 2002. Home is where the habitat is: an ecosystem foundation for wildlife distribution and behavior. Arctic Research of the United States. 16: 6–17.

Stephens, S.L.; Collins, B.M.; Fettig, C.J. [and others]. 2018. Drought, tree mortality, and wildfire in forests adapted to frequent fire. BioScience. 68(2): 77–88. https://doi.org/10.1093/biosci/bix146.

Templeton, A. 2020. Two people remain missing in Oregon's devastating wildfires. Oregon Public Broadcasting. https://www.opb.org/article/2020/09/24/only-two-people-remain-missing-in-oregons-devastating-wildfires/. [Date accessed: June 22, 2021].

Thom, D.; Seidl, R. 2016. Natural disturbance impacts on ecosystem services and biodiversity in temperate and boreal forests. Biological Reviews. 91(3): 760–781. https://doi.org/10.1111/brv.12193.

Tonini, M.; Tuia, D.; Ratle, F. 2009. Detection of clusters using space-time scan statistics. International Journal of Wildland Fire. 18(7): 830–836. https://doi.org/10.1071/WF07167.

U.S. Department of Agriculture (USDA) Forest Service. 2008. National forest type data development. http://svinetfc4.fs.fed.us/rastergateway/forest_type/. [Date accessed: May 13, 2008].

U.S. Department of Agriculture (USDA) Forest Service. 2021. Fire detection GIS data. https://fsapps.nwcg.gov/afm/gisdata.php. [Date accessed: June 23, 2021].

Wade, D.D.; Brock, B.L.; Brose, P. [and others]. 2000. Fire in eastern ecosystems. In: Brown, J.K.; Kapler, J., eds. Wildland fire in ecosystems: effects of fire on flora. Gen. Tech. Rep. RMRS-42-vol. 2. Ogden, UT: U.S. Department of Agriculture Forest Service, Rocky Mountain Research Station: 53–96.

White, D.; Kimerling, A.J.; Overton, W.S. 1992. Cartographic and geometric components of a global sampling design for environmental monitoring. Cartography and Geographic Information Systems. 19(1): 5–22. https://doi.org/10.1559/152304092783786636.

CHAPTER 4

Drought and Moisture Surplus Patterns in the Conterminous United States: 2020, 2018–2020, and 2016–2020

Frank H. Koch
John W. Coulston

INTRODUCTION

Droughts can have significant impacts on forests. They can give rise to considerable tree stress, particularly when they co-occur with heat waves (L.D.L. Anderegg and others 2013, Peters and others 2015, Williams and others 2013). While trees and other plants can defend against this stress by restricting fundamental growth processes and photosynthesis (Kareiva and others 1993, Mattson and Haack 1987), prolonged drought stress can lead to failure of a tree's hydraulic system, causing crown death and eventual tree mortality (Choat and others 2018). Research suggests that large trees may be more sensitive to drought stress than small trees and experience comparatively higher rates of growth decline and mortality (Bennett and others 2015, Stovall and others 2019). Furthermore, drought stress can make trees vulnerable to damaging insects and diseases (Clinton and others 1993, Kolb and others 2016, Mattson and Haack 1987, Raffa and others 2008). In addition, droughts heighten the risk of more frequent and more severe wildfires by hindering organic matter breakdown and reducing the moisture content of downed woody debris, leading to higher fuel loads (Clark 1989, Collins and others 2006, Keetch and Byram 1968, Schoennagel and others 2004, Trouet and others 2010). Regional-scale relationships between drought and fire occurrence are complex, but generally, projections of increased drought frequency and severity under a warming climate imply that wildfires will be more prevalent and extensive in many U.S. forest systems, especially in the Western United States (Abatzoglou and Williams 2016, Dennison and others 2014, Littell and others 2016).

Ecologists define the concept of drought inconsistently and disagree about the best way to measure its severity (Slette and others 2019, 2020; Zang and others 2020). For example, in a review of 564 ecological drought studies, Slette and others (2019) found that less than one-third explicitly defined drought or cited a definition from another source. Furthermore, about 30 percent of the studies merely treated the term "drought" as synonymous with "dry conditions" without characterizing or quantifying how dry the conditions were relative to normal conditions. Bearing these issues in mind, a meaningful definition applicable to forests is that a drought is a period of precipitation deficit that persists long enough to deplete available soil water, resulting in impacts to trees and other plants that may include injury or death (Anderegg and others 2012, Hanson and Weltzin 2000). By this definition, droughts affect most forests in the United States, although there are regional variations in drought frequency, timing, and intensity (Hanson and Weltzin 2000). These variations characterize the regions' predominant drought regimes. In the Western United States, most forests receive a large majority of their precipitation during a relatively brief period of 2–3 months, so they experience seasonal droughts each year. By comparison, forests in the Eastern United States usually exhibit a pattern of random (i.e., occurring at any time of year) but occasional droughts, as observed in the Appalachian Mountains and the Northeast, or frequent late-summer droughts, as commonly observed in the Southeastern Coastal Plain and the eastern Great Plains (Hanson and Weltzin 2000).

How to cite this chapter:

Koch, Frank H.; Coulston, John W. 2022. Drought and moisture surplus patterns in the conterminous United States: 2020, 2018–2020, and 2016–2020. In: Potter, Kevin M.; Conkling, Barbara L., eds. Forest Health Monitoring: national status, trends, and analysis 2021. Gen. Tech. Rep. SRS-266. Asheville, NC: U.S. Department of Agriculture Forest Service, Southern Research Station: 79–99. https://doi.org/10.2737/SRS-GTR-266-Chap4.

Most forests can tolerate short-term droughts, although individual tree species differ in their level of tolerance (Archaux and Wolters 2006, Berdanier and Clark 2016, Peters and others 2015). Because of this tolerance, drought duration may be more important for forests than drought intensity (Archaux and Wolters 2006). For example, forests that endure multiple consecutive years of drought are likelier to experience high tree mortality or other negative impacts than forests subject to a single year of extreme drought (Bigler and others 2006, Guarín and Taylor 2005, Jenkins and Pallardy 1995, Millar and others 2007). Indeed, effects on tree growth and function from 1 year of drought are probably still reversible for many forests (Bigler and others 2006). In other words, forests may not encounter significant deleterious effects until they undergo a prolonged period of comparatively intense drought conditions. Hence, comprehensive evaluations of drought impact in forests should include analyses of moisture conditions at multiple timescales. Such approaches were once rare among broad-scale assessments (Norman and others 2016), but multiscale drought indices such as the Standardized Precipitation Evaporation Index (SPEI) have grown in popularity (Vicente-Serrano and others 2010).

In the 2010 FHM national report, we described a method for mapping drought conditions across the conterminous United States (Koch and others 2013b). Our objective was to generate fine-scale, drought-related spatial datasets that build upon products available from sources such as the National Centers for Environmental Information (e.g., Vose and others 2014) or the U.S. Drought Monitor program (Svoboda and others 2002). The primary inputs are gridded climate data (i.e., monthly raster maps of precipitation and temperature over a 100-year period) created with the Parameter-elevation Regressions on Independent Slopes (PRISM) climate mapping system (Daly and others 2002). The method uses a standardized indexing approach that facilitates comparison of a given location's moisture status during different time windows, regardless of their length. The index is more straightforward to calculate than the commonly used Palmer Drought Severity Index, or PDSI (Palmer 1965), and avoids some criticisms of the PDSI (see Alley 1984) regarding its underlying assumptions and limited comparability across space and time. Here, we applied the method outlined in the 2010 FHM Report to the most currently available climate data (i.e., the monthly PRISM data through 2020), thereby providing the twelfth installment in an ongoing series of annual drought assessments for the conterminous United States (Koch and Coulston 2015, 2016, 2017, 2018, 2019, 2020, 2021; Koch and others 2013a, 2013b, 2014, 2015).

This is the seventh year in which we also mapped levels of moisture surplus across the conterminous United States during multiple time windows. While recent refereed literature (Adams and others 2009, Allen and others 2010, Martínez-Vilalta and others 2012, Peng and others 2011, Williams and others 2013) has typically focused on reports of regional-scale forest decline and mortality due to persistent drought conditions, surplus moisture availability can likewise affect forests. Unusually high moisture can be a short-term stressor (e.g., an extreme rainfall event with subsequent flooding) or a long-term stressor (e.g., persistent wetness caused by a macroscale climatic pattern such as the El Niño-Southern Oscillation), either of which may lead to tree dieback and mortality (Rozas and García-González 2012, Rozas and Sampedro 2013). Such impacts have been observed in tropical, temperate, and boreal forest systems (Hubbart and others 2016, Laurance and others 2009, Rozas and García-González 2012). For example, larch (*Larix*) species that predominate in eastern Siberian forests appear to be drought-resistant yet highly sensitive to excessively wet conditions (Tei and others 2019). While surplus-induced impacts in forests may be less common than drought-induced impacts, a single index that depicts moisture surplus as well as deficit conditions provides a more comprehensive indicator of potential forest health issues.

METHODS

We acquired grids for monthly precipitation and monthly mean temperature for the conterminous United States from the PRISM Climate Group website (PRISM Climate Group 2021). At the time of these analyses, gridded datasets were available for all years from 1895 to 2020. The spatial resolution of the grids was approximately 4 km (cell area = 16 km^2). For future applications and to ensure better compatibility with other spatial datasets, output grids were resampled to a spatial resolution of approximately 2 km (cell area = 4 km^2) using a nearest neighbor approach. The nearest neighbor approach is a computationally simple resampling method that avoids the smoothing of data values observed with methods such as bilinear interpolation or cubic convolution.

Potential Evapotranspiration (PET) Maps

As in our previous drought mapping efforts (in particular, see Koch and others 2013b), we adopted an approach in which a moisture index value is calculated for each location of interest (i.e., each grid cell in a map of the conterminous United States) during a given time period. Moisture indices are intended to reflect the amount of water available in a location (e.g., to support plant growth). In our case, the index is computed using an approach that considers both the amount of precipitation that falls on a location during the period of interest as well as the level of potential evapotranspiration during this period. Potential evapotranspiration measures the loss of soil moisture through plant uptake and transpiration (Akin 1991). It does not measure actual moisture loss, but rather the loss that would occur if there was no possible shortage of moisture for plants to transpire (Akin 1991, Thornthwaite 1948). Potential evapotranspiration serves as a basic measure of moisture demand. By incorporating potential evapotranspiration along with precipitation, our index thus documents the long-term balance between moisture demand and supply for each location of interest.

To complement the available PRISM monthly precipitation grids, we computed monthly potential evapotranspiration (*PET*) grids using Thornthwaite's formula (Akin 1991, Thornthwaite 1948):

$$PET_m = 1.6 L_{l\,m} (10 \frac{T_m}{I})^a \qquad (1)$$

where

PET_m = the potential evapotranspiration for a given month *m* in cm

L_{lm} = a correction factor for the mean possible duration of sunlight during month *m* for all locations (i.e., grid cells) at a particular latitude *l* (see Table V in Thornthwaite [1948] for a list of *L* correction factors by month and latitude)

T_m = the mean temperature for month *m* in degrees C

I = an annual heat index ranging from 0 to 160, calculated as, $I = \sum_{m=1}^{12} \left(\frac{T_m}{5}\right)^{1.514}$ where T_m is the mean temperature for each month *m* of the year

a = an exponent calculated as $a = 6.75 \times 10^{-7} I^3 - 7.71 \times 10^{-5} I^2 + 1.792 \times 10^{-2} I + 0.49239$ [see Appendix I in Thornthwaite (1948) regarding calculation of *I* and the empirical derivation of *a* in relation to *I*]

Although only a simple approximation, a key advantage of Thornthwaite's formula is that it has modest input data requirements (i.e., mean temperature values) compared to more sophisticated methods of estimating PET such as the Penman-Monteith equation (Monteith 1965), which requires less readily available data on factors such as humidity, radiation, and wind speed. While the Thornthwaite method is considered less accurate than Penman-Monteith and some other PET estimation methods (Amatya and others 1995, Sentelhas and others 2010), it is coupled with the moisture index that serves as the foundation for our analysis (see equation [2]). If we used another PET estimation method, we would have to recalibrate and potentially revise the moisture index to conform to the expected distribution of PET values under that method. We intend to address this aspect in future work.

To implement equation (1) spatially, we created a grid of latitude values for determining the *L* adjustment for any given grid cell (and any given month) in the conterminous United States. We extracted the T_m values for the grid cells from the corresponding PRISM mean monthly temperature grids.

Moisture Index Maps

To estimate baseline conditions, we used the precipitation (P) and PET grids to generate monthly moisture index grids for the past 100 years (i.e., 1921–2020) for the conterminous United States. We used a moisture index described by Willmott and Feddema (1992), which has been applied in a variety of contexts, including global vegetation modeling (Potter and Klooster 1999) and climate change analysis (Grundstein 2009). Willmott and Feddema (1992) devised the index as a refinement of one described earlier by Thornthwaite (1948) and Thornthwaite and Mather (1955). Their revised index, MI', has the following form:

$$MI' = \begin{cases} P/PET - 1 & , \quad P < PET \\ 1 - PET/P & , \quad P \geq PET \\ 0 & , \quad P = PET = 0 \end{cases} \qquad (2)$$

where

P = precipitation

PET = potential evapotranspiration, as calculated using equation (1)

(P and PET must be in equivalent measurement units, e.g., mm.)

This set of equations yields a symmetric, dimensionless index scaled between -1 and 1. A primary advantage of this symmetry is that it enables valid comparisons between any set of locations in terms of their balance between moisture demand and supply. MI' can be calculated for any time period but is commonly calculated on an annual basis using P and PET values summed across the entire year (Willmott and Feddema 1992). An alternative to this summation approach is to calculate MI' on a monthly basis (i.e., from total measured precipitation and estimated potential evapotranspiration in each month), and then, for a given time window of interest, calculate its moisture index as the mean of the MI' values for all months in the time window. This “mean-of-months” approach limits the ability of short-term peaks in either precipitation or potential evapotranspiration to negate corresponding short-term deficits, as would happen under a summation approach.

For each year in our study period (i.e., 1921–2020), we used the mean-of-months approach to calculate moisture index grids for three different time windows: 1 year (MI_1'), 3 years (MI_3'), and 5 years (MI_5'). Briefly, the MI_1' grids are the mean (i.e., the mean value for each grid cell) of the 12 monthly MI' grids for each year in the study period, the MI_3' grids are the mean of the 36 monthly grids from January 2 years prior through December of the target year, and the MI_5' grids are the mean of the 60 consecutive monthly MI' grids from January 4 years prior through December of the target year. Thus, the MI_1' grid for the year 2020 is the mean of the monthly MI' grids from January to December 2020, while the MI_3' grid is the mean of the grids from January 2018 to December 2020, and the MI_5' grid is the mean of the grids from January 2016 to December 2020.

Annual and Multiyear Drought Maps

To determine degree of departure from typical moisture conditions, we first created a normal grid, $MI'_{i\,norm}$, for each of our time windows, representing the mean (i.e., the mean value for each grid cell) of the 100 corresponding moisture index grids (i.e., the MI_1', MI_3', or MI_5' grids, depending on the window; see fig. 4.1). We also created a standard deviation grid, $MI'_{i\,SD}$, for each time window, calculated from the window's 100 individual moisture index grids as well as its $MI'_{i\,norm}$ grid. We subsequently calculated moisture difference *z*-scores, MDZ_{ij}, for each time window using these derived datasets:

$$MDZ_{ij} = \frac{MI_i' - MI'_{i\;norm}}{MI'_{i\;SD}} \qquad (3)$$

where

> i = the analytical time window (i.e., 1, 3, or 5 years) and j = a particular target year in our 100-year study period (i.e., 1921–2020)

MDZ scores may be classified in terms of degree of moisture deficit or surplus (table 4.1). The classification scheme includes categories (e.g., severe drought, extreme drought) like those associated with the PDSI. The scheme has also been adopted for other drought indices such as the Standardized Precipitation Index, or SPI (McKee and others 1993). Moreover, the breakpoints between *MDZ* categories resemble those used for the SPI, such that we expect the *MDZ* categories to have theoretical frequencies of occurrence that are similar to their SPI counterparts (e.g., approximately 2.3 percent of the time for extreme drought; see McKee and others 1993, Steinemann 2003). More importantly, because of the standardization in equation (3), the breakpoints between categories remain the same regardless of the size of the time window of interest. For comparative analysis, we generated and classified *MDZ* maps of the conterminous United States, based on 1-, 3-, and 5-year windows, for the target year 2020.

Table 4.1—Moisture difference *z*-score *(MDZ)* value ranges for nine wetness and drought categories, along with each category's approximate theoretical frequency of occurrence

MDZ	Category	Frequency
		percent
≤-2	Extreme drought	2.3
-1.999 to -1.5	Severe drought	4.4
-1.499 to -1	Moderate drought	9.2
-0.999 to -0.5	Mild drought	15
-0.499 to 0.5	Near normal conditions	38.2
0.501 to 1	Mild moisture surplus	15
1.001 to 1.5	Moderate moisture surplus	9.2
1.501 to 2	Severe moisture surplus	4.4
>2	Extreme moisture surplus	2.3

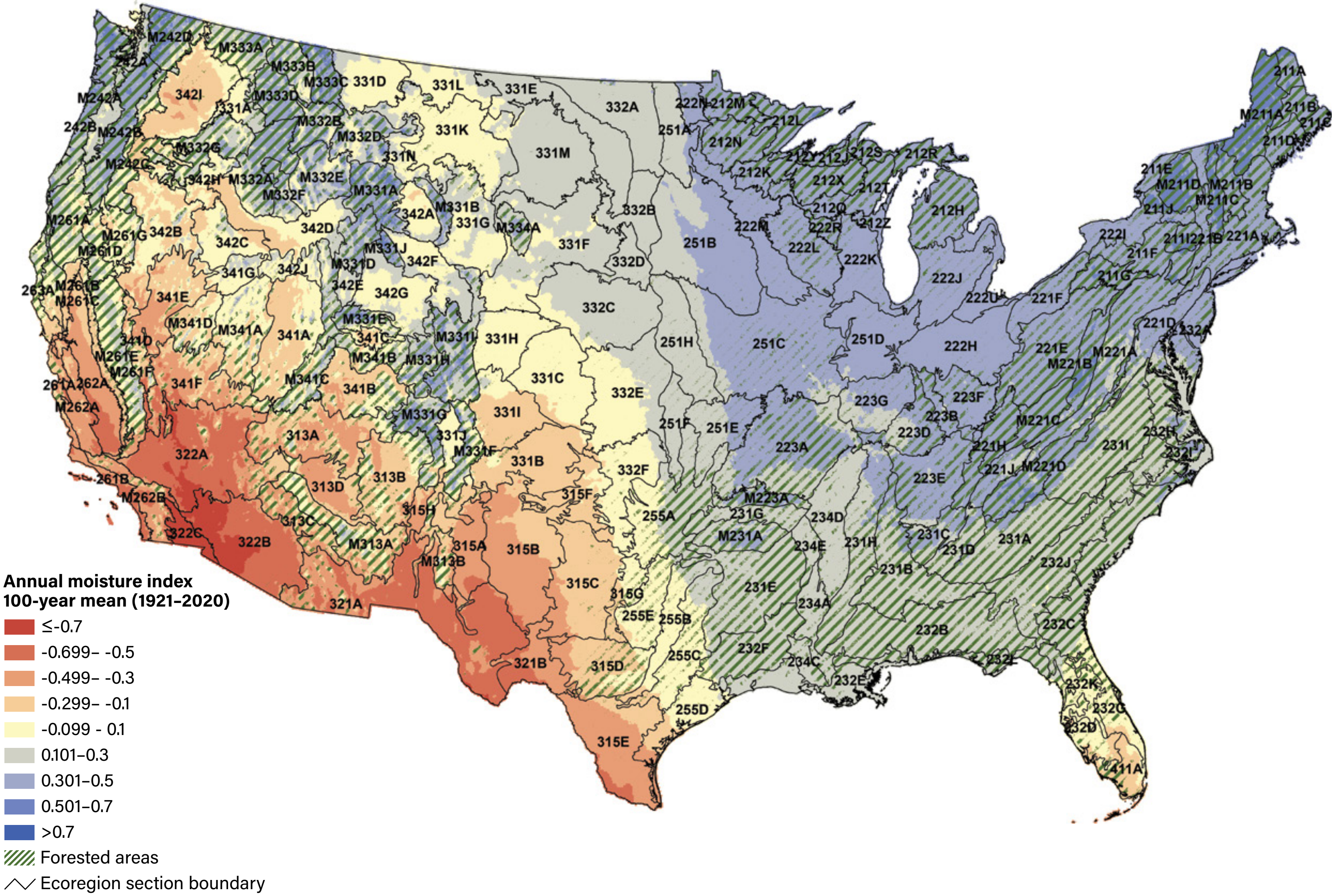

Figure 4.1—The 100-year (1921–2020) mean annual moisture index, or $MI'_{1\,norm}$, for the conterminous United States. Ecoregion section (Cleland and others 2007) boundaries and labels are included for reference. Forest cover data (overlaid green hatching) derived from Moderate Resolution Imaging Spectroradiometer (MODIS) imagery by the U.S. Department of Agriculture Forest Service, Geospatial Technology and Applications Center. (Data source: PRISM Climate Group, Oregon State University)

RESULTS AND DISCUSSION

The 100-year (1921–2020) mean annual moisture index, or $MI_1{}'_{norm}$, grid (fig. 4.1) provides a summary of long-term moisture regimes in the conterminous United States. (The 100-year $MI_3{}'_{norm}$ and $MI_5{}'_{norm}$ grids were very similar to the mean $MI_1{}'_{norm}$ grid, and so are not shown here.) Wet climates ($MI' > 0$) are typical in the Eastern United States, especially the Northeast. An exception worth noting is southern Florida, primarily ecoregion sections (Cleland and others 2007) 232D–Florida Coastal Lowlands-Gulf, 232G–Florida Coastal Lowlands-Atlantic, and 411A–Everglades. This region appears to be dry relative to other parts of the East, which is an effect of its tropical climate, which has distinct wet (primarily summer months) and dry (late fall to early spring) seasons. Although southern Florida usually receives a high level of precipitation during the wet season, it can be insufficient to offset the region's lengthy dry season (Duever and others 1994) or its high level of temperature-driven evapotranspiration, especially during the late spring and summer months, resulting in negative MI' values. This differs from the pattern observed in the driest parts of the Western United States, especially the Southwest (e.g., sections 322A–Mojave Desert, 322B–Sonoran Desert, and 322C–Colorado Desert), where potential evapotranspiration is very high, as in southern Florida, but precipitation levels are typically very low. In fact, because of generally lower precipitation than the East, dry climates ($MI' < 0$) are typical across much of the Western United States. Nonetheless, some mountainous areas in the Pacific Northwest as well as the central and northern Rocky Mountains, such as ecoregion sections M242A–Oregon and Washington Coast Ranges, M242B–Western Cascades, M331G–South Central Highlands, and M333C–Northern Rockies, have been wetter historically than other parts of the West. Principally, this has been driven by large amounts of winter snowfall (Hanson and Weltzin 2000). Under warming climatic conditions, many of these areas are expected to shift toward markedly drier moisture regimes due to a decrease in winter snowpack (Fyfe and others 2017).

Figure 4.2 shows the annual (i.e., 1-year) MDZ map for 2020 for the conterminous United States. Moderate to extreme drought conditions ($MDZ \leq -1$) were common across much of the Western United States in 2020, including forested areas in the central Rocky Mountains (e.g., ecoregion sections M331G, mentioned above, and M331I–Northern Parks and Ranges) and California (e.g., ecoregion sections M261B–Northern California Coast Ranges and M261E–Sierra Nevada). However, forested portions of the northern Rocky Mountains (e.g., M332B–Northern Rockies and Bitterroot Valley) and Pacific Northwest (e.g., M242D–Northern Cascades) experienced near normal or moisture surplus conditions. On the other side of the country, moderate to extreme surplus conditions were widespread throughout the Southeast and Mid-Atlantic regions in 2020, maybe most distinctly in sections 232H–Middle Atlantic Coastal Plains and Flatwoods and 232I–Central Appalachian Piedmont, although there were exceptions (e.g., 232K–Florida Coastal Plains Central Highlands). Areas of extreme moisture surplus also appeared in the Great Lakes region (e.g., 212H–Northern Lower Peninsula). In contrast, nearly all of New England experienced drought conditions, including areas of severe to

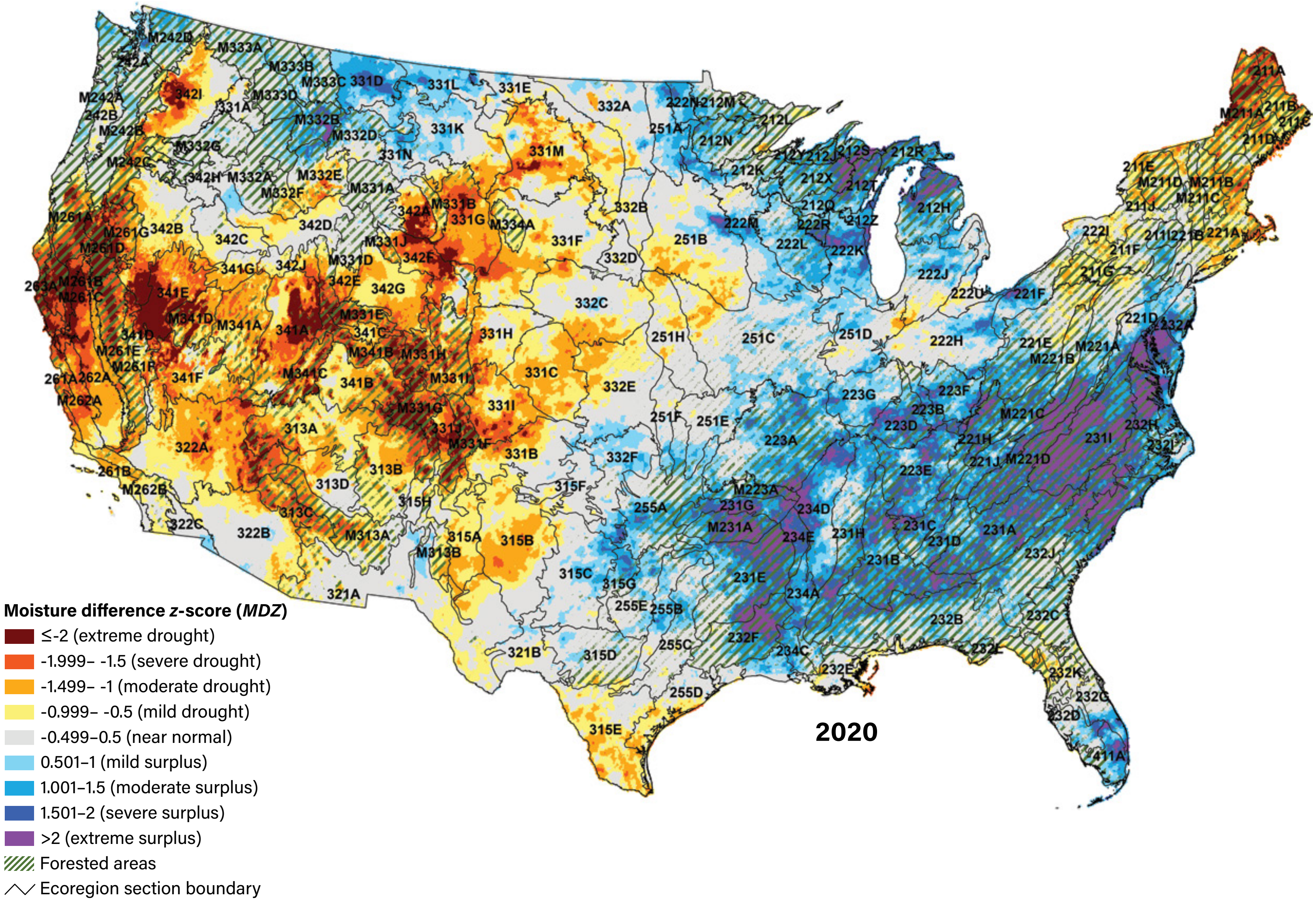

Figure 4.2—The 2020 annual (i.e., 1-year) moisture difference z-score, or MDZ, *for the conterminous United States. Ecoregion section (Cleland and others 2007) boundaries and labels are included for reference. Forest cover data (overlaid green hatching) derived from MODIS imagery by the U.S. Department of Agriculture Forest Service, Geospatial Technology and Applications Center. (Data source: PRISM Climate Group, Oregon State University)*

extreme drought (*MDZ* ≤-1.5) in the northern portions of sections 211A–Aroostook Hills and Lowlands and M211A–White Mountains.

The 2020 *MDZ* map is consistent with summary statistics reported elsewhere. According to the U.S. Drought Monitor, the percentage of area of the conterminous United States with drought conditions peaked at 49.0 percent in December (NOAA National Centers for Environmental Information 2021b). In the Western United States, the percentage of area experiencing moderate or worse drought conditions exceeded 75 percent for the last 3 months of 2020. In terms of climatological ranks relative to the historical record, it was the third driest and fourth warmest year for the Western United States since 1895, and the second driest and third warmest year for the Southwest region, specifically (NOAA National Centers for Environmental Information 2021a, 2021b). On the other side of the country, the Southeast experienced its third wettest year on record, but 2020 was also its second warmest year in terms of average temperature. It was a similarly warm year in the Northeast—the region's third warmest since 1895—but unlike in the Southeast, precipitation levels remained close to historical averages, enabling the development of drought conditions across the region.

Comparing the 2020 *MDZ* map with the 2019 *MDZ* map (fig. 4.3), much of the conterminous United States shifted from surplus to deficit conditions, or vice versa, between the 2 years. For example, the Southeast and Mid-Atlantic regions saw scattered areas of mild to moderate drought during 2019, but these were replaced by surplus conditions in 2020 (fig. 4.2). Conversely, areas of severe to extreme moisture surplus that appeared in the Desert Southwest in 2019 (i.e., 322A–Mojave Desert, 322B–Sonoran Desert, and 322C–Colorado Desert) were nearly gone in 2020. (Note that none of these ecoregion sections contains significant forest.) There is some evidence that a rapid swing between drought and surplus conditions can induce tree mortality directly (Tei and others 2019), although this is presumably influenced by the swing's magnitude (e.g., from extreme drought to extreme surplus over the course of a few months). Regardless, the observed disparities between 2019 and 2020 are partly explained by the fact that the former was an anomalously wet year: the second wettest nationally since 1895, and the wettest ever across the Midwest and the Northern Great Plains (NOAA National Centers for Environmental Information 2021a, 2021b). Furthermore, the Northeast and a large share of the West had precipitation levels that were above average (sometimes well above average) in 2019; the only regions with average or below average precipitation were the Southeast and Pacific Northwest. It is also important to recognize that, alongside this high degree of moisture variability, most of the country experienced temperatures that were significantly above average in both years (NOAA National Centers for Environmental Information 2021a, 2021b). This is in keeping with a steady warming trend that has been observed worldwide since the 1970s, signaling future climatic conditions that are expected to feature greater drought frequency, severity, and

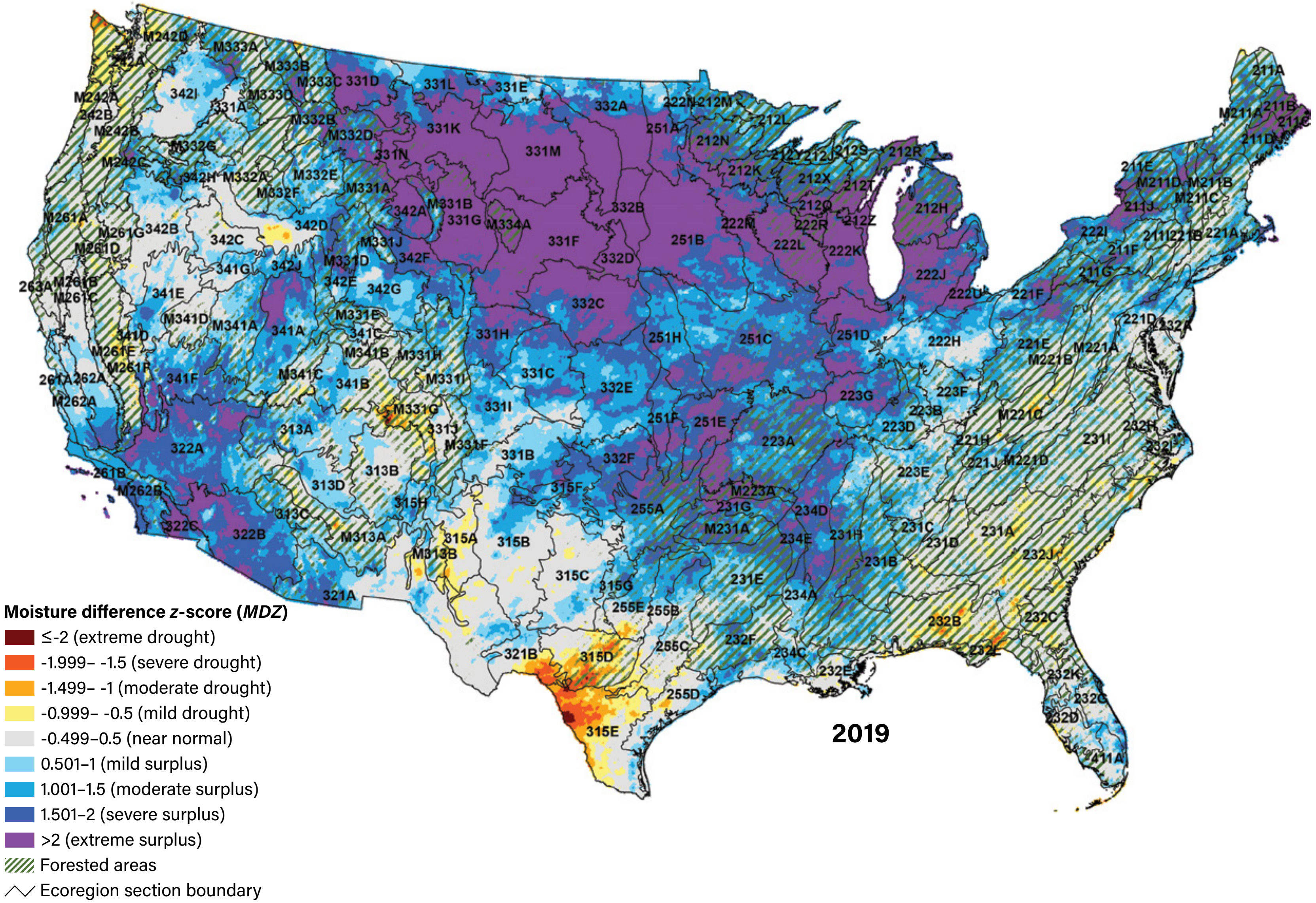

Figure 4.3—The 2019 annual (i.e., 1-year) moisture difference z-score, or MDZ, for the conterminous United States. Ecoregion section (Cleland and others 2007) boundaries and labels are included for reference. Forest cover data (overlaid green hatching) derived from MODIS imagery by the U.S. Department of Agriculture Forest Service, Geospatial Technology and Applications Center. (Data source: PRISM Climate Group, Oregon State University)

duration, particularly in drier locales such as the Western United States (Peltier and Ogle 2019, Rahmstorf and others 2017, Williams and others 2013). Indeed, warmer temperatures have the capacity to magnify moderate droughts into "megadroughts" that can have highly destructive impacts on forest systems (Brodribb and others 2020, Williams and others 2020). In fact, this may already be happening in the Southwest (Williams and others 2020).

With their longer time windows, the 3-year (2018–2020; fig. 4.4) and 5-year (2016–2020; fig. 4.5) *MDZ* maps are less influenced by year-to-year variation in moisture status. Thus, they can highlight areas where drought or surplus conditions have been persistent and intense, at least in the short term. Taken together, the two maps show an obvious disparity between the East and West. From the Rocky Mountains westward, few areas with severe to extreme moisture surpluses (*MDZ* >1.5) appeared in both maps (i.e., persisted for 5 years). Furthermore, only two of these surplus areas extended appreciably into forested ecoregion sections (i.e., M332B–Northern Rockies and Bitterroot Valley and M333A–Okanogan Highland). Perhaps more concerning are areas of severe to extreme drought that appeared in both the 3- and 5-year *MDZ* maps. These occurred primarily in southwestern Colorado and northern New Mexico (including parts of M331F–Southern Parks and Rocky Mountain Range, M331G–South Central Highlands, M331H–North Central Highlands and Rocky Mountains, and M331I–Northern Parks and Ranges) and in northern California (parts of M261A–Klamath Mountains, M261B–Northern California Coast Ranges, M261D–Southern Cascades, and M261E–Sierra Nevada). As noted, the occurrence of severe to extreme drought in both the 3- and 5-year maps indicates persistence, but it also points to minimal improvement in drought status during the last couple of years and downplays the significance of the near normal to surplus conditions that many of these areas experienced in 2019 (see fig. 4.3).

In the Eastern United States, only a few isolated hot spots of moderate or worse drought conditions appeared in both the 3- and 5-year *MDZ* maps (figs. 4.4 and 4.5): in northern Maine (ecoregion sections 211A–Aroostook Hills and Lowlands and M211A–White Mountains) and southern Florida (411A–Everglades and 232G–Florida Coastal Lowlands-Atlantic). The relative rarity of drought hot spots at the 3- and 5-year timescales provides support for the idea that prolonged droughts may not be a major issue for eastern forests (but see Clark and others 2016, Swanston and others 2018). Areas of prolonged moisture surplus were far more common and tended to be more extensive and spatially contiguous. While both the 3- and 5-year *MDZ* maps showed areas of surplus in the Ozark Mountains (e.g., ecoregion sections 231G–Arkansas Valley and M223A–Boston Mountains) and throughout the Mid-Atlantic (e.g., 231I–Central Appalachian Piedmont), the most notable area was in the Great Lakes region. This contiguous area of extreme surplus extended across almost every forested ecoregion section near Lakes Huron, Michigan, and Superior, including 212H–Northern Lower Peninsula, 212J–Southern Superior Uplands, 212K–Western Superior

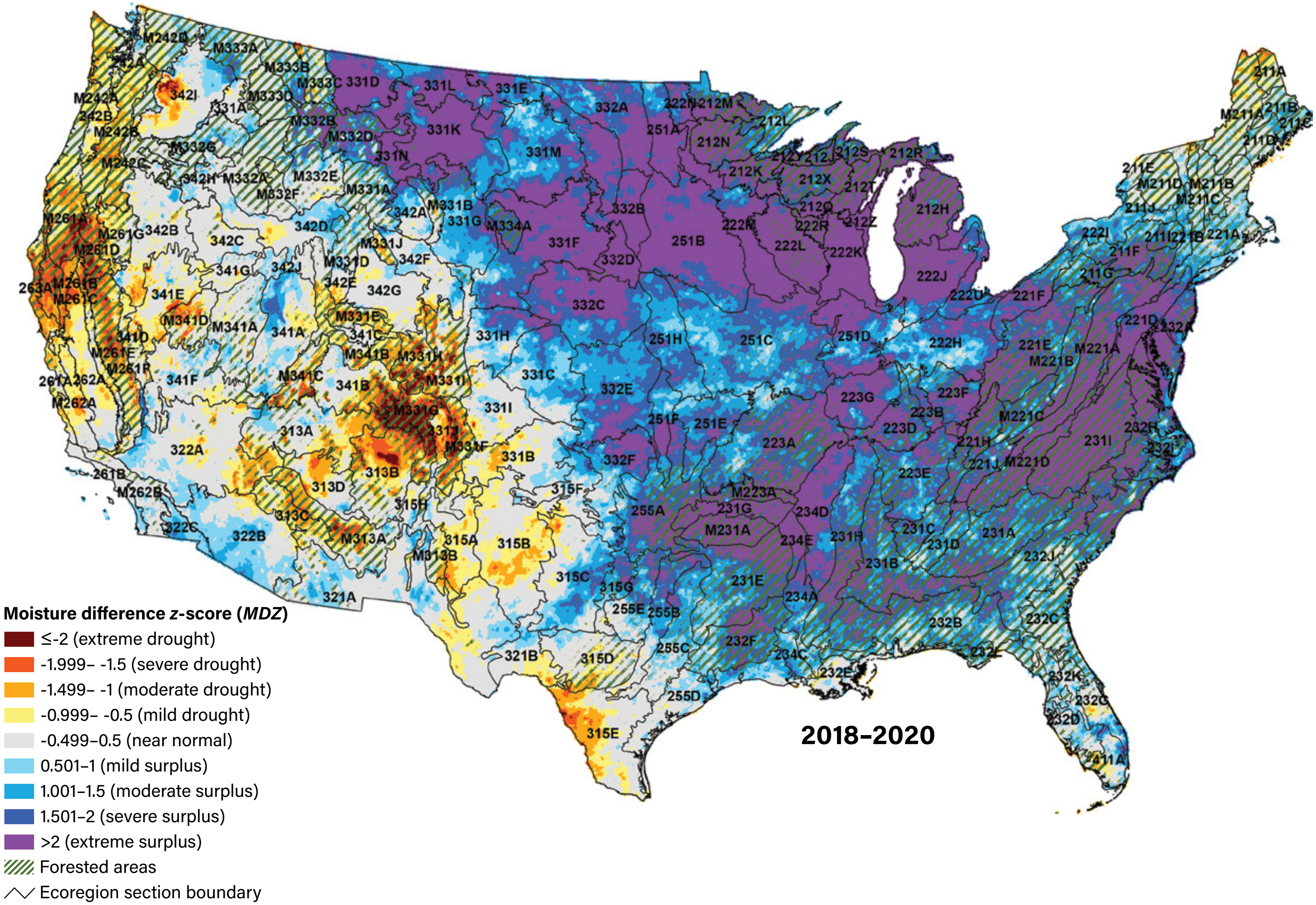

Figure 4.4—The 2018–2020 (i.e., 3-year) moisture difference z-score, or MDZ, *for the conterminous United States. Ecoregion section (Cleland and others 2007) boundaries are included for reference. Forest cover data (overlaid green hatching) derived from MODIS imagery by the U.S. Department of Agriculture Forest Service, Geospatial Technology and Applications Center. (Data source: PRISM Climate Group, Oregon State University)*

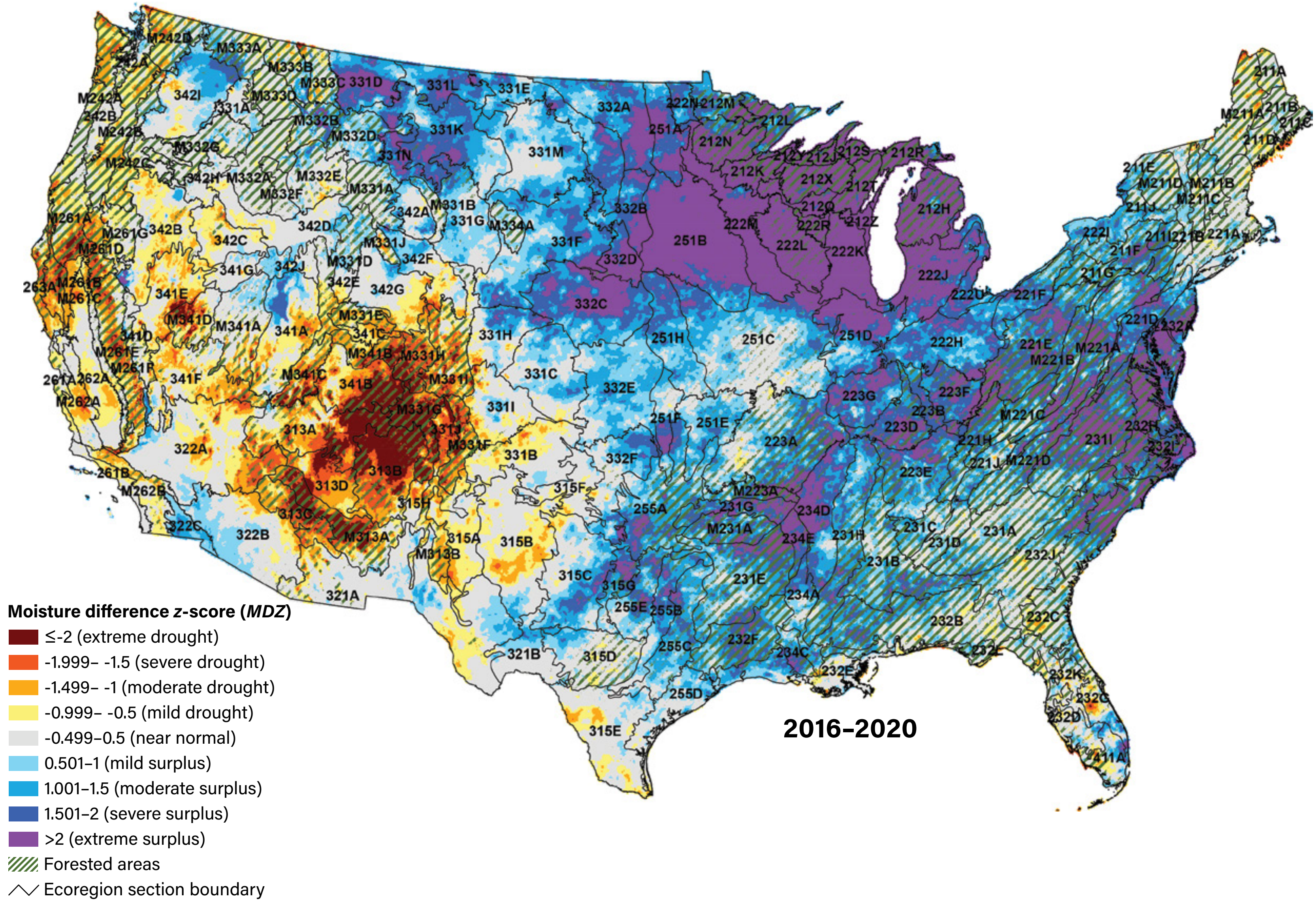

Figure 4.5—The 2016–2020 (i.e., 5-year) moisture difference z-score, *or* MDZ, *for the conterminous United States. Ecoregion section (Cleland and others 2007) boundaries are included for reference. Forest cover data (overlaid green hatching) derived from MODIS imagery by the U.S. Department of Agriculture Forest Service, Geospatial Technology and Applications Center. (Data source: PRISM Climate Group, Oregon State University)*

Uplands, 212N–Northern Minnesota Drift and Lake Plains, 212Q–North Central Wisconsin Uplands, 212R–Eastern Upper Peninsula, 212T–Northern Green Bay Lobe, and 222R–Wisconsin Central Sands. The implications of this major surplus, which was essentially uniform across the region, are not entirely clear, but persistent excess moisture can make forests more vulnerable to pathogens and other disease-causing agents, especially when wet and warm conditions co-occur (Hubbart and others 2016). Moisture surpluses can also present a challenge for forest management. For example, wet conditions can act as a barrier to prescribed burning by restricting burn windows, i.e., the times when conditions are appropriate for implementing prescribed fire treatments (Chiodi and others 2018).

When attempting to understand the significance of conditions captured in the *MDZ* maps, it may be useful to consider them in the context of longer term moisture trajectories. Figure 4.6 shows full trajectories for the 1921–2020 period for eight ecoregion sections in the conterminous United States. The values on the y-axis of each plot are the mean 5-year *MDZ* values, by year, across an ecoregion section. A benefit of using 5-year *MDZ* is that it yields smoother trajectory curves than the 1-year and 3-year *MDZ*, and thus makes it easier to discern trends through time. A few notable aspects emerge from figure 4.6. Foremost, moisture conditions have been highly variable through time. All eight ecoregion sections have seen pronounced periods of deficit and surplus in the last 100 years. In some cases, these periods have been of relatively long duration, such as the period of moisture surplus that lasted through the 1960s and 1970s in 232J–Southern Atlantic Coastal Plains and Flatwoods. In other cases, the periods have been of very high intensity, such as the drought periods in the mid-1950s and mid-1960s in M231A–Ouachita Mountains and in the mid-1960s in 221A–Lower New England; these droughts are noted as the worst in recent history for their respective regions (Haavik and others 2011, Seager and others 2012, Xue and Ullrich 2021).

Although their long-term trajectories differ, the four ecoregion sections in the Eastern United States (i.e., 212H–Northern Lower Peninsula, as well as 221A–Lower New England, 232J–Southern Atlantic Coastal Plains and Flatwoods, and M231A–Ouachita Mountains) generally have been wetter during the last 50 years than the 50 years prior. The most distinctive case is 212H, which just experienced its wettest year as well as its wettest decade. By comparison, parts of the West have seen their worst drought conditions develop over the last 20 years. In section M331G–South Central Highlands, drought conditions have persisted since 2000 but reached their most extreme level in 2020. This may foretell prevalent tree mortality in pinyon-juniper (*Pinus-Juniperus* spp.) woodlands, as has already been reported in nearby regions (Kannenberg and others 2021). In M261E–Sierra Nevada, the drought conditions that have developed during the last several years are significantly more severe than at any other time in the last century. Broad-scale forest mortality associated with these conditions has been well documented in this and neighboring ecoregion sections (Fettig and others 2019, Goulden and Bales 2019).

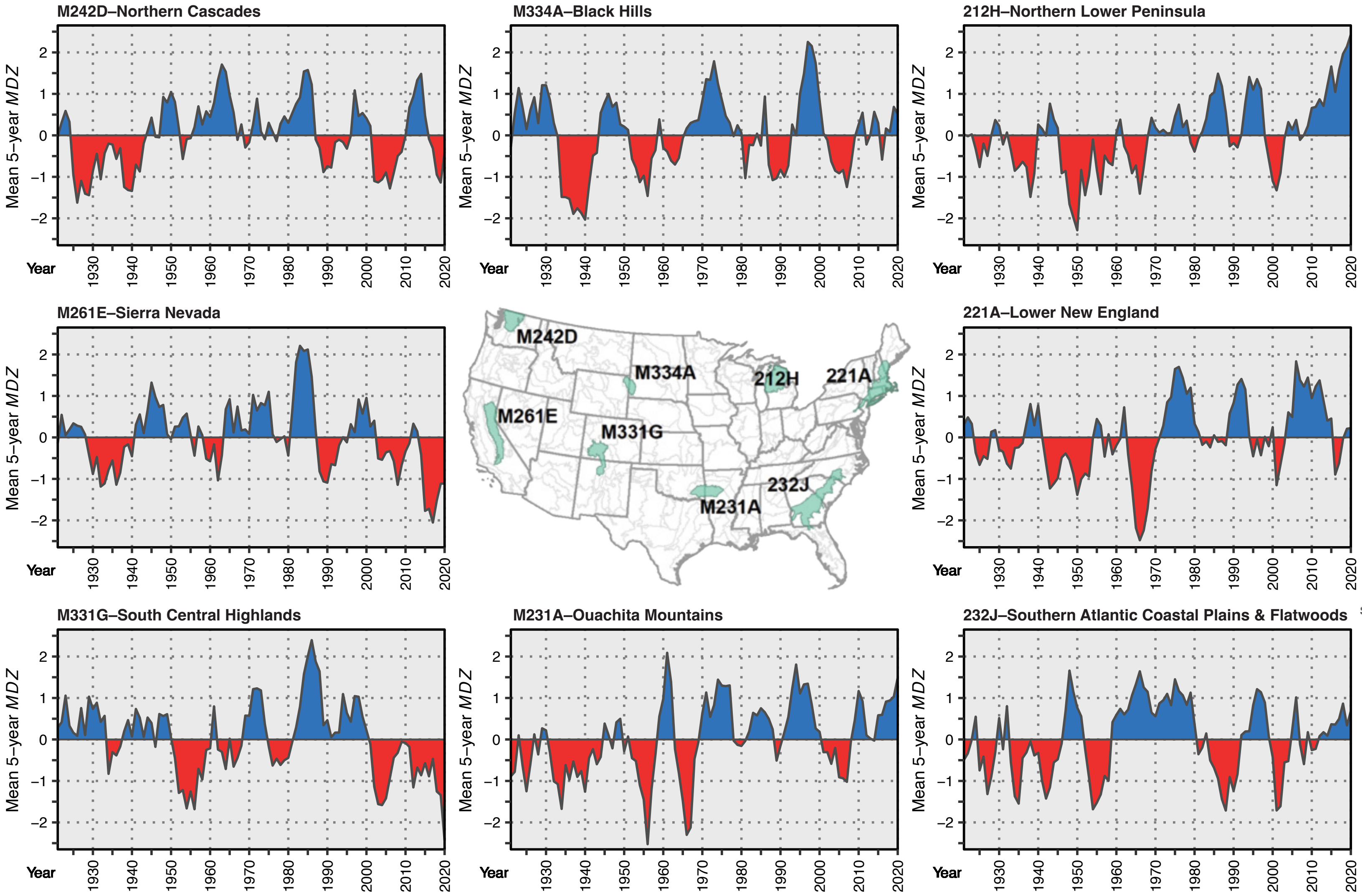

Figure 4.6—Long-term (1921–2020) trajectories in mean 5-year moisture difference z-score, or MDZ, *for eight ecoregion sections (Cleland and others 2007) in the conterminous United States. Periods of moisture deficit are shown in red and moisture surplus in blue. Sections are shown in green on the map for reference. (Data source: PRISM Climate Group, Oregon State University)*

Future Efforts

One-year, 3-year, and 5-year *MDZ* maps of the conterminous United States are a recurring component of national forest health reporting. For interpretive purposes, it is critical to understand their limitations. Most notably, the *MDZ* approach omits certain factors that influence a location's moisture supply at finer spatial and temporal scales, such as winter snowpack, surface runoff, or ground water storage. Furthermore, while the maps use a standardized index scale that can be used with time windows of any size, it is still important to choose a window size that is analytically appropriate. For example, an extreme drought that lasts for 5 years will have different forest health ramifications than an extreme drought that ends after only 1 year. While the 1-year, 3-year, and 5-year *MDZ* maps provide a reasonably complete short-term picture, a region's longer term moisture trajectory may also be meaningful with respect to forest health. For instance, in regions where droughts have been historically frequent, some tree species are more drought-adapted than others (McDowell and others 2008). At any rate, long periods of persistent moisture extremes could initiate changes in regional forest composition (McEwan and others 2011, Mueller and others 2005). Such changes are likely to affect responses to future drought or surplus conditions, fire regimes, and the status of ecosystem services such as nutrient cycling and wildlife habitat (W.R.L. Anderegg and others 2013, DeSantis and others 2011). In future reporting, we hope to provide forest managers and other decision makers with quantitative evidence about relationships between moisture extremes and significant forest health impacts such as regional-scale tree mortality (e.g., Edgar and others 2019, Mitchell and others 2014). Deciphering such relationships can be difficult at broader spatial scales. Nonetheless, we also intend to investigate the capacity of moisture extremes to serve as inciting factors for other forest threats such as wildfire or pest outbreaks.

LITERATURE CITED

Abatzoglou, J.T.; Williams, A.P. 2016. Impact of anthropogenic climate change on wildfire across Western US forests. Proceedings of the National Academy of Sciences. 113(42): 11770–11775. https://doi.org/10.1073/pnas.1607171113.

Adams, H.D.; Guardiola-Claramonte, M.; Barron-Gafford, G.A. [and others]. 2009. Temperature sensitivity of drought-induced tree mortality portends increased regional die-off under global-change-type drought. Proceedings of the National Academy of Sciences. 106(17): 7063–7066. https://doi.org/10.1073/pnas.0901438106.

Akin, W.E. 1991. Global patterns: climate, vegetation, and soils. Norman, OK: University of Oklahoma Press. 370 p.

Allen, C.D.; Macalady, A.K.; Chenchouni, H. [and others]. 2010. A global overview of drought and heat-induced tree mortality reveals emerging climate change risks for forests. Forest Ecology and Management. 259(4): 660–684. https://doi.org/10.1016/j.foreco.2009.09.001.

Alley, W.M. 1984. The Palmer Drought Severity Index: limitations and assumptions. Journal of Climate & Applied Meteorology. 23(7): 1100–1109. https://doi.org/10.1175/1520-0450(1984)023<1100:TPDSIL>2.0.CO;2.

Amatya, D.M.; Skaggs, R.W.; Gregory, J.D. 1995. Comparison of methods for estimating REF-ET. Journal of Irrigation and Drainage Engineering. 121(6): 427–435. https://doi.org/10.1061/(ASCE)0733-9437(1995)121:6(427).

Anderegg, L.D.L.; Anderegg, W.R.L.; Berry, J.A. 2013. Not all droughts are created equal: translating meteorological drought into woody plant mortality. Tree Physiology. 33(7): 701–712. https://doi.org/10.1093/treephys/tpt044.

Anderegg, W.R.L.; Berry, J.A.; Field, C.B. 2012. Linking definitions, mechanisms, and modeling of drought-induced tree death. Trends in Plant Science. 17(12): 693–700. https://doi.org/10.1016/j.tplants.2012.09.006.

Anderegg, W.R.L.; Kane, J.M.; Anderegg, L.D.L. 2013. Consequences of widespread tree mortality triggered by drought and temperature stress. Nature Climate Change. 3(1): 30–36. https://doi.org/10.1038/nclimate1635.

Archaux, F.; Wolters, V. 2006. Impact of summer drought on forest biodiversity: what do we know? Annals of Forest Science. 63: 645–652. https://doi.org/10.1051/forest:2006041.

Bennett, A.C.; McDowell, N.G.; Allen, C.D.; Anderson-Teixeira, K.J. 2015. Larger trees suffer most during drought in forests worldwide. Nature Plants. 1(10): 15139. https://doi.org/10.1038/nplants.2015.139.

Berdanier, A.B.; Clark, J.S. 2016. Multiyear drought-induced morbidity preceding tree death in Southeastern U.S. forests. Ecological Applications. 26(1): 17–23. https://doi.org/10.1890/15-0274.

Bigler, C.; Bräker, O.U.; Bugmann, H. [and others]. 2006. Drought as an inciting mortality factor in Scots pine stands of the Valais, Switzerland. Ecosystems. 9(3): 330–343. https://doi.org/10.1007/s10021-005-0126-2.

Brodribb, T.J.; Powers, J.; Cochard, H.; Choat, B. 2020. Hanging by a thread? Forests and drought. Science. 368(6488): 261–266. https://doi.org/10.1126/science.aat7631.

Chiodi, A.M.; Larkin, N.S.; Varner, J.M. 2018. An analysis of Southeastern US prescribed burn weather windows: seasonal variability and El Niño associations. International Journal of Wildland Fire. 27(3): 176–189. https://doi.org/10.1071/WF17132.

Choat, B.; Brodribb, T.J.; Brodersen, C.R. [and others]. 2018. Triggers of tree mortality under drought. Nature. 558(7711): 531–539. https://doi.org/10.1038/s41586-018-0240-x.

Clark, J.S. 1989. Effects of long-term water balances on fire regime, north-western Minnesota. Journal of Ecology. 77: 989–1004. https://doi.org/10.2307/2260818.

Clark, J.S.; Iverson, L.; Woodall, C.W. [and others]. 2016. The impacts of increasing drought on forest dynamics, structure, and biodiversity in the United States. Global Change Biology. 22(7): 2329–2352. https://doi.org/10.1111/gcb.13160.

Cleland, D.T.; Freeouf, J.A.; Keys, J.E. [and others]. 2007. Ecological subregions: sections and subsections for the conterminous United States. Gen. Tech. Rep. WO-76D. Washington, DC: U.S. Department of Agriculture Forest Service. Map; Sloan, A.M., cartographer; presentation scale 1:3,500,000; colored. https://doi.org/10.2737/WO-GTR-76D.

Clinton, B.D.; Boring, L.R.; Swank, W.T. 1993. Canopy gap characteristics and drought influences in oak forests of the Coweeta Basin. Ecology. 74(5): 1551–1558. https://doi.org/10.2307/1940082.

Collins, B.M.; Omi, P.N.; Chapman, P.L. 2006. Regional relationships between climate and wildfire-burned area in the Interior West, USA. Canadian Journal of Forest Research. 36(3): 699–709. https://doi.org/10.1139/x05-264.

Daly, C.; Gibson, W.P.; Taylor, G.H. [and others]. 2002. A knowledge-based approach to the statistical mapping of climate. Climate Research. 22: 99–113. https://doi.org/10.3354/cr022099.

Dennison, P.E.; Brewer, S.C.; Arnold, J.D.; Moritz, M.A. 2014. Large wildfire trends in the Western United States, 1984–2011. Geophysical Research Letters. 41: 2928–2933. https://doi.org/10.1002/2014GL059576.

DeSantis, R.D.; Hallgren, S.W.; Stahle, D.W. 2011. Drought and fire suppression lead to rapid forest composition change in a forest-prairie ecotone. Forest Ecology and Management. 261(11): 1833–1840. https://doi.org/10.1016/j.foreco.2011.02.006.

Duever, M.J.; Meeder, J.F.; Meeder, L.C.; McCollum, J.M. 1994. The climate of south Florida and its role in shaping the Everglades ecosystem. In: Davis, S.M.; Ogden, J.C., eds. Everglades: the ecosystem and its restoration. Delray Beach, FL: St. Lucie Press: 225–248.

Edgar, C.B.; Westfall, J.A.; Klockow, P.A. [and others]. 2019. Interpreting effects of multiple, large-scale disturbances using national forest inventory data: a case study of standing dead trees in east Texas, USA. Forest Ecology and Management. 437: 27–40. https://doi.org/10.1016/j.foreco.2019.01.027.

Fettig, C.J.; Mortenson, L.A.; Bulaon, B.M.; Foulk, P.B. 2019. Tree mortality following drought in the central and southern Sierra Nevada, California, U.S. Forest Ecology and Management. 432: 164–178. https://doi.org/10.1016/j.foreco.2018.09.006.

Fyfe, J.C.; Derksen, C.; Mudryk, L. [and others]. 2017. Large near-term projected snowpack loss over the Western United States. Nature Communications. 8: 1–7. https://doi.org/10.1038/ncomms14996.

Goulden, M.L.; Bales, R.C. 2019. California forest die-off linked to multi-year deep soil drying in 2012–2015 drought. Nature Geoscience. 12(8): 632–637. https://doi.org/10.1038/s41561-019-0388-5.

Grundstein, A. 2009. Evaluation of climate change over the continental United States using a moisture index. Climatic Change. 93(1–2): 103–115. https://doi.org/10.1007/s10584-008-9480-3.

Guarín, A.; Taylor, A.H. 2005. Drought triggered tree mortality in mixed conifer forests in Yosemite National Park, California, USA. Forest Ecology and Management. 218: 229–244. https://doi.org/10.1016/j.foreco.2005.07.014.

Haavik, L.J.; Stahle, D.W.; Stephen, F.M. 2011. Temporal aspects of *Quercus rubra* decline and relationship to climate in the Ozark and Ouachita Mountains, Arkansas. Canadian Journal of Forest Research. 41(4): 773–781. https://doi.org/10.1139/x11-018.

Hanson, P.J.; Weltzin, J.F. 2000. Drought disturbance from climate change: response of United States forests. Science of the Total Environment. 262: 205–220. https://doi.org/10.1016/S0048-9697(00)00523-4.

Hubbart, J.A.; Guyette, R.; Muzika, R.-M. 2016. More than drought: precipitation variance, excessive wetness, pathogens and the future of the western edge of the Eastern Deciduous Forest. Science of the Total Environment. 566–567: 463–467. https://doi.org/10.1016/j.scitotenv.2016.05.108.

Jenkins, M.A.; Pallardy, S.G. 1995. The influence of drought on red oak group species growth and mortality in the Missouri Ozarks. Canadian Journal of Forest Research. 25(7): 1119–1127. https://doi.org/10.1139/x95-124.

Kannenberg, S.A.; Driscoll, A.W.; Malesky, D.; Anderegg, W.R.L. 2021. Rapid and surprising dieback of Utah juniper in the Southwestern USA due to acute drought stress. Forest Ecology and Management. 480: 118639. https://doi.org/10.1016/j.foreco.2020.118639.

Kareiva, P.M.; Kingsolver, J.G.; Huey, B.B., eds. 1993. Biotic interactions and global change. Sunderland, MA: Sinauer Associates, Inc. 559 p.

Keetch, J.J.; Byram, G.M. 1968. A drought index for forest fire control. Res. Pap. SE-38. Asheville, NC: U.S. Department of Agriculture Forest Service, Southeastern Forest Experiment Station. 35 p.

Koch, F.H.; Coulston, J.W. 2015. 1-year (2013), 3-year (2011–2013), and 5-year (2009–2013) drought maps for the conterminous United States. In: Potter, K.M.; Conkling, B.L., eds. Forest Health Monitoring: national status, trends, and analysis 2014. Gen. Tech. Rep. SRS-209. Asheville, NC: U.S. Department of Agriculture Forest Service, Southern Research Station: 57–71.

Koch, F.H.; Coulston, J.W. 2016. 1-year (2014), 3-year (2012–2014), and 5-year (2010–2014) maps of drought and moisture surplus for the conterminous United States. In: Potter, K.M.; Conkling, B.L., eds. Forest Health Monitoring: national status, trends, and analysis 2015. Gen. Tech. Rep. SRS-213. Asheville, NC: U.S. Department of Agriculture Forest Service, Southern Research Station: 61–78.

Koch, F.H.; Coulston, J.W. 2017. Moisture deficit and surplus in the conterminous United States for three time windows: 2015, 2013–2015, and 2011–2015. In: Potter, K.M.; Conkling, B.L., eds. Forest Health Monitoring: national status, trends, and analysis 2016. Gen. Tech. Rep. SRS-222. Asheville, NC: U.S. Department of Agriculture Forest Service, Southern Research Station: 63–80.

Koch, F.H.; Coulston, J.W. 2018. Moisture deficit and surplus in the conterminous United States for three time windows: 2016, 2014–2016, and 2012–2016. In: Potter, K.M.; Conkling, B.L., eds. Forest Health Monitoring: national status, trends, and analysis 2017. Gen. Tech. Rep. SRS-233. Asheville, NC: U.S. Department of Agriculture Forest Service, Southern Research Station: 65–84.

Koch, F.H.; Coulston, J.W. 2019. Drought and moisture surplus patterns in the conterminous United States: 2017, 2015–2017, and 2013–2017. In: Potter, K.M.; Conkling, B.L., eds. Forest Health Monitoring: national status, trends, and analysis 2018. Gen. Tech. Rep. SRS-239. Asheville, NC: U.S. Department of Agriculture Forest Service, Southern Research Station: 77–96.

Koch, F.H.; Coulston, J.W. 2020. Drought and moisture surplus patterns in the conterminous United States: 2018, 2016–2018, and 2014–2018. In: Potter, K.M.; Conkling, B.L., eds. Forest Health Monitoring: national status, trends, and analysis 2019. Gen. Tech. Rep. SRS-250. Asheville, NC: U.S. Department of Agriculture Forest Service, Southern Research Station: 83–102.

Koch, F.H.; Coulston, J.W. 2021. Spatial patterns of drought and moisture surplus in the conterminous United States: 2019, 2017–2019, and 2015–2019. In: Potter, K.M.; Conkling, B.L., eds. Forest Health Monitoring: national status, trends, and analysis 2020. Gen. Tech. Rep. SRS-261. Asheville, NC: U.S. Department of Agriculture Forest Service, Southern Research Station: 85–104.

Koch, F.H.; Smith, W.D.; Coulston, J.W. 2013a. Recent drought conditions in the conterminous United States. In: Potter, K.M.; Conkling, B.L., eds. Forest Health Monitoring: national status, trends, and analysis 2011. Gen. Tech. Rep. SRS-185. Asheville, NC: U.S. Department of Agriculture Forest Service, Southern Research Station: 41–58.

Koch, F.H.; Smith, W.D.; Coulston, J.W. 2013b. An improved method for standardized mapping of drought conditions. In: Potter, K.M.; Conkling, B.L., eds. Forest Health Monitoring: national status, trends, and analysis 2010. Gen. Tech. Rep. SRS-176. Asheville, NC: U.S. Department of Agriculture Forest Service, Southern Research Station: 67–83.

Koch, F.H.; Smith, W.D.; Coulston, J.W. 2014. Drought patterns in the conterminous United States and Hawaii. In: Potter, K.M.; Conkling, B.L., eds. Forest Health Monitoring: national status, trends, and analysis 2012. Gen. Tech. Rep. SRS-198. Asheville, NC: U.S. Department of Agriculture Forest Service, Southern Research Station: 49–72.

Koch, F.H.; Smith, W.D.; Coulston, J.W. 2015. Drought patterns in the conterminous United States, 2012. In: Potter, K.M.; Conkling, B.L., eds. Forest Health Monitoring: national status, trends, and analysis 2013. Gen. Tech. Rep. SRS-207. Asheville, NC: U.S. Department of Agriculture Forest Service, Southern Research Station: 55–69.

Kolb, T.E.; Fettig, C.J.; Ayres, M.P. [and others]. 2016. Observed and anticipated impacts of drought on forest insects and diseases in the United States. Forest Ecology and Management. 380: 321–334. https://doi.org/10.1016/j.foreco.2016.04.051.

Laurance, S.G.W.; Laurance, W.F.; Nascimento, H.E.M. [and others]. 2009. Long-term variation in Amazon forest dynamics. Journal of Vegetation Science. 20(2): 323–333. https://doi.org/10.1111/j.1654-1103.2009.01044.x.

Littell, J.S.; Peterson, D.L.; Riley, K.L. [and others]. 2016. A review of the relationships between drought and forest fire in the United States. Global Change Biology. 22(7): 2353–2369. https://doi.org/10.1111/gcb.13275.

Martínez-Vilalta, J.; Lloret, F.; Breshears, D.D. 2012. Drought-induced forest decline: causes, scope and implications. Biology Letters. 8(5): 689–691. https://doi.org/10.1098/rsbl.2011.1059.

Mattson, W.J.; Haack, R.A. 1987. The role of drought in outbreaks of plant-eating insects. BioScience. 37(2): 110–118. https://doi.org/10.2307/1310365.

McDowell, N.; Pockman, W.T.; Allen, C.D. [and others]. 2008. Mechanisms of plant survival and mortality during drought: why do some plants survive while others succumb to drought? New Phytologist. 178: 719–739. https://doi.org/10.1111/j.1469-8137.2008.02436.x.

McEwan, R.W.; Dyer, J.M.; Pederson, N. 2011. Multiple interacting ecosystem drivers: toward an encompassing hypothesis of oak forest dynamics across eastern North America. Ecography. 34: 244–256. https://doi.org/10.1111/j.1600-0587.2010.06390.x.

McKee, T.B.; Doesken, N.J.; Kliest, J. 1993. The relationship of drought frequency and duration to time scales. In: Eighth conference on applied climatology, Anaheim, CA. Boston, MA: American Meteorological Society: 179–184.

Millar, C.I.; Westfall, R.D.; Delany, D.L. 2007. Response of high-elevation limber pine (*Pinus flexilis*) to multiyear droughts and 20th-century warming, Sierra Nevada, California, USA. Canadian Journal of Forest Research. 37: 2508–2520. https://doi.org/10.1139/X07-097.

Mitchell, P.J.; O'Grady, A.P.; Hayes, K.R.; Pinkard, E.A. 2014. Exposure of trees to drought-induced die-off is defined by a common climatic threshold across different vegetation types. Ecology and Evolution. 4(7): 1088–1101. https://doi.org/10.1002/ece3.1008.

Monteith, J.L. 1965. Evaporation and environment. Symposia of the Society for Experimental Biology. 19: 205–234.

Mueller, R.C.; Scudder, C.M.; Porter, M.E. [and others]. 2005. Differential tree mortality in response to severe drought: evidence for long-term vegetation shifts. Journal of Ecology. 93: 1085–1093. https://doi.org/10.1111/j.1365-2745.2005.01042.x.

NOAA National Centers for Environmental Information. 2021a. National temperature and precipitation. https://www.ncdc.noaa.gov/temp-and-precip/us-maps/. [Date accessed: August 20, 2021].

NOAA National Centers for Environmental Information. 2021b. State of the climate: drought for annual 2020. https://www.ncdc.noaa.gov/sotc/drought/202013. [Date accessed: August 23, 2021].

Norman, S.P.; Koch, F.H.; Hargrove, W.W. 2016. Review of broad-scale drought monitoring of forests: toward an integrated data mining approach. Forest Ecology and Management. 380: 346–358. https://doi.org/10.1016/j.foreco.2016.06.027.

Palmer, W.C. 1965. Metereological drought. Res. Pap. No. 45. Washington, DC: U.S. Department of Commerce, Weather Bureau. 58 p.

Peltier, D.M.P.; Ogle, K. 2019. Legacies of more frequent drought in ponderosa pine across the Western United States. Global Change Biology. 25(11): 3803–3816. https://doi.org/10.1111/gcb.14720.

Peng, C.; Ma, Z.; Lei, X. [and others]. 2011. A drought-induced pervasive increase in tree mortality across Canada's boreal forests. Nature Climate Change. 1(9): 467–471. https://doi.org/10.1038/nclimate1293.

Peters, M.P.; Iverson, L.R.; Matthews, S.N. 2015. Long-term droughtiness and drought tolerance of Eastern US forests over five decades. Forest Ecology and Management. 345: 56–64. https://doi.org/10.1016/j.foreco.2015.02.022.

Potter, C.S.; Klooster, S.A. 1999. Dynamic global vegetation modelling for prediction of plant functional types and biogenic trace gas fluxes. Global Ecology and Biogeography. 8(6): 473–488. https://doi.org/10.1046/j.1365-2699.1999.00152.x.

PRISM Climate Group. 2021. 2.5-arcmin (4 km) gridded monthly climate data. https://prism.oregonstate.edu. [Date accessed: August 20, 2021].

Raffa, K.F.; Aukema, B.H.; Bentz, B.J. [and others]. 2008. Cross-scale drivers of natural disturbances prone to anthropogenic amplification: the dynamics of bark beetle eruptions. BioScience. 58(6): 501–517. https://doi.org/10.1641/B580607.

Rahmstorf, S.; Foster, G.; Cahill, N. 2017. Global temperature evolution: recent trends and some pitfalls. Environmental Research Letters. 12(5): 54001. https://doi.org/10.1088/1748-9326/aa6825.

Rozas, V.; García-González, I. 2012. Too wet for oaks? Inter-tree competition and recent persistent wetness predispose oaks to rainfall-induced dieback in Atlantic rainy forest. Global and Planetary Change. 94–95: 62–71. https://doi.org/10.1016/j.gloplacha.2012.07.004.

Rozas, V.; Sampedro, L. 2013. Soil chemical properties and dieback of *Quercus robur* in Atlantic wet forests after a weather extreme. Plant and Soil. 373(1–2): 673–685. https://doi.org/10.1007/s11104-013-1835-5.

Schoennagel, T.; Veblen, T.T.; Romme, W.H. 2004. The interaction of fire, fuels, and climate across Rocky Mountain forests. BioScience. 54(7): 661–676. https://doi.org/10.1641/0006-3568(2004)054[0661:TIOFFA]2.0.CO;2.

Seager, R.; Pederson, N.; Kushnir, Y. [and others]. 2012. The 1960s drought and the subsequent shift to a wetter climate in the Catskill Mountains region of the New York City watershed. Journal of Climate. 25(19): 6721–6742. https://doi.org/10.1175/JCLI-D-11-00518.1.

Sentelhas, P.C.; Gillespie, T.J.; Santos, E.A. 2010. Evaluation of FAO Penman-Monteith and alternative methods for estimating reference evapotranspiration with missing data in Southern Ontario, Canada. Agricultural Water Management. 97(5): 635–644. https://doi.org/10.1016/j.agwat.2009.12.001.

Slette, I.J.; Post, A.K.; Awad, M. [and others]. 2019. How ecologists define drought, and why we should do better. Global Change Biology. 25(10): 3193–3200. https://doi.org/10.1111/gcb.14747.

Slette, I.J.; Smith, M.D.; Knapp, A.K. [and others]. 2020. Standardized metrics are key for assessing drought severity. Global Change Biology. 26(2): e1–e3. https://doi.org/10.1111/gcb.14899.

Steinemann, A. 2003. Drought indicators and triggers: a stochastic approach to evaluation. Journal of the American Water Resources Association. 39(5): 1217–1233. https://doi.org/10.1111/j.1752-1688.2003.tb03704.x.

Stovall, A.E.L.L.; Shugart, H.; Yang, X. 2019. Tree height explains mortality risk during an intense drought. Nature Communications. 10(1): 4385. https://doi.org/10.1038/s41467-019-12380-6.

Svoboda, M.; LeComte, D.; Hayes, M. [and others]. 2002. The drought monitor. Bulletin of the American Meteorological Society. 83(8): 1181–1190. https://doi.org/10.1175/1520-0477-83.8.1181.

Swanston, C.; Brandt, L.A.; Janowiak, M.K. [and others]. 2018. Vulnerability of forests of the Midwest and Northeast United States to climate change. Climatic Change. 146(1): 103–116. https://doi.org/10.1007/s10584-017-2065-2.

Tei, S.; Sugimoto, A.; Yonenobu, H. [and others]. 2019. Effects of extreme drought and wet events for tree mortality: insights from tree-ring width and carbon isotope ratio in a Siberian larch forest. Ecohydrology. 12(8): e2143. https://doi.org/10.1002/eco.2143.

Thornthwaite, C.W. 1948. An approach towards a rational classification of climate. Geographical Review. 38(1): 55–94. https://doi.org/10.2307/210739.

Thornthwaite, C.W.; Mather, J.R. 1955. The water balance. Publications in Climatology. 8(1): 1–104.

Trouet, V.; Taylor, A.H.; Wahl, E.R. [and others]. 2010. Fire-climate interactions in the American West since 1400 CE. Geophysical Research Letters. 37(4): L04702. https://doi.org/10.1029/2009GL041695.

Vicente-Serrano, S.M.; Beguería, S.; López-Moreno, J.I. 2010. A multiscalar drought index sensitive to global warming: the Standardized Precipitation Evapotranspiration Index. Journal of Climate. 23(7): 1696–1718. https://doi.org/10.1175/2009JCLI2909.1.

Vose, R.S.; Applequist, S.; Squires, M. [and others]. 2014. Improved historical temperature and precipitation time series for U.S. climate divisions. Journal of Applied Meteorology and Climatology. 53(5): 1232–1251. https://doi.org/10.1175/jamc-d-13-0248.1.

Williams, A.P.; Allen, C.D.; Macalady, A.K. [and others]. 2013. Temperature as a potent driver of regional forest drought stress and tree mortality. Nature Climate Change. 3(3): 292–297. https://doi.org/10.1038/nclimate1693.

Williams, A.P.; Cook, E.R.; Smerdon, J.E. [and others]. 2020. Large contribution from anthropogenic warming to an emerging North American megadrought. Science. 368(6488): 314–318. https://doi.org/10.1126/science.aaz9600.

Willmott, C.J.; Feddema, J.J. 1992. A more rational climatic moisture index. Professional Geographer. 44(1): 84–88. https://doi.org/10.1111/j.0033-0124.1992.00084.x.

Xue, Z.; Ullrich, P. 2021. A retrospective and prospective examination of the 1960s U.S. Northeast drought. Earth's Future. 9(7): e2020EF001930. https://doi.org/10.1029/2020EF001930.

Zang, C.S.; Buras, A.; Esquivel-Muelbert, A. [and others]. 2020. Standardized drought indices in ecological research: why one size does not fit all. Global Change Biology. 26(2): 322–324. https://doi.org/10.1111/gcb.14809.

CHAPTER 5

Tree Mortality

MARK J. AMBROSE
RYAN HANAVAN
TOM SMITH

INTRODUCTION

Tree mortality is a natural process in all forest ecosystems. High rates of tree mortality can be an indicator of greater forest health problems. On a regional scale, high mortality levels may indicate widespread insect or disease impacts. High rates of tree mortality may also occur if a large proportion of the forest in a particular region is made up of older, senescent stands. The approach presented here seeks to detect mortality patterns that might reflect changes to ecosystem processes at large (e.g., regional) scales. In many cases, the proximate cause of mortality may be discernable. Understanding proximate causes of mortality may provide insight into whether the mortality level is within the range of natural variation or reflects more fundamental changes to ecological processes.

DATA

Forest Inventory and Analysis (FIA) phase 2 (P2) data were the basis of the mortality analysis. The FIA P2 data are collected across forested land throughout the United States, with approximately one plot per 6,000 acres of forest, using a rotating panel sample design (Bechtold and Patterson 2005). Field plots are divided into spatially balanced panels, with one panel being measured each year. A single cycle of measurements consists of measuring all panels. This "annualized" method of inventory was adopted, State by State, beginning in 1999. The cycle length (i.e., number of years required to measure all plot panels) ranges from 5 to 10 years, with Western States measured on a 10-year cycle and Eastern States measured on a 5-year or 7-year cycle.

An analysis of mortality rates requires data collected at a minimum of two points in time. Therefore, mortality analysis was possible for areas where data from repeated plot measurements using consistent sampling protocols were available (i.e., where one cycle of measurements had been completed and at least one panel of the next cycle had been measured, and where there had been no changes to the protocols affecting measurements of trees or saplings).

In the West, plots are remeasured on a 10-year cycle. Thus, estimates of growth and mortality from several Western States are based on less than a complete cycle of remeasurement. Working from an incomplete cycle of remeasurement, the effective sampling intensity for growth and mortality estimates is lower than FIA's standard of one plot per 6,000 acres (table 5.1). Therefore, the sampling error percentage on growth and mortality estimates tends to be larger in States with the lowest effective sampling intensities. Results are not presented for ecoregions where fewer than 25 plots had been remeasured.

Due to the COVID-19 pandemic, FIA data collection slowed during 2020. As a result, no new data were available from many Eastern States (i.e., the available datasets are the same as those used for the 2020 FHM report). Therefore, for this report, we focus our analysis on Western and some South-central States. Figure 5.1 shows the States included in the analysis as well as the forested area in those States.

How to cite this chapter:

Ambrose, Mark J.; Hanavan, Ryan; Smith, Tom. 2022. Tree mortality. In: Potter, Kevin M.; Conkling, Barbara L., eds. Forest Health Monitoring: national status, trends, and analysis 2021. Gen. Tech. Rep. SRS-266. Asheville, NC: U.S. Department of Agriculture Forest Service, Southern Research Station: 101–115. https://doi.org/10.2737/SRS-GTR-266-Chap5.

Table 5.1—States from which repeated Forest Inventory and Analysis (FIA) Phase 2 measurements were available, the time period spanned by the data, and the effective sample intensity (based on the proportion of plots that had been remeasured) in the available datasets

State	Time period	Effective sample intensity
Arizona	2001–2019	one plot: 6,667 acres
California	2001–2019	one plot: 6,667 acres
Colorado	2002–2019	one plot: 7,500 acres
Idaho	2004–2019	one plot: 10,000 acres
Kansas	2009–2019	one plot: 6,000 acres
Louisiana	2004–2018	one plot: 6,000 acres
Montana	2003–2019	one plot: 8,571 acres
Nevada	2004–2019	one plot: 10,000 acres
New Mexico	2005–2019	one plot: 12,000 acres
Oklahoma[a]	2010–2020	one plot: 6,000 acres
Oregon	2001–2019	one plot: 6,000 acres
Texas	2004–2020	one plot: 6,000 acres (eastern Texas)[b] one plot: 15,000 acres (western Texas)
Utah	2000–2019	one plot: 6,000 acres
Washington	2002–2019	one plot: 7,500 acres
Wyoming[c]	2000–2019	one plot: 6,667 acres

[a] Mortality data are only available for eastern Oklahoma. Eastern Oklahoma includes those counties in FIA Survey Units 1 and 2 (see Appendix B in Burrill and others 2018).

[b] Eastern Texas consists of those counties in FIA Survey Units 1 and 2 (see Appendix B in Burrill and others 2018).

[c] Mortality estimates for Wyoming are based on a comparison of annualized inventory data with data from the final periodic inventory.

METHODS

Forest Inventory and Analysis calculates the growth, mortality, and removal volume on each plot over the interval between repeated measurements. These values are stored in the FIA Database (version 8.0) (Burrill and others 2018). EVALIDator (version 1.8.0.01), an online tool for querying the FIA Database and generating area-based reports on forest characteristics (USDA Forest Service FIA program 2021), was used to obtain mortality rates over the most recent measurement cycle for each ecoregion section (Cleland and others 2007, McNab and others 2007). For most States, the most recent cycle of available data ran through 2018[1] (e.g., data collected from 2012 through 2018).

To compare mortality across forest types and climate zones, mortality as a percentage of live growing stock was calculated:

$$\text{Mortality percent} = m \,/\, v * 100$$

where

m = average annual mortality of sound bole volume of trees (at least 5 inches in diameter) on forest land (cubic feet per year)

v = sound bole volume of live trees (at least 5 inches in diameter) on forest land (cubic feet)

The temporal basis for all EVALIDator estimates is "Current."

To identify causal agents for the observed mortality, EVALIDator was also used to summarize mortality by the reported "cause of death" associated with the observed mortality. Causes of death are reported as general categories (e.g., insects, fire, weather). For each ecoregion section, EVALIDator also was used to generate a table of annual mortality volume by FIA species group (Burrill and others 2018) and cause of death. From these tables, it is possible to make reasonable assumptions about the particular insects or diseases that may be affecting particular regions. Care must be used in interpreting these causes because tree mortality may actually be caused by a combination of factors such as drought and insects. Further information about the causes of mortality is provided by the aerial survey of insects and disease (see ch. 2 in this report). It is difficult to directly match aerial survey data to mortality observed on FIA plots due to both the difference in timing when mortality is recorded and difficulty matching plot locations with aerial survey mortality polygons. However, aerial survey information has been incorporated into the discussion by referencing State Forest Health Highlights, which reflect in large part the results of aerial surveys.

In addition, mortality rates were derived for each forest type group (Burrill and others 2018, USDA Forest Service 2008) for each ecoregion section. At times, identifying the forest type experiencing high mortality can be more useful than identifying the species group, especially when the cause of death is abiotic.

---

[1] *Overall, the most recent data available for any State ranged from 2016 to 2019.*

RESULTS AND DISCUSSION

Figure 5.2 shows the ratio of annual mortality to standing live tree volume for the United States. Results are not presented for ecoregions that had fewer than 25 remeasured plots. The majority of ecoregions omitted from the analysis were mostly nonforest (see fig. 5.1) (mostly desert or grassland, heavily urbanized, or converted to agriculture). Table 5.2 summarizes the mortality results for those ecoregion sections having the highest mortality relative to live tree volume (>2 percent), showing the species groups that had the highest mortality as well as the major causes of mortality, if they could be identified.

In the South-central part of the country, ecoregion section 255C–Oak Woods and Prairies in Texas had the highest mortality relative to live volume. About 49 percent of the mortality occurred in the red and white oak species groups,[2] and another 15 percent occurred in the loblolly and shortleaf pine species group. The majority (67 percent) of mortality in this ecoregion section was identified as weather-related (table 5.2). Weather was responsible for 65 percent of oak mortality and 44 percent of pine mortality. Disease was the reported cause of another 21 percent of mortality (table 5.2). Disease was reported as responsible for 32 percent of oak mortality. Fire was responsible for 51 percent of loblolly and shortleaf pine mortality.

Similarly, in ecoregion 255A–Cross Timbers and Prairies in Kansas, Oklahoma, and northern Texas, most (43 percent) of the mortality occurred in oaks (red and white oak species groups). Thirty-two percent of overall mortality was due to diseases, 31 percent was due to adverse weather, and 13 percent was due to fire (table 5.2).[3]

A record-setting drought in 2011 affected Oklahoma and Texas (Oklahoma Forestry Services 2014, 2015, 2016). It was reported as weakening both pines and hardwoods in Texas, making them susceptible to a variety of pests and pathogens (McBride and Appel 2016; Smith 2013, 2014). Oak wilt has been a major problem in oak woodlands in central Texas (Smith 2014; Texas A & M Forest Service 2015, 2016, 2019) and probably contributed to the red and white oak mortality. Pine engraver beetle (*Ips* spp.) has been a problem in Texas' pine forests and may have contributed to mortality in the loblolly and shortleaf pine species group (Smith 2014; Texas A & M Forest Service 2015, 2016, 2017).

In ecoregion section 321B–Stockton Plateau in southwestern Texas, 74 percent of mortality was related to adverse weather and another 25 percent was due to fire (table 5.2). About 92 percent of mortality occurred in the western woodland softwoods species group (i.e., pinyon pines [*Pinus* spp.] and junipers [*Juniperus* spp.]). Presumably, the fire as well as the direct weather-induced

---

[2] *Overall mortality of the FIA select red oaks, select white oaks, other red oaks, and other white oaks species groups have been combined.*

[3] *Mortality data were not available from a large portion of ecoregion section 255A because much of the ecoregion is in western Oklahoma (as designated by FIA). Nevertheless, enough data were available from the portions of the ecoregion in Kansas, Texas, and eastern Oklahoma that we are able to report results for the ecoregion section.*

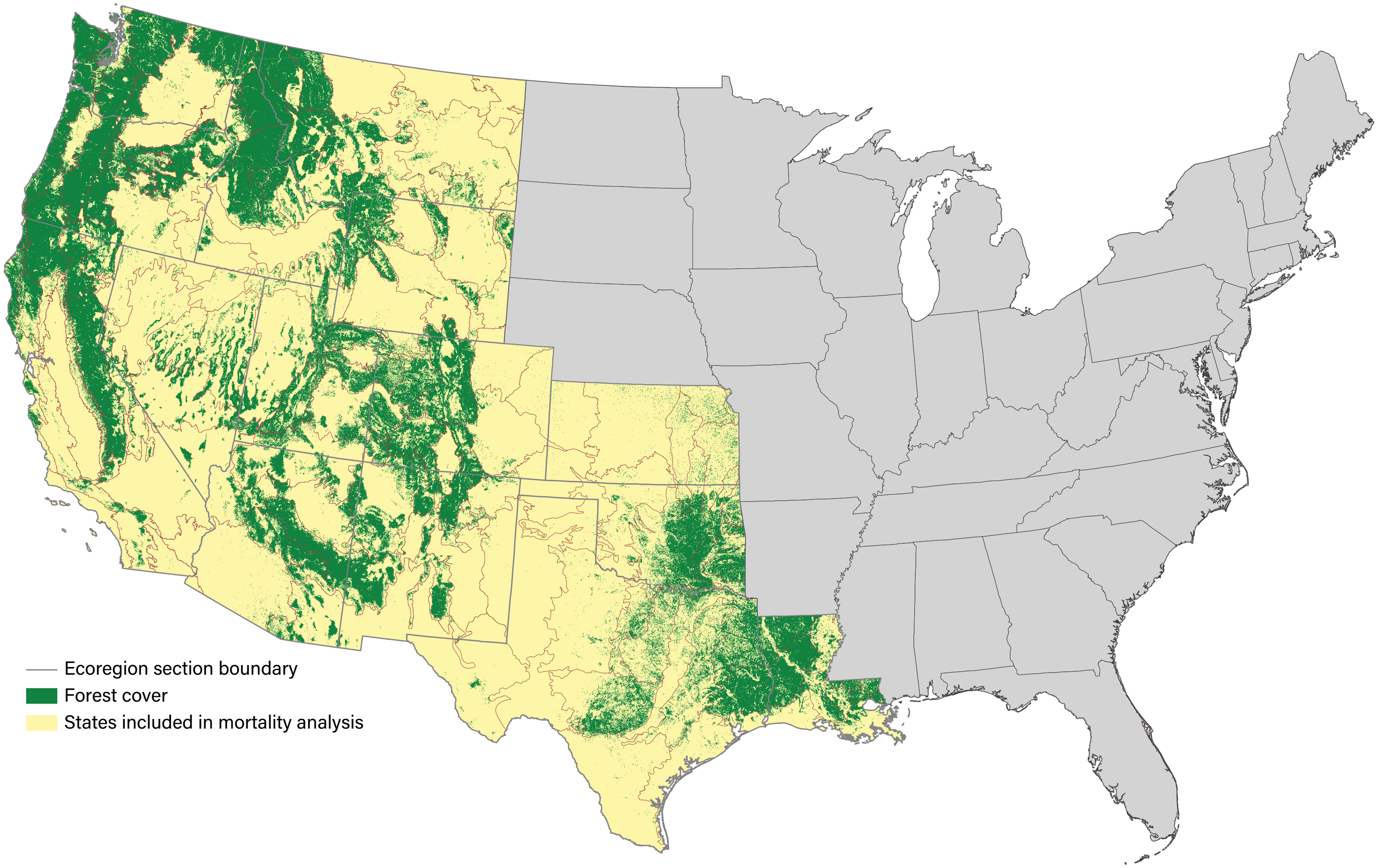

Figure 5.1—Forest cover in the States where mortality was analyzed by ecoregion section (Cleland and others 2007). Forest cover was derived from MODIS satellite imagery (U.S. Department of Agriculture Forest Service 2008).

Table 5.2—Ecoregion sections having the highest mortality relative to live tree volume, annual mortality rates, live volume, species groups having the highest mortality relative to growth, and associated causes of mortality

Ecoregion section	Average annual mortality	Live volume	Mortality relative to live volume	Species groups[a] having the highest mortality[b]	Major causes of mortality[c]
	cubic feet per year	*cubic feet*	*percent*		
341G–Northeastern Great Basin	6,684,440	100,898,913	6.62	True firs (57%)	Fire (55%), insects (30%)
M332F–Challis Volcanics	120,658,604	2,058,620,613	5.86	Douglas-fir (41%), lodgepole pine (26%)	Fire (49%), insects (40%)
M331J–Wind River Mountains	51,241,545	1,004,282,891	5.10	Lodgepole pine (50%), other western softwoods (26%)	Insects (69%), fire (18%)
M332D–Belt Mountains	198,200,487	4,864,386,519	4.07	Lodgepole pine (71%)	Insects (86%)
M331A–Yellowstone Highlands	321,755,288	8,122,990,167	3.96	Lodgepole pine (30%), Engelmann and other spruces (26%), other western softwoods (22%)	Insects (58%), fire (26%)
255C–Oak Woods and Prairies	128,117,245	3,344,147,442	3.83	Oaks[d] (49%), loblolly and shortleaf pine (15%)	Weather-related (67%), disease (21%)
M331I–Northern Parks and Ranges	467,198,325	12,353,152,165	3.78	Lodgepole pine (58%), Engelmann and other spruces (22%)	Insects (82%), disease (11%)
M331E–Uinta Mountains	104,048,591	2,802,315,890	3.71	Lodgepole pine (58%), Engelmann and other spruces (20%)	Insects (73%), disease (17%)
342A–Bighorn Basin	3,833,210	103,464,368	3.70	Lodgepole pine (66%)	Fire (67%), insects (17%), disease (15%)
M331G–South-Central Highlands	334,248,138	9,120,912,071	3.66	Engelmann and other spruces (65%)	Insects (69%), fire (13%), disease (10%)
M332B–Northern Rockies and Bitterroot Valley	202,003,412	5,865,620,498	3.44	Lodgepole pine (52%)	Insects (47%), fire (38%)
M262B–Southern California Mountain and Valley	29,449,257	916,788,218	3.21	Ponderosa and Jeffrey pine (26%), other western softwoods (18%), western woodland softwoods (13%)	Fire (65%), insects (12%), weather-related (11%)
M332A–Idaho Batholith	532,704,187	17,438,304,531	3.05	Lodgepole pine (32%), true firs (26%), Douglas-fir (23%)	Fire (54%), insects (26%), disease (12%)
M332E–Beaverhead Mountains	143,761,933	5,282,301,861	2.72	Lodgepole pine (55%), other western softwoods (18%)	Insects (79%), fire (13%)

(*Continued*)

Table 5.2 ***(Continued)*****—Ecoregion sections having the highest mortality relative to live tree volume, annual mortality rates, live volume, species groups having the highest mortality relative to growth, and associated causes of mortality**

Ecoregion section	Average annual mortality	Live volume	Mortality relative to live volume	Species groups[a] having the highest mortality[b]	Major causes of mortality[c]
	cubic feet per year	*cubic feet*	*percent*		
321B–Stockton Plateau	9,297,589	384,623,307	2.42	Western woodland softwoods (92%)	Weather-related (74%), fire (25%)
M333C–Northern Rockies	189,675,948	7,885,114,636	2.41	Engelmann and other spruces (24%), lodgepole pine (23%), true firs (23%)	Fire (51%), disease (25%), insects (16%)
342F–Central Basin and Hills	3,847,809	165,862,120	2.32	Lodgepole pine (22%), cottonwood and aspen (22%), ponderosa and Jeffrey pine (19%)	Insects (64%), disease (16%), vegetation[e] (11%)
321A–Basin and Range	23,829,502	1,041,097,106	2.29	Western woodland hardwoods (48%), western woodland softwoods (22%)	Fire (56%), disease (15%), insects (12%)
331K–North Central Highlands	20,305,814	907,138,797	2.24	Ponderosa and Jeffrey pine (57%), lodgepole pine (27%)	Fire (54%), insects (27%)
331G–Powder River Basin	16,659,252	767,361,244	2.17	Ponderosa and Jeffrey pine (93%)	Fire (87%)
255A–Cross Timbers and Prairie	16,127,155	748,440,827	2.15	Oaks[d] (43%), other eastern soft hardwoods (28%)	Disease (32%), weather-related (31%), fire (13%)

[a] For the species included in each species group, see Appendices E and F in Burrill and others 2018.

[b] The value in parentheses is the proportion of average annual mortality volume in the ecoregion section occurring in the species group.

[c] The value in parentheses is the proportion of average annual mortality volume in the ecoregion section attributed to the causal agent.

[d] Overall mortality of the FIA select red oaks, select white oaks, other red oaks, and other white oaks species groups have been combined.

[e] Mortality caused by suppression, competition, vines/kudzu (Burrill and others 2018).

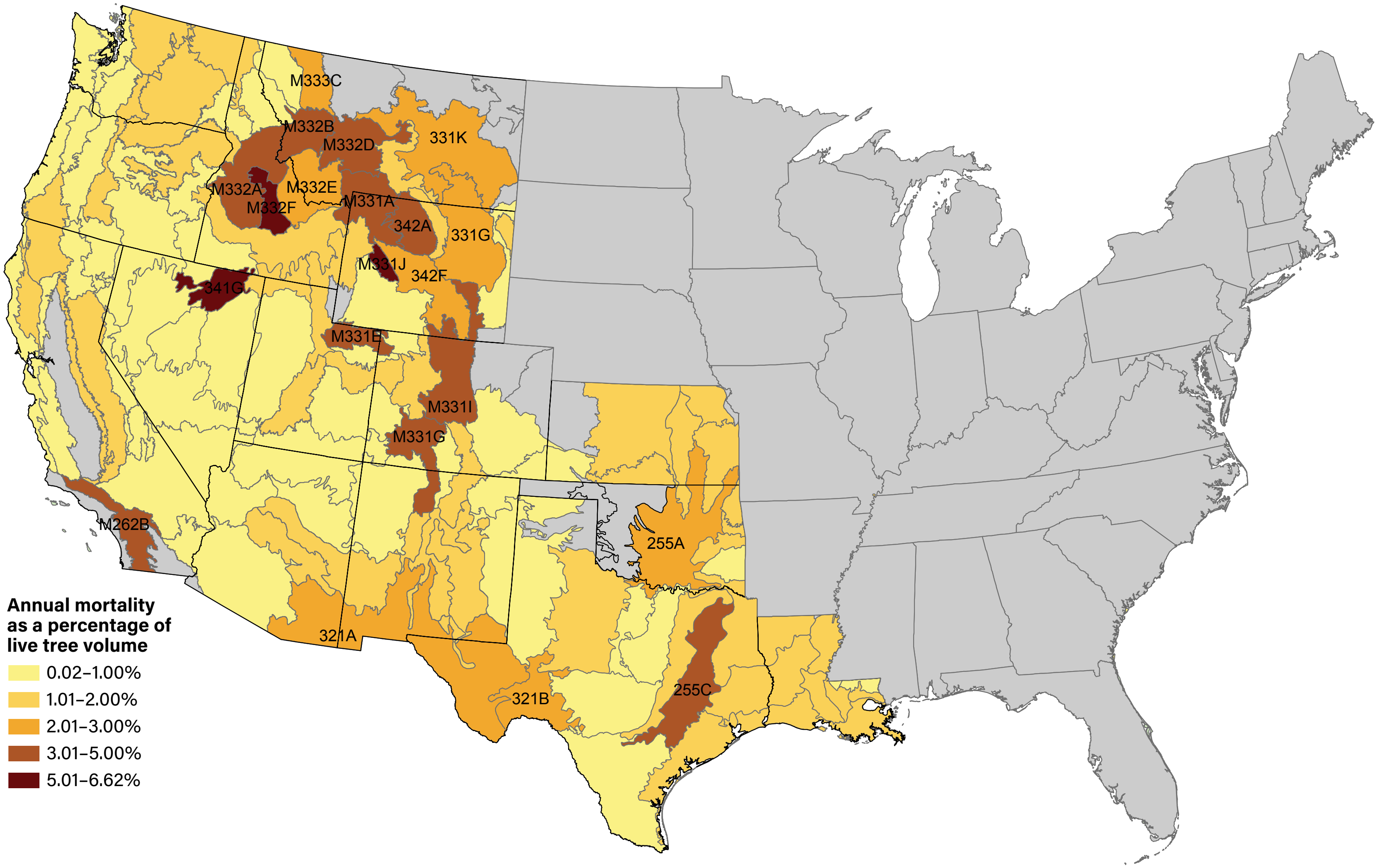

Figure 5.2—Annual tree mortality expressed as a percentage of live tree volume by ecoregion section (Cleland and others 2007). (Data source: U.S. Department of Agriculture Forest Service, Forest Inventory and Analysis program). Areas shown in gray are States not analyzed for this report and ecoregion sections with too few remeasured forested plots to include in the analysis.

mortality were related to the droughts that have affected much of Texas over the past decade.

As mentioned above, in most Western States, less than the full cycle of plots have been remeasured, reducing the precision of mortality estimates. Also, one must be aware that, because of the longer 10-year measurement cycle in the West, results shown represent mortality that may have occurred any time during the period spanned by the data (see table 5.1), which may have been as long as 20 years.

Of the ecoregions of the West Coast States, ecoregion section M262B–Southern California Mountain and Valley stands out, with an annual mortality rate of 3.21 percent. Fire was responsible for 65 percent of this mortality (table 5.2). About 57 percent of the mortality in this ecoregion section occurred in the Western Oak forest type group, and most of that mortality (79 percent) was due to fire. Fire was also responsible for most of the mortality (76 percent) in the Pinyon/juniper forest type group, where 7 percent of the ecoregion's mortality occurred. This ecoregion was severely impacted by the Thomas fire, which started in late 2017 and burned into 2018. At the time, it was the largest fire in the history of California (Chavez 2017), covering 281,893 acres (440 square miles). Other smaller fires have also affected the region.

While fire was the major cause of mortality within the region, ecoregion section M262B–Southern California Mountain and Valley was also impacted significantly by insects and diseases (12 percent of mortality) and adverse weather (11 percent of mortality). Insects were responsible for almost all the mortality in the Ponderosa Pine forest type group and about 43 percent of the mortality in the California Mixed Conifer forest type group; they were responsible for about 21 percent of the mortality in the ponderosa and Jeffrey pine species group and about 17 percent of the other western softwoods species group. Bark and engraver beetle outbreaks related to drought conditions and overstocked stands resulted in considerable conifer mortality in the past 20-year period. Seventeen percent of pine mortality was caused by insects. The ecoregion has also been a center of nonnative insect and insect/disease complex activities in California. The goldspotted oak borer (*Agrilus auroguttatus*) has killed various oak (*Quercus* spp.) species within the ecoregion, and the invasive shot hole borer complexes (two species of *Euwallacea* ambrosia beetles combined with their associated *Fusarium* species) have attacked and killed oaks and many other species of hardwoods. Although most activity was in urban forests and riparian zones, the invasive shot hole borer complexes have spread into woodlands and neighboring forested areas, leading to mortality.

In much of California, tree mortality has often been related to a combination of prolonged drought (2011–2015 statewide; 2011–2017 in parts of the State), bark beetles, and fire (California Forest Pest Council 2015, 2016, 2017). These factors have interacted, leading to high mortality, especially in southern California. Overstocked stands have contributed to the drought stress and susceptibility of forests to insects and wildfires (California Forest Pest Council 2015, 2016, 2017, 2018).

Turning to the Interior West, we see two clusters of ecoregion sections where mortality is high relative to standing live volume: a cluster of mountain ecoregions in western Montana, central Idaho, and northwestern Wyoming (M331A–Yellowstone Highlands, M331J–Wind River Mountains, M332A–Idaho Batholith, M332B–Northern Rockies and Bitterroot Valley, M332D–Belt Mountains, M332E–Beaverhead Mountains, and M332F–Challis Volcanics), together with the Northeastern Great Basin in northern Nevada (341G–Northeastern Great Basin), and a cluster including the Front Range of Colorado and southern Wyoming (M331I–Northern Parks and Ranges) and the South-Central Highlands of Colorado and northern New Mexico (M331G–South-Central Highlands) together with the Uinta Mountains of Utah (M331E–Uinta Mountains). In all of these regions, except M332E–Beaverhead Mountains, annual mortality exceeded 3 percent of live volume (table 5.2, fig. 5.2).

Spruce beetle (*Dendroctonus rufipennis*) epidemics have continued to expand over the last 20 years in the spruce (*Picea* spp.) forests of these ecoregions, particularly near areas of recent blowdown in Colorado, Idaho, Utah, New Mexico, and Wyoming. Spruce beetle-attacked trees tend to fade from green (healthy) to red (dying) more slowly than those attacked by other bark beetles, and damage estimates can be underestimated as a result. Chronic drought and repeated years of heavy western spruce budworm (*Choristoneura freemani*) defoliation have stressed Douglas-fir (*Pseudotsuga menziesii*) forests, making them more susceptible to bark beetle attacks. This has resulted in an increase in Douglas-fir beetle (*D. pseudotsugae*) in the Douglas-fir forests of these regions, which, in turn, is associated with the high Douglas-fir mortality observed in several of these ecoregions (table 5.2).

In Colorado and Wyoming, 58 percent of the mortality in ecoregion section M331I–Northern Parks and Ranges was in the lodgepole pine species group, and another 22 percent was in the Engelmann and other spruces species group; most (82 percent) of the mortality was attributed to insects. Western spruce budworm continued to cause significant defoliation in the Bighorn Mountains. Major outbreaks of mountain pine beetle (*D. ponderosae*) as well as spruce beetle (Colorado State Forest Service 2016, 2020; Wyoming State Forestry Division 2016, 2017, 2020; USDA Forest Service 2020) have occurred in the region over the last 20 years. These same pests have been affecting ecoregion section M331E–Uinta Mountains, (USDA Forest Service [N.d]; Utah Department of Natural Resources, Forestry, Fire, & State Lands 2016, 2019) where 58 percent of mortality was in the lodgepole pine species group and 20 percent was in the Engelmann and other spruces species group. Here, also, most (73 percent) of the mortality was caused by insects.

In ecoregion section M331G–South-Central Highlands, about 69 percent of mortality overall was caused by insects. In this ecoregion, about 65 percent of mortality was in the Engelmann and other spruces species group; 88 percent of spruce mortality was due to insects. In this area, spruce beetle has caused significant mortality (Colorado State Forest Service 2016, 2017; Formby 2020;

USDA Forest Service 2019, 2020; Zegler 2015, 2016; Zegler and Formby 2017). Also, severe drought is starting to cause visible discoloration in ponderosa pine (*Pinus ponderosa*) in this region with no visible signs of insects or diseases yet. Bark beetle-induced mortality, across most host species, is expected to increase in this ecoregion over the next few years (Formby 2020).

In most of the areas of high mortality in Montana, Idaho, and northwestern Wyoming (ecoregion sections M331A, M331J, M332A, M332B, M332D, M332E, and M332F) as well as the Northeastern Great Basin (341G) of Nevada, insects and fire were the most significant causes of mortality (table 5.2). This region includes areas suffering outbreaks of mountain pine beetle (Idaho Department of Lands 2010, 2019; Montana Department of Natural Resources and Conservation 2014, 2016) as well as major fires (Idaho Department of Lands 2014). However, several other insect and disease issues have been identified in this region and may have contributed to the mortality. In most of these ecoregion sections (M331A, M331J, M332A, M332B, M332D, M332E), lodgepole pine was the species group suffering the highest mortality, mostly from mountain pine beetle attacks. However, many other species groups, including Douglas-fir, true firs, and Engelmann and other spruces also suffered nontrivial mortality. Douglas-fir beetle is the primary causal agent impacting Douglas-fir in these regions while the nonnative balsam woolly adelgid (*Adelges piceae*) and fir engraver are impacting the true firs (Idaho Department of Lands 2017, 2018, 2019, 2020; Montana Department of Natural Resources and Conservation 2019, 2020). In contrast with the other ecoregions in this cluster, in ecoregion section M332F–Challis Volcanics in Idaho, most mortality occurred in the Douglas-fir species group (41 percent) rather than lodgepole pine (26 percent). However, the causes of mortality were the same—fire and insects, especially Douglas-fir beetle and mountain pine beetle.

The highest mortality in the Interior West occurred in occurred in ecoregion section 341G–Northeastern Great Basin in northern Nevada, where mortality was 6.62 percent of live volume. Here, fire was responsible for 55 percent of mortality while insects caused another 30 percent of mortality. Most (57 percent) of this mortality occurred in the true firs species group. In this ecoregion, forested area is very low (fig. 5.1); all of this is high-elevation forest (Bryce and others 2003). Only 31 forested plots were included in the analysis (only slightly above our cut-off of 25 plots). It is hard to interpret how important this high mortality rate is. While it affects a relatively small area of forest, that forest may be very important ecologically because of the rarity of forested ecosystems in this region.

Though it is difficult to point to particular, major fires associated with much of the observed mortality in the Interior West, the cumulative impact of fires in the region cannot be overstated. Over the past decade, the Interior West has experienced numerous extreme fire seasons with large, high-severity fires. The year 2017 stands out, with over 4.4 million acres burned in wildfires across the region (National Interagency Fire Center 2017). In 2018 and 2019, another 2.9

million and 1.1 million acres burned (National Interagency Fire Center 2018, 2019). Fires not only kill trees directly but also leave trees near the fire perimeter stressed and damaged, making them susceptible to bark beetle attacks. These beetle populations can then reach levels high enough that the outbreak spreads to undamaged stands.

SUMMARY

Throughout the portions of the United States analyzed for this report, drought and fire have been primary drivers of mortality. They have been directly responsible for mortality in many areas. They have also stressed forests, leaving them susceptible to the insect and disease outbreaks responsible for much of the observed mortality.

Based on current trends, we expect that fire and drought will continue to cause significant mortality throughout many of the areas analyzed. California and Colorado experienced their largest fires in history in 2020 when the August Complex in California burned 1,032,648 acres and the Cameron Peak Fire in Colorado burned 208,913 acres. Extended periods of drought are now causing significant mortality, apparently as a direct result of moisture stress, from Arizona up through Colorado, Nevada, and Utah.

The analyses presented in this chapter alone do not tell the complete story regarding tree mortality. Mortality that occurred in highly fragmented forest or treed areas adjacent to or circumscribed by human development may not have been detected because the FIA inventory does not cover most urban areas or other places not defined as forest by FIA.[4] Also, these analyses are unlikely to detect a pest or pathogen attacking a particular tree species in a mixed-species forest where other species are growing vigorously.

To gain a more complete understanding of mortality, one should consider the results of this analysis together with other indicators of forest health. Forest Inventory and Analysis tree damage data (Burrill and others 2018), as well as Evaluation Monitoring projects that focus on particular mortality-causing agents (ch. 7–13 in this report) can provide insight into smaller scale or species-specific mortality issues. Large-scale analyses of forest stressors, including insect and disease activity (ch. 2), fire (ch. 3), and drought (ch. 4) are also important for understanding mortality patterns.

---

[4] *For a detailed explanation of FIA's definition of forest, see Burrill and others 2018, section 2.4.*

LITERATURE CITED

Bechtold, W.A.; Patterson, P.L., eds. 2005. The enhanced Forest Inventory and Analysis program—national sampling design and estimation procedures. Gen. Tech. Rep. SRS-80. Asheville, NC: U.S. Department of Agriculture Forest Service, Southern Research Station. 85 p.

Bryce, S.A.; Woods, A.J.; Morefield, J.D. [and others]. 2003. Ecoregions of Nevada [color poster with map, descriptive text, summary tables, and photographs]. Reston, VA: U.S. Department of the Interior, U.S. Geological Survey. Map presentation scale 1:1,350,000. https://gaftp.epa.gov/EPADataCommons/ORD/Ecoregions/nv/nv_front.pdf. [Date accessed: October 1, 2021].

Burrill, E.A.; Wilson, A.M.; Turner, J.A. [and others]. 2018. The Forest Inventory and Analysis Database: database description and user guide for Phase 2 (version 8.0). Washington, DC: U.S. Department of Agriculture Forest Service. 946 p. http://fia.fs.fed.us/library/database-documentation/. [Date accessed: July 16, 2019].

California Forest Pest Council. 2015. 2015 California forest health highlights. 21 p. https://www.fs.fed.us/foresthealth/protecting-forest/forest-health-monitoring/monitoring-forest-highlights.shtml. [Date accessed: May 9, 2018].

California Forest Pest Council. 2016. 2016 California forest health highlights. 31 p. https://www.fs.fed.us/foresthealth/protecting-forest/forest-health-monitoring/monitoring-forest-highlights.shtml. [Date accessed: May 9, 2018].

California Forest Pest Council. 2017. 2017 California forest health highlights. 38 p. https://www.fs.usda.gov/Internet/FSE_DOCUMENTS/fseprd578578.pdf. [Date accessed: May 9, 2018].

California Forest Pest Council. 2018. 2018 California forest health highlights. 32 p. https://www.fs.usda.gov/Internet/FSE_DOCUMENTS/fseprd617798.pdf. [Date accessed: May 19, 2021].

Chavez, N. 2017. Thomas Fire is now the largest blaze in California history. https://www.cnn.com/2017/12/23/us/thomas-fire-california/index.html. [Date accessed: September 1, 2021].

Cleland, D.T.; Freeouf, J.A.; Keys, J.E. [and others]. 2007. Ecological subregions: sections and subsections for the conterminous United States. Gen. Tech. Rep. WO-76D. Washington, DC: U.S. Department of Agriculture Forest Service. Map; Sloan, A.M., cartographer; presentation scale 1:3,500,000; colored. https://doi.org/10.2737/WO-GTR-76D.

Colorado State Forest Service. 2016. 2015 report on the health of Colorado's forests: 15 years of change. Fort Collins, CO: Colorado State Forest Service. 32 p. https://csfs.colostate.edu/media/sites/22/2016/02/ForestHealthReport-2015.pdf. [Date accessed: July 30, 2019].

Colorado State Forest Service. 2017. 2016 report on the health of Colorado's forests: fire and water. Fort Collins, CO: Colorado State Forest Service. 36 p. https://csfs.colostate.edu/media/sites/22/2017/02/CSU_304464_ForestReport-2016-www.pdf. [Date accessed: July 30, 2019].

Colorado State Forest Service. 2020. 2020 report on the health of Colorado's forests: protecting our future after a historic wildfire year. Fort Collins, CO: Colorado State Forest Service. 36 p. https://csfs.colostate.edu/forest-management/forest-health-report/. [Date accessed: June 27, 2020].

Formby, J.P. 2020. New Mexico forest health conditions 2020. 20 p. http://www.emnrd.state.nm.us/SFD/FWHPlan/documents/2020NMForestHealthReport.FINAL.pdf. [Date accessed: June 30, 2020].

Idaho Department of Lands. 2010. 2010 forest health highlights. 5 p. https://www.fs.fed.us/foresthealth/docs/fhh/ID_FHH_2010.pdf. [Date accessed: May 26, 2020].

Idaho Department of Lands. 2014. 2014 forest health highlights. 7 p. https://www.fs.fed.us/foresthealth/docs/fhh/ID_FHH_2014.pdf. [Date accessed: May 26, 2020].

Idaho Department of Lands. 2017. 2017 forest health highlights. 9 p. https://www.fs.fed.us/foresthealth/docs/fhh/ID_FHH_2017.pdf. [Date accessed: May 29, 2020].

Idaho Department of Lands. 2018. 2018 forest health highlights. 9 p. https://www.idl.idaho.gov/wp-content/uploads/sites/2/2020/04/2018-Idaho-Forest-Health-Highlights.pdf. [Date accessed: May 29, 2020].

Idaho Department of Lands. 2019. 2019 forest health highlights. 9 p. https://www.idl.idaho.gov/wp-content/uploads/sites/116/2020/04/2019-Idaho-Forest-Health-Highlights.pdf. [Date accessed: May 29, 2020].

Idaho Department of Lands. 2020. 2020 forest health highlights. 9 p. https://www.idl.idaho.gov/wp-content/uploads/sites/116/2020/04/2019-Idaho-Forest-Health-Highlights.pdf. [Date accessed: June 24, 2020].

McBride, S.; Appel, D. 2016. Hypoxylon canker of oaks. College Station, TX: Texas A & M AgriLife Extension Service. 4 p. https://cdn-ext.agnet.tamu.edu/wp-content/uploads/2018/10/EPLP-030-hypoxylon-canker-of-oaks.pdf. [Date accessed: May 20, 2021].

McNab, W.H.; Cleland, D.T.; Freeouf, J.A. [and others], comps. 2007. Description of ecological subregions: sections of the conterminous United States. Gen. Tech. Report WO-76B. Washington, DC: U.S. Department of Agriculture Forest Service. 80 p. https://doi.org/10.2737/WO-GTR-76B.

Montana Department of Natural Resources and Conservation. 2014. Montana forest health highlights 2014. 4 p. https://www.fs.fed.us/foresthealth/docs/fhh/MT_FHH_2014.pdf. [Date accessed: May 28, 2021].

Montana Department of Natural Resources and Conservation. 2016. Montana forest health highlights 2016. 4 p. http://dnrc.mt.gov/divisions/forestry/docs/assistance/pests/conditions-highlights/fhh_2016.pdf. [Date accessed: May 28, 2021].

Montana Department of Natural Resources and Conservation. 2019. Montana forest health highlights 2019. 3 p. http://dnrc.mt.gov/divisions/forestry/docs/assistance/pests/conditions-highlights/fhh2019_compliant.pdf. [Date accessed: May 28, 2021].

Montana Department of Natural Resources and Conservation. 2020. Montana forest insect and disease conditions and program highlights 2020. 4 p. https://www.fs.fed.us/foresthealth/docs/fhh/MT_FHH_2020.pdf. [Date accessed: 5/28/2021].

National Interagency Fire Center. 2017. National report of wildland fires and acres burned by State (2017). https://www.predictiveservices.nifc.gov/intelligence/2017_statssumm/fires_acres17.pdf. [Date accessed: August 29, 2021].

National Interagency Fire Center. 2018. National report of wildland fires and acres burned by State (2018). https://www.predictiveservices.nifc.gov/intelligence/2018_statssumm/fires_acres18.pdf. [Date accessed: August 29, 2021].

National Interagency Fire Center. 2019. National report of wildland fires and acres burned by State (2019). https://www.predictiveservices.nifc.gov/intelligence/2019_statssumm/fires_acres19.pdf. [Date accessed: August 29, 2021].

Oklahoma Forestry Services. 2014. Oklahoma forest health highlights 2014. 5 p. https://www.fs.fed.us/foresthealth/protecting-forest/forest-health-monitoring/monitoring-forest-highlights.shtml. [Date accessed: April 2, 2018].

Oklahoma Forestry Services. 2015. Oklahoma forest health highlights 2015. 6 p. https://www.fs.fed.us/foresthealth/protecting-forest/forest-health-monitoring/monitoring-forest-highlights.shtml. [Date accessed: April 3, 2018].

Oklahoma Forestry Services. 2016. Oklahoma forest health highlights 2016. 6 p. https://www.fs.fed.us/foresthealth/protecting-forest/forest-health-monitoring/monitoring-forest-highlights.shtml. [Date accessed: April 2, 2018].

Smith, L.A. 2013. Forest health insects and diseases conditions Texas 2013. Longview, TX: Texas A & M Forest Service. 5 p. https://www.fs.fed.us/foresthealth/protecting-forest/forest-health-monitoring/monitoring-forest-highlights.shtml. [Date accessed: April 27, 2018].

Smith, L.A. 2014. Forest health highlights in Texas 2014. Longview, TX: Texas A & M Forest Service. 1 p. https://www.fs.fed.us/foresthealth/protecting-forest/forest-health-monitoring/monitoring-forest-highlights.shtml. [Date accessed: April 27, 2018].

Texas A & M Forest Service. 2015. Forest health highlights in Texas 2015. Longview, TX: Texas A & M Forest Service. 1 p. https://www.fs.fed.us/foresthealth/protecting-forest/forest-health-monitoring/monitoring-forest-highlights.shtml. [Date accessed: April 20, 2018].

Texas A & M Forest Service. 2016. Forest health highlights in Texas 2016. Longview, TX: Texas A & M Forest Service. 1 p. https://www.fs.fed.us/foresthealth/protecting-forest/forest-health-monitoring/monitoring-forest-highlights.shtml. [Date accessed: April 20, 2018].

Texas A & M Forest Service. 2017. Forest health highlights 2017. Longview, TX: Texas A & M Forest Service. 2 p. https://www.fs.fed.us/foresthealth/protecting-forest/forest-health-monitoring/monitoring-forest-highlights.shtml. [Date accessed: May 21, 2018].

Texas A & M Forest Service. 2019. Forest health highlights 2019. Longview, TX: Texas A & M Forest Service. 2 p. https://www.fhm.fs.fed.us/foresthealth/docs/fhh/TX_FHH_2019.pdf. [Date accessed: May 21, 2020].

U.S. Department of Agriculture (USDA) Forest Service. 2008. National forest type dataset. http://data.fs.usda.gov/geodata//rastergateway/forest_type/index.php. [Date accessed: September 13, 2016].

U.S. Department of Agriculture (USDA) Forest Service. 2019. Forest insect and disease conditions in the Southwestern Region, 2018. Forest Health PR-R3-16-18. 49 p. https://www.fs.usda.gov/Internet/FSE_DOCUMENTS/fseprd663788.pdf. [Date accessed: August 10, 2021].

U.S. Department of Agriculture (USDA) Forest Service. 2020. Forest insect and disease conditions in the Rocky Mountain Region, 2019. Forest Health R2-RO-20-01. 40 p. https://www.fs.usda.gov/Internet/FSE_DOCUMENTS/fseprd700752.pdf. [Date accessed: July 25, 2021].

U.S. Department of Agriculture (USDA) Forest Service, Forest Inventory and Analysis (FIA) program. 2021. Forest Inventory EVALIDator web-application version 1.8.0.01. St. Paul, MN: U.S. Department of Agriculture Forest Service, Northern Research Station. http://apps.fs.fed.us/Evalidator/evalidator.jsp. [Date accessed: May 20, 2021]

U.S. Department of Agriculture (USDA) Forest Service, Uinta-Wasatch-Cache National Forest. [N.d.]. Beetle activity on the Uinta-Wasatch-Cache National Forest. http://www.fs.usda.gov/detail/uwcnf/home/?cid=STELPRDB5145143. [Date accessed: July 25, 2017].

Utah Department of Natural Resources, Forestry, Fire, & State Lands. 2016. Utah forest health highlights 2016. 3 p. https://www.fs.fed.us/foresthealth/protecting-forest/forest-health-monitoring/monitoring-forest-highlights.shtml. [Date accessed: April 24, 2018].

Utah Department of Natural Resources, Forestry, Fire, & State Lands. 2019. Utah forest health highlights 2019. 3 p. https://ffsl.utah.gov/wp-content/uploads/StateHighlights2019-final.pdf. [Date accessed: June 20, 2020].

Wyoming State Forestry Division. 2016. 2016 Wyoming forest health highlights. 16 p. https://www.fs.fed.us/foresthealth/docs/fhh/WY_FHH_2016.pdf. [Date accessed: August 25, 2018].

Wyoming State Forestry Division. 2017. 2017 Wyoming forest health highlights. 17 p. https://www.fs.fed.us/foresthealth/docs/fhh/WY_FHH_2017.pdf. [Date accessed: August 25, 2018].

Wyoming State Forestry Division. 2020. 2020 Wyoming forest health highlights. 9 p. https://www.fs.fed.us/foresthealth/docs/fhh/WY_FHH_2020. [Date accessed: June 26, 2020].

Zegler, T. 2015. New Mexico forest health conditions, 2015. 17 p. http://www.emnrd.state.nm.us/SFD/FWHPlan/documents/2015_NMconditionsreport_low_shortIIpdf.pdf. [Date accessed: July 30, 2019].

Zegler, T. 2016. New Mexico forest health conditions, 2016. 18 p. http://www.emnrd.state.nm.us/SFD/FWHPlan/documents/2016_NMconditionsreport_short.pdf. [Date accessed: July 30, 2019].

Zegler, T.; Formby, J.P. 2017. New Mexico forest health conditions 2017. 35 p. http://www.emnrd.state.nm.us/SFD/FWHPlan/documents/NMForestHealthConditionsReportComplete.pdf. [Date accessed: July 30, 2019].

SECTION 2

Analyses of Long-Term Forest Health Trends and Presentations of New Techniques

CHAPTER 6

Precise Mapping of Disturbance Impacts to U.S. Forests Using High-Resolution Satellite Imagery

Steven P. Norman
William M. Christie

INTRODUCTION

Aerial mapping of forest disturbances has contributed to monitoring efforts in the United States since aircraft were first used to detect wildfire and insect mortality after World War I. In the century since, routine aircraft patrols with field examinations have successfully documented disturbances with increasing effectiveness. There remain conspicuous discrepancies among States, jurisdictions, and forest types, however, and this is further complicated by shifting mapping methods over time (e.g., Housman and others 2018).

Satellite-based remote sensing provides a complementary approach for aerial surveys as it brings efficient, cross-jurisdictional standardization to change detection. Systematic observations from satellite data taken over months to decades provide substance for programmatic forest monitoring, and this approach gives us a rigorous understanding of status and change over time using the satellite data archive.

Until recently, integration of satellite-based remote sensing with field and aircraft efforts was impeded by data processing constraints, given the large and unwieldy datasets involved. With the rise of cloud computing such as Google Earth Engine (hereafter referred to as EE), data access and image processing are no longer constraining (Gorelick and others 2017, Hanson and others 2013). Other game changers have been the opening of satellite data archives for free use (Wulder and others 2012) and the launch of new satellites with higher resolution than existed before. Imagery from the Sentinel-2 satellites in particular has nine times more spatial detail than Landsat and about 600 times more detail than Moderate Resolution Imaging Spectroradiometer (MODIS) imagery. Mapping forest change at this more precise resolution gives insights into the pattern and texture of disturbances that are helpful for accurate mapping and interpretation. Despite these technological advances, causal attribution can still be challenging, so field observations are needed to resolve insect defoliation or when multiple causes contribute to tree stress or mortality.

This chapter reports on the broad patterns of forest anomalies across the conterminous United States for 2020 as detected from remote sensing. A prior effort used the summer persistence of anomalies in 240-m MODIS imagery across this same extent (Norman and Christie 2020). Leveraging the computational power of EE, this current effort summarizes conditions over that same area using forested 10-m grid cells. As hexagons have been proposed as a standardized unit for forest reporting (Potter and others 2016), we demonstrate how these precise gridded observations can be filtered and summarized into coarser reporting units.

METHODS

Imagery from the European Space Community's Sentinel-2 satellites were accessed using EE to produce national maps of the Normalized Difference Vegetation Index (NDVI) for summer 2019 and 2020. Data were corrected for surface reflectance and filtered for clouds. The NDVI captures canopy vegetation vigor and has well-

How to cite this chapter:

Norman, Steven P.; Christie, William M. 2022. Precise mapping of disturbance impacts to U.S. forests using high-resolution satellite imagery. In: Potter, Kevin M.; Conkling, Barbara L., eds. Forest Health Monitoring: national status, trends, and analysis 2021. Gen. Tech. Rep. SRS-266. Asheville, NC: U.S. Department of Agriculture Forest Service, Southern Research Station: 119–133. https://doi.org/10.2737/SRS-GTR-266-Chap6.

understood limitations (Norman and Christie 2020). Compared to some other vegetation-sensitive indices, Sentinel-2's NDVI relies on the 10-m resolution red and infrared bands—a resolution which approximates the footprint of a single large canopy tree. We used a maximum NDVI value compositing technique to select the best imagery available for a designated period of time, and this minimized the influence of clouds and shadows that lower NDVI (Spruce and others 2011).

Growing season NDVI was defined as the maximum NDVI observed over a 2.5-month period for 2019 and 2020. For areas east of the 100th meridian, the compositing period was May 15 to July 31, which is generally the best season for detecting early spring defoliators and when summer NDVI reaches its phenological high in the East (Norman and others 2017). For the West, we used the highest NDVI between July 15 and September 30 to reduce the influence of variable spring timing and mountain snowpack. We acknowledge that local phenological factors and the timing of some disturbances before or after these dates could interfere with some mapping objectives, but for this national-scale effort, our primary objective is to have a transparent and standardized methodology.

We calculated 1-year absolute change in summer NDVI (dNDVI) by comparing the 2019 and 2020 maps. The 1-year baseline ensures that the detected changes are recent as it avoids persistent effects from prior years. A shortcoming of using the 1-year baseline is that in areas with sequential year disturbances such as year-on-year defoliation, the 2020 dNDVI may mischaracterize impacts when 2019 was also anomalous. A 1-year baseline provides the most clarity for industrially logged regions, as multiyear artifacts accumulate there and these obscure other disturbances (Norman and Christie 2020).

In EE, we distinguished likely forest from nonforest using the 2016 National Land Cover Database (NLCD) (https://www.mrlc.gov/). While the NLCD product is at 30-m resolution and its cover type designation is outdated where severe fire or logging activity occurred immediately prior to 2019, this was the best nationally consistent land cover source available.

For our national overview, we used EE to summarize forest-only changes below a threshold of -0.1 NDVI, and we summarized these in hexagons of 834 km^2. This nationwide NDVI departure threshold was chosen because declines that are less are more likely to have minor or ephemeral impacts to the canopy. Based on observations in the Eastern United States where thresholding is challenging due to the dominance of mixed deciduous cover, this threshold usually captures growing season canopy stress from moderate to severe fire and wind and insect defoliation, as well as tree mortality. This effort gave us approximately 9,810 hexagons for the conterminous United States with each having 8.34 million 10-m Sentinel-2 grid cells. We calculated the percentage of each hexagon with forest and the percentage of forest cells departed at or below the specified threshold. For our finer scale assessment, we relied on the same 10-m Sentinel-2 NDVI change product and the same

NLCD forest mask. This seamless approach allowed us to visualize regional and fine-resolution patterns of departures efficiently using the *HiForm.org* script in EE.

RESULTS AND DISCUSSION

At the national scale, broadly coherent patterns of growing season change generally conform to ecological or climatological regions. The central and southern Interior West exhibit more NDVI departure than the northern Interior West or Pacific Northwest coast (fig. 6.1). Across the East, the Southeast Piedmont and Coastal Plain show more NDVI departure than most of the Northeast, but there are pockets of stronger departure such as in northern Michigan, northeastern New England, and southern Pennsylvania. There is additional variability among hexagons within each broad region. Together, these multistate and hexagon-scale patterns suggest stress at the regional and landscape scale for 2020.

Even at this coarse hexagonal resolution, regional causes of disturbance can be inferred. In particular, the coherence of the Interior West's summer NDVI departure and that of much of New England is generally consistent with the U.S. Drought Monitor for late September 2020 (https://droughtmonitor.unl.edu/Maps/MapArchive.aspx). The areas of moderate departure across the Southeast's Coastal Plain and Piedmont region, Maine, and portions of the Pacific Northwest are consistent with where intensive forest harvesting occurs, which along with drought ranks as a leading cause of summer NDVI variability for the conterminous United States (Norman and Christie 2020, Norman and others 2016).

As the national hexagon map is assembled from 10-m source imagery, we see local patterns and textures of disturbances by zooming in. With this precision, we also gain further insights into the local causes of forest NDVI departure. Figure 6.2 includes the U.S. Department of Energy Savannah River Site, and it shows prominent patterns of linear streaks, rectangular blocks (in dark blue indicating recovery and red indicating extreme decline), and separate amorphous areas (in light yellow indicating low NDVI change). The streaks were caused by spring 2020 tornadoes, and the blocky areas of disturbance and recovery are from recent logging. The yellow areas likely represent areas of low-severity prescribed fire or thinning that had a minor effect on the overstory canopy. The extent, shape, edge attributes, and intensity or texture help us interpret these patterns, often with a high degree of certainty even when ancillary data such as storm tracks and treatment dates are not utilized. These ancillary datasets can serve a confirmational role, but the drop in NDVI can result from more than one cause, such as wildfire and beetles, beetles and logging, wind damage, and prescribed fire.

Situated in the northern Lower Peninsula of Michigan, figure 6.3 shows a large, amorphous area of moderately severe disturbance caused by *Lymantria dispar dispar* (formerly known as European gypsy moth) defoliation. This 2020 outbreak was documented by field observations, and this map is particularly adept at showing

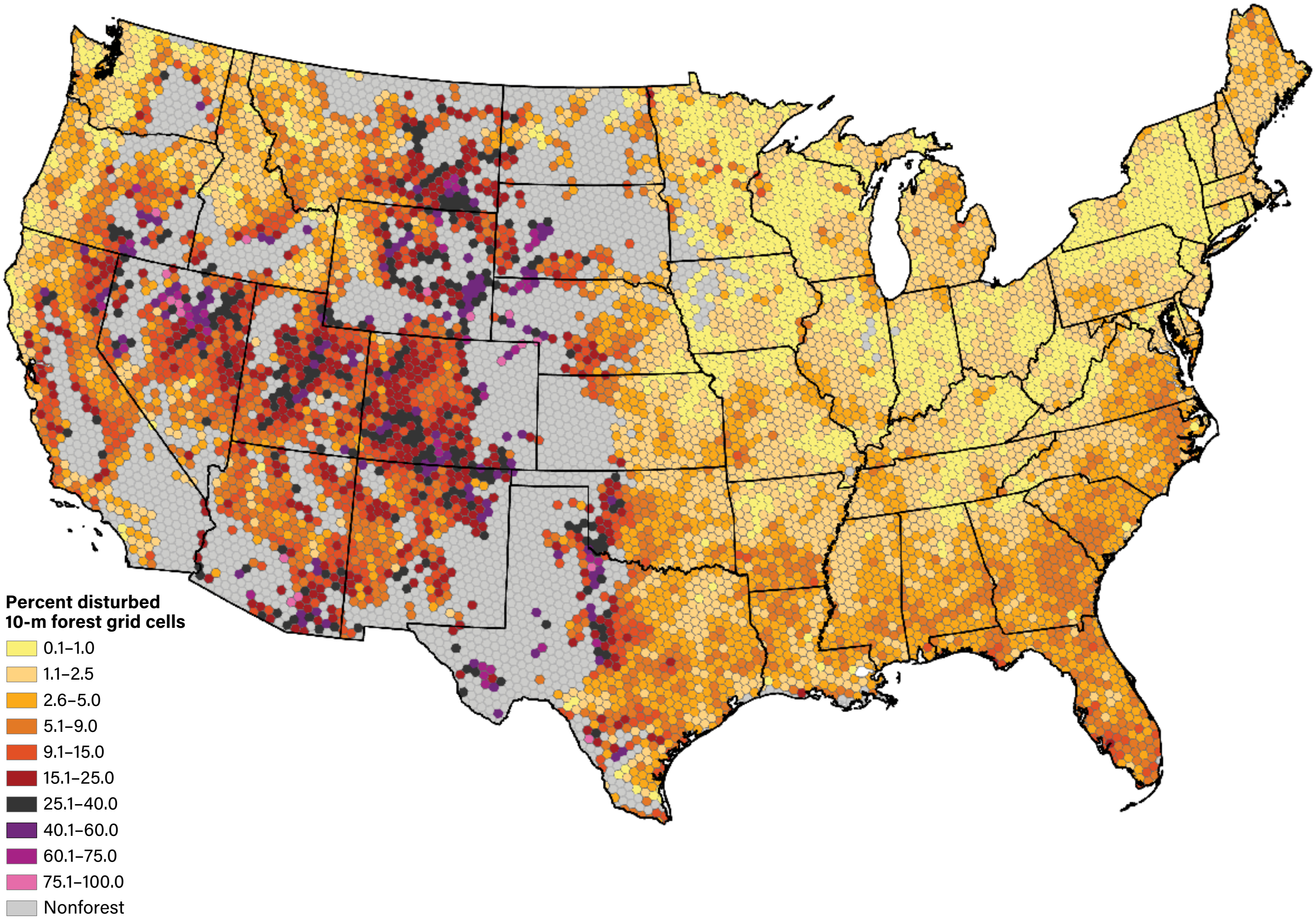

Figure 6.1—Percentage of 10-m forest grid cells within 834-km² hexagons that were disturbed below a threshold Normalized Difference Vegetation Index (NDVI) departure of -0.11 from the 2019 to the 2020 growing seasons for the conterminous United States. Grey hexagons have little to no forest cover.

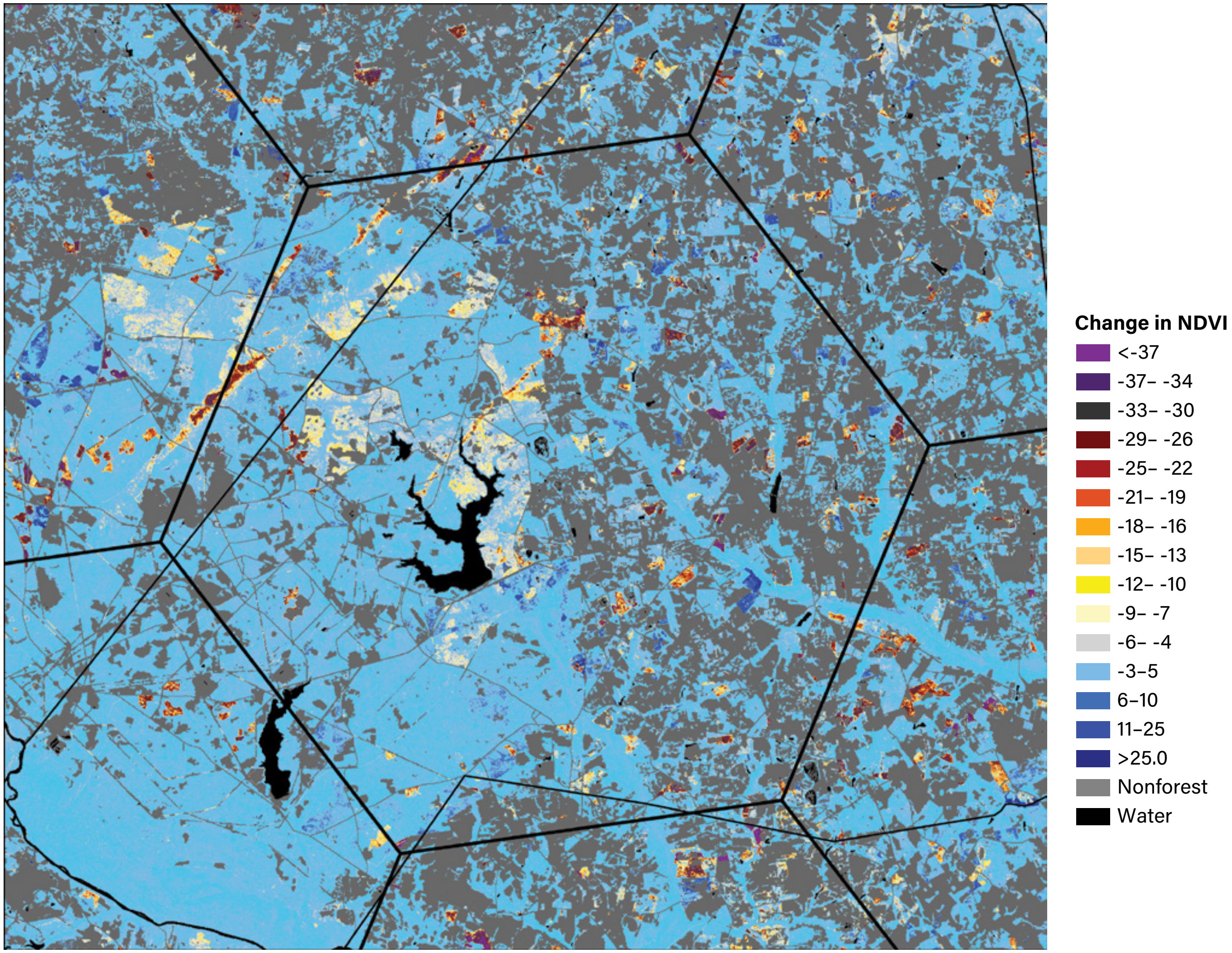

Figure 6.2—Forest disturbances near the U.S. Department of Energy Savannah River Site, SC. Areas in yellow to red show the severity of recent disturbances, while light blue shows forests with no change. Dark blue is recovery from earlier disturbances.

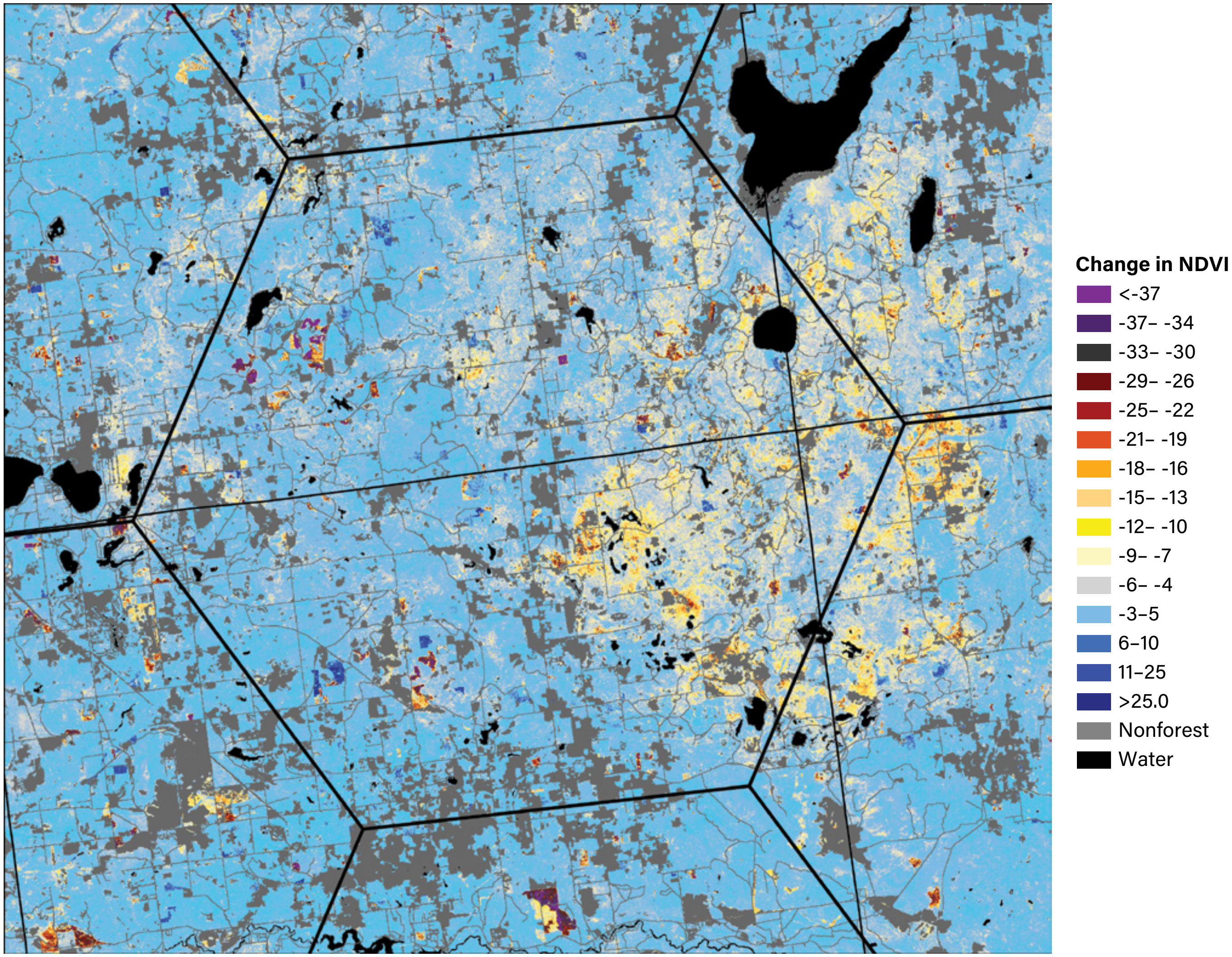

Figure 6.3—Change in Normalized Difference Vegetation Index (NDVI) in northeastern Michigan. Areas in yellow to red show the severity of recent disturbances, while light blue shows forests with no change. Dark blue is recovery from earlier disturbances.

subtle differences in defoliation intensity. As recurrent gypsy moth defoliations can occur over multiple years, impact assessment may need to be calculated using a baseline year that had no defoliation as part of a local exploration process. Such multiyear impacts are difficult to accurately map as is gradational intensity without the benefit of remote sensing.

Just east of Portland, OR, and south of the Columbia River Gorge, figure 6.4 shows relatively few acres of late summer NDVI decline, but these are readily mapped using 10-m NDVI change imagery. The area of the September 2017 Eagle Creek wildfire now in post-fire recovery is shown in dark blue at the top of the figure, while areas of local NDVI declines shown in yellow at the southern and eastern edge of that fire are likely from delayed mortality from insects. It is notable that there has been gradual migrating NDVI decline near these sites each year since the fire. Also note the extreme NDVI declines from logging near the western edge of the hexagon in purple that lie amid areas of NDVI recovery in dark blue. The co-occurrence of similarly shaped rectangular blocks of decline and recovery is indicative of industrial logging.

Figure 6.5 shows change in NDVI for a high elevation (8,000–12,000 feet) subalpine spruce-fir forest in the San Juan National Forest in Mineral County, CO. Both figure 6.1 and the status of the late summer 2020 U.S. Drought Monitor suggest that the primary cause of this broad NDVI departure is drought. This is particularly likely here because in 2020, most areas showing NDVI departure marginally fall under the definition of forest due to prior mortality. The June 2013 West Fork Complex burned the eastern portion of the hexagon in figure 6.5, and while this area has had limited mapped insect activity recently, significant mortality occurred during the last decade. Inspecting these areas more closely in EE using background imagery, nearly all the NDVI departures in yellow and the majority of the NDVI departures in red on figure 6.5 are those areas of prior mortality. As drought-sensitive grass is not the intended target for mapping, a more recent and higher resolution forest mask would isolate recent tree impacts from nonwoody drought responses here.

Tools for Disturbance Assessment

With technological advances improving the accessibility of satellite data, analytical needs shift toward disturbance assessment. That is, detections may or may not be real disturbances, and when they are, analysts need to know exactly what caused them. In practical terms, attribution comes down to likelihoods based on the weight of the evidence available.

In many cases, the most likely cause of a disturbance is suggested by available ancillary datasets. Thanks to numerous independent governmental efforts, we generally know where drought, major storms, large wildfires, and extensive insect defoliations are occurring before their precise impacts are mapped (Norman and Christie 2020). Assessment refines the disturbance footprint, maps severity, and tracks the disturbance's duration or recovery over time. Where disturbances appear unexpectedly, the

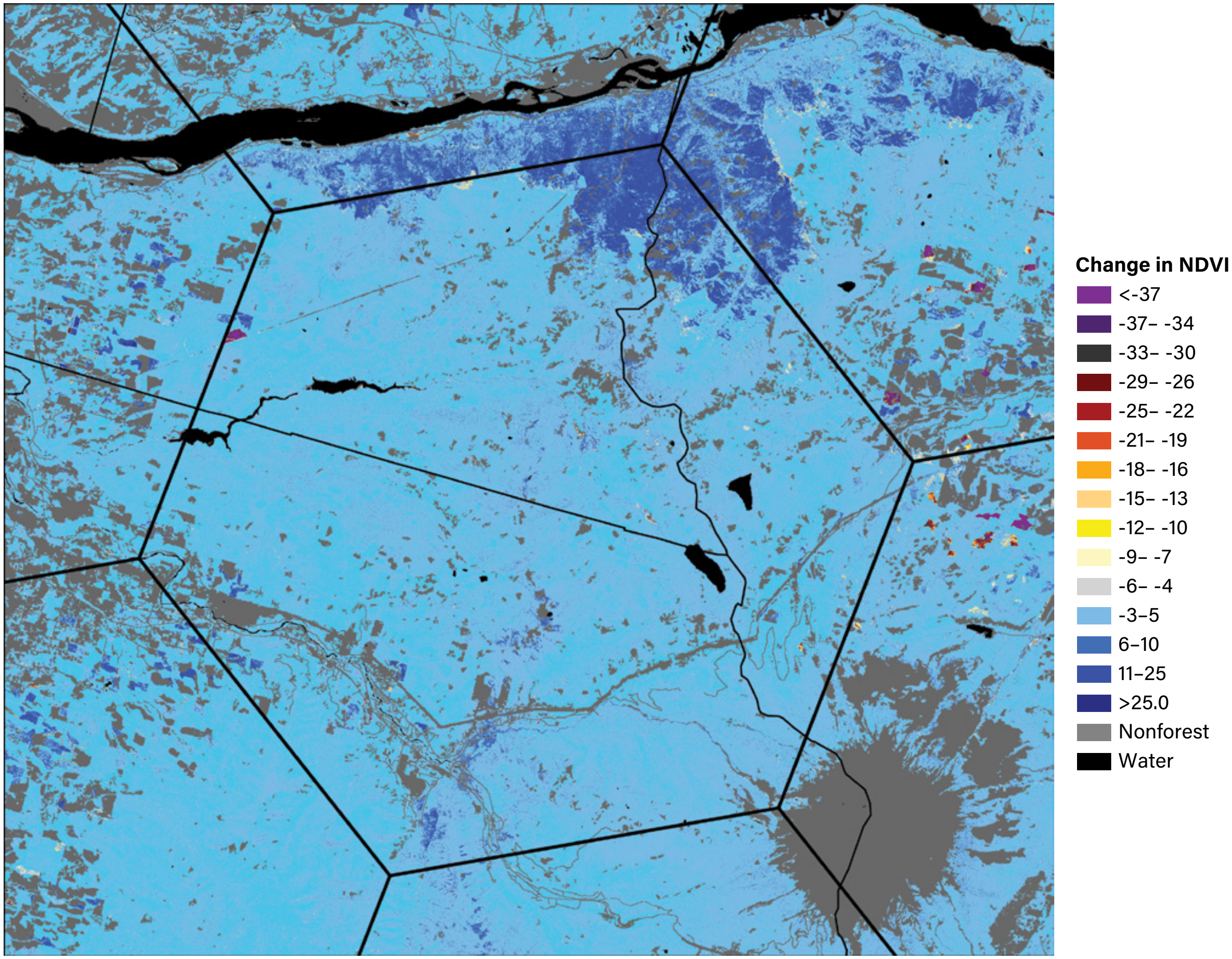

Figure 6.4—Change in Normalized Difference Vegetation Index (NDVI) east of Portland, OR. Mount Hood lies just outside this hexagon at lower right. Areas in yellow to red show the severity of recent disturbances, while light blue shows forests with no change. Dark blue is recovery from earlier disturbances.

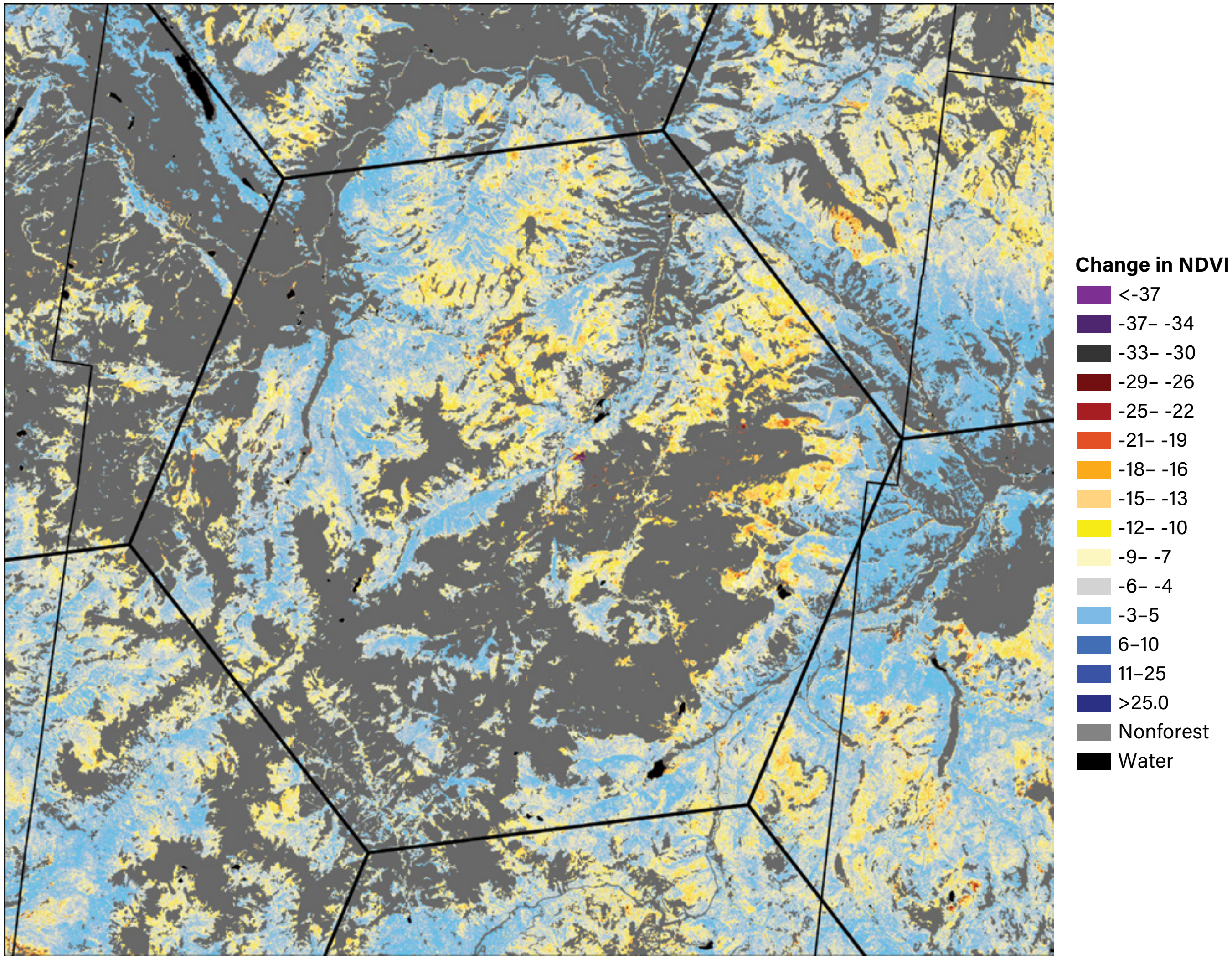

Figure 6.5—Change in Normalized Difference Vegetation Index (NDVI) for a high-elevation (8,000–12,000 feet) portion of the San Juan National Forest in Mineral County, CO. Areas in yellow to red show the severity of recent disturbances, while light blue shows forests with no change. Dark blue is recovery from earlier disturbances.

spatial and temporal attributes of the disturbance become critical for attributing cause.

The field of landscape ecology has devised numerous ways to characterize the spatial attributes of landscape features, and these are useful for characterizing the processes that give rise to them (Costanza and others 2019, Gustafson 1998). Critical attributes include extent, shape, edge, texture, and intensity. The precision of these measures is reduced by coarse-resolution imagery such as MODIS, particularly in heterogeneous forests with diverse cover or fragmented landscapes.

Fine-resolution imagery is more likely to reveal these disturbance attributes accurately, but texture, shape, edge, and intensity also reflect vegetation susceptibility. In mixed stands, disturbances that preferentially affect one species can create spotty or dispersed textures, while fragmented land use and a homogenous forest type can create aggregations. The underlying patterns of susceptibility from exposure or host vulnerability can result in shapes that would not otherwise occur, which means that pattern interpretation needs to reflect both this underlying condition and the diagnostic characteristics of a particular disturbance. Situational context is key.

The behavior of remotely sensed measures over time can also be useful for attributing cause. Algorithms such as LCMS (Landscape Change Monitoring System), LandTrendr (Landsat-based detection of Trends in Disturbance and Recovery), and VerDET (Vegetation Regeneration and Disturbance Estimates) evaluate multiyear responses using time series data, and these temporal patterns are often indicative of general classes of disturbances (Cohen and others 2018, Hughes and others 2017, Kennedy and others 2018, Schroeder and others 2017). For near-real-time evaluations, weekly streaming MODIS satellite data are particularly adept at documenting onset timing, progression, and duration in particular (Hargrove and others 2009). Recurrent observations within and across growing seasons at any grid resolution can help distinguish ephemeral defoliation from actual tree mortality (Norman and Christie 2020).

Indicators

Most indicators in common use by remote sensing analysts are informal, but a more standardized approach is critical for communication and machine learning approaches that could someday support attribution efforts. As shown below, four spatial indicators include extent, shape, edge character, and texture and intensity. Three temporal indicators are the seasonal onset date, the speed of development or weekly progression, and the duration of the impact. These indicators can differ among disturbances (as shown in tables 6.1 and 6.2):

1. **Extent** (local, landscape, regional)—Extensive disturbances often suggest a weather or phenological cause, although the manifestation of the anomaly is often confined to susceptible vegetation types. Extensive disturbances result from drought, hurricanes, spring freezes, and derechos, but delayed spring green-up, an early leaf senescence, and variation in snowpack can create similarly broad-scale anomalies at certain times of year.

Table 6.1—Common spatial indicators for assessing the causes of Normalized Difference Vegetation Index (NDVI) decline that link pattern with process

Cause	Extent	Shape	Edge	Texture and intensity
Drought	Broadly regional extending across multiple counties or States	Amorphous	Gradational, usually over tens to hundreds of kilometers	Depends on the sensitivity of vegetation types to drought stress
Tornadoes	Local to landscape depending on storm track	Strongly linear patch, in a consistent direction as storm tracks	Moderately sharp, with steep wind speed gradients over hundreds of meters	Generally highly intense along the midline with lateral reductions with reduced wind speed
Hurricanes	Multicounty or multistate, particularly from more intense storms	Broad impacts often with narrowing breadth inland as wind speeds fall	Generally decreasing inland; sharp-edged only with differences in cover type, such as at flood plains or harvest boundaries	Valleys show strong post-storm decline from flooding; damage intensity varies by hardwood/deciduous type
Freezes	Multicounty to regional consistent with extreme low temperatures	Broadly evident but locally constrained by elevation and topographic position	Gradational regionally but locally abrupt with cover, topography or the freeze line	Usually low intensity; textural impacts vary with cover type and terrain
Downbursts /hail	Local to landscape	Often oblong and directionally consistent with storm tracks	Gradational to fuzzy except where core impacts persist	Usually has an epicenter of concentrated impact surrounded by lower impact areas
Defoliating insects	Local to landscape	Amorphous	Gradational	Often with areas of concentrated high impact in areas of modest decline; rash-like
Bark beetles	Local to landscape	Gap to patch sized; clustered	Sharp or gradual	Can show a leading edge of progressive migrating decline or highly textured variation; sometimes rash-like
Diseases/ pathogens	Local	Spotty; constrained by affected host distribution	Sharp or gradational	Depends on the density of the affected host and size of the infestation
Prescribed fire	Local, confined to management units	Usually limited to a distinct management unit or confined by roads or streams	Usually gradational, often with minimal detectability; severe patches are often sharp-edged	Variable; usually of lower intensity with fewer discrete patches than area wildfires
Wildfire	Local to landscape	High-intensity patch shape often conforms to topography	Usually soft or gradational due to operational backfires or managed edges	Variable severity is common with high-intensity patches conforming to topography
Thinning	Local, confined to a management unit	Patchy	Gradual to sharp depending on the intensity	Strong fine-scale textural variation; sometimes rash-like
Logging	Local, confined to a management unit	Patchy	Very sharp where canopy patches are removed	Generally extreme with variation from exposed soil or persistent slash
Landslides	Highly localized	Patchy and linear, especially with downslope flow	Very sharp	Depends on size and severity; extreme where bare rock or soil
Flooding	Occurrence is generally confined to waterways or valley bottoms	Linear or branching along valley networks	Generally sharp, conforming with the topography	Microtopography affects depth and overstory canopy affects the apparent intensity

Table 6.2—Common temporal indicators for assessing the cause of Normalized Difference Vegetation Index (NDVI) decline that link pattern with process

Cause	Onset date	Development speed	Duration
Drought	Regionally specific; sometimes only evident during drought-sensitive seasons; affects snowpack and the timing of spring and fall phenology	Usually gradual; behavior is sensitive to phenology, particularly that of grass	Usually seasonal; duration is often consistent with meteorological drought, but mortality can create a multiyear legacy
Tornadoes	Spring or early summer when these storms occur	Rapid	Multiyear with mortality
Hurricanes	Late summer or fall when these storms occur	Rapid	Seasonal to multiyear
Frost	Mid- to late spring when this weather occurs; in spring, often manifest as a delayed or slowed spring; in fall manifest as early senescence	Rapid	Weeks; severe frost damage can extend through the entire growing season
Downbursts/hail	Anytime during the growing season; usually spring or summer	Rapid	When severe, effects can persist through the remaining growing season
Defoliating insects	Region and defoliator-dependent; early spring through mid-summer	Gradual, over a period of weeks	When severe, effects can persist through the remaining growing season
Bark beetles	Region- and insect-specific; mortality can be year-round in the Southeast	Rapid to gradual over a period of weeks	Multiyear with mortality
Diseases/pathogens	Recognition can depend on the host tree's seasonal leaf phenology	Often gradual; the outbreak can evolve over several growing seasons	Multiyear with mortality
Prescribed fire	During the region's prescribed fire season; winter prescribed fires may not emerge until spring	Rapid	Multiyear; often only visible soon after the event
Wildfire	Normally emerge during the region's wildfire season	Rapid	Multiyear with mortality
Thinning	Anytime	Rapid to gradual over a period of weeks to months	Multiyear with mortality
Logging	Anytime	Rapid to gradual over a period of weeks to months	Multiyear with mortality
Landslides	Anytime; usually triggered by a heavy rain event	Usually rapid unless actively expanding	Multiyear with mortality
Flooding	Anytime; usually triggered by a heavy rain event	Rapid	Weeks to months

2. **Shape** (amorphous, linear, blocky, conformal)—Shape is particularly useful for isolating intense weather events such as tornadoes and downbursts. At high resolution, shape often depends on the susceptibility of the available vegetation or land cover type as much as the physical attributes of the disturbance itself, and this is particularly complicated in mixed deciduous-evergreen forests.

3. **Edge** (sharp, gradual, conformal)—Natural disturbances such as wind, hail, and insect defoliations often have gradational edges because the stress grades naturally, but severe fire patches can be as abruptly edged as clearcut logging units. Fragmented landscapes often have conformal disturbance edges due to how different cover types respond.

4. **Texture and intensity** (uniform, patchy, rash-like)—These attributes reflect both the behavior of the disturbance and the vulnerability of the vegetation involved. In heterogenous mixed evergreen-deciduous forests, textural variation in intensity can reflect topography and host density. In homogenous forests, it can reveal unfolding disturbance processes, such as local epicenters of spreading beetle mortality.

5. **Onset date** (winter, spring, summer, fall)—Onset date provides important evidence when analysts know when different disturbances emerge locally. Many insect defoliators are diagnosed by when they erupt. Importantly, the canopy effects of some disturbances that occur during the fall, winter, or early spring may not be detected by remote sensing until leaves emerge, and this delay in manifestation can limit the usefulness of onset date.

6. **Speed of development** (rapid, gradual)—Most severe forest disturbances occur suddenly, but some evolve over the course of weeks, such as progressive pine beetle mortality or the gradual logging of a unit. After windstorms, the manifestation of a disturbance can be slow to show up even when the event is rapid, possibly because downed canopies take time to brown.

7. **Duration** (weeks, season, multiyear)—Disturbance duration is particularly useful in eastern hardwood forests for distinguishing among ephemeral defoliations or minor damage from hail, wind, or frost effects, and tree mortality. In some cases, severe canopy damage can occur that is only detectable for a few weeks due to compensatory growth, and this limitation may only be overcome through field examinations.

The grid resolution of remote sensing products can affect how clearly these first four indicators—extent, shape, edge, and texture and intensity—can be recognized. Meanwhile, the temporal frequency of imagery can affect how precisely we can resolve onset date, speed of development, and duration. As a result, daily coarse-resolution imagery such as 250-m MODIS may best document temporal behavior, while high-resolution imagery that is 10 m or less can most reliably show shape, edge, and textural variation. A precise understanding of spatial pattern is most important in areas with complex terrain, cover types, or mixed species as that helps isolate what caused NDVI departures.

High-resolution imagery can even be important for attributing cause to extensive disturbances such as drought, given the different sensitivities of cover types (Norman and others 2016).

CONCLUSIONS

Cloud-based remote sensing provides forest monitoring solutions for near-real-time tracking purposes and as part of a broader forest monitoring program. The flexibility of cloud-based analyses allows efficient use of high-resolution imagery, such as Sentinel-2, for national-scale summary efforts while retaining the fine spatial resolution needed to effectively attribute cause. At 10 m, small disturbances that involve just a few trees are often detectable. This use of fine-resolution imagery as the foundation for national assessments efficiently satisfies the local demand for precision and accuracy and the landscape, regional, and national need for context and generalization, all using a common indicator—change in growing season NDVI at 10 m.

The persistent challenge of remote sensing for landscape monitoring is causal assessment. That is, when the purpose of monitoring is to resolve impacts to a known disturbance, the cause is usually established from the start, but when the objective is to systematically track forests more broadly, attribution can be difficult. Our use of a single remote sensing measure reflects the need to capture vegetation dynamics broadly, and this includes disturbance recognition, attribution, quantification of impacts, and recovery.

The science of disturbance attribution can be advanced through use of a standard set of spatial and temporal indicators, such as those shown on tables 6.1 and 6.2. Yet without use of ancillary datasets and aerial or field confirmation, such indicators can only shift the likelihood of different causes, as their attributes overlap. For confirmation of the cause of an NDVI departure observed from remote sensing, storm, fire, and management activity datasets are useful. Field observations are sometimes also critical, such as with the need to resolve which defoliating insect is responsible when multiple species are possible. For precise characterization of disturbance impacts, aerial surveys and field observations are generally required. Local expertise is, therefore, a critical part of monitoring, and advances in remote sensing are best used in support of an integrated monitoring program.

ACKNOWLEDGMENTS

Jeff Bliss and Dave Michaelson of the University of North Carolina, Asheville's National Environmental Modeling and Analysis Center (NEMAC), and Ian Housman, contractor with the Forest Service, U.S. Department of Agriculture, provided Google Earth Engine programming support that was used in this effort. Two anonymous reviewers commented on an earlier draft of this chapter.

LITERATURE CITED

Cohen, W.B.; Yang, Z.; Healey, S.P. [and others]. 2018, A LandTrendr multispectral ensemble for forest disturbance detection. Remote Sensing of Environment. 205: 131–140. https://doi.org/10.1016/j.rse.2017.11.015.

Costanza, J.K.; Riitters, K.; Vogt, P.; Wickham, J. 2019. Describing and analyzing landscape patterns: where are we now, and where are we going? Landscape Ecology. 34: 2049–2055. https://doi.org/10.1007/s10980-019-00889-6.

Gorelick, N.; Hancher, M.; Dixon, M. [and others]. 2017. Google Earth Engine: planetary-scale geospatial analysis for everyone. Remote Sensing of Environment. 202: 18–27. https://doi.org/10.1016/j.rse.2017.06.031.

Gustafson, E.J. 1998. Quantifying landscape spatial pattern: what is the state of the art? Ecosystems. 1: 143–156. https://doi.org/10.1007/s100219900011.

Hansen, M.C.; Potapov, P.V.; Moore, R. [and others]. 2013. High-resolution global maps of 21st-century forest cover change. Science. 342: 850–853. https://doi.org/10.1126/science.1244693.

Hargrove, W.W.; Spruce, J.P.; Gasser, G.E.; Hoffman, F.M. 2009. Toward a national early warning system for forest disturbances using remotely sensed canopy phenology. Photogrammetric Engineering & Remote Sensing. 75: 1150–1156.

Housman, I.W.; Chastain, R.A.; Finco, M.V. 2018. An evaluation of forest health Insect and Disease Survey data and satellite-based remote sensing forest change detection methods: case studies in the United States. Remote Sensing. 10: 1184. https://doi.org/10.3390/rs10081184.

Hughes, M.; Kaylor, S.; Hayes, D. 2017. Patch-based forest change detection from Landsat time series. Forests. 8: 166. https://doi.org/10.3390/f8050166.

Kennedy, R.E.; Yang, Z.; Gorelick, N. [and others]. 2018. Implementation of the LandTrendr algorithm on Google Earth Engine. Remote Sensing. 10: 691. https://doi.org/10.3390/rs10050691.

Norman, S.P.; Christie, W.M. 2020. Satellite-based evidence of forest stress and decline across the conterminous United States for 2016, 2017, and 2018. In: Potter, K.M.; Conkling, B.L., eds. Forest Health Monitoring: national status, trends, and analysis 2019. Gen. Tech. Rep. SRS-250. Asheville, NC: U.S. Department of Agriculture Forest Service, Southern Research Station: 151–166.

Norman, S.P.; Koch, F.; Hargrove, W.W. 2016. Review of broad-scale drought monitoring of forests: toward an integrated data mining approach. Forest Ecology and Management. 380: 346–358. https://doi.org/10.1016/j.foreco.2016.06.027.

Norman, S.P.; Hargrove, W.W.; Christie, W.M. 2017. Spring and autumn phenological variability across environmental gradients of Great Smoky Mountains National Park. Remote Sensing. 9(5): 407. https://doi.org/10.3390/rs9050407.

Potter, K.M.; Koch, F.H.; Oswalt, C.M.; Iannone, B.V. 2016. Data, data everywhere: detecting spatial patterns in fine-scale ecological information collected across a continent. Landscape Ecology. 31: 67–84. https://doi.org/10.1007/s10980-015-0295-0.

Schroeder, T.A.; Schleeweis, K.G.; Moisen, G.G. [and others]. 2017. Testing a Landsat-based approach for mapping disturbance causality in U.S. forests. Remote Sensing of Environment. 195: 230–243. https://doi.org/10.1016/j.rse.2017.03.033.

Spruce, J.P.; Sader, S.; Ryan, R.E. [and others]. 2011. Assessment of MODIS NDVI time series data products for detecting forest defoliation by gypsy moth outbreaks. Remote Sensing of Environment. 1152: 427–437. https://doi.org/10.1016/j.rse.2010.09.013.

Wulder, M.A.; Masek, J.G.; Cohen, W.B. [and others]. 2012. Opening the archive: how free data has enabled the science and monitoring promise of Landsat. Remote Sensing of Environment. 122: 2–10. https://doi.org/10.1016/j.rse.2012.01.010.

SECTION 3

Evaluation Monitoring Project Summaries

Each year, the Forest Health Monitoring (FHM) program funds a variety of Evaluation Monitoring (EM) projects, which are projects to determine the extent, severity, and causes of undesirable changes in forest health identified through Detection Monitoring (see the FHM website: https://www.fs.fed.us/foresthealth/protecting-forest/forest-health-monitoring/index.shtml). In addition, EM projects can produce information about forest health improvements. The EM projects are submitted, reviewed, and selected through an established process. More detailed information about how EM projects are selected, the most recent call letter, and reporting responsibilities are listed on the Forest Health Protection Grants website (https://www.fs.fed.us/foresthealth/working-with-us/index.shtml).

Beginning in 2008, each FHM National Status, Trends, and Analysis report contains summaries of recently completed EM projects. Each summary provides an overview of the project and results, citations for products and other relevant information, and a contact for questions or further information. The summaries provide an introduction to the kinds of monitoring projects supported by FHM and include enough information for readers to pursue specific interests. Seven project summaries are included in this report.

CHAPTER 7

Monitoring Eastern White Pine Decline and Its Causes in New England and New York through Enhanced Survey Methods

Aaron Bergdahl
Isabel A. Munck
Rebecca Lilja
Jessica Cancelliere
Robert Cole
Josh Halman
Nicole Keleher
Kyle Lombard
Jen Weimer
Paul Ricard
John Stanovick

How to cite this chapter:

Bergdahl, Aaron; Munck, Isabel A.; Lilja, Rebecca; Cancelliere, Jessica; Cole, Robert; Halman, Josh; Keleher, Nicole; Lombard, Kyle; Weimer, Jen; Ricard, Paul; Stanovick, John. 2022. Monitoring eastern white pine decline and its causes in New England and New York through enhanced survey methods. In: Potter, Kevin M.; Conkling, Barbara L., eds. Forest Health Monitoring: national status, trends, and analysis 2021. Gen. Tech. Rep. SRS-266. Asheville, NC: U.S. Department of Agriculture Forest Service, Southern Research Station: 137–144. https://doi.org/10.2737/SRS-GTR-266-Chap7.

INTRODUCTION

Eastern white pine (EWP) is a major component of forest types in New England and New York where it is found on 4.1 million acres, supporting its ecological importance as key habitat for many organisms. Representing EWP's regional economic importance, the estimated stumpage value of the resource in the Northeast likely exceeds $4.3 billion (USDA Forest Service, FIA program 2021).[1] In the decade prior to 2018, regionally prevailing cool and moist weather patterns during key infection periods for needle diseases and other fungal pathogens of EWP have led to a noticeable regional increase in EWP decline.

The need for this project came from calls to address regional EWP health issues identified as prominent concerns in the Forest Health Highlights reports from Massachusetts, Maine, New Hampshire, New York, Rhode Island, and Vermont since 2009. It was suspected that many cases of EWP decline were tied to chronic stress from repeated defoliation by the white pine needle damage (WPND) complex. In 2016, the documented acreage of WPND was 24,000 acres in New Hampshire and 30,600 in Vermont. However, it is understood that these numbers only partially represented the impacted acreage due to limited aerial surveys that were not always conducted at a time of peak WPND symptoms and the difficulty of viewing symptomology from top-down vantage points. Of further concern was that existing regeneration is often severely affected by WPND in the understory environment. This was viewed as a threat to sustaining EWP, as most of the region's EWP resource is mature with very little acreage in the seedling/sapling stand size class (Ken Laustsen, personal communication[2]).

To address this, a collaborative effort involving personnel from Massachusetts, Maine, New Hampshire, New York, Rhode Island, and Vermont led to the creation of a white pine decline survey and identification of the resources needed to accomplish it. The effort was made possible by funding from the U.S. Department of Agriculture Forest Service, Forest Health Monitoring program. The resources to complete both in-field plot work and surveys were in place by 2018, and field work was completed in that year. The project had diagnostic support from the Forest Service State and Private Forestry field office in Durham, NH, Cornell University, University of Massachusetts Amherst, and University of Rhode Island. For further analysis, long-term climate data were used from regional weather stations.

The objectives of this project were to (1) identify EWP stands with high- and low-intensity

---

[1] *Estimate comes from sawlog and merchantable volume estimates using U.S. Department of Agriculture Forest Service, Forest Inventory and Analysis (FIA) data and reported stumpage values (Maine Forest Service 2021; Vermont Department of Forest, Parks, and Recreation 2019–2021; New Hampshire Department of Revenue Administration 2021; New York Department of Environmental Conservation 2021; University of Massachusetts Amherst 2021). The FIA estimate is 31 million mbf (thousand board feet) sawlog volume across the States in question. We used a weighted estimate of $127 per mbf across all seven States. At $3 per green ton and less, the remaining merchantable volume in the tree (considered pulp here) adds relatively little to the overall stumpage value.*

[2] *Personal communication. 2021. Ken Laustsen, Biometrician, Maine Forest Service (retired), 17 Perennial Way, Oakland, ME 04963-5240.*

white pine needle damage (WPND) using a variety of data sources, survey methods, and tools such as aerial survey, on-the-ground survey, and existing remote sensing products; (2) assess site factors associated with disease severity levels adversely affecting overall EWP forest health leading to increasing mortality; (3) determine the disease complexes, in addition to WPND, associated with general EWP decline and reduced regeneration; and (4) develop management practices to lessen future mortality.

METHODS

Sites were selected prior to plot work based on species composition of at least 50-percent EWP by basal area. States used various survey methods to identify suitable sites that were selected based on a known history of WPND (unhealthy), or rarely, perceived absence of disease (healthy). Selected stands needed to be large enough to accommodate at least three of the four total inventory plots (prism plots, ≥5 acres). Prism plots (20-factor) were established based on Forest Service Forest Inventory and Analysis (FIA) methods. Plot IDs were labelled, and each plot center was marked with a pin, where latitude/longitude, slope, and aspect were recorded. A monument tree was then selected and marked.

All measurable trees were tallied and the following measurements were taken for living EWP trees: diameter at breast height (d.b.h.); crown position (dominant, co-dominant, intermediate, suppressed, or dead); live crown ratio estimated as 10-percent intervals; crown density estimated as 10-percent intervals; and crown transparency estimated as 10-percent intervals, all based on FIA methods. A WPND severity rating was assigned to each tree, generalizing the location of symptoms in the crown in thirds as bottom, middle, and top. This information was reinforced with estimates of WPND crown symptoms using the following ratings: 0 = no WPND symptoms; 1 = <1/3 crown affected; 2 = ≥1/3–2/3 crown affected; 3 = >2/3 crown affected. Other symptoms observed in the crown such as necrosis, flagging, insect defoliation, symptoms and signs of Caliciopsis canker (*Caliciopsis pinea*), and fungal fruiting bodies (such as decay fungi) were also recorded in the comments. Lastly, the species of the five closest seedlings (consistent with FIA definitions) and their distance to plot center were recorded for future estimation of per-acre seedling density as done in previous studies (Munck and others 2016). Presence/absence of disease on EWP seedlings was evaluated, paying special attention to the presence of WPND symptomatic needles and *Caliciopsis* fruiting structures. On some plots, this presented the best opportunity to collect WPND needle samples. Collected needle samples included branches with symptomatic needles, including current growth and up to 3-year-old needles if present, from several locations on the tree and at different plot locations. Collected samples were placed in separate 1-quart plastic bags and kept on ice in coolers in the field and refrigerated before being sent to cooperating diagnostic labs for fungal identification.

In most cases, data were recorded electronically using a data form created in the Survey123 application (app) by the Forest Service Durham, NH, field office. When survey crews were within cell range and able to access the internet, data were automatically uploaded to a remote server, securing data in real time and reducing the time needed for data entry. The Survey123 app also had a built-in function for recording images at the sites, so crews were encouraged to take pictures of the site and symptomatic trees.

RESULTS

A total of 122 stands (4 subplots each) were identified, and 4,419 trees were surveyed across the 6 participating States. Naturally established stands comprised 64 percent (78) of the plots, and 36 percent (44) were plantations. Highlighting the extent of particular and significant stressors impacting the region's EWP resource, WPND symptoms were recorded on 95 percent of stands, and Caliciopsis canker symptoms were recorded on 71 percent of stands (see fig. 7.1 for WPND and Caliciopsis canker symptoms).

The data presented in tables 7.1 and 7.2 show significant relationships between basal area and crown density and represent the main findings of this project. White pine needle damage severity was shown to increase with increasing stand basal area. Also, increased WPND severity was related to lower crown density in overstory trees. Further, and as expected, presence of causal agents of WPND was correlated with a decrease in crown density. The results suggest WPND symptoms increase within overstocked stands and WPND causal agents are associated with thinner crowns. The majority of samples submitted to diagnostic clinics were positive for the brown spot needle blight pathogen, *Lecanosticta acicola*. The second most frequently recovered pathogen was *Septorioides strobi*, with needle cast pathogens *Lophophacidium dooksii* and *Bifusella linearis* also recovered from symptomatic needles (see fig. 7.2).

DISCUSSION

Defoliation of EWP caused by the complex of WPND foliar fungi has been reported throughout the Northeast for over 10 years. Repeated defoliation has impacted the vigor and growth of EWP (McIntire and others 2018b). In combination with diseases such as Caliciopsis canker and unfavorable environmental factors, thousands of acres have been negatively impacted. The 122 EWP stands included in this work throughout New England and New York were identified using a variety of techniques including on-the-ground and enhanced aerial survey and the National Insect and Disease Risk Map (NIDRM) EWP host layer. This combination of techniques proved to be satisfactory for plot selection given the differing resources available to the participating States.

The results of this survey, the characteristics of EWP as a timber species, and long-term climatic conditions of wet spring seasons suggest the positive potential of low-density management for EWP. Eastern white pine is a species of intermediate shade tolerance that competes well with other vegetation, especially on sites with deep, sandy soils. Once established, EWP exhibits excellent height and diameter growth (Livingston and others 2019). Low-density management would reduce competition for water and light, enhancing establishment and making trees more resilient to

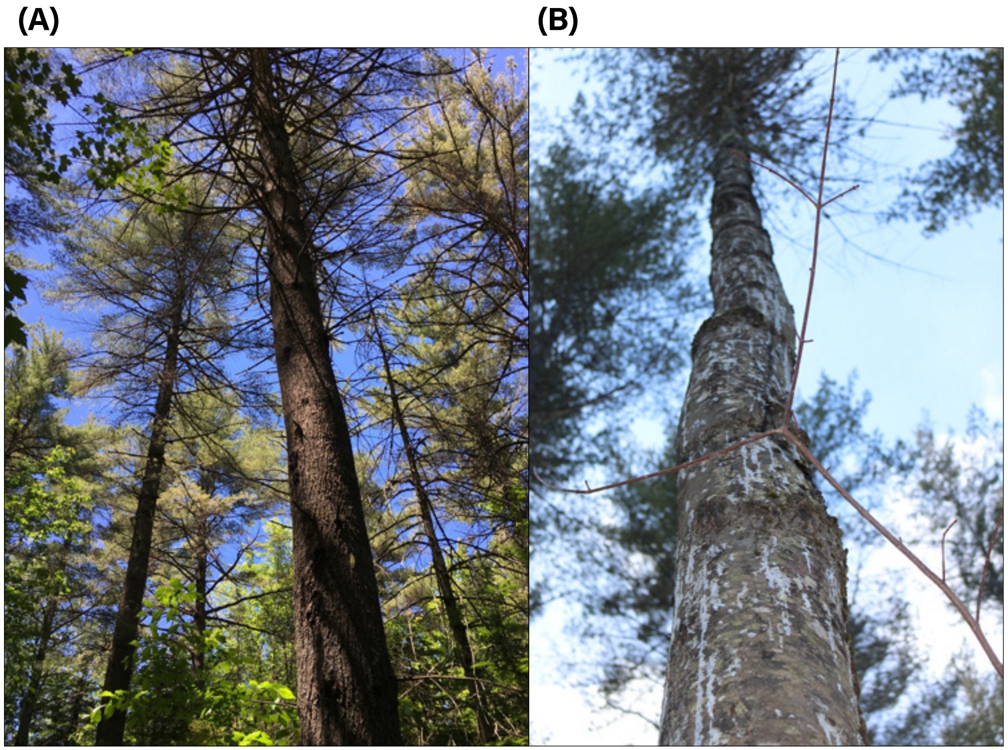

Figure 7.1—(A) White pine trees impacted by white pine needle damage with small, thin crowns and lower branch dieback. (B) Internodal sap streaking, a symptom of Caliciopsis canker. (Courtesy photo by A. Bergdahl, Maine Forest Service)

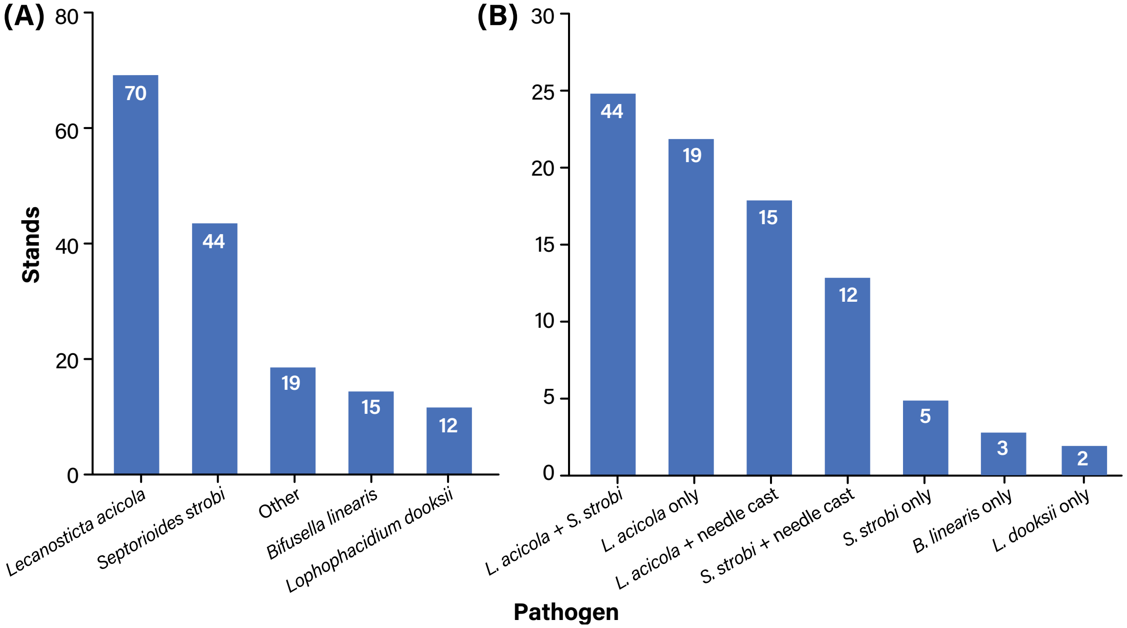

Figure 7.2—Pathogenic fungi recovered from eastern white pine samples collected from 92 stands of 112 in New England and New York. (A) Total number of plots where each pathogen was present. (B) Number of plots with different pathogen combinations. Bifusella linearis *and* Lophophacidium dooksii *are needle cast pathogens (from Munck and others, in preparation [see footnote 3]).*

Table 7.1—Descriptive statistics associated with collected variables (from Munck and others, in preparation [see footnote 3])

Variable	Mean	Standard deviation	Minimum	Maximum
White pine needle damage (WPND) severity rating (0–3) of trees	1.7	0.8	0	3
Proportion of trees with Caliciopsis canker symptoms	0.1	0.2	0	0.9
Live crown ratio	31.3	12.7	11.1	67.1
Crown density	45.7	8.5	27.6	66.8
Total basal area (square feet per acre)	272.2	136.5	33.1	767.5
Eastern white pine basal area (square feet per acre)	247.8	130.8	23.3	584
Proportion of basal area in white pine	88.8	12.4	34	100
White pine seedlings per acre	1,446	3,575	0	21,424
Proportion of white pine seedlings per acre with Caliciopsis canker	0.1	0.2	0	1
Proportion of white pine seedlings per acre with WPND	0.4	0.4	0	1
Longitude	-72	1.8	-76.6	-68.6
Latitude	43.5	0.8	41.5	45
Elevation (m)	224.9	149.2	20	645
Diameter at breast height (inches)	17.7	4.2	5.8	36.8

Table 7.2—Pearson Correlation Coefficients and Prob > |r| under H0: Rho = 0, between stand variables and disease variables, with significant relationships shown in bold (from Bergdahl and others 2020)

Variables	WPND severity for trees	Proportion of trees with Caliciopsis canker symptoms (percent)	Live crown ratio	Crown density	Total basal area (square feet per acre)	White pine basal area (square feet per acre)	Basal area in white pine (percent)	White pine seedlings per acre	White pine seedlings with Caliciopsis canker symptoms (percent)	White pine seedlings with WPND (percent)	Longitude	Latitude	Elevation (m)
Proportion of trees with Caliciopsis canker symptoms (percent)	-0.01188	1											
	0.8967												
Live crown ratio	0.01606	0.13297	1										
	0.8606	0.1443											
Crown density	**-0.33355**	-0.0825	0.09819	1									
	0.0002	0.3724	0.2881										
Total basal area (square feet per acre)	**0.20295**	-0.07971	-0.0427	-0.1496	1								
	0.0256	0.3848	0.642	0.1058									
White pine basal area (square feet per acre)	**0.23578**	-0.0656	-0.0255	-0.1488	0.98116	1							
	0.0089	0.4729	0.7804	0.1062	<.0001								
Basal area in white pine (percent)	0.12957	-0.0377	-0.0263	0.03626	**0.18573**	**0.32443**	1						
	0.1549	0.6801	0.7741	0.6954	**0.0414**	**0.0003**							
White pine seedlings per acre	**-0.20659**	-0.00882	-0.0205	-0.0148	**-0.2299**	**-0.2415**	-0.1314	1					
	0.0224	0.9232	0.8223	0.873	**0.0112**	**0.0074**	0.149						
White pine seedlings with Caliciopsis canker symptoms (percent)	**-0.18904**	0.03263	**0.22841**	-0.0222	**-0.2758**	**-0.279**	-0.1458	0.10076	1				
	0.037	0.7212	**0.0114**	0.811	**0.0022**	**0.0019**	0.109	0.2694					
White pine seedlings with WPND (percent)	0.10487	-0.16084	**0.25387**	0.08893	**-0.2481**	**-0.2395**	-0.0495	0.04954	**0.47433**	1			
	0.2503	0.0768	**0.0048**	0.3362	**0.0061**	**0.0079**	0.5885	0.5879	**<.0001**				
Longitude	0.16952	-0.15541	**0.55729**	-0.0259	-0.0805	-0.0698	-0.0614	-0.0014	**0.22035**	**0.5939**	1		
	0.0619	0.0874	**<.0001**	0.7802	0.3801	0.445	0.5021	0.9876	**0.0147**	**<.0001**			
Latitude	**0.23432**	0.14839	**0.50305**	0.0835	-0.0044	0.04887	0.14675	-0.1529	-0.07614	**0.16692**	**0.41854**	1	
	0.0094	0.1028	**<.0001**	0.3666	0.9615	0.5929	0.1068	0.0927	0.4045	**0.0661**	**<.0001**		
Elevation (m)	**-0.17461**	0.11577	**-0.2793**	0.08881	0.05778	0.06901	0.14756	-0.0407	**-0.19285**	**-0.5124**	**-0.7652**	**-0.1773**	1
	0.0544	0.2042	**0.0018**	0.3368	0.529	0.45	0.1048	0.6565	**0.0333**	**<.0001**	**<.0001**	**0.0508**	
Diameter at breast height (inches)	0.15475	-0.12722	**0.22937**	0.08311	**0.76916**	**0.75558**	**0.21177**	-0.1685	**-0.25065**	-0.06813	0.13658	0.14317	-0.08091
	0.0888	0.1626	**0.011**	0.3689	**<.0001**	**<.0001**	**0.0192**	0.0636	**0.0054**	0.4559	0.1336	0.1157	0.3757

WPND = white pine needle damage.

drought conditions. Reduced disease pressure from the causal agents of WPND associated with lower density stands described in this work would favor higher live crown ratios, increased growth (Livingston and others 2019), and resilience to other agents of decline. For example, stress reduction via lower density stands is thought to reduce incidence and severity of Caliciopsis canker. Reduced impacts of needle loss from WPND are also favored by low-density management, as this study showed that stand basal area was negatively correlated with WPND severity, and presence of WPND causal agents was correlated with decreased crown density. This further suggests that managing stand density would increase resilience to foliar diseases and decrease their incidence. This stands to reason, as increased spacing reduces dispersal of inoculum to adjacent trees (Wyka and others 2018) and enhances drying of foliage, therefore reducing colonization by WPND causal agents and preservation of higher live crown ratios, a strong indicator of tree vigor (McIntire and others 2018a). Further, due to the positive contributions to tree vigor mentioned here, faster growth leads to reduced rotation times, subsequently reducing exposure, impacts, and losses due to decay (Livingston and others 2019).

Stand basal area was found to be negatively correlated with number of seedlings, indicating the positive effect of this style of management on regeneration, and thus, future sustainability of the EWP resource (Munck and others, in preparation[3]).

CONCLUSIONS

The findings of this study support the idea that, under current climatic conditions which dictate disease conditions via increased prolonged periods of moisture during the infection period of WPND, low stand density leads to improved growing conditions, improved stand health, improved tree vigor, and improved regeneration. Thus, managing for lower stand density would not only increase resilience to foliar diseases but have additional positive impacts on the overall sustainability of the regional EWP resource. Although low-density management of EWP does not apply to all growing situations, it should be considered in areas with conditions conducive to disease, on drought-prone sites/soils, and on sites where agents of decline like pine bast scale (*Matsucoccus macrocicatrices*) and Caliciopsis canker are issues of concern. As a final conclusion, aerial survey, interstate coordination, and data collection with the Survey123 app was an efficient way to collect data from a wide geographic range, leading to the interesting results of this study.

For more information, contact:
Isabel A. Munck, Isabel.munck@usda.gov
Aaron Bergdahl, aaron.bergdahl@maine.gov

---

[3] *Munck, I.A.; Bergdahl, A.; Cancelliere, J. [and others]. Site factors associated with foliar diseases and Caliciopsis canker causing declining health of eastern white pine in Northeastern USA. Manuscript in preparation. Author can be reached at U.S. Department of Agriculture Forest Service, State and Private Forestry, 271 Mast Rd., Durham, NH 03824.*

LITERATURE CITED

Bergdahl, A.; Cancelliere, J.; Cole, R. [and others]. 2020. Monitoring eastern white pine decline and its causes in New England and New York: NE-EM-17-04 [poster]. 2020 Forest Health Monitoring Workshop, Raleigh, North Carolina, February 24–27, 2020.

Livingston, W.H.; Munck, I.; Lombard, K. [and others]. 2019. Field manual for managing eastern white pine health in New England. Maine Agricultural and Forest Experiment Station Misc. Publ. 764. Orono, ME: The University of Maine, College of Natural Sciences, Forestry, and Agriculture. 15 p.

Maine Forest Service. 2021. 2019 stumpage price report. Augusta, ME: Maine Department of Agriculture, Conservation & Forestry, Maine Forest Service, Forest Policy and Management Division. 17 p. https://www.maine.gov/dacf/mfs/publications/index.html. [Date last accessed: October 21, 2021].

McIntire C.D.; Munck, I.A.; Ducey, M.J.; Asbjrosen, H. 2018a. Thinning treatments reduce severity of foliar pathogens in eastern white pine. Forest Ecology and Management. 423: 106–113. https://doi.org/10.1016/j.foreco.2018.03.032.

McIntire, C.D.; Munck, I.A.; Vadeboncoeur, M.A. [and others]. 2018b. Impacts of white pine needle damage on seasonal litterfall dynamics and wood growth of eastern white pine (*Pinus strobus*) in northern New England. Forest Ecology and Management. 423: 27–36. https://doi.org/10.1016/j.foreco.2018.02.034.

Munck, A.I.; Luther, T.; Wyka, S. [and others]. 2016. Soil and stocking effects on Caliciopsis canker of *Pinus strobus* L. Forests. 7(11): 269. https://doi.org/10.3390/f7110269.

New Hampshire Department of Revenue Administration. 2021. Property average stumpage prices. Concord, NH: New Hampshire Department of Revenue Administration. https://www.revenue.nh.gov/mun-prop/property/stumpage-values.htm. [Date last accessed: October 21, 2021].

New York Department of Environmental Conservation. 2021. Stumpage price reports. Albany, NY: New York Department of Environmental Conservation. https://www.dec.ny.gov/lands/5259.html. [Date last accessed: October 21, 2021].

University of Massachusetts Amherst. 2021. Southern New England stumpage price report. Amherst, MA: Cooperative Extension at the Universities of Massachusetts and Connecticut, and the State forestry agencies in Connecticut, Massachusetts, and Rhode Island. https://masswoods.org/southern-new-england-stumpage-price-report. [Date last accessed: October 21, 2021].

U.S. Department of Agriculture (USDA) Forest Service, Forest Inventory and Analysis (FIA) program. 2021. Forest Inventory EVALIDator web-application version 1.8.0.01. St. Paul, MN: USDA Forest Service, FIA program. [Date accessed: July 15, 2021].

Vermont Department of Forests, Parks and Recreation, 2019–2021. Stumpage price reports. Montpelier, VT: Vermont Department of Forests, Parks, and Recreation, Division of Forests. https://fpr.vermont.gov/stumpage-price-reports. [Date last accessed: October 21, 2021].

Wyka, S.A.; McIntire, C.D.; Smith, C. [and others]. 2018. Effect of climatic variables on abundance and dispersal of *Lecanosticta acicola* spores and their impact on defoliation on eastern white pine. Phytopathology. 108(3): 374–383. https://doi.org/10.1094/PHYTO-02-17-0065-R.

CHAPTER 8

Evaluating the Effects of Nonnative Grass Invasion on Fuels, Fire Behavior, and Tree Regeneration in the Central Hardwoods Region

Jennifer Fraterrigo
Ron Salemme

INTRODUCTION

Nonnative grass invasions can increase fire intensity by increasing the loading, continuity, and flammability of fine fuels (Balch and others 2013, Fuentes-Ramirez and others 2016, Fusco and others 2019, Setterfield and others 2010). Increased fire intensity, in turn, can shift ecosystem dynamics by promoting nonnative, invasive grasses over native plants, creating a positive feedback between fire and invasion (D'Antonio and Vitousek 1992). Although this grass-fire feedback has been documented in temperate deciduous forests (Flory and others 2015, Kerns and others 2020, Wagner and Fraterrigo 2015), the consequences for regeneration dynamics remain uncertain.

In temperate deciduous forests, fire favors the establishment of species with fire-adapted traits, such as hypogeal germination, resprouting ability, and thick bark (Arthur and others 2012; Brose and Van Lear 1998, 2004). However, the responses of fire-adapted and other temperate deciduous species to increases in fire intensity are poorly understood. On the one hand, seedlings may tolerate increased fire intensity because they have well-developed root systems and stores of carbohydrates that promote resprouting (Bond and Midgley 2001, Bowen and Pate 1993). On the other hand, invasive grasses can outcompete native woody vegetation for resources owing to their dense roots, high nutrient efficiencies, and rapid growth rates (Grice and others 2013, Marshall and others 2009). Strong resource competition could reduce tree carbohydrate reserves, especially in small individuals, thereby limiting resprouting ability (Villar-Salvador and others 2015). Additionally, small individuals are more prone to fire-induced injuries (Brando and others 2012) and may therefore experience higher mortality rates. With fire increasingly used to maintain and restore temperate forests (Stephens 2005) and with widespread grass invasions in forests (Iannone and others 2016), there is a critical need to determine how invasion affects post-fire tree persistence to guide management and anticipate future forest dynamics.

We examined how invasion by the shade-tolerant, C4 grass *Microstegium vimineum* (Nepalese browntop, or stiltgrass) interacts with prescribed fire to affect the regeneration of naturally established seedlings and saplings of varying sizes. *M. vimineum* is widespread in temperate forests in the Eastern United States, currently spanning 26 States (USDA NRCS 2020). Previous studies show that once established, *M. vimineum* can strongly compete with native understory plants for resources (Ehrenfeld and others 2001, Flory and Clay 2009, Marshall and others 2009), although this effect diminishes with canopy closure (Daniels and Larson 2020, Flory and others 2017). *M. vimineum* has also been found to increase fire intensity and the mortality of planted tree seedlings (Flory and others 2015), yet the interactive effects of fire and invasion on naturally established juvenile trees are less clear. We expected that naturally established juvenile trees would be resilient to grass-fire interactions because of their ability to resprout. However, because size influences resprouting ability and vigor (Gilbert and others 2003, Matula and others 2019) as well as vulnerability to heating-induced

How to cite this chapter:

Fraterrigo, Jennifer; Salemme, Ron. 2022. Evaluating the effects of nonnative grass invasion on fuels, fire behavior, and tree regeneration in the Central Hardwoods Region. In: Potter, Kevin M.; Conkling, Barbara L., eds. Forest Health Monitoring: national status, trends, and analysis 2021. Gen. Tech. Rep. SRS-266. Asheville, NC: U.S. Department of Agriculture Forest Service, Southern Research Station: 145–153. https://doi.org/10.2737/SRS-GTR-266-Chap8.

mortality, we expected smaller trees would be less resilient than larger trees, potentially leading to long-term shifts in regeneration dynamics. We tested these predictions in the context of the following three objectives: (1) quantify differences in fire intensity and its drivers between invaded and uninvaded plots; (2) determine how fire intensity and *M. vimineum* invasion affect the regeneration of tree seedlings and saplings with respect to size; and (3) evaluate the potential long-term effects of prescribed fire and *M. vimineum* invasion on stand development using a forest growth and yield simulation model.

METHODS

As described in Salemme and Fraterrigo (2021), in August 2015 we established twenty 0.04-ha pairs of invaded and uninvaded (control) plots (n = 40 plots total) spanning the range in soil moisture conditions present and distributed across six Forest Service, U.S. Department of Agriculture, management units at Shawnee National Forest in southern Illinois. Stands were dominated by oak (*Quercus* spp.) and hickory (*Carya* spp.) in drier areas and shortleaf pine (*Pinus echinata*) and tuliptree (*Liriodendron tulipifera*) in wetter areas. Prescribed fire had previously been applied in each of the management units one to three times. Invaded plots had at least 70-percent *M. vimineum* surface cover. In the fall prior to prescribed fire application, we determined surface litter, *M. vimineum* biomass, and coarse woody fuel biomasses in each plot. Woody fuel samples were collected immediately prior to burning to determine fuel moisture content. Volumetric soil moisture was measured monthly throughout the growing season. Additionally, tree seedlings (≤1 m in height) in each plot were identified to species, tagged, and measured for stem height and diameter at ground level (seedlings) or breast height (saplings). Overall, we tagged 419 seedlings and 157 saplings.

Between October 2015 and February 2017, prescribed fire was applied to all management units. To quantify fire behavior, we recorded fire temperature and residence time using a K-type thermocouple coupled with a data logger and determined flame length by measuring the maximum height of scorch marks. Weather conditions preceding fires and on fire days were determined from nearby weather stations. Fuels were resampled following fire to determine consumption. To determine post-fire seedling and sapling persistence, defined here as trees that survived or resprouted post-fire, we relocated tagged trees in July of the following growing season and recorded their survival status (survived, resprouted, or other). Seedlings that did not survive or resprout in the growing season following fire were reassessed after an additional growing season; if they still showed no signs of growth, they were considered dead.

We simulated post-fire tree regeneration decadally from 2016–2066 using the Central States variant of the Forest Service Forest Vegetation Simulator (FVS) and the Fire and Fuels Extension (FFE) to the FVS (Rebain 2010). Simulated stands were initialized using field data for each plot. To examine the effects of grass invasion and prescribed fire on tree regeneration, we modeled four different scenarios: low-intensity, uninvaded; low-intensity, invaded; moderate-intensity, uninvaded; and moderate-intensity, invaded. For each scenario, we adjusted the following parameters: flame height, percentage of stand area burned, and the number of sprouts multiplier using field data from our study and from a similar study involving *M. vimineum* and prescribed fire in a midwestern temperate forest (Flory and others 2015).

To evaluate the relationships between grass invasion, fuel conditions, and fire behavior, we used linear mixed effects models. To test for differences in post-fire seedling and sapling persistence and resprouting probabilities, we used generalized linear mixed models. In both cases, we included burn unit as a random effect. We used structural equation modeling to quantify the relative magnitude of direct and indirect effects of *M. vimineum* invasion and fire intensity on seedling survival. Finally, to evaluate the effects of invasion status and prescribed burning on FVS-simulated tree resprouting, we compared the average number of resprouts per time step (decadal) by invasion status for each fire intensity scenario described above using paired t-tests. All analyses were performed in R.

RESULTS

Total fuel loading and woody fuel moisture did not differ with invasion status; however, nonwoody surface litter moisture was nearly 50 percent higher in invaded than uninvaded plots (Salemme and Fraterrigo 2021). *M. vimineum* biomass accounted for roughly 10 percent of nonwoody litter biomass in invaded plots and was significantly higher in areas of high soil moisture. As a result of these moisture differences, fires in invaded plots had 33-percent-lower flame length, 45-percent-lower percentage of area burned, and 40-percent-shorter fire residence time than uninvaded plots (fig. 8.1). Fire-weather and site conditions, mainly air temperature and soil moisture, were the strongest predictors of fire behavior (Salemme and Fraterrigo 2021).

Prior to fire, invaded plots had significantly lower seedling densities than uninvaded plots, with 43.5 percent fewer seedlings on average. Invaded plots also had significantly fewer small-sized individuals than uninvaded plots (table 8.1). Pre-fire sapling density did not vary between invaded and uninvaded plots.

Fire reduced seedling persistence by 40 percent compared to unburned plots. There was no statistical interaction between fire and invasion. Among burned plots, however, invaded plots had 54-percent-lower seedling persistence than uninvaded plots, despite experiencing lower fire intensity and having larger individuals (fig. 8.2). On average, the diameter of seedlings with a 50-percent probability of persistence was 2.8 times higher in invaded than uninvaded plots, suggesting invasion reduced the resilience of smaller individuals to fire. Supporting this, resprouting probability was positively related to diameter, while invasion had a marginal negative effect. The structural equation model indicated a direct negative effect of *M. vimineum* biomass and an indirect negative effect of fire intensity on seedling persistence, with the effect size of

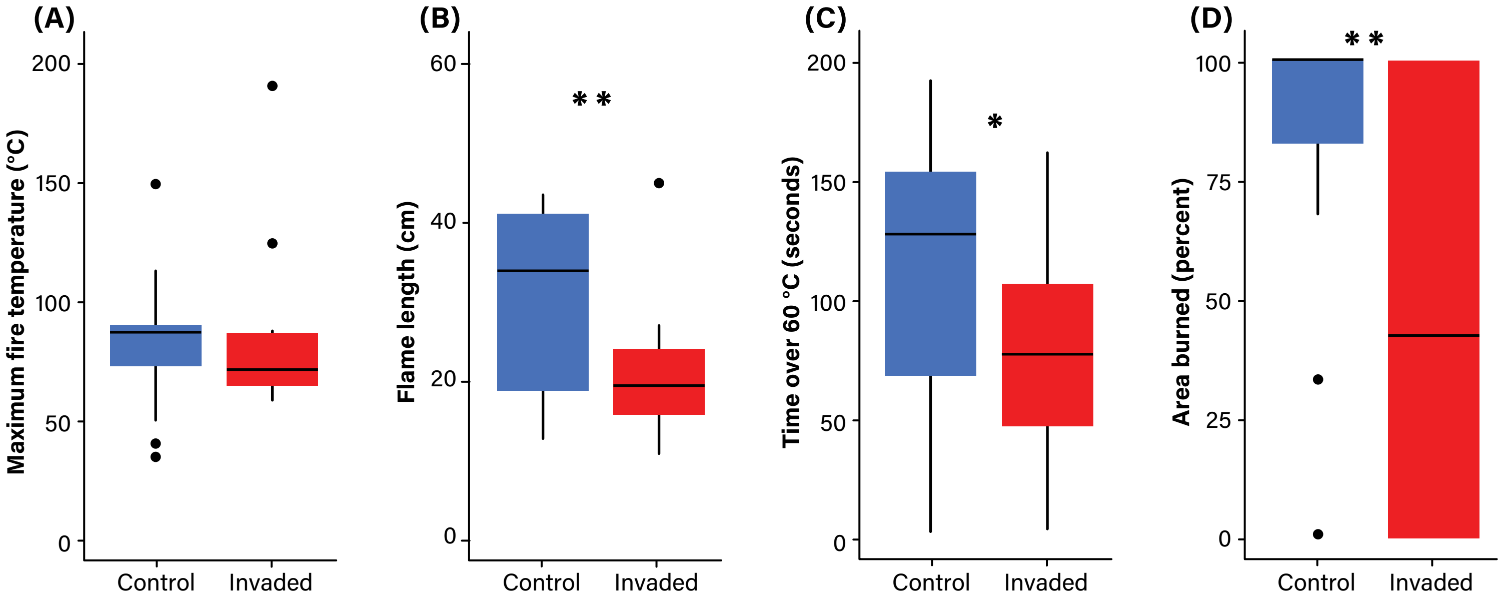

Figure 8.1—Boxplots of (A) maximum fire temperature, (B) flame length, (C) residence time over 60 °C, and (D) percentage of area burned in uninvaded (control) and Microstegium vimineum*-invaded plots. Data are averaged across 2015–2017 prescribed fires. Asterisks indicate statistical significance (** = $p < 0.05$; * = $p < 0.10$).*

Table 8.1—Pre-fire diameter-class distribution for tagged seedlings in control and invaded plots

	Seedling diameter class						
	0–2 cm	*>2–4 cm*	*>4–6 cm*	*>6–8 cm*	*>8–10 cm*	*>10–12 cm*	*>12 cm*
Control	52	98	65	36	17	5	0
Invaded	13	43	51	23	12	3	1

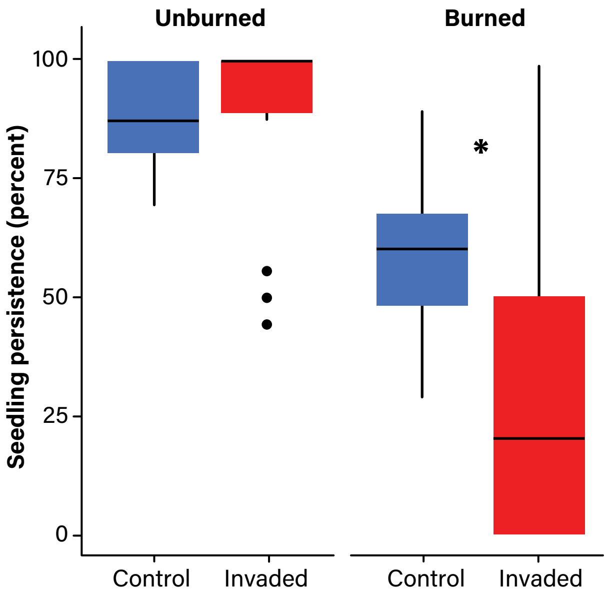

Figure 8.2—Boxplots of seedling persistence by invasion and fire status. Data are averaged across 2015–2017 prescribed fires. While there was no interactive effect of fire and invasion, persistence in burned-invaded plots was lower than in burned-uninvaded plots. Asterisk indicates statistical significance (= p <0.01).*

M. vimineum more than twice that of fire. There was also a direct positive effect of seedling diameter on persistence. Although fire reduced sapling persistence by 28 percent compared to unburned plots, there were no significant differences in sapling survival by invasion or diameter among burned plots.

The partial establishment model in the FVS Central States variant simulates resprouting from stumps or roots based on stand density, parent tree size, and species resprouting potential (FVS Staff 2008). We parameterized the number of sprouts multiplier within FVS to further reflect observed differences in post-fire tree regeneration. Averaged over a 10-year time step, we found that FVS-simulated resprouting differed with invasion under both low- and moderate-intensity fires. Invasion resulted in a 63-percent reduction in resprout density compared to uninvaded plots.

DISCUSSION AND CONCLUSIONS

Previous studies show that invasive grass-fire feedbacks can increase fire intensity in temperate deciduous forests (Wagner and Fraterrigo 2015), resulting in decreased survival of recently planted but not naturally established juvenile trees (Flory and others 2015). In contrast, we found that grass invasion reduced the intensity of prescribed fire. Despite having lower fire intensity, post-fire persistence and resprouting of naturally established seedlings was lower in invaded than uninvaded plots, whereas persistence was unaffected by invasion in the absence of fire (Salemme and Fraterrigo 2021). Structural equation modeling also demonstrated that the magnitude of the direct negative effect of invasion on post-fire seedling persistence was greater than the negative indirect effect via fire intensity. Collectively, these results suggest that grass invasion can reduce forest resilience to fire by inhibiting the regeneration and growth of seedlings. Consequently, temperate deciduous forests that have historically been maintained or restored by periodic fire may no longer experience the same benefits from burning when invaded by nonnative grasses.

Our results reveal that soil moisture was a strong driver of fire intensity and that the moisture content of nonwoody surface fuels was considerably higher in invaded than uninvaded plots. These patterns coincided with 11-percent-greater precipitation during the spring 2016 burn season than the 15-year average (WARM/ICN 2019). A previous study conducted at comparable sites in Shawnee National Forest demonstrated that burning under drier conditions resulted in higher fire residence times in *M. vimineum*-invaded plots (Wagner and Fraterrigo 2015). Collectively, these findings underscore the overarching effect of climate and meteorological events on fire intensity regardless of invasion status and suggest we may have observed more intense fires and possibly lower tree survival if fires were conducted under drier conditions.

Despite lower intensity fires, fewer seedlings persisted following fire in invaded plots, with stem diameter moderating this effect. The observed post-fire persistence rate in invaded plots averaged 31 ± 7 percent. Similarly, grass invasion reduced post-fire survival of planted seedlings by 54 percent in southeastern Indiana (Flory and others 2015) and significantly reduced species richness of naturally recruited woody species in a northern Mississippi oak-hickory woodland (Brewer and others 2015). The difference in seedling survival rate by invasion, together with the difference in resprouting rate, suggests that *M. vimineum* invasion has both direct and indirect effects on post-fire seedling persistence, a hypothesis supported by the results of the standard error of the mean. The marginal difference in resprouting could be caused by prolonged nitrogen immobilization, associated with both grass invasion (Ehrenfeld and others 2001) and repeated burning (Fraterrigo and Rembelski 2021, Hernández and Hobbie 2008), which has been shown to reduce the storage of nonstructural carbohydrates in woody plants and decrease seedling resprouting capabilities (Villar-Salvador and others 2015). Additionally, grass invasion may have resulted in fire burning closer to the root collar of seedlings by increasing within-plot fuel continuity, as even the low flame temperatures observed in invaded areas were high enough to damage root collars (Levitt 1980). In line with other studies (Flory and Clay 2010, Oswalt and Oswalt 2010, Oswalt and others 2007), we observed significantly lower pre-fire seedling densities and reduced numbers of small trees in invaded plots. All the management units in our study had previously been burned, so this pattern may be the result of past filtering of small individuals by grass-fire interactions.

Our results have important implications for managing grass-invaded temperate forests with fire. This study and others show that invasion can have varying effects on fire intensity depending on weather conditions, with dry conditions resulting in increased fire intensity and high mortality rates for planted seedlings (Flory and others 2015) and wet conditions having the opposite effect (Pilliod and others 2017, Poulos and Roy 2015). We further demonstrate that grass invasion can negatively affect tree regeneration by inhibiting the recovery of small seedlings from fire, likely through a combination of increasing resource competition and fine-scale increases in fire intensity. Further, our FVS simulations suggest that the interactive effects of fire and invasion on seedling resprouting alter long-term tree regeneration dynamics. Therefore, if a management goal is to promote the regeneration of shade-intolerant tree species, the time between fire applications may need to be lengthened to allow juvenile trees in invaded areas to reach a "safe" size (i.e., 7–10-mm stem diameter), at which the likelihood of persistence is higher.

For more information, contact:
Jennifer Fraterrigo, jmf@illinois.edu

REFERENCES

Arthur, M.A.; Alexander, H.D.; Dey, D.C. [and others]. 2012. Refining the oak-fire hypothesis for management of oak-dominated forests of the Eastern United States. Journal of Forestry. 110: 257–266. https://doi.org/10.5849/jof.11-080.

Balch, J.K.; Bradley, B.A.; D'Antonio, C.M.; Gómez-Dans, J. 2013. Introduced annual grass increases regional fire activity across the arid Western USA (1980–2009). Global Change Biology. 19:173–183. https://doi.org/10.1111/gcb.12046.

Bond, W.J.; Midgley, J.J. 2001. Ecology of sprouting in woody plants: the persistence niche. Trends in Ecology & Evolution. 16: 45–51. https://doi.org/10.1016/S0169-5347(00)02033-4.

Bowen, B.J.; Pate, J.S. 1993. The significance of root starch in post-fire shoot recovery of the resprouter *Stirlingia latifolia* R. Br. (Proteaceae). Annals of Botany. 72: 7–16. https://doi.org/10.1006/anbo.1993.1075.

Brando, P.M.; Nepstad, D.C.; Balch, J.K. [and others]. 2012. Fire-induced tree mortality in a neotropical forest: the roles of bark traits, tree size, wood density and fire behavior. Global Change Biology. 18: 630–641. https://doi.org/10.1111/j.1365-2486.2011.02533.x.

Brewer, J.S.; Abbott, M.J.; Moyer, S.A. 2015. Effects of oak-hickory woodland restoration treatments on native groundcover vegetation and the invasive grass, *Microstegium vimineum*. Ecological Restoration. 33: 256–265. https://doi.org/10.3368/er.33.3.256.

Brose, P.H.; Van Lear, D.H. 1998. Responses of hardwood advance regeneration to seasonal prescribed fires in oak-dominated shelterwood stands. Canadian Journal of Forest Research. 28: 331–339. https://doi.org/10.1139/x97-218.

Brose, P.; Van Lear, D. 2004. Survival of hardwood regeneration during prescribed fires: the importance of root development and root collar location. In: Spetich, M.A., ed. Upland oak ecology symposium: history, current conditions, and sustainability. Gen. Tech. Rep. SRS-73. Asheville, NC: U.S. Department of Agriculture Forest Service, Southern Research Station: 123–127.

D'Antonio, C.M.; Vitousek, P.M. 1992. Biological invasions by exotic grasses, the grass/fire cycle, and global change. Annual Review of Ecology and Systematics. 23: 63–87. https://doi.org/10.1146/annurev.es.23.110192.000431.

Daniels, M.K.; Larson, E.R. 2020. Effects of forest windstorm disturbance on invasive plants in protected areas of southern Illinois, USA. Journal of Ecology. 108: 199–211. https://doi.org/10.1111/1365-2745.13254.

Ehrenfeld, J.G.; Kourtev, P.; Huang, W. 2001. Changes in soil functions following invasions of exotic understory plants in deciduous forests. Ecological Applications. 11: 1287–1300. https://doi.org/10.1890/1051-0761(2001)011[1287:CISFFI]2.0.CO;2.

Flory, S.; Bauer, J.; Phillips, R.P.; Clay, K. 2017. Effects of a non-native grass invasion decline over time. Journal of Ecology. 105: 1475–1484. https://doi.org/10.1111/1365-2745.12850.

Flory, S.; Clay, K. 2010. Non-native grass invasion suppresses forest succession. Oecologia. 164: 1029–1038. https://doi.org/10.1007/s00442-010-1697-y.

Flory, S.L.; Clay, K. 2009. Invasive plant removal method determines native plant community responses. Journal of Applied Ecology. 46: 434–442. https://doi.org/10.1111/j.1365-2664.2009.01610.x.

Flory, S.L.; Clay, K.; Emery, S.M. [and others]. 2015. Fire and non-native grass invasion interact to suppress tree regeneration in temperate deciduous forests. Journal of Applied Ecology. 52: 992–1000. https://doi.org/10.1111/1365-2664.12437.

Fraterrigo, J.M.; Rembelski, M.K. 2021. Frequent fire reduces the magnitude of positive interactions between an invasive grass and soil microbes in temperate forests. Ecosystems. https://doi.org/10.1007/s10021-021-00615-x.

Fuentes-Ramirez, A.; Veldman, J.W.; Holzapfel, C.; Moloney, K.A. 2016. Spreaders, igniters, and burning shrubs: plant flammability explains novel fire dynamics in grass-invaded deserts. Ecological Applications. 26: 2311–2322. https://doi.org/10.1002/eap.1371.

Fusco, E.J.; Finn, J.T.; Balch, J.K. [and others]. 2019. Invasive grasses increase fire occurrence and frequency across US ecoregions. Proceedings of the National Academy of Sciences. 116: 23594–23599. https://doi.org/10.1073/pnas.1908253116.

FVS Staff. 2008. Central States (CS) variant overview - Forest Vegetation Simulator. Internal Rep. Revised June 28, 2021. Fort Collins, CO: U.S. Department of Agriculture Forest Service, Forest Management Service Center. 78 p.

Gilbert, N.L.; Johnson, S.L.; Gleeson, S.K. [and others]. 2003. Effects of prescribed fire on physiology and growth of *Acer rubrum* and *Quercus* spp. seedlings in an oak-pine forest on the Cumberland Plateau, KY. Journal of the Torrey Botanical Society. 130(4): 253–264. https://doi.org/10.2307/3557544.

Grice, A.; Vanderduys, E.P.; Perry, J.J.; Cook, G.D. 2013. Patterns and processes of invasive grass impacts on wildlife in Australia. Wildlife Society Bulletin. 37: 478–485. https://doi.org/10.1002/wsb.314.

Hernández, D.L.; Hobbie, S.E. 2008. Effects of fire frequency on oak litter decomposition and nitrogen dynamics. Oecologia. 158: 535–543. https://doi.org/10.1007/s00442-008-1162-3.

Iannone, B.V.; Potter, K.M.; Guo, Q. [and others]. 2016. Biological invasion hotspots: a trait-based perspective reveals new sub-continental patterns. Ecography. 39: 961–969. https://doi.org/10.1111/ecog.01973.

Kerns, B.K.; Tortorelli, C.; Day, M.A. [and others]. 2020. Invasive grasses: a new perfect storm for forested ecosystems? Forest Ecology and Management. 463: 117985. https://doi.org/10.1016/j.foreco.2020.117985.

Levitt, J. 1980. Responses of plants to environmental stress, volume 1: chilling, freezing, and high temperature stresses. New York, NY: Academic Press. 497 p. https://doi.org/10.1016/B978-0-12-445501-6.50016-6.

Marshall, J.M.; Buckley, D.S.; Franklin, J.A. 2009. Competitive interaction between *Microstegium vimineum* and first-year seedlings of three central hardwoods. The Journal of the Torrey Botanical Society. 136: 342–349. https://doi.org/10.3159/09-RA-006.1.

Matula, R.; Šrámek, M.; Kvasnica, J. [and others]. 2019. Pre-disturbance tree size, sprouting vigour and competition drive the survival and growth of resprouting trees. Forest Ecology and Management. 446: 71–79. https://doi.org/10.1016/j.foreco.2019.05.012.

Oswalt, C.M.; Oswalt, S.N. 2010. The facilitation and impacts of *Microstegium vimineum* colonization in an eastern hardwood forest. In: Stanturf, J.A., ed. 2010. Proceedings of the 14th biennial southern silvicultural research conference. Gen. Tech. Rep. SRS-121. Asheville, NC: U.S. Department of Agriculture Forest Service, Southern Research Station: 103–106.

Oswalt, C.M.; Oswalt, S.N.; Clatterbuck, W.K. 2007. Effects of *Microstegium vimineum* (Trin.) A. Camus on native woody species density and diversity in a productive mixed-hardwood forest in Tennessee. Forest Ecology and Management. 242: 727–732. https://doi.org/10.1016/j.foreco.2007.02.008.

Pilliod, D.S.; Welty, J.L.; Arkle, R.S. 2017. Refining the cheatgrass–fire cycle in the Great Basin: precipitation timing and fine fuel composition predict wildfire trends. Ecology and Evolution. 7: 8126–8151. https://doi.org/10.1002/ece3.3414.

Poulos, L.P.; Roy, B.A. 2015. Fire and false brome: how do prescribed fire and invasive *Brachypodium sylvaticum* affect each other? Invasive Plant Science and Management. 8: 122–130. https://doi.org/10.1614/IPSM-D-14-00024.1.

Rebain, S.A., comp. 2010. The fire and fuels extension to the Forest Vegetation Simulator: updated model documentation. Internal Rep. Revised 2015. Fort Collins, CO: U.S. Department of Agriculture Forest Service, Forest Management Service Center. 403 p.

Salemme, R.K.; Fraterrigo, J.M. 2021. Grass invasion reduces the resilience of tree regeneration to fire in the Central Hardwoods Region. Forest Ecology and Management. 491: 119202. https://doi.org/10.1016/j.foreco.2021.119202.

Setterfield, S.A.; Rossiter-Rachor, N.A.; Hutley, L.B. [and others]. 2010. Biodiversity research: turning up the heat: the impacts of *Andropogon gayanus* (gamba grass) invasion on fire behaviour in northern Australian savannas. Diversity and Distributions. 16: 854–861. https://doi.org/10.1111/j.1472-4642.2010.00688.x.

Stephens, S.L. 2005. Forest fire causes and extent on United States Forest Service lands. International Journal of Wildland Fire. 14: 213–222. https://doi.org/10.1071/WF04006.

U.S. Department of Agriculture (USDA) Natural Resources Conservation Service (NRCS). 2020. The PLANTS Database. National Plant Data Team, Greensboro, NC. https://plants.usda.gov/home [Date accessed: May 1, 2020].

Villar-Salvador, P.; Uscola, M.; Jacobs, D.F. 2015. The role of stored carbohydrates and nitrogen in the growth and stress tolerance of planted forest trees. New Forests. 46: 813–839. https://doi.org/10.1007/s11056-015-9499-z.

Wagner, S.A.; Fraterrigo, J.M. 2015. Positive feedbacks between fire and non-native grass invasion in temperate deciduous forests. Forest Ecology and Management. 354: 170–176. https://doi.org/10.1016/j.foreco.2015.06.024.

Water and Atmospheric Resources Monitoring Program (WARM)/Illinois Climate Network (ICN). 2019. Dixon Springs RAWS data. Champaign, IL: Illinois State Water Survey. https://www.isws.illinois.edu/warm [Date accessed: January 10, 2019].

CHAPTER 9

Ice Storm Impacts on Forest Health: Monitoring and Predicting the Growth and Mortality of Ice-Damaged Trees in Southern Forests

Brittany DiRienzo
G. Geoff Wang

INTRODUCTION

Ice storms are among the most frequent and injurious disturbances in temperate forests (Irland 2000), but they are less studied compared with other major disturbances such as fire or drought. On a global scale, forests in the Eastern United States witness the most ice storms because the region's terrain and coastline configurations encourage freezing rains (Changnon and Karl 2003). There exists a "glaze belt" extending from north Texas to southern New England, where major ice storms are expected once every 3 years (Bennett 1959). Although less frequent, major ice storms also periodically strike the South beyond the "glaze belt" (Bragg and others 2003, Changnon and Karl 2003), causing significant damage to southern forests. For example, the February 2014 ice storm in South Carolina impacted 1.5 million acres of timberland and resulted in a loss of $360 million, second only to damages from Hurricane Hugo (South Carolina Forestry Commission 2014). Following this severe ice storm, the National Science Foundation funded a rapid response study aimed at characterizing and modeling species-specific damage and mortality by assessing the immediate responses of different species (Lu and others 2020). The objective of the study was to monitor the long-term growth and mortality of trees in Beidler Forest after the initial ice damage in 2014.

METHODS

This study was conducted at Beidler Forest in southeastern South Carolina. Beidler Forest experienced between 9.9 and 19.6 mm (between 0.39 and 0.77 inches) of ice accumulation during the February 2014 ice storm (fig. 9.1).

Three forest types were identified along a decreasing moisture gradient: cypress-tupelo swamp, bottomland hardwood, and upland forest. Post-ice storm measurement was conducted during the growing season after the 2014 ice storm on 11 permanent plots that were established after Hurricane Hugo in 1989. A detailed description of the initial assessment method is given in Lu and others (2020). On each plot, trees were remeasured in 2016 and 2018 to record diameter at breast height (d.b.h.) growth and status changes (dead, alive, or missing). Additional data were collected in 2018 to assess individual tree health through the visual description and to determine diameter growth by taking an increment core at breast height. Cored species include bald cypress (*Taxodium distichum* [L.] Rich.), blackgum (*Nyssa sylvatica* Marshall), green ash (*Fraxinus pennsylvanica* Marshall), scarlet oak (*Quercus coccinea* Münchh), red maple (*Acer rubrum* L.), white oak (*Quercus alba* L.), laurel oak (*Quercus laurifolia* Michx.), and water tupelo (*Nyssa aquatica* L.).

We tested the effects of forest type, lifeform, damage category, damage severity, and diameter size on tree mortality, mean annual basal area growth after the storm, and recovery using analysis of variance (ANOVA). Based on changes in basal area growth from d.b.h. measurements between 2014 and 2018, the recovery status of each live tree was classified as in recovery (increase in growth), no change, or decline (decrease in growth). Using ANOVA, we also tested the effect of percentage of crown damage on the

How to cite this chapter:

DiRienzo, Brittany; Wang, G. Geoff. 2022. Ice storm impacts on forest health: monitoring and predicting the growth and mortality of ice-damaged trees in southern forests. In: Potter, Kevin M.; Conkling, Barbara L., eds. Forest Health Monitoring: national status, trends, and analysis 2021. Gen. Tech. Rep. SRS-266. Asheville, NC: U.S. Department of Agriculture Forest Service, Southern Research Station: 155–158. https://doi.org/10.2737/SRS-GTR-266-Chap9.

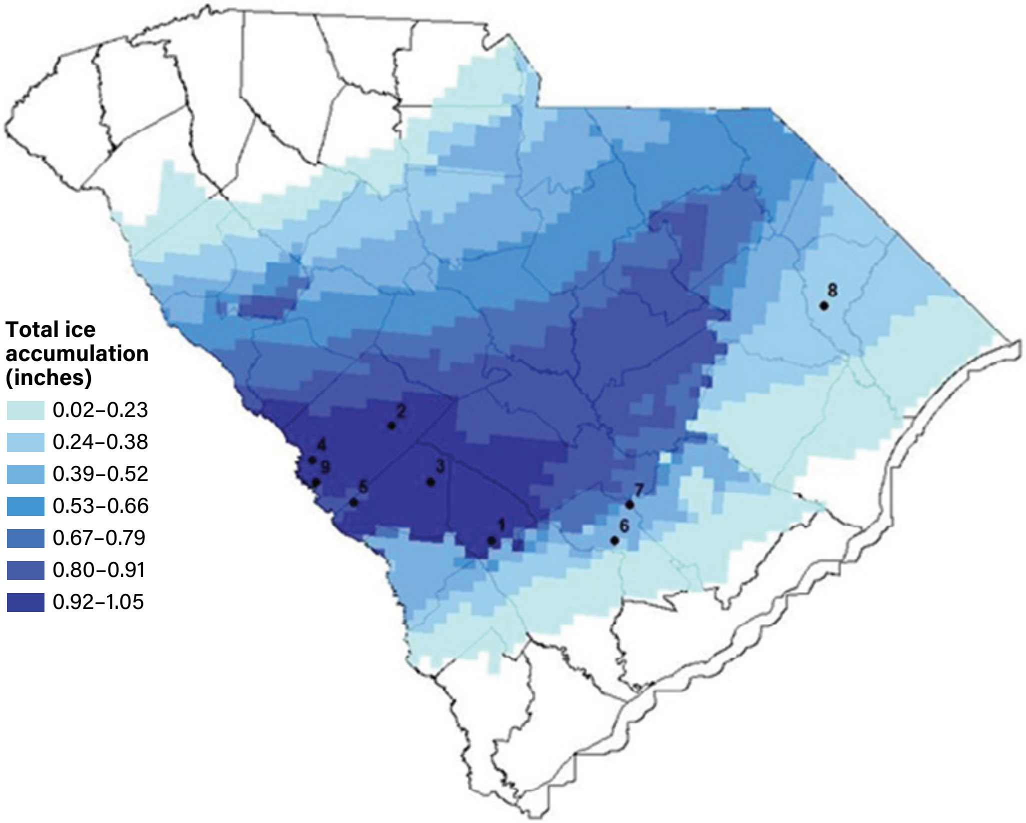

Figure 9.1—Levels of ice accumulation in South Carolina from the 2014 ice storm denoted by different colors (Data source: South Carolina Forestry Commission). Nine sites (1–9) were sampled immediately after the ice storm (Lu and others 2020). Study site 7 is Beidler Forest, where permanent plots were set up for long-term monitoring.

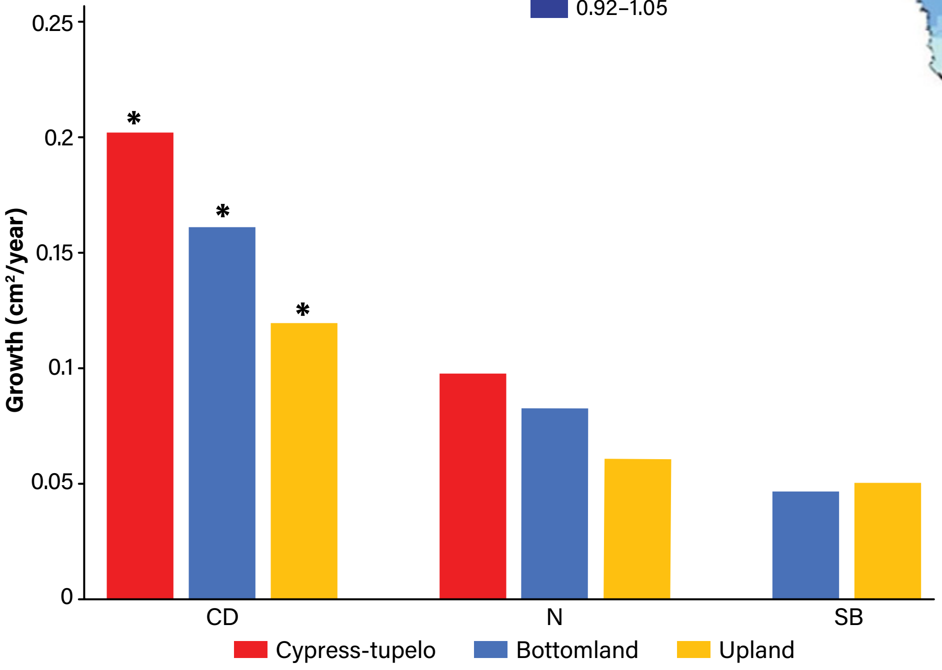

Figure 9.2—Mean annual basal area growth among forest types and damage categories are compared at Beidler Forest in 2018. CD = crown damage; N = no damage; SB = snapped bole. An asterisk indicates mean annual growth is significantly different between the damage categories at $\alpha = 0.05$.

radial growth index, which was calculated as the annualized mean increment for the 4 years after storm injury (2014–2017) divided by the annualized mean increment for the 4 years before the storm injury (2010–2013) determined through tree core analyses. Tree health was analyzed using only descriptive statistics because of the low frequency of observations.

RESULTS AND DISCUSSION

Damage and Mortality

Ice storm damage can have lasting effects on the mortality of southern forests, with an increase from 3.4 percent immediately after the storm to 13.1 percent 4 years later. The mortality rate was much higher than the mean annual mortality of <1 percent in the Southeastern United States (Klos and others 2009). For trees >5 cm d.b.h., mortality from damage was dependent upon the category of damage sustained from the ice storm and the forest type. Root-sprung trees and snapped trees were more likely to perish over time than those with crown damage. Crown damage, the most common type of damage sustained from an ice storm, does not impact the probability of mortality, suggesting that trees with crown damage recovered during the 4 years after the ice storm. The cypress-tupelo community was the most resistant to ice storm damage because of dominant species such as bald cypress showing storm-resistant traits, including narrow, symmetrical crowns, deciduous leaves, and strong buttressed stems. The dominant species in the bottomland and upland forest types, such as laurel oak, had qualities associated with higher susceptibility to ice damage such as asymmetry, winter phenology with larger surface area (marcescent and evergreen broadleaf trees), and sprawling crowns. A positive correlation with diameter size and damage was found, which is consistent with Lafon (2004). Smaller trees are more likely to die from severe damage as these trees may face more competition from other larger trees. Future research could include tree height as an additional measure of size to study the impact of ice storms.

Growth

Diameter size and growth rate were positively correlated, which is consistent with Bragg and others (2010). Surprisingly, the highest annual growth rates were found in trees that sustained crown damage in all forest types (fig. 9.2), which may be due to the probability of these trees being in the vicinity of other crown-damaged trees or areas with higher tree mortality due to the ice storm. The increase in light level must have been large enough to overcome the loss of photosynthetic area from crown damage. However, crown damage intensity affected neither basal area (by d.b.h. measurement) nor radial growth (by analyzing tree cores). We note that our sample size was limited by a low number of live trees with severe crown damage, which likely decreased the statistical power of the test.

Recovery

Overall, 14.2 percent of surviving trees are in growth decline, while 65.3 percent experienced no change, and 20.5 percent are in recovery since the storm in 2014. The forest type with the most trees in decline is the bottomland community at 18.9 percent. Interestingly, the bottomland community also has the highest number of recovering trees at 22.2 percent. Large trees (d.b.h. >11 cm) were the most impacted by the ice storm, with 30 percent having experienced growth changes (recovery or decline), while small trees were almost entirely unaffected due to their position in the canopy, suggesting that canopy position should also be evaluated with diameter size.

Forest Health

Overall, 6.1 percent (184 of 3,032) of surviving trees had some sort of implication to their health. However, the visual health data were skewed toward smaller (shorter) trees since visual estimations of foliar damage were difficult for taller trees.

CONCLUSIONS

Ice storms may be infrequent, but their impacts can have a lasting legacy on the remaining trees for years. The accumulated mortality increased by about 10 percent over the 4 years after the ice storm. Damage severity had a positive correlation with mortality, and trees with damage categories of uprooting and snapped bole were more likely to perish than those with crown damage. Evergreen broadleaf and marcescent trees were significantly more likely to perish than deciduous trees. Small-diameter trees were also more likely to perish than larger ones. The cypress-tupelo swamp is the community that is most resistant to ice storms, with significantly lower mortality in trees >5 cm d.b.h. than the two drier (bottomland and upland) communities. Trees with d.b.h >11 cm are the most dynamic in changes in growth after the storm, with >30 percent experiencing recovery and >30 percent experiencing decline, while most smaller trees remain steady in post-storm growth rates.

For more information, contact:
G. Geoff Wang, gwang@clemson.edu

LITERATURE CITED

Bennett, I. 1959. Glaze: its meteorology and climatology, geographical distribution, and economical effects. Tech. Rep. EP-105. Natick, MA: U.S. Army Quartermaster Research & Engineering Center, Environmental Protection Research Division. 217 p.

Bragg, D.C.; Shelton, M.G. 2010. Recovery of planted loblolly pine 5 years after severe ice storms in Arkansas. Southern Journal of Applied Forestry. 34(1): 13–20. https://doi.org/10.1093/sjaf/34.1.13.

Bragg, D.C.; Shelton, M.G.; Zeide, B. 2003. Impacts and management implications of ice storms on forests in the Southern United States. Forest Ecology and Management. 186: 99–123. https://doi.org/10.1016/S0378-1127(03)00230-5.

Changnon, S.A.; Karl, T.R. 2003. Temporal and spatial variations of freezing rain in the contiguous United States: 1948–2000. Journal of Applied Meteorology. 42: 1302–1315. https://doi.org/10.1175/1520-0450(2003)042<1302:TASVOF>2.0.CO;2.

Irland, L.C. 2000. Ice storms and forest impacts. Science of the Total Environment. 262: 231–242. https://doi.org/10.1016/S0048-9697(00)00525-8.

Klos, R.J.; Wang, G.G.; Bauerle, W.L.; Rieck, J.R. 2009. Drought impact on forest growth and mortality in Southeast USA: an analysis using Forest Health and Monitoring data. Ecological Applications. 19: 699–708. https://doi.org/10.1890/08-0330.1.

Lafon, C.W. 2004. Ice-storm disturbance and long-term forest dynamics in the Adirondack Mountains. Journal of Vegetation Science. 15: 267–276. https://doi.org/10.1111/j.1654-1103.2004.tb02261.x.

Lu, D.L.; Pile, L.S.; Yu, D. [and others]. 2020. Differential responses of tree species to a severe ice storm and their implications to forest composition in the Southeast United States. Forest Ecology and Management. 468: 118177. https://doi.org/10.1016/j.foreco.2020.118177.

South Carolina Forestry Commission. 2014. Timber damage assessment. https://www.state.sc.us/forest/2014winterstorm.htm [Date accessed: January 4, 2022].

CHAPTER 10

Investigating the Extent, Severity, and Causes of Sugarberry Mortality in the Southeastern United States

Michael Ulyshen
Emilee Poole

INTRODUCTION

Numerous instances of sugarberry (*Celtis laevigata*) mortality or dieback have been reported over the last 75 years in Europe and North America (Poole and others 2021). While most events were brief and thought to be caused by physical damage, environmental stress, or temporary eruptions of native pest species, more protracted episodes of mortality have also been reported. In Europe, European hackberry (*C. australis* L.) decline has been reported since 1949, and several pathogens (phytoplasma and fungi) as well as their interactions with insect damage and drought have been implicated in recent mortality events (Bertaccini and others 1996, Linaldeddu and others 2016). Louisiana was the location of an estimated 3 million acres affected by *Celtis* mortality between 1988 and 1990, which was the worst episode previously reported from North America. Similar symptoms were reported in Mississippi during the same period (Solomon and others 1997). A specific cause was not identified in that study, although a nonnative plant-feeding insect was suspected to play a role in the mortality.

The Southeastern United States is currently experiencing the worst episode of *Celtis* mortality ever reported in North America. Based on observations of dead and dying sugarberry from Columbia, SC, in 2009 (Andy Boone, personal communication[1]), this problem has been developing and expanding for more than 10 years. Sugarberry, one of six *Celtis* species native to North America, is common in riparian areas. It can grow as tall as 24–30 m and live an average of 150 years (Duncan and Duncan 2000, Tirmenstein 1990). To our knowledge, mortality is currently limited to sugarberry, and although sugarberry is not widely used for timber, there are multiple reasons to be concerned about widespread mortality (Poole and others 2021). This species produces berries that provide mast to wildlife species such as multiple bird species, small game, and deer. It is also a host plant used by several butterfly species. While sugarberry is a common riparian species, it is also now an urban species planted for shade in parks and yards, and is found as street trees and fencerows. Sugarberry also is considered of value for pulp production (Duncan and Duncan 2000, Tirmenstein 1990). Although mortality is most obvious among urban and residential trees, forest trees are also affected and even those growing in riparian zones are dying at alarming rates.

Here we summarize findings from ongoing research aimed at (1) describing patterns of sugarberry dieback and mortality at a single site in North Augusta, SC, (2) determining the spatial extent and spread of the mortality in the Southeastern United States, and (3) investigating what role, if any, insects are playing in the death of trees. These three study areas are described separately below.

---

[1] *Personal communication. 2021. A. Boone, President, DendroDiasnostics, Inc., 1901 Martin Rd., Chapin, SC 29036.*

How to cite this chapter:

Ulyshen, Michael; Poole, Emilee. 2022. Investigating the extent, severity, and causes of sugarberry mortality in the Southeastern United States. In: Potter, Kevin M.; Conkling, Barbara L., eds. Forest Health Monitoring: national status, trends, and analysis 2021. Gen. Tech. Rep. SRS-266. Asheville, NC: U.S. Department of Agriculture Forest Service, Southern Research Station: 159–165. https://doi.org/10.2737/SRS-GTR-266-Chap10.

METHODS

Patterns of Sugarberry Dieback and Mortality

Beginning in October 2015, we established a long-term monitoring site at a single location in North Augusta, SC. We selected a total of 131 trees (11–69 cm in diameter) for long-term monitoring of dieback and mortality. All trees that could be relocated were used to assess mortality after 5 years. A subset of 72 trees was selected, and the trees were monitored monthly during the years 2016–2018. We monitored canopy conditions over time using a crown class rating system adapted from Solomon and others (1997) with the following rating categories (illustrations of the categories can be seen in fig. 2 in Poole and others [2021]):

1. No discernable crown loss
2. <10-percent crown loss
3. 11–33-percent crown loss
4. 34–66-percent crown loss
5. 67–99-percent crown loss
6. Dead

Spatial Extent and Spread of Sugarberry Mortality

Although it was not possible to systematically assess the health of sugarberry populations throughout the range of the species, we attempted to identify areas experiencing high sugarberry mortality in parts of South Carolina and Georgia. This included trips around Columbia, SC, Savannah, GA, and several locations along the Savannah River south of Augusta, GA. Because the crown conditions of sugarberry were highly variable, in part due to damage caused by the hackberry woolly aphid (*Shivaphis celti* Das) (see below), we were very conservative in classifying a site as affected.

Role of Insects

Our research on insects potentially contributing to sugarberry mortality has focused on two species that are common across the affected area. First, insect egg masses found on the bark of dying sugarberry trees were determined to be from a native species of buprestid beetle, *Agrilus macer* LeConte. Very little was known about the biology or distribution of this species, so we carried out several studies to better understand its biology and native range (Poole and others 2019). First, we felled five sugarberry trees to determine the number of egg masses per unit bark area. We used this data along with information on the number of eggs laid per egg mass (based on laboratory dissections) to determine the density of beetle larvae attacking declining trees in our area. We also obtained museum records to better understand the known distribution of the species.

The second insect species we are studying is the hackberry woolly aphid. This nonnative species was first detected in North America in the 1990s and often attacks sugarberry in great numbers. The density of aphids is often high enough to cause obvious stress to trees, including the formation of thick layers of sooty mold that grows as a result of copious honeydew production and premature leaf fall. Research is underway to determine cumulative effects on sugarberry health from repeated attacks by this species. More specifically, we are comparing the carbohydrate reserves in the roots and phenolic profiles of leaves of potted sugarberry trees that have been chemically protected (imidacloprid and Ecotrol® Plus, a broad spectrum botanical insecticide) from the aphids to those of control trees that are not protected from these insects.

RESULTS AND DISCUSSION

Patterns of Sugarberry Dieback and Mortality

The canopy conditions of trees at the beginning of our monitoring period ranged widely, with 4, 29, 21, 33, and 44 trees receiving initial ratings of 1, 2, 3, 4, and 5, respectively. To understand inter- and intra-annual variation in crown conditions, monthly evaluations were conducted by the same individual for 3 years thereafter (2016–2018). Final mortality was recorded for all tagged trees after 5 years in September 2020.

As shown in figure 2 in Poole and others (2021), symptomatic trees were characterized by thinning canopies, small and chlorotic leaves, and branch dieback. Of the original 131 trees monitored in North Augusta, SC, 36 trees had been cut down before mortality could be confirmed. Of the remaining 95 trees, 51.6 percent had died by the end of the 5 years.

After 5 years, 13 of the original 72 monitoring trees had been cut down. Of the 59 remaining trees, 30 (50.8 percent) had died. Figure 10.1A shows that trees died throughout the 5-year study with a steady decrease in tree survivorship. Average crown rating over time (fig. 10.1B) indicates some seasonality in crown conditions with fall ratings tending to be higher (greater deterioration of crown conditions) with observable improvement in crown conditions (lower crown rating) in the spring. This was observed even with considerable variability in ratings among dates of observation.

The tree death rate was highly variable after first receiving a crown rating of 3 or higher, which was the point at which a tree was considered symptomatic. A total of 25 trees that were monitored monthly became symptomatic after May 2016 and died by September 2020. Over half of these (52 percent) died within 1 year of appearing symptomatic, six (24 percent) of which died within 3 months of first appearing symptomatic. Another 32 percent died within 1 to 2 years, 12 percent died within 2 to 3 years, and 4 percent died within 3 to 4 years. By contrast, 28 trees were alive but symptomatic at the end of the 5-year monitoring period. These remaining trees were symptomatic for more than 2 years, and 28.6 percent were symptomatic for at least 4 years (Poole and others 2021).

Spatial Extent and Spread of Sugarberry Mortality

Mortality appears to be most noticeable along the Savannah River near Augusta, GA, and near Columbia, SC. More recently, high mortality has been observed in Savannah, GA, and in neighboring coastal regions (Poole and others 2021) (fig. 10.2). Although dead sugarberry trees

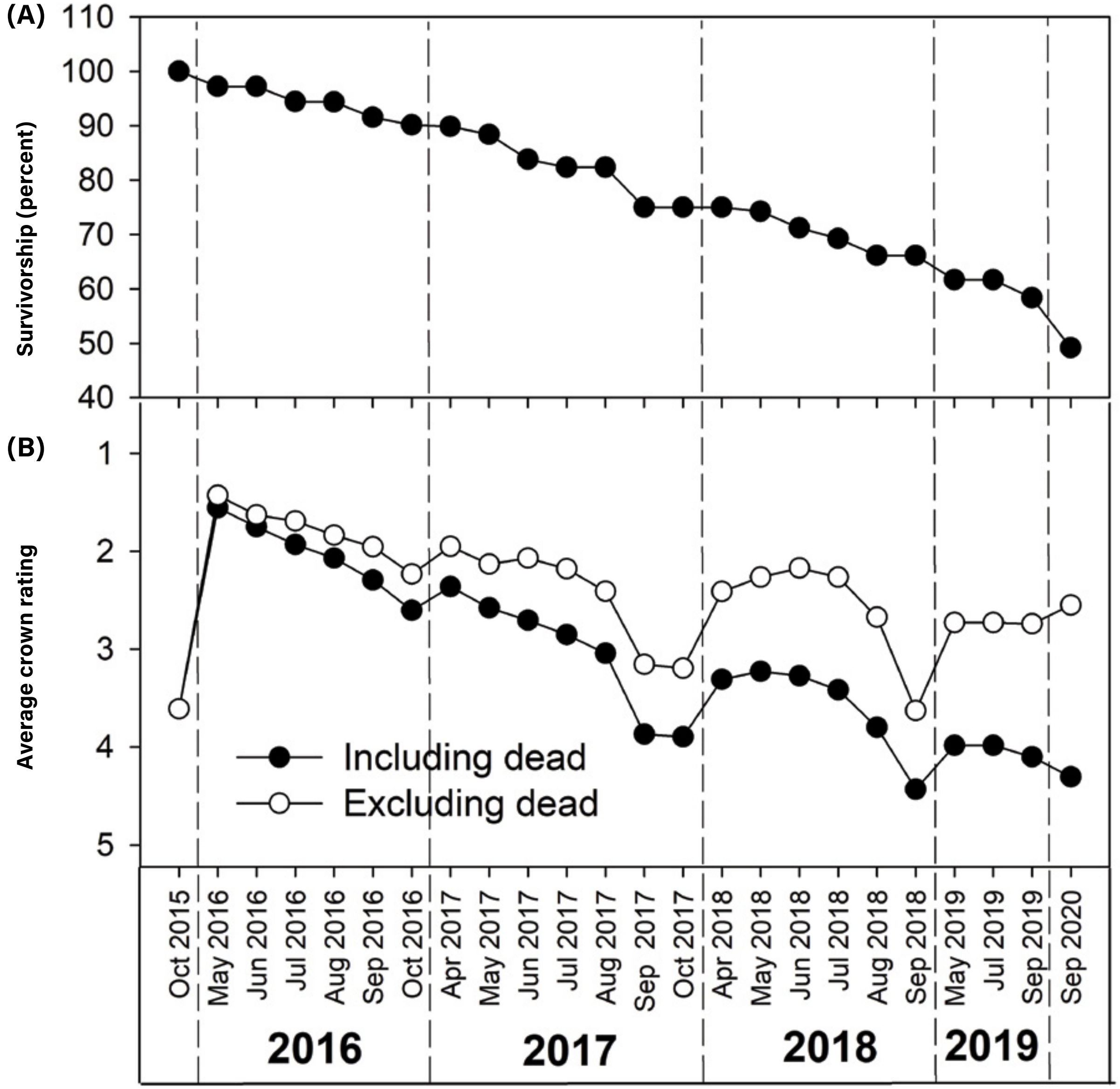

Figure 10.1—Long-term (2015–2020) monitoring data from North Augusta, SC. (A) Percentage of survivorship over time; (B) average crown rating of trees based on scores ranging from 1 (no discernable crown loss) to 6 (dead). Trees that were cut down before we could confirm mortality were not included in these calculations. Average ratings were calculated both including and excluding dead trees (black and white symbols, respectively). Vertical dashed lines separate calendar years. (From Poole and others 2021)

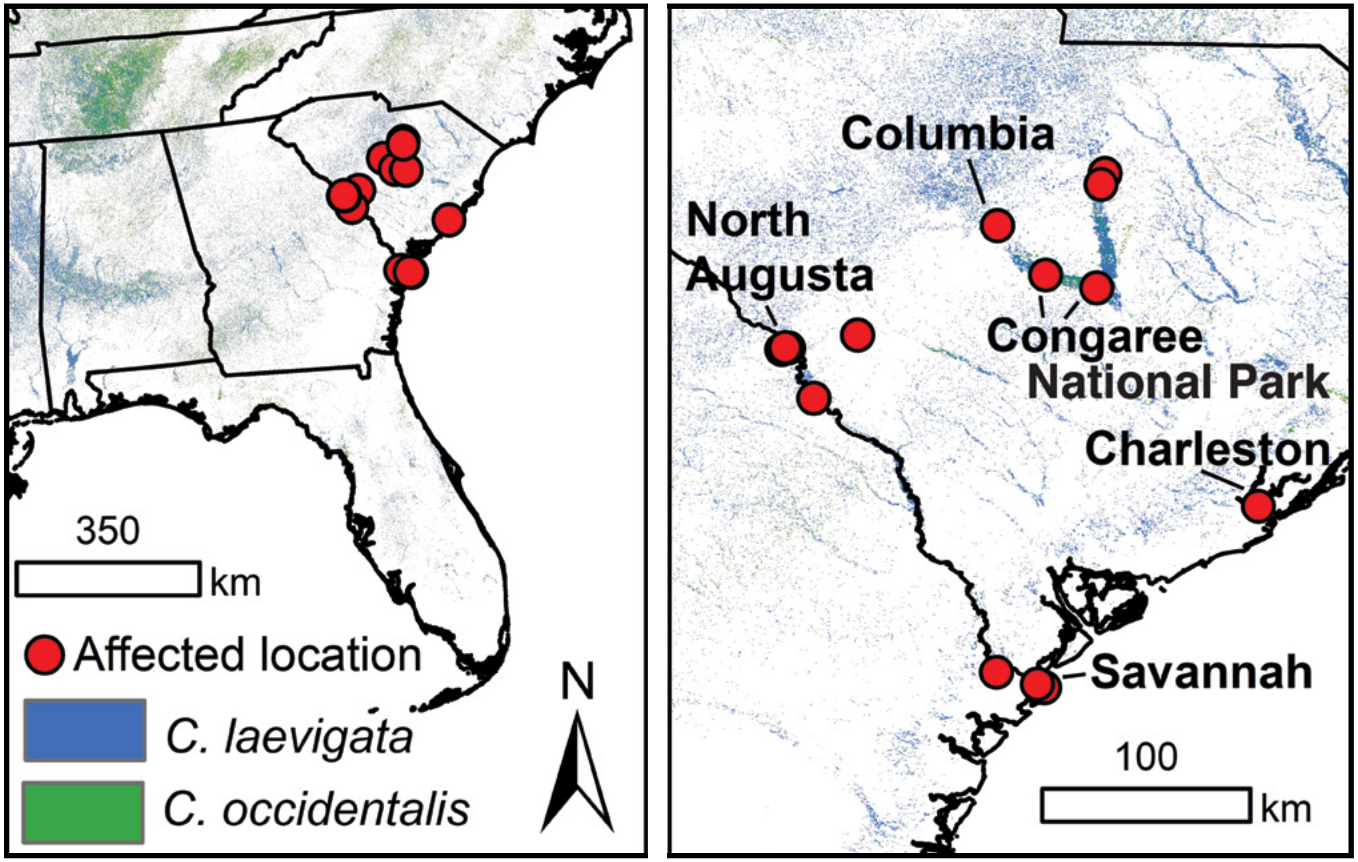

*Figure 10.2—Locations in South Carolina and Georgia known to be experiencing high levels of sugarberry mortality. Areas shaded in blue and green reflect the distributions of sugarberry (*Celtis laevigata*) and hackberry (*Celtis occidentalis*), respectively. (From Poole and others 2021)*

are more easily observed in urban areas, mortality is not limited to such areas. Indeed, trips to heavily forested places like Congaree National Park confirm that this is a serious issue facing forests as well. Because the mortality cause is still unknown, the beginning and rate of spread of the problem in the Southeast cannot currently be determined. We do know, however, that unusual sugarberry mortality was first observed in Columbia, SC, and Savannah, GA, in 2009 (Andrew Boone, personal communication [see footnote 1]) and 2019 (Bates and others 2020), respectively. With about 200 km separating these two cities, this suggests the problem is either expanding rapidly or is caused by widespread factors. Based on our observations, we suspect the problem has reached far beyond the areas depicted in figure 10.2. Because sugarberry is found throughout the Southeastern United States, this problem has the potential to spread throughout other States, which could already be occurring unnoticed. Furthermore, if other species of *Celtis* are also susceptible, this problem with mortality could become a forest health challenge throughout much of North America.

Role of Insects

We found the buprestid beetle, *A. macer*, was attacking some trees at incredible densities, with some trees having hundreds of thousands of eggs (Poole and others 2019). We made dissections of logs to observe the different larval stages of the beetle and made observations of females preparing egg masses. We also collected data on the seasonality of the adult beetles using flight-intercept traps. A survey of museum records found that this beetle has formerly been captured throughout the Southern United States, including the Southeast and is thus not new to this area (Poole and others 2019). Our observations indicate that it only attacks weakened or dying trees and that relatively healthy trees are able to overcome attacks from this species. Taken together, our results indicate that *A. macer* is only a secondary pest on sugarberry and this species has experienced a large population increase in response to the high availability of suitable host material within the affected area. As our latest research on how the aphid *S. celti* affects potted sugarberry health is ongoing and unpublished, we do not yet have data to share from this work.

CONCLUSIONS

The mortality reported here from the Southeastern United States represents the most severe, protracted, and extensive episode of *Celtis* mortality ever reported from North America. Mortality has been observed for at least 10 years, and large parts of Georgia and South Carolina are being affected. The mortality data reported in this summary are from one site, North Augusta, SC. The patterns of mortality, however, appear to be consistent with the rest of the affected area. It is concerning that 51.6 percent of our monitoring trees died after 5 years. Moreover, the crown conditions of the remaining trees continue to deteriorate. If the trees that were cut before we could determine mortality had died, or would have died, the mortality would have been nearly 65 percent over this period of time. It is important to note that based on the canopy class ratings we recorded, trees showed high variability in how quickly they died after first symptoms were observed. Some died in a few months while others continued to live for several years. A question requiring continued monitoring is whether affected trees can recover, specifically when competition may be reduced if neighboring trees die (Zhang and others 2017).

This problem has the potential to impact much of the Southeast, since sugarberry occurs throughout the region and its loss will cause many negative ecological and economic impacts. For example, loss of sugarberry trees has the potential to exacerbate the spread and dominance of invasive shrubs such as Chinese privet (*Ligustrum sinense* [Lour.]) in the forest understory.

For more information, contact:
Michael Ulyshen, michael.d.ulyshen@usda.gov

ACKNOWLEDGMENTS

We thank our collaborators and many others who helped with this project either directly or indirectly. We are particularly grateful to Scott Horn, Steve Fraedrich, Michelle Cram, Rabiu Olatinwo, David Shelley, David Jenkins, Chip Bates, Chris Barnes, Roy Kibler, Patrick Anderson, Lynne Womack, Caterina Villari, Afaq Niyas, and Kris Braman. We also thank Chris Asaro and Kevin Chase for providing helpful comments on an early draft of this report.

LITERATURE CITED

Bates, C.; McClure, M.; Womack, L.; Barnes, C. 2020. Georgia Forestry Commission forest health highlights. Dry Branch, GA: Georgia Forestry Commission. 14 p.

Bertaccini, A.; Mittempergher, L.; Vibio, M. 1996. Identification of phytoplasmas associated with a decline of European hackberry (*Celtis australis*). Annals of Applied Biology. 128(2): 245–253. https://doi.org/10.17660/ActaHortic.1996.432.38.

Duncan, W.H.; Duncan, M.B. 2000. Trees of the Southeastern United States. Athens, GA: University of Georgia Press. 336 p.

Linaldeddu, B.; Alves, A.; Phillips, A.J.L. 2016. *Sardiniella urbana* gen. *et* sp. nov., a new member of the Botryosphaeriaceae isolated from declining *Celtis australis* trees in Sardinian streetscapes. Mycosphere. 7(7): 893–905. https://doi.org/10.5943/mycosphere/si/1b/5.

Poole, E.M.; Ulyshen, M.D.; Horn, S. [and others]. 2019. Distribution and biology of *Agrilus macer* (Coleoptera: Buprestidae), a species associated with sugarberry (*Celtis laevigata*) mortality in the Southeastern United States. Annals of Forest Science. 76: 7. https://doi.org/10.1007/s13595-018-0794-7.

Poole, E.M.; Ulyshen, M.D.; Horn, S. [and others]. 2021. Progression of sugarberry (*Celtis laevigata*) dieback and mortality in the Southeastern United States. Journal of Forestry. 119: 266–274.

Solomon, J.D.; Wilson, A.D.; Leininger, T.D. [and others]. 1997. Sugarberry dieback and mortality in southern Louisiana: cause, impact, and prognosis. Res. Pap. SRS-9. Asheville, NC: U.S. Department of Agriculture Forest Service, Southern Research Station. 19 p. https://doi.org/10.2737/SRS-RP-009.

Tirmenstein, D.A. 1990. *Celtis laevigata* var. *reticulata*. In: Fire Effects Information System. Missoula, MT: U.S. Department of Agriculture Forest Service, Rocky Mountain Research Station, Missoula Fire Sciences Laboratory. https://www.fs.fed.us/database/feis/plants/tree/cellaer/all.html. [Date last accessed: October 22, 2021].

Zhang, Z.; Papaik, M.J.; Wang, X. [and others]. 2017. The effect of tree size, neighborhood competition and environment on tree growth in an old-growth temperate forest. Journal of Plant Ecology. 10(6): 970–980.

CHAPTER 11

Ecological Consequences of Mountain Pine Beetle Outbreaks in the Intermountain West

Christopher J. Fettig
A. Steven Munson
Justin B. Runyon
Leif A. Mortenson
Brytten E. Steed
Kenneth E. Gibson
Carl L. Jørgensen
Stephen R. McKelvey
Joel D. McMillin
Jackson P. Audley
Jose F. Negrón

INTRODUCTION

Mountain pine beetle (*Dendroctonus ponderosae*) is the most notable forest insect in western North America, where it colonizes at least 15 pine species but primarily lodgepole pine (*Pinus contorta*). Since 2000, >10 million ha have been affected by mountain pine beetle, which represents almost half of the total area impacted by all bark beetles combined in the Western United States during this period (Fettig and others 2021). In addition to mountain pine beetle playing an important role in the ecology of western forests, extensive levels of tree mortality resulting from outbreaks may have many other impacts affecting, for example, aesthetics, recreation, fire risk and severity, human safety, and timber production. As such, the extent and severity of 21st century outbreaks have triggered concerns about short- and long-term impacts to forests and the many ecosystem goods and services they provide. The primary objective of our study (INT-EM-17-01) was to determine the causes and rates of tree mortality during and after mountain pine beetle outbreaks based on a network of plots in five States (Colorado, Idaho, Montana, Utah, and Wyoming) and to describe changes in forest conditions from 2004–2019.

METHODS

A network of 125 circular plots (0.081 ha each) was established across Colorado, Idaho, Montana, Utah, and Wyoming (*n* = 25 per State) in 2010 (see fig. 1 in Audley and others 2020). For inclusion in the network, plots were required to be >50-percent lodgepole pine by basal area, and to contain a minimum of 10 lodgepole pines >13.9 cm diameter at breast height (d.b.h.) with evidence of at least 2 of these trees being colonized and/or killed by mountain pine beetle within the last 3 years. Plots meeting these criteria were randomly selected in groups of five, with plots within groups separated by ≥100 m. Within States, groups were separated by >1.6 km (mean distance ± standard error of the mean [SEM] = 23.4 ± 3.0 km). Fifteen plots were lost to high-severity wildfires in Idaho, and three plots were lost to tree cutting in Wyoming. These plots were excluded from our analyses.

After plot establishment, all trees ≥7.62 cm d.b.h. were tagged and the species, d.b.h., total height, height to the base of the live crown, status (live or dead), causal agent of mortality (when applicable), and year of death (when applicable) were recorded. For trees that died prior to plot establishment in 2010, year of death was estimated based on the color of faded needles in the crown and degree of needle and twig retention based on Klutsch and others (2009) (i.e., 1 year prior, >90-percent retention of yellow and/or red needles; 2 years prior, ≥50–90-percent retention of red needles; 3 years prior, <50-percent retention of red needles; 4 years prior, no needle retention but small and large [5–7.62 cm diameter] twigs remain; 5 years prior, only large twigs remain; 6 years prior, both small and large twigs no longer remain). For trees that died prior to 2004, year of death could not be estimated by twig retention. As such, these trees were ignored and excluded from our analyses. A section of bark ~625 cm^2 was removed from dead trees with a hatchet at ~1.7 m in height to determine if bark beetle galleries were

How to cite this chapter:

Fettig, Christopher J.; Munson, A. Steven; Runyon, Justin B.; Mortenson, Leif A.; Steed, Brytten E.; Gibson, Kenneth E.; Jørgensen, Carl L.; McKelvey, Stephen R.; McMillin, Joel D.; Audley, Jackson P.; Negrón, Jose F. 2022. Ecological consequences of mountain pine beetle outbreaks in the Intermountain West. In: Potter, Kevin M.; Conkling, Barbara L., eds. Forest Health Monitoring: national status, trends, and analysis 2021. Gen. Tech. Rep. SRS-266. Asheville, NC: U.S. Department of Agriculture Forest Service, Southern Research Station: 167–175. https://doi.org/10.2737/SRS-GTR-266-Chap11.

present. The shape, distribution, and orientation of galleries are commonly used to distinguish among bark beetle species. In some cases, the presence of entrance holes, boring dust, pitch tubes, and deceased bark beetles was used to supplement identifications based on galleries. We attributed tree mortality to colonization by bark beetles only when these diagnostic characteristics were observed. Trees were partitioned into 5-cm d.b.h. classes with midpoints of 10, 15, 20, 25, 30, and >32.5 cm in order to analyze tree density and tree mortality by causal agent within d.b.h. class.

Three 16.1-m Brown's transects (Brown 1974) were established on each plot at 0°, 120°, and 240° from plot center to measure fuels (data not shown). At the end of each transect, a 1-m^2 subplot was established to estimate forest floor composition, and, beginning in 2012, a complete census of each plot was conducted for nonnative invasive plants (hereafter invasive weeds). A 3.6-m radius (0.004-ha) subplot was established at each plot center to estimate tree regeneration. All seedlings and saplings within the 0.004-ha subplot were identified to species and designated as seedlings (≤0.3 m tall) or saplings (>0.3 m tall and <7.6 cm d.b.h.). Tree mortality and snag fall occurrences were recorded each year (2010–2019) while all other metrics were remeasured every fourth year (2010, 2014, 2018). In 2014 and 2018, we also surveyed all plots by walking linear transects (about 5 m apart) spanning each plot and recorded the presence, identity, and abundance (number of aboveground stems) of invasive weeds.

More detailed information concerning methods can be found in Audley and others (2020) for study of seedlings, saplings, and trees; in Runyon and others (2020) for study of understory vegetation, including invasive weeds; and in Audley and others (2021) for study of lodgepole pine snags, including snag longevity, factors influencing snag longevity, and modeling of survival and hazard functions.

RESULTS AND DISCUSSION

Across our network of plots, tree mortality attributed to mountain pine beetle peaked in 2007 in all States except Colorado (fig. 11.1). A total of 5,107 trees died; 98.6 percent were lodgepole pine. We identified 15 mortality agents, including mountain pine beetle (3,512 trees); unknown causes (941 trees); pine engraver (*Ips pini*) (265 trees); wind breakage and/or adjacent tree fall (258 trees); *Pityogenes knechteli*/*Pityophthorus confertus* bark beetles (242 trees); suppression (53 trees); spruce beetle (*D. rufipennis*) (32 trees); root disease (22 trees); western balsam bark beetle (*Dryocoetes confusus*) (10 trees); lodgepole pine dwarf mistletoe (*Arceuthobium americanum*) (9 trees); stem diseases (6 trees); woodborers (5 trees); North American porcupine (*Erethizon dorsatum*) (4 trees); mule deer (*Odocoileus hemionus*) (2 trees); and lodgepole pine beetle (*D. murrayanae*) (1 tree). On occasion, more than one agent was identified for the same tree, and therefore the total above (among agents) exceeds the total number of trees killed. While we were unable to confidently identify a mortality agent (unknown causes) for 18.4 percent of trees, mountain pine beetle was likely a contributing

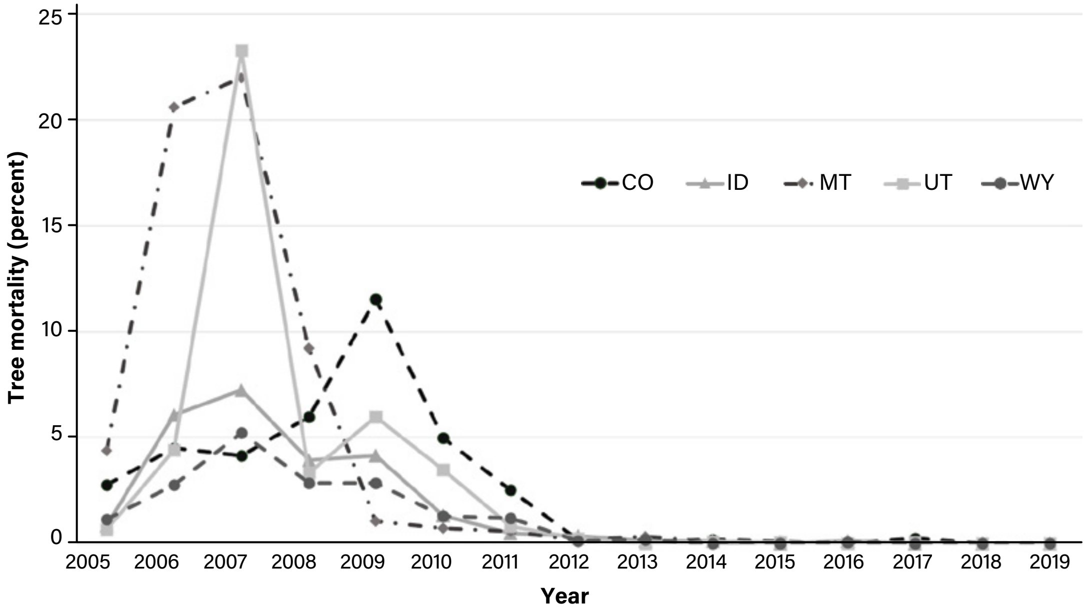

Figure 11.1—Mean percentage of pines killed during and after mountain pine beetle outbreaks in Colorado, Idaho, Montana, Utah, and Wyoming, 2005–2019. (Adapted from Audley and others 2020)

factor in many of these deaths as sampling for bark beetle galleries was limited to a small portion of the lower bole. No patterns were observed among trees with the mortality agent classified as unknown causes.

Data describing forest conditions in 2004, 2010, 2014, and 2018, and comparisons among States are provided in table 11.1. Overall, significant reductions in mean d.b.h. (by 5.3 percent), mean quadratic mean diameter (q.m.d.) (by 8.6 percent), mean tree height (by 15.9 percent), mean number of trees (by 40.8 percent), mean basal area (by 52.9 percent), and mean stand density index (SDI) (by 51.8 percent) were observed (Audley and others 2020). Despite the high levels of mortality in lodgepole pine, lodgepole pine remained the dominant tree species, and no difference was observed in the overall prevalence (percentage) of lodgepole pine between 2004 and 2018. Notably, subalpine fir (*Abies lasiocarpa*) significantly increased in prevalence on plots where it occurred prior to the outbreak (Audley and others 2020).

Significant reductions in tree abundance were observed for all d.b.h. classes except the smallest (10 cm d.b.h). Compared to all other causes of tree mortality combined, mountain pine beetle killed a significantly greater percentage

Table 11.1—Changes in forest structure and composition (mean ± standard error of the mean [SEM]) during and after mountain pine beetle outbreaks in lodgepole pine forests in the Intermountain West

	Colorado	Idaho	Montana	Utah	Wyoming	All
2004						
d.b.h. (cm)	18.2 ± 0.2 a	17.8 ± 0.2 a	16.4 ± 0.1 b	16.6 ± 0.1 b	17.1 ± 0.3 b	17.1 ± 0.1
q.m.d. (cm)	21.1 ± 0.5 a	19.9 ± 0.8 a	19.4 ± 1.0 a	21.7 ± 1.9 a	21.9 ± 0.9 a	20.9 ± 0.5
Tree height (m)	13.5 ± 0.1 d	17.2 ± 0.2 b	18.0 ± 0.1 a	15.0 ± 0.1 c	15.1 ± 0.2 c	15.7 ± 0.1
Trees/ha	1,169.8 ± 87.4 ab	1,364.0 ± 96.1 a	1,390.2 ± 112.1 a	1,493.0 ± 181.1 a	772.2 ± 68.6 b	1,233.2 ± 63.3
Snags/ha	11.4 ± 1.7 b	71.7 ± 21.9 a	32.1 ± 7.9 ab	44.5 ± 9.9 a	16.8 ± 3.5 ab	30.7 ± 4.2
Basal area (m^2/ha)	38.4 ± 1.8 a	41.1 ± 2.3 a	36.1 ± 1.8 a	40.1 ± 2.5 a	26.8 ± 1.2 b	36.1 ± 1.0
Stand density index	822.9 ± 41.7 a	895.7 ± 46.2 a	802.7 ± 39.4 a	854.3 ± 41.5 a	561.9 ± 21.5 b	778.7 ± 20.4
Pinus contorta (percent)	84.7 ± 3.0 bc	81.6 ± 3.5 c	98.2 ± 0.5 a	89.8 ± 2.9 abc	94.5 ± 1.6 ab	90.8 ± 1.2
Pinus ponderosa (percent)	0.7 ± 0.5 a	0.0 ± 0.0 a	0.0 ± 0.0 a	0.0 ± 0.0 a	0.0 ± 0.0 a	0.2 ± 0.1
Pinus flexilis (percent)	5.1 ± 2.2 a	0.0 ± 0.0 b	0.0 ± 0.0 b	0.0 ± 0.0 b	0.3 ± 0.3 b	1.3 ± 0.5
Abies lasiocarpa (percent)	3.4 ± 1.0 b	16.7 ± 3.2 a	0.3 ± 0.9 c	4.9 ± 1.7 b	3.7 ± 1.3 bc	4.3 ± 0.7
Populus tremuloides (percent)	1.4 ± 0.8 a	0.0 ± 0.0 ab	0.0 ± 0.0 b	3.4 ± 2.4 ab	0.5 ± 0.5 ab	1.2 ± 0.6
Pseudotsuga menziesii (percent)	0.3 ± 0.2 a	0.1 ± 0.1 a	0.7 ± 0.3 a	0.0 ± 0.0 a	0.5 ± 0.3 a	0.4 ± 0.1
Picea engelmannii (percent)	4.5 ± 1.5 a	1.6 ± 0.6 a	0.8 ± 0.3 a	1.8 ± 1.0 a	0.4 ± 0.2 a	1.9 ± 0.4
2010						
d.b.h. (cm)	15.3 ± 0.2 b	16.8 ± 0.3 a	13.4 ± 0.2 c	14.4 ± 0.1 d	14.3 ± 0.2 d	14.7 ± 0.1
q.m.d. (cm)	16.9 ± 0.4 a	18.7 ± 0.8 a	17.5 ± 1.7 a	20.3 ± 2.7 a	19.0 ± 1.3 a	18.4 ± 0.8
Tree height (m)	11.2 ± 0.1 d	14.6 ± 0.2 a	14.3 ± 0.1 a	12.5 ± 0.1 b	12.1 ± 0.2 c	12.8 ± 0.1
Trees/ha	813.0 ± 71.3 a	952.5 ± 60.8 a	717.1 ± 88.7 a	988.4 ± 144.7 a	586.3 ± 72.7 a	798.0 ± 48.0
Snags/ha	363.2 ± 30.8 b	464.5 ± 53.3 ab	680.5 ± 50.3 a	563.9 ± 54.8 ab	199.9 ± 18.6 c	460.1 ± 25.9
Basal area (m^2/ha)	18.1 ± 1.6 ab	25.7 ± 1.4 a	13.5 ± 1.7 b	18.4 ± 2.2 ab	14.1 ± 1.3 b	17.0 ± 0.9
Stand density index	419.7 ± 37.0 ab	570.9 ± 28.2 a	309.1 ± 35.0 b	396.3 ± 40.6 b	312.6 ± 25.0 b	380.5 ± 17.6
Pinus contorta (percent)	81.8 ± 3.9 b	78.7 ± 4.4 ab	95.9 ± 1.2 a	84.1 ± 3.9 ab	91.6 ± 2.2 ab	86.8 ± 1.6
Pinus ponderosa (percent)	0.6 ± 0.6 a	0.0 ± 0.0 a	0.0 ± 0.0 a	0.0 ± 0.0 a	0.0 ± 0.0 a	0.1 ± 0.1
Pinus flexilis (percent)	4.9 ± 2.3 a	0.0. ± 0.0 ab	0.0 ± 0.0 b	0.0 ± 0.0 b	1.1 ± 1.1 b	1.7 ± 0.7
Abies lasiocarpa (percent)	4.9 ± 1.6 b	18.9 ± 4.0 a	0.6 ± 0.5 c	8.3 ± 2.6 b	5.1 ± 1.7 bc	6.1 ± 1.0
Populus tremuloides (percent)	0.9 ± 0.5 a	0.0 ± 0.0 a	0.0 ± 0.1 a	4.1 ± 2.8 a	0.8 ± 0.8 a	1.5 ± 0.7
Pseudotsuga menziesii (percent)	0.5 ± 0.3 a	0.0 ± 0.0 a	2.2 ± 1.1 a	0.0 ± 0.0 a	0.8 ± 0.4 a	0.8 ± 0.3
Picea engelmannii (percent)	6.4 ± 2.4 a	2.3 ± 0.8 a	1.4 ± 0.6 a	3.6 ± 1.8 a	0.6 ± 0.3 a	3.1 ± 0.7

d.b.h. = diameter at breast height; q.m.d. = quadratic mean diameter.

Means ± SEMs followed by the same letter within rows are not significantly different (p >0.05).

(Continued)

Table 11.1 ***(Continued)*****—Changes in forest structure and composition (mean ± standard error of the mean [SEM]) during and after mountain pine beetle outbreaks in lodgepole pine forests in the Intermountain West**

	Colorado	Idaho	Montana	Utah	Wyoming	All
2014						
d.b.h. (cm)	15.5 ± 0.2 b	17.3 ± 0.3 a	14.4 ± 0.2 d	14.9 ± 0.1 cd	15.3 ± 0.2 bc	15.3 ± 0.1
q.m.d. (cm)	17.6 ± 0.4 a	19.0 ± 0.8 a	18.4 ± 2.0 a	20.8 ± 2.8 a	19.3 ± 1.4 a	19.0 ± 0.8
Tree height (m)	11.4 ± 0.1 d	14.9 ± 0.2 a	14.5 ± 0.1 a	12.8 ± 0.1 b	12.2 ± 0.2 c	13.0 ± 0.1
Trees/ha	696.3 ± 77.8 a	879.7 ± 59.6 a	718.6 ± 88.6 a	934.0 ± 135.6 a	567.2 ± 71.0 a	747.7 ± 46.6
Snags/ha	435.9 ± 29.1 b	481.8 ± 49.0 ab	695.3 ± 50.4 a	620.7 ± 61.4 ab	211.2 ± 16.6 c	497.8 ± 26.6
Basal area (m^2/ha)	16.3 ± 1.7 ab	24.3 ± 1.4 a	14.3 ± 1.7 b	18.2 ± 2.1 ab	14.1 ± 1.3 b	16.6 ± 0.8
Stand density index	373.4 ± 39.2 b	537.8 ± 27.7 a	323.2 ± 35.2 b	390.0 ± 37.3 ab	309.9 ± 27.1 b	367.8 ± 17.1
Pinus contorta (percent)	79.6 ± 4.2 b	75.5 ± 4.2 b	94.9 ± 1.4 a	84.8 ± 3.9 ab	88.3 ± 3.1 ab	85.8 ± 1.7
Pinus ponderosa (percent)	0.3 ± 0.3 a	0.0 ± 0.0 a	0.0 ± 0.0 a	0.0 ± 0.0 a	0.0 ± 0.0 a	0.1 ± 0.1
Pinus flexilis (percent)	6.7 ± 2.9 a	0.0 ± 0.0 b	0.0 ± 0.0 b	0.0 ± 0.0 b	1.3 ± 1.3 b	1.8 ± 0.8
Abies lasiocarpa (percent)	5.4 ± 1.8 bc	21.8 ± 3.8 a	0.7 ± 0.4 c	7.5 ± 2.5 b	7.1 ± 2.2 bc	6.7 ± 1.1
Populus tremuloides (percent)	1.2 ± 0.8 a	0.0 ± 0.0 a	0.0 ± 0.1 a	4.0 ± 2.7 a	1.2 ± 1.2 a	1.5 ± 0.7
Pseudotsuga menziesii (percent)	0.5 ± 0.3 a	0.1 ± 0.1 a	2.7 ± 1.4 a	0.0 ± 0.0 a	0.9 ± 0.4 a	0.9 ± 0.3
Picea engelmannii (percent)	6.2 ± 2.2 a	2.6 ± 0.9 a	1.7 ± 0.7 a	3.7 ± 1.8 a	1.3 ± 0.7 a	3.2 ± 0.7
2018						
d.b.h. (cm)	16.5 ± 0.2 b	17.8 ± 0.3 a	15.6 ± 0.1 c	15.5 ± 0.1 c	16.8 ± 0.2 b	16.2 ± 0.1
q.m.d. (cm)	17.9 ± 0.4 a	19.1 ± 0.7 a	18.7 ± 1.7 a	20.7 ± 2.6 a	19.4 ± 1.3 a	19.1 ± 0.8
Tree height (m)	11.4 ± 0.1 d	15.0 ± 0.2 a	14.5 ± 0.1 a	13.2 ± 0.1 b	12.4 ± 0.2 c	13.2 ± 0.1
Trees/ha	699.3 ± 81.2 a	842.6 ± 51.1 a	716.6 ± 85.7 a	861.9 ± 121.3 a	577.9 ± 67.4 a	729.8 ± 43.3
Snags/ha	389.9 ± 29.1 a	453.4 ± 35.5 a	547.6 ± 50.3 a	606.9 ± 66.7 a	166.2 ± 15.7 b	437.4 ± 26.2
Basal area (m^2/ha)	16.6 ± 1.8 ab	23.8 ± 1.5 a	15.4 ± 1.7 ab	17.9 ± 2.0 ab	15.0 ± 1.4 b	17.0 ± 0.8
Stand density index	379.4 ± 41.7 ab	524.6 ± 29.4 a	344.7 ± 35.7 b	383.7 ± 36.0 ab	326.7 ± 27.5 b	375.0 ± 17.0
Pinus contorta (percent)	78.2 ± 4.3 b	73.4 ± 4.5 b	93.1 ± 2.0 a	85.2 ± 3.7 ab	85.7 ± 3.6 ab	84.4 ± 1.7
Pinus ponderosa (percent)	1.0 ± 0.7 a	0.0 ± 0.0 a	0.0 ± 0.0 a	0.0 ± 0.0 a	0.0 ± 0.0 a	0.2 ± 0.2
Pinus flexilis (percent)	6.5 ± 2.8 a	0.0 ± 0.0 b	0.0 ± 0.0 b	0.0 ± 0.0 b	2.3 ± 2.3 b	2.0 ± 0.8
Abies lasiocarpa (percent)	5.9 ± 1.9 b	23.4 ± 3.7 a	0.9 ± 0.6 c	7.9 ± 2.6 b	8.5 ± 2.6 b	7.4 ± 1.1
Populus tremuloides (percent)	1.6 ± 1.2 a	0.0 ± 0.0 a	0.0 ± 0.0 a	4.0 ± 2.8 a	1.6 ± 1.4 a	1.6 ± 0.8
Pseudotsuga menziesii (percent)	0.5 ± 0.3 a	0.5 ± 0.4 a	2.9 ± 1.5 a	0.0 ± 0.0 a	0.8 ± 0.4 a	1.0 ± 0.4
Picea engelmannii (percent)	6.2 ± 2.2 a	2.7 ± 0.9 a	3.1 ± 1.1 a	2.9 ± 1.3 a	1.1 ± 0.5 a	3.3 ± 0.7

d.b.h. = diameter at breast height; q.m.d. = quadratic mean diameter.

Means ± SEMs followed by the same letter within rows are not significantly different ($p > 0.05$).

of all trees (all d.b.h. classes) and trees in each individual d.b.h. class except for the smallest (10 cm d.b.h.). These results are consistent with the beetle's propensity to colonize larger diameter trees (Shepherd 1966) and that of other mortality agents observed (above, e.g., pine engraver) that disproportionally affect smaller diameter trees. Tree mortality was positively correlated with number of live trees, basal area of live trees, and SDI of live trees (Audley and others 2020), which is not surprising as density management has long been advocated as a measure to reduce stand susceptibility to mountain pine beetle (Fettig and others 2014). Significant increases in the number of subalpine fir seedlings and subalpine fir saplings were observed, but a long-term shift in tree composition is unlikely (Audley and others 2020).

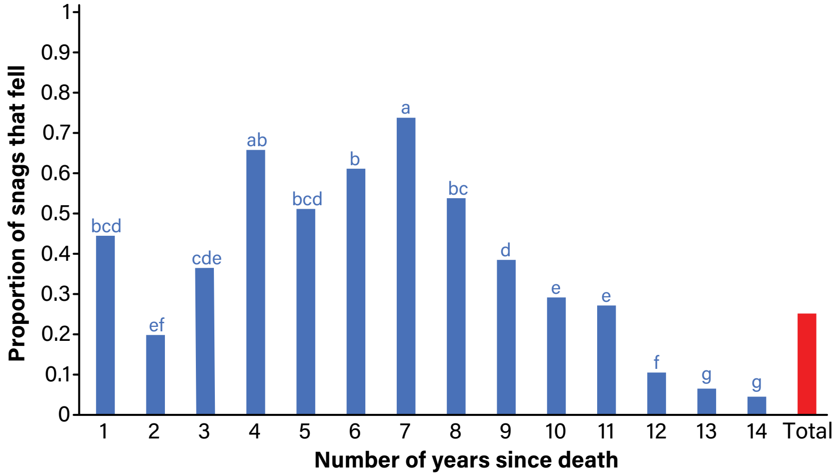

*Figure 11.2—Proportion of lodgepole pine snags within each year since death class (number of years since tree death occurred) that fell to the forest floor. Means followed by the same letter are not significantly different (*p *>0.05). (Adapted from Audley and others 2021)*

Among lodgepole pine snag age classes (number of years since tree death), the highest number of snags (1,046) were 12 years since death (YSD), and those 13 and 14 YSD exhibited the lowest fall rates (<10 percent) despite being the oldest in our study (Audley and others 2021). Snag fall occurred in every snag age class from 1–14 YSD, with the greatest proportion of snag fall events occurring 4–8 YSD (fig. 11.2). In our modeling of snag longevity, covariates of interest were informed from prior modeling efforts and included: elevation (m), latitude (°), slope aspect (categorical, N, S, E, W), slope (percent), tree density (number of live trees/ha), canopy cover (percent), snag d.b.h. (cm), snag height (m), and snag height (m):d.b.h. (m) ratio. Slope aspect had the strongest influence on fall rates. Northern aspects, greater canopy cover, and taller snag heights decreased the probability of snag fall. Conversely, southern aspects and greater height:d.b.h. ratios (taller, skinnier snags) increased the probability of snag fall. The predicted half-life (the amount of time since death required for 50 percent of the snag population to fall to the forest floor) was ~16 YSD, after which a linear, ~0.04-per-year decline in snag survival (i.e., snag remains standing) probability was observed for 15–30 YSD (Audley and others 2021). The observed longevity of snags in our study confers important ecological benefits for some wildlife and may offer opportunities for extended periods of salvage but lengthens concerns regarding hazard trees, human safety, and protection of critical infrastructure.

*Figure 11.4—The disturbance created when mountain pine beetle-killed trees tip up and fall appears prone to establishment and spread of invasive weeds, including Canada thistle (*Cirsium arvense*). (USDA Forest Service photo by J. Runyon, Rocky Mountain Research Station)*

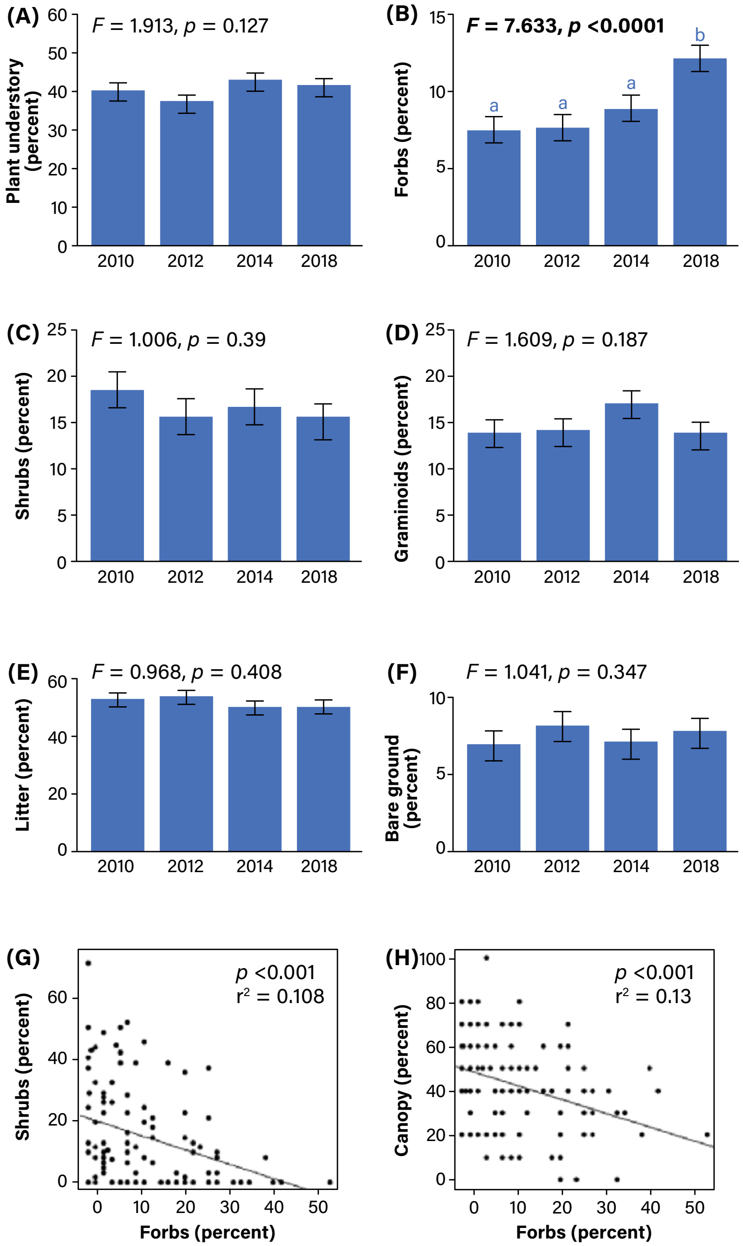

Figure 11.3—Percent cover of (A) total understory vegetation, (B) forbs, (C) shrubs, (D) graminoids, (E) litter, and (F) bare ground from 2010–2018 (about 2–10 years after peak levels of tree mortality), and relationships between (G) forb cover and shrub cover (H) and forb cover and canopy cover in 2018. Significant differences ($p < 0.05$) are denoted in bold for changes in understory conditions over time (forbs only). Adapted from Runyon and others (2020).

Total understory cover and cover of shrubs and graminoids remained unchanged while cover of forbs increased (fig. 11.3). Forb cover was negatively correlated with shrub and canopy cover (fig. 11.3). Approximately 20 percent of plots contained weeds, and weed abundance increased over time. Canada thistle (*Cirsium arvense*) represented 95 percent of total weed abundance. Presence of weeds was negatively correlated with graminoid cover and positively correlated with tree mortality and snag fall. However, by 2018, weed abundance was positively correlated only with snag fall. The localized soil disturbance created when snags uproot and fall appears to facilitate invasion by Canada thistle (fig. 11.4), which is of concern as the majority of snags (75 percent) have yet to fall in our study.

Given the substantial reductions in stand density, we conclude that the mountain pine beetle outbreak has effectively thinned these forests and shifted the age-class distributions of lodgepole pine in a manner sufficient to reduce susceptibility to future generations of mountain pine beetle for several decades. This is not to suggest that the trees killed by mountain pine beetle were the same trees that would have been selected for removal during thinning operations to reduce stand susceptibility to mountain pine beetle (Fettig and others 2014), or to diminish the many ecosystem goods and services that have been negatively impacted by the outbreak. Additional results and the implications of these results to recovery and management of lodgepole pine forests are available in Audley and others (2020, 2021) and Runyon and others (2020). All variables are scheduled to be remeasured in 2022, immediately after which we will report on changes in fuel profiles over time.

For more information, contact:
Christopher J. Fettig,
christopher.fettig@usda.gov

ACKNOWLEDGMENTS

We thank Chris Asaro (U.S. Department of Agriculture Forest Service, Forest Health Protection) and Robert Progar (Forest Service Sustainable Forest Management Research) for their helpful reviews of an earlier version of this summary, and the numerous colleagues who contributed to various aspects of the work described. We also thank the Forest Service Forest Health Monitoring program and Forest Health Protection (Regions 1 and 4) for their continued support.

LITERATURE CITED

Audley, J.P.; Fettig, C.J.; Munson, A.S. [and others]. 2020. Impacts of mountain pine beetle outbreaks on lodgepole pine forests in the Intermountain West, U.S., 2004–2019. Forest Ecology and Management. 475: 118403. https://doi.org/10.1016/j.foreco.2020.118403.

Audley, J.P.; Fettig, C.J.; Munson, A.S. [and others]. 2021. Dynamics of beetle-killed snags following mountain pine beetle outbreaks in lodgepole pine forests. Forest Ecology and Management. 482: 118870. https://doi.org/10.1016/j.foreco.2020.118870.

Brown, J.K. 1974. Handbook for inventorying downed woody material. Gen. Tech. Rep. INT-16. Ogden, UT: U.S. Department of Agriculture Forest Service, Intermountain Research Station. 24 p.

Fettig, C.J.; Gibson, K.E.; Munson, A.S.; Negrón, J.F. 2014. Cultural practices for prevention and mitigation of mountain pine beetle infestations. Forest Science. 60: 450–463. https://doi.org/10.5849/forsci.13-032.

Fettig, C.J.; Progar, R.A.; Paschke, J.; Sapio, F.J. 2021. Forest insects. In: Barrett, T.; Robertson, G., eds. Gen. Tech. Rep. PNW-992. Disturbance and sustainability in forests of the Western United States. Portland, OR: U.S. Department of Agriculture Forest Service, Pacific Northwest Research Station: 81–122.

Klutsch, J.G.; Negrón, J.F.; Costello, S.L. [and others]. 2009. Stand characteristics and downed woody debris accumulations associated with a mountain pine beetle (*Dendroctonus ponderosae* Hopkins) outbreak in Colorado. Forest Ecology and Management. 258: 641–649. https://doi.org/10.1016/j.foreco.2009.04.034.

Runyon, J.B.; Fettig, C.J.; Trilling, J.A. [and others]. 2020. Changes in understory vegetation including invasive weeds following mountain pine beetle outbreaks. Trees, Forests and People. 2: 100038. https://doi.org/10.1016/j.tfp.2020.100038.

Shepherd, R.F. 1966. Factors influencing the orientation and rates of activity of *Dendroctonus ponderosae* Hopkins (Coleoptera: Scolytidae). The Canadian Entomologist. 98: 507–518. https://doi.org/10.4039/Ent98507-5.

CHAPTER 12

Limber Pine Condition Along Montana's Rocky Mountain Front

Christy Cleaver
Amy Gannon
Dave Hanna
Katie McKeever
Marcus Jackson
August Kramer
Tanya Murphy
Drew Sovilla
Matt Voigt

INTRODUCTION

White pine blister rust (WPBR) (*Cronartium ribicola*) has caused extensive crown dieback and mortality along Montana's Rocky Mountain Front since its introduction to limber pine (*Pinus flexilis*) east of the Continental Divide in the 1930s. The combined impacts of WPBR, mountain pine beetle (*Dendroctonus ponderosae*), and changing climate patterns are suspected to be contributing to mortality and the alteration of limber pine stands occupying the grassland-montane ecotone throughout this region. Few studies have monitored low-elevation limber pine in Montana (Jackson and others 2010). Information on stand conditions is needed to inform management and restoration efforts. The objectives of this study were to (1) assess site and stand characteristics that describe limber pine along Montana's Rocky Mountain Front, (2) determine the status and health of limber pine trees and regeneration, and (3) characterize the major damage agents on limber pine trees and regeneration and determine the occurrence, incidence, and severity of WPBR on limber pine.

METHODS

Limber pine-dominated stands, spanning multiple land ownerships along Montana's Rocky Mountain Front, were identified with aerial imagery supplied by The Nature Conservancy, and random plot locations were located using Region One Plot Locator (ROPL) software. To ensure an adequate sample of limber pine, plots included at least 30 limber pine stems ≤4.5 feet tall. Plot direction was determined using a random compass bearing that placed the plot within the limber pine stand. Plots were 200 x 50 feet and divided into three sections with three circular, fixed-area understory vegetation subplots (1/100 acre, 11.8-foot radius) at equal increments along the central transect. Survey methods were adapted from Burns and others (2011) and the Whitebark Pine Ecosystem Foundation's published methods (Tomback and others 2004).

Plot data collected included GPS coordinates, elevation, aspect, slope, slope position, stand structure, canopy cover using a line intercept method, and disturbance history. All trees ≥4.5 feet tall were permanently tagged; tree assessments included species, diameter at breast height (d.b.h.), height, status (healthy, up to 5-percent damage; declining, 6–50-percent damage; dying, >50 percent damage; recent dead [0–5 years], red needles and fine twigs present; old dead [>5 years], no needles or fine twigs present), crown class, crown ratio, canopy kill, height to green crown, ground cover at tree base, and damage agents with associated severities. Limber pines were additionally assessed for WPBR, including crown and stem impacts, number of cankers, and canker lengths. White pine blister rust severity was assessed by dividing both the crown and bole into thirds and counting individual branch and stem cankers within each third. Percentage of branches with WPBR cankers was estimated for each crown third. Stem canker severity was quantified by percentage of the stem circumference girdled. All regeneration <4.5 feet tall was assessed for species, height, and status, while limber pines were examined for WPBR within the entire plot. In each subplot, we recorded ground cover

How to cite this chapter:

Cleaver, Christy; Gannon, Amy; Hanna, Dave; McKeever, Katie; Jackson, Marcus; Kramer, August; Murphy, Tanya; Sovilla, Drew; Voigt, Matt. 2022. Limber pine condition along Montana's Rocky Mountain Front. In: Potter, Kevin M.; Conkling, Barbara L., eds. Forest Health Monitoring: national status, trends, and analysis 2021. Gen. Tech. Rep. SRS-266. Asheville, NC: U.S. Department of Agriculture Forest Service, Southern Research Station: 177–181. https://doi.org/10.2737/SRS-GTR-266-Chap12.

type (vegetation, wood, mineral soil, rock, litter), shrub species, and WPBR alternate host (*Ribes, Castilleja,* and *Pedicularis* spp.), and estimated associated percent covers of each.

RESULTS

In 2017 and 2018, a total of 74 long-term monitoring plots were established in limber pine-dominated stands along a 50-mile latitudinal gradient west of Choteau, MT (fig 12.1). Plots ranged in elevation from 4,499–6,185 feet and were located on a variety of aspects and slope positions. Mean slope was 15 percent and ranged from 0–40 percent.

We assessed 6,065 trees, of which 4,427 were limber pine. Limber pine was found in association with Douglas-fir (*Pseudotsuga menziesi*) on 82 percent of plots and subalpine fir (*Abies lasiocarpa*) and lodgepole pine (*Pinus contorta*) on <1 percent of plots. On 18 percent of plots, limber pine was the only tree species present. Plot density of live limber pine ranged from 35–475 trees per acre, and mean density was 150 trees per acre. Average d.b.h. of live limber pine was 4.3 inches (range = 0.1–33.3 inches), and average height was 10.4 feet (range = 4.5–42.6 feet). Thirty-seven percent of limber pines were classified as healthy, 21 percent were declining or dying, and 43 percent were dead (fig. 12.2). The most common damage agents affecting live limber pine were WPBR and twig beetles. Of the 2.7 percent of recent limber pine mortality, 40 percent was attributed to WPBR and <1 percent was attributed to bark beetles. Nearly 40 percent of limber pine were old dead, and cause of mortality was difficult to discern on most trees. Alternate hosts of WPBR were observed on 32 percent of plots with *Ribes* spp. on 22 plots, *Castilleja* spp. on 3 plots, and *Pedicularis* spp. on 2 plots.

White pine blister rust occurred in 100 percent of plots with a mean incidence of 36 percent (range = 4–90 percent). Incidence of WPBR was highest in the large (>8 inches) d.b.h. class at 48 percent (table 12.1). The mean number of branch and stem cankers per tree was 3.0 but was higher in the large d.b.h. class. Of all live infected trees, 88 percent had fewer than five branch cankers per tree. Most (55 percent) branch cankers were in the largest size category (>12 inches length) with only 15 percent of cankers in the smallest size category (1–3 inches length) (table 12.2). Half of all live infected trees had stem cankers. The incidence of stem cankers was highest in trees in the small (0–2 inches) d.b.h. class.

We assessed 5,899 seedlings (trees <4.5 feet tall), of which 65 percent were limber pine and 34 percent were Douglas-fir. Live limber pine seedlings occurred on 93 percent of plots, and density averaged 170 stems per acre (range = 0–985 trees per acre). Only one plot had no seedlings of any species. Of all limber pine seedlings, 69 percent were alive, 31 percent were dead, and WPBR occurred on 5 percent of live seedlings.

DISCUSSION AND CONCLUSIONS

White pine blister rust, the primary damage agent, has been established in the study area for >80 years. It is widespread, occurring on all plots in the study area. While incidence of WPBR on

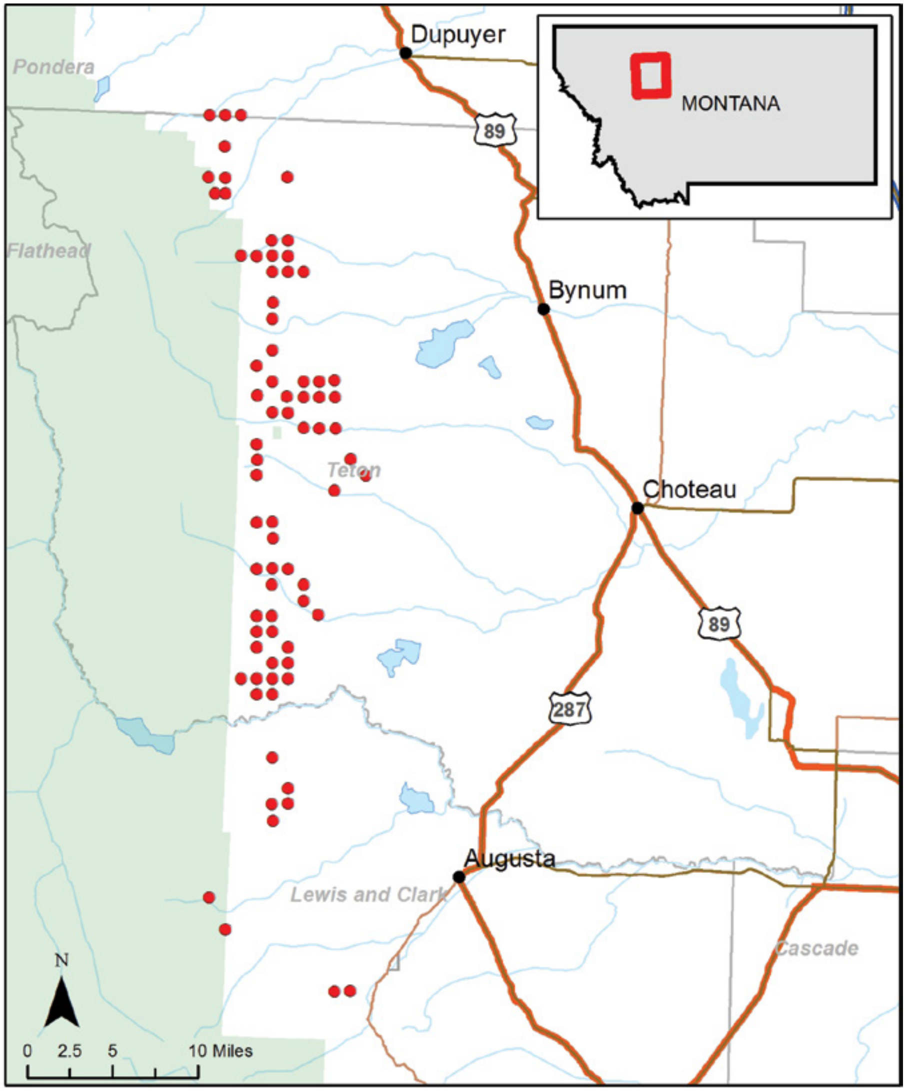

Figure 12.1—Location of limber pine monitoring plots along the Rocky Mountain Front in Montana, installed in 2017 and 2018.

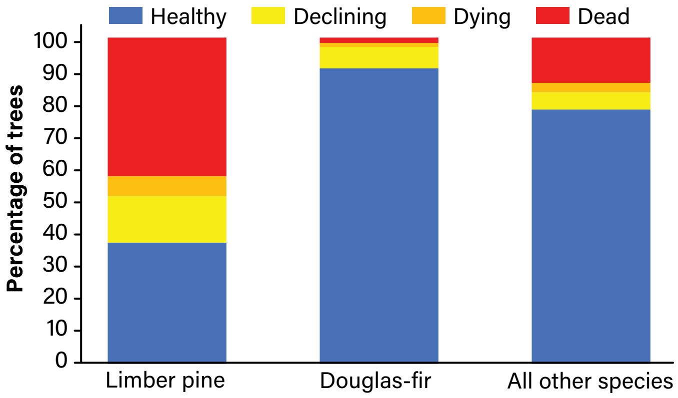

Figure 12.2—Health status of limber pine in comparison with Douglas-fir and all other tree species (all trees ≥4.5 feet tall) in 74 plots installed along the Rocky Mountain Front in Montana in 2017 and 2018. Healthy trees are those with up to 5-percent visual damage to crown or stem. Declining trees are those with 6–50-percent damage to the crown or stem. Dying trees are those with >50-percent damage to the crown or stem. Dead trees include both recent and older mortality.

Table 12.1—Proportion of living limber pine trees with white pine blister rust (WPBR), mean number of WPBR cankers per live limber pine with WPBR, and proportion of live limber pine with WBPR stem cankers, each by diameter at breast height (d.b.h.) size class

d.b.h. class	Number of limber pines	Trees with WPBR		Mean cankers per tree (SD)	Trees with stem cankers
		number	*percent*		*percent*
Small (0–2 inches)	614	162	26	1.9 (1.6)	62
Medium (2.1–8 inches)	1,636	622	38	2.7 (3.3)	48
Large (>8 inches)	292	140	48	3.7 (5.0)	46

SD = standard deviation.

Table 12.2—Proportion of white pine blister rust cankers in canker length categories

Canker length category	Proportion of cankers
inches	*percent*
1–3	15
3–6	12
6–9	11
9–12	6
>12	55

live limber pine was comparable to incidence in other areas farther south in the Rocky Mountains (Burns and others 2011, Cleaver and others 2015), mortality in this study was higher, likely due to WPBR being established earlier in the northern Rocky Mountains. Recent mortality, however, was low, and bark beetles did not have a major impact on limber pine stands in this study area in recent years. About half of live limber pine with WPBR in each d.b.h. class had stem cankers. Fewer WPBR cankers in all the smaller size classes combined versus the largest size class suggest the possibility that there may have been a lack of recent wave years or that WPBR infections have plateaued beyond the wave of initial infections. Incidence of WPBR on seedlings was low and comparable with other studies in the Rocky Mountains (Burns and others 2011, Cleaver and others 2017, Smith and others 2013). The latitudinal gradient of the study area was relatively small, and there was no relationship between latitude and density of live limber pine or incidence of WPBR on live limber pine.

Density of live limber pine was consistent with limber pine stands farther south in the Rocky Mountains, but mean seedling density was three times higher in this study as compared to Cleaver and others (2017). While WPBR is well established in this study area and a high level of mortality has occurred, the lack of recent bark beetle mortality and impact from other stressors like dwarf mistletoe (*Arceuthobium americanum*) has allowed for relatively good regeneration.

This study established baseline conditions for low-elevation limber pine stands along Montana's Rocky Mountain Front. Continued monitoring will help to assess impacts of WPBR and bark beetles, monitor effects of future climate change, assist resource managers in forecasting WPBR impacts in areas more recently invaded by the disease, and inform future restoration activities for limber pine.

For more information, contact:
Christy Cleaver, christy.cleaver@usda.gov

ACKNOWLEDGMENTS

This study was funded by The Nature Conservancy, Montana Department of Natural Resources and Conservation, and the U.S. Department of Agriculture Forest Service, Forest Health Monitoring program through the Evaluation Monitoring program.

LITERATURE CITED

Burns, K.S.; Blodgett, J.; Jackson, M. [and others]. 2011. Monitoring limber pine health in the Rocky Mountains and North Dakota. In: Keane, R.E.; Tomback, D.F.; Murray, M.P.; Smith, C.M., eds. The future of high-elevation, five-needle white pines in western North America: proceedings of the high five symposium, 28–30 June 2010; Missoula, MT. Proc. RMRS-63. Fort Collins, CO: U.S. Department of Agriculture Forest Service, Rocky Mountain Research Station. 376 p.

Cleaver, C.M.; Jacobi, W.R.; Burns, K.S.; Means, R.E. 2015. Limber pine in the central and southern Rocky Mountains: stand conditions and interactions with blister rust, mistletoe, and bark beetles. Forest Ecology and Management. 358: 139–153. https://doi.org/10.1016/j.foreco.2015.09.010.

Cleaver, C.M.; Jacobi, W.R.; Burns, K.S.; Means, R.E. 2017. Limber pine regeneration and white pine blister rust in the central and southern Rocky Mountains. Forest Science. 63(2): 151–164. https://doi.org/10.5849/forsci.16-052.

Jackson, M.; Gannon, A.: Kearns, H.: Kendall, K. 2010. Current status of limber pine in Montana. Report 10-06. [Place of publication unknown]: U.S. Department of Agriculture Forest Service, Forest Health Protection. 14 p.

Smith, C.M.; Langor, D.W.; Myrholm, C. [and others]. 2013. Changes in white pine blister rust infection and mortality in limber pine over time. Canadian Journal of Forest Research. 43(10): 919–928. https://doi.org/10.1139/cjfr-2013-0072.

Tomback, D.F.; Keane, R.E.; McCaughey, W.W.; Smith, C. 2004. Methods for surveying and monitoring whitebark pine for blister rust infection and damage. Missoula, MT: Whitebark Pine Ecosystem Foundation. 28 p.

INTRODUCTION

Balsam woolly adelgid (*Adelges piceae*) (BWA) is a nonnative pest of true firs (*Abies* spp.) in North America. Subalpine fir (*A. lasiocarpa*), grand fir (*A. grandis*), and white fir (*A. concolor*) are common hosts for this insect within the Intermountain West. These species contribute to societal and ecosystem services. Subalpine fir forests provide benefits to water quantity and quality, outdoor recreation, wood products, and food and shelter for wildlife (Colorado State Forest Service 2009, Lalande and others 2020). Subalpine fir may become more valuable in filling ecosystem services in high-elevation forests, because other common species have declined, such as whitebark pine (*Pinus albicaulis*), killed by mountain pine beetle (*Dendroctonus ponderosae*) and white pine blister rust, and Engelman spruce (*Picea engelmannii*), killed by past spruce beetle (*D. rufipennis*) outbreaks.

Since BWA established in Idaho (Livingston and others 2000) and expanded its range into Montana and Utah (Davis and others 2020), land managers working in these States have requested local information on potential losses from this insect upon infestation, and over time, to inform expected timeframes for applying possible management options. They have also requested information on expected future forest composition if no management for BWA occurs. We addressed their questions through long-term monitoring of tree decline and death in BWA-infested stands. We also begin to explore the complexities of climate influences on the pest-host relationship under differing stand conditions.

METHODS

Twenty-eight monitoring sites were selected in 2008 and 2009 across Idaho, where BWA populations were not detected or detected only in low densities, and were measured on 5-year intervals. In 2018 and 2019, plots were established at 12 and 26 sites in Montana and Utah, respectively. Site-selection criteria, plot design, and metrics that evaluated BWA infestation and expected tree and stand decline are detailed in Davis and others (2022). Woody and live surface ground fuel load metrics were recorded at all the Utah sites (41 plots total across all sites) and 15 sites in southern Idaho during 2018 (Brown 1974).

Weather-induced stress on fir species was considered using (1) temperature and precipitation metrics spanning 5 years prior to plot installation through 2018 and (2) stand density at plot establishment. Weather influence on the insect was not evaluated because it requires annual BWA population data and would benefit from applying onsite weather data. Multiple gridded weather climate datasets were evaluated due to sparseness of weather stations and elevational variability with an emphasis on temperature and precipitation metrics. PRISM data (Daly and others 2008) were selected because they were available for 2018 and offered finer resolution that allowed more accurate elevational representation than the other evaluated datasets. Analyses of climate metrics, stand structure, host density, and BWA pressure on BWA damage class and tree mortality are presented in Hicke and others (in preparation).[1]

CHAPTER 13

Influences of Balsam Woolly Adelgid and Climate on True Fir: A Baseline for Utah and Montana and a 10-year Assessment for Idaho

Gina A. Davis
Laura Lowrey
Danielle Malesky
Tom Eckberg
Amy Gannon
Jeffrey Hicke

How to cite this chapter:

Davis, Gina A.; Lowrey, Laura; Malesky, Danielle; Eckberg, Tom; Gannon, Amy; Hicke, Jeffrey. 2022. Influences of balsam woolly adelgid and climate on true fir: a baseline for Utah and Montana and a 10-year assessment for Idaho. In: Potter, Kevin M.; Conkling, Barbara L., eds. Forest Health Monitoring: national status, trends, and analysis 2021. Gen. Tech. Rep. SRS-266. Asheville, NC: U.S. Department of Agriculture Forest Service, Southern Research Station: 183–187. https://doi.org/10.2737/SRS-GTR-266-Chap13.

---

[1] *Hicke, J.A.; Davis, G.A.; Smirnova, E. [and others]. An evaluation of climate and stand structure influences on balsam woolly adelgid damage in Idaho. Manuscript in preparation. Author can be reached at the University of Idaho, 875 Perimeter Dr., Moscow, ID 83844.*

RESULTS AND DISCUSSION

Baseline Observations

Host trees of BWA composed between 26 and 77 percent of basal area at the Montana sites, and a relatively low amount of BWA was observed at four sites. Defoliation from western spruce budworm (*Choristoneura occidentalis*) was moderate to extensive at all sites except at Emery Creek, Showdown, and Portal, possibly complicating observations of low BWA populations. In Utah, Powder Mountain high and low stands and Big Mountain were well infested with BWA, and eight other sites had lesser amounts of BWA. Host trees composed between 10 and 99 percent of the total basal area (table 13.1). The Soapstone low stand was the only site where trees <5 inches diameter at breast height (d.b.h.) were infested while larger trees were not also infested. Abundant subalpine fir seedlings grew at all sites in both States and were only infested with BWA at sites with moderate to high prevalence of BWA in Utah. Host seedlings were infested at most of the heavily infested sites in northern Utah, but none were infested at Montana sites.

10-Year Observations

In Idaho, annual mortality rates of host trees increased from 1.3 percent (SD 2.3 percent) 5 years after plot establishment to 2.2 percent (SD 3.1 percent) after 10 years. The reported mortality rates are likely conservative because greater losses have been reported in other stands in Idaho (Lowrey 2015). By 2018, the proportion of subalpine fir that died at a site (mean = 0.355, SD = 0.175) was significantly greater than the proportion of grand fir that died (mean = 0.157, SD = 0.216) (Kruskal-Wallis chi-square statistic 4.041, $p = 0.044$, $n = 8$), although there was not a significant difference between the proportion of the two host species infested with BWA (Kruskal-Wallis chi-square statistic 0.177, $p = 0.674$, $n = 8$) (Davis and others, in review [see footnote 1]). Based on multivariate statistical modeling, the proportion of stands infested with BWA in the prior 5 years was the most important predictor variable of severe decline and mortality of host trees, followed by basal area of host species. Both variables had linear, positive relationships with BWA damage. Climate variables were not as important and exhibited nonlinear and uncertain relationships with BWA damage (Hicke and others, in preparation [see footnote 2]).

Further Evaluation

These plot networks allow for a deeper assessment of the ecological effects from BWA across three States. Because plots in Utah, Montana, and Idaho were established using methods similar to Spiegel and others (2013), future studies across a range of environmental conditions will be possible. One difference in the methods was that Spiegel and others (2013) rated BWA damage as the average of three crown section estimates while we applied the BWA damage class to the entire tree. However, the same tree symptoms were considered and rated within the same ranges of percentage of the crown affected (BWA damage class 1 = none; class 2 = light, 1–24 percent; class 3 = moderate, 25–50 percent; class 4 = severe, >50 percent; and class 4 = dead). Other assessments that utilize this dataset are underway or pending

Table 13.1—Balsam woolly adelgid (BWA) monitoring site descriptions during plot establishment in Montana and Utah ordered from higher to lower latitudes

	Trees per acre			Basal area		Host trees		Elevation	Habitat type[e]
Site[a]	Total[b]	Host	Infested with BWA	Total[c]	Host	q.m.d.[d]	d.b.h. range		
			percent	*square feet per acre*	*percent*	*inches*		*feet*	
Montana									
China Mountain	303	273	0	125	73	7.7	1.1–18.3	5,757	ABLA/VAME
Quartz Mountain	800	637	0	187	52	5.5	1.0–18.9	5,150	ABLA/XETE
Emery Creek	303	190	0	184	38	8.1	1.1–16.3	4,285	ABLA/VAME
Blacktail	1,357	1,180	0	135	77	4.7	1.0–16.4	6,405	ABLA/XETE
Cottonwood Lakes	363	263	5	197	46	8.5	1.0–19.5	4,760	ABLA/CLUN
Sunset	720	603	0	156	57	5.2	1.1–13.7	6,250	Not available
Kings Hill	413	280	NA[h]	162	26	5.7	1.0–12.8	8,020	ABLA/VACA
Showdown	1,213	993	NA[h]	211	48	4.5	1.0–12.6	7,235	ABLA/VACA
Twin Lakes	307	267	15	134	69	7.9	1.0–19.9	6,625	ABLA/MEFE
Lost Horse	407	233[f]	14	105	61	7.9	2.3–16.0	5,270	ABLA/XETE
Portal	470	237	0	92	49	6.0	1.5–11.1	8,135	ABLA/VAGL
Hyalite	480	243	11	123	41	6.7	1.0–13.6	6,825	ABLA/VASC
Utah									
Logan Canyon high	480	273	20[i]	268	28	9.6	1.0–22.7	8,398	ABLA/PERA
Logan Canyon low	257	170	2	176	46	8.9	1.1–20.5	6,844	ABLA/PERA
Monte Cristo high	308	213	18	225	49	9.4	1.2–30.6	8,769	ABLA/RIMO
Monte Cristo low	505	295	39[i]	171	82	9.1	1.0–27.2	8,087	ABLA/RIMO
Powder Mountain high	278	260	96[i]	144	79	9.2	1.0–21.0	8,196	ABLA/RIMO

d.b.h. = diameter at breast height; q.m.d. = quadratic mean diameter.

Data averaged across three plots at all sites except Powder Mountain hi and lo and Monte Cristo hi and lo, which included four plots.

[a] Sites installed in 2018 except Wasatch Plateau high and low, Fishlake Plateau high and low, Manti-LaSal high and low, Tushar Mountains high and low, Aquarius Plateau high and low, Abajo Mountains high and low, and Markagunt Plateau high and low, which were installed in 2019.

[b] Includes all tree species and diameters.

[c] Includes all species averaged across plots.

[d] q.m.d. of host trees ≥5 inches d.b.h.

[e] See Mauk and Henderson 1984 and Youngblood and Mauk 1985 for habitat type details.

[f] Includes 30 trees per acre of grand fir. No grand firs were infested with BWA.

[g] Includes 10 trees per acre of white fir infested with BWA.

[h] NA = inconclusive adelgid species collected.

[i] Some or all true fir seedlings were infested with BWA. Seedlings of true fir species occupied all sites.

(Continued)

Table 13.1 ***(Continued)*****—Balsam woolly adelgid (BWA) monitoring site descriptions during plot establishment in Montana and Utah ordered from higher to lower latitudes**

	Trees per acre			Basal area		Host trees		Elevation	Habitat type[e]
Site[a]	Total[b]	Host	Infested with BWA	Total[c]	Host	q.m.d.[d]	d.b.h. range		
			percent	*square feet per acre*	*percent*	*inches*		*feet*	
Powder Mountain low	338	223	82[i]	132	83	10.4	1.0–23.2	7,426	ABLA/BERE
Big Mountain	273	123[g]	97[i]	184	73	14.3	1.7–45.5	7,351	ABLA/ACRU
Guardsman's Pass	243	130	0	160	38	9.6	3.0–17.7	9,750	ABLA/BERE
Ashley National Forest high	817	327	21[i]	81	17	2.8	1.0–7.0	9,715	ABLA/VASC
Ashley National Forest low	650	123	32[i]	168	10	6.3	1.0–12.4	9,329	ABLA/VASC
Soapstone Basin high	460	353	1	135	93	8.3	1.8–24.5	9,216	ABLA/RIMO
Soapstone Basin low	1,133	830	2	147	74	5.0	1.0–14.4	8,432	ABLA/BERE
Wasatch Plateau high	263	260	0	149	99	10.5	1.3–21.4	10,006	ABLA/RIMO
Wasatch Plateau low	583	423	0	112	41	4.9	1.1–19.7	8,941	ABLA/OSCH
Fishlake Plateau high	1,053	697	0	130	60	4.9	1.1–15.7	10,577	ABLA/RIMO
Fishlake Plateau low	603	343	0	208	39	7.2	1.0–19.9	9,687	ABLA/RIMO
Manti-LaSal high	347	243	0	183	23	6.1	1.3–18.6	10,142	ABLA/RIMO
Manti-LaSal low	377	73	0	151	38	13.9	2.2–19.9	9,209	ABLA/BERE
Tushar Mountains high	573	333	0	156	33	5.2	1.0–23.2	10,252	ABLA/RIMO
Tushar Mountains low	470	340	0	174	52	7.4	1.0–18.3	9,189	ABLA/RIMO
Aquarius Plateau high	677	477	0	102	31	3.8	1.0–10.6	9,706	ABLA/CAGE
Aquarius Plateau low	620	263	0	149	26	5.4	1.0–17.7	8,914	ABLA/BERE
Abajo Mountains high	487	320	0	186	59	8.1	1.0–32.6	10,373	ABLA/RIMO
Abajo Mountains low	460	366	0	225	56	8.8	1.2–32.6	9,066	ABLA/RIMO
Markagunt Plateau high	427	380	0	101	84	6.4	1.1–19.6	10,408	ABLA/RIMO
Markagunt Plateau low	387	280	0	94	42	5.3	1.0–16.7	9,183	ABLA/BERE

d.b.h. = diameter at breast height; q.m.d. = quadratic mean diameter.

Data averaged across three plots at all sites except Powder Mountain hi and lo and Monte Cristo hi and lo, which included four plots.

[a] Sites installed in 2018 except Wasatch Plateau high and low, Fishlake Plateau high and low, Manti-LaSal high and low, Tushar Mountains high and low, Aquarius Plateau high and low, Abajo Mountains high and low, and Markagunt Plateau high and low, which were installed in 2019.

[b] Includes all tree species and diameters.

[c] Includes all species averaged across plots.

[d] q.m.d. of host trees ≥5 inches d.b.h.

[e] See Mauk and Henderson 1984 and Youngblood and Mauk 1985 for habitat type details.

[f] Includes 30 trees per acre of grand fir. No grand firs were infested with BWA.

[g] Includes 10 trees per acre of white fir infested with BWA.

[h] NA = inconclusive adelgid species collected.

[i] Some or all true fir seedlings were infested with BWA. Seedlings of true fir species occupied all sites.

funding. Fuel monitoring within Utah and southern Idaho sites in 2018 are being evaluated under a project led by Sharon Hood, Research Ecologist at the U.S. Department of Agriculture Forest Service, Rocky Mountain Research Station, that will evaluate potential fire behavior (Forest Health Protection - Special Technology Development Program R4-2020-01). Tree cores from host species at sites in all three States have been mounted for preliminary evaluation at the Center for Dendrochronology at the University of Minnesota. These tree cores may be valuable in understanding relationships between growth rates with BWA infestation density or with severity of BWA damage class, deepening our understanding of climate variables in this complex system and possibly identifying actual year(s) of BWA infestation if rotholz (similar to compression wood) can be differentiated.

For more information, contact:
Gina A. Davis, gina.davis@usda.gov

LITERATURE CITED

Brown, J.K. 1974. Handbook for inventorying downed woody material. Gen. Tech. Rep. INT-16. Ogden, UT: U.S. Department of Agriculture Forest Service, Intermountain Forest and Range Experimental Station. 32 p.

Colorado State Forest Service. 2009. 2008 report: the health of Colorado's forests – special issue: high elevation forests. Fort Collins, CO: Colorado State Forest Service. 40 p.

Daly, C.; Halbleib, M.; Smith, J.I. [and others] 2008. Physiographically sensitive mapping of climatological temperature and precipitation across the conterminous United States. International Journal of Climatology. 28: 2031–2064. https://doi.org/10.1002/joc.1688.

Davis, G.; Lowrey, L.; Eckberg, T. [and others]. 2020. Notes on balsam woolly adelgid, *Adelges piceae* (Ratzeburg, 1844) (Hemiptera: Adelgidae), range expansion in Idaho, Montana and Utah. The Pan-Pacific Entomologist. 93(3): 129–133. https://doi.org/10.3956/2020-96.3.129.

Davis, G.A.; Lowrey, L.; Eckberg, T. [and others]. 2022. Characterizing balsam woolly adelgid infestations and associated tree mortality in Idaho. Journal of Forestry. fvac007. https://doi.org/10.1093/jofore/fvac007.

Lalande, B.M; Hughes, K.; Jacobi, W.R. [and others]. 2020. Subalpine fir mortality in Colorado is associated with stand density, warming climates and interactions among fungal diseases and the western balsam bark beetle. Forest Ecology and Management. 466: 118–133. https://doi.org/10.1016/j.foreco.2020.118133.

Livingston, R.L.; Dewey, J.E.; Beckman, D.P; Stipe, L.E. 2000. Distribution of the balsam woolly adelgid in Idaho. Western Journal of Applied Forestry. 15(4): 227–231. https://doi.org/10.1093/wjaf/15.4.227.

Lowrey, L. 2015. Monitoring high severity damages to subalpine fir-dominated forests caused by balsam woolly adelgid on the Boise and Payette National Forests. BFO-TR-2015-29. Boise, ID: U.S. Department of Agriculture Forest Service, Forest Health Protection. 9 p.

Mauk, R.; Henderson, J. 1984. Coniferous forest habitat types of northern Utah. Gen. Tech. Rep. INT-170. Ogden, UT: U.S. Department of Agriculture Forest Service, Intermountain Forest and Range Experiment Station. 89 p. https://doi.org/10.5962/bhl.title.100096.

Spiegel, L.H.; Chadwick, K.; Mehmel, C. 2013. Assessment of balsam woolly adelgid damage to eastern Washington and Oregon subalpine fir (Project WC-F-07-01). In: Potter, K.M.; Conkling, B.L., eds. Forest Health Monitoring: national status, trends, and analysis 2010. Gen. Tech. Rep. SRS-176. Asheville, NC: U.S. Department of Agriculture Forest Service, Southern Research Station: 129–134.

Youngblood, A.P.; Mauk, R.L. 1985. Coniferous forest habitat types of central and southern Utah. Gen. Tech. Rep. INT-187. Ogden, UT: U.S. Department of Agriculture Forest Service, Intermountain Research Station. 89 p. https://doi.org/10.5962/bhl.title.100042.

ACKNOWLEDGMENTS

This research presented in this report was supported in part through the project "Forest Health Monitoring, Assessment, and Analysis" of Cost Share Agreement 20-CS-11330180-020 (June 20, 2020 through August 31, 2021) and the project "Forest Health Monitoring and Assessment" of Cost Share Agreement (July 19, 2021 through September 15, 2022) between North Carolina State University (this institution is an equal opportunity provider) and the U.S. Department of Agriculture Forest Service, Southern Research Station, Asheville, NC. This research was supported by funds provided by the U.S. Department of Agriculture Forest Service, Southern Research Station, Asheville, NC.

The editors and authors of this report thank the following for their reviews and constructive comments: Chris Asaro, Jeff Bliss, Ryan Bracewell, Stephen Burr, Kevin Chase, Stephen Cook, Jennifer Costanza, Daniel Dey, Joel Egan, Robbie Flowers, Betsy Goodrich, Ian Housman, Allison Kanoti, Holly Kearns, Frank Krist, Cameron McIntire, Dave Michaelson, Robert Progar, KaDonna Randolph, Matthew Reilly, Tim Shearman, Robert Warren, and Denys Yemshanov.

AUTHOR INFORMATION

Sections 1 and 2, Forest Health Monitoring Research

MARK J. AMBROSE, Research Assistant, North Carolina State University, Department of Forestry and Environmental Resources, Raleigh, NC 27695.

WILLIAM M. CHRISTIE, Biological Scientist, U.S. Department of Agriculture Forest Service, Southern Research Station, Eastern Forest Environmental Threat Assessment Center, Asheville, NC 28804.

JOHN W. COULSTON, Supervisory Research Forester, U.S. Department of Agriculture Forest Service, Southern Research Station, Blacksburg, VA 24060.

RYAN HANAVAN, Region 1 and 4 Coordinator, U.S. Department of Agriculture Forest Service, Forest Health Monitoring program, Missoula, MT 59807.

FRANK H. KOCH, Research Ecologist, U.S. Department of Agriculture Forest Service, Southern Research Station, Eastern Forest Environmental Threat Assessment Center, Research Triangle Park, NC 27709.

STEVEN P. NORMAN, Research Ecologist, U.S. Department of Agriculture Forest Service, Southern Research Station, Eastern Forest Environmental Threat Assessment Center, Asheville, NC 28804.

JEANINE L. PASCHKE, Geographic Information Systems Analyst, RedCastle Resources, Inc., Fort Collins, CO 80526.

KEVIN M. POTTER, Research Professor, North Carolina State University, Department of Forestry and Environmental Resources, Raleigh, NC 27695.

TOM SMITH, Forest Pest Management Specialist, California Department of Forestry and Fire Protection, Sacramento, CA 94244.

AUTHOR INFORMATION

Section 3, Evaluation Monitoring Project Summaries

Jackson P. Audley, Postdoctoral Scholar, U.S. Department of Agriculture Forest Service, Pacific Southwest Research Station, Davis, CA 95618.

Aaron Bergdahl, Forest Pathologist, Maine Department of Agriculture, Conservation & Forestry, Maine Forest Service, Augusta, ME 04333-0168.

Jessica Cancelliere, Research Scientist, New York State Department of Environmental Conservation, Bureau of Invasive Species and Ecosystem Health, Delmar, NY 12054.

Christy Cleaver, Plant Pathologist, U.S. Department of Agriculture Forest Service, Forest Health Protection, Coeur d'Alene, ID 83815.

Robert Cole, Forester, New York State Department of Environmental Conservation, Bureau of Invasive Species and Ecosystem Health, Albany, NY 12233.

Gina A. Davis, Supervisory Entomologist, U.S. Department of Agriculture Forest Service, Region 1, State and Private Forestry, Coeur d'Alene, ID 83815.

Brittany DiRienzo, Graduate Student, Clemson University, Department of Forestry and Environmental Conservation, Clemson, SC 29634.

Tom Eckberg, Forest Health Program Manager, Idaho Department of Lands, Coeur d'Alene, ID 83815.

Christopher J. Fettig, Research Entomologist, U.S. Department of Agriculture Forest Service, Pacific Southwest Research Station, Davis, CA 95618.

Jennifer Fraterrigo, Associate Professor, University of Illinois, Department of Natural Resources and Environmental Sciences, Urbana, IL 61801.

Amy Gannon, Forest Pest Management Program Manager, Montana Department of Natural Resources, Missoula, MT 59804.

Kenneth E. Gibson, Entomologist (retired), U.S. Department of Agriculture Forest Service, Forest Health Protection, Missoula, MT 59807.

Josh Halman, Forest Health Lead, Vermont Department of Forests, Parks and Recreation, Essex Junction, VT 05452.

AUTHOR INFORMATION

Dave Hanna, Crown of the Continent Program Director, The Nature Conservancy, Choteau, MT 59436.

Jeffrey Hicke, Professor, University of Idaho, Moscow, ID 83844.

Marcus Jackson, Staff Officer, U.S. Department of Agriculture Forest Service, Forest Health Protection, Bismarck, ND 58501.

Carl L. Jørgensen, Supervisory Entomologist and Group Leader, U.S. Department of Agriculture Forest Service, Forest Health Protection, Boise, ID 83709.

August Kramer, Graduate Student, University of Minnesota, St. Paul, MN 55108.

Nicole Keleher, Forest Health Program Director, Massachusetts Department of Conservation & Recreation, Bureau of Forest Fire Control and Forestry, Amherst, MA 01002.

Rebecca Lilja, Data Service Specialist (GIS), U.S. Department of Agriculture Forest Service, State and Private Forestry, Durham, NH 03824.

Kyle Lombard, Forest Health Program Coordinator, New Hampshire Division of Forests and Lands, Concord, NH 03001.

Laura Lowrey, Entomologist, U.S. Department of Agriculture Forest Service, Forest Health Protection, Medford, OR 97504.

Danielle Malesky, Entomologist, U.S. Department of Agriculture Forest Service, Forest Health Protection, Coeur d'Alene, ID 83815.

Katie McKeever, Plant Pathologist, Resistance Screening Center Manager, U.S. Department of Agriculture Forest Service, Forest Health Protection, Asheville, NC 28806.

Stephen R. McKelvey, Biological Science Technician (retired), U.S. Department of Agriculture Forest Service, Pacific Southwest Research Station, Placerville, CA 95667.

Joel D. McMillin, Supervisory Entomologist and Zone Leader, U.S. Department of Agriculture Forest Service, Forest Health Protection, Flagstaff, AZ 86001.

Leif A. Mortenson, Biological Science Technician, U.S. Department of Agriculture Forest Service, Pacific Southwest Research Station, Placerville, CA 95667.

AUTHOR INFORMATION

Isabel A. Munck, Forest Pathologist, U.S. Department of Agriculture Forest Service, State and Private Forestry, Durham, NH 03824.

A. Steven Munson, Supervisory Entomologist and Group Leader (retired), U.S. Department of Agriculture Forest Service, Forest Health Protection, Ogden, UT 84403.

Tanya Murphy, Forest Silviculturist, U.S. Department of Agriculture Forest Service, National Forest System, Region 1, Great Falls, MT 59405.

Jose F. Negrón, Research Entomologist, U.S. Department of Agriculture Forest Service, Rocky Mountain Research Station, Fort Collins, CO 80526.

Emilee Poole, Graduate Student, University of Georgia, Athens, GA 30602.

Paul Ricard, Principal Biologist, Forest Health Program Coordinator, Rhode Island Department of Environmental Management, Providence, RI 02908.

Justin B. Runyon, Research Entomologist, U.S. Department of Agriculture Forest Service, Rocky Mountain Research Station, Bozeman, MT 59717.

Ron Salemme, Graduate Student (doctoral candidate), University of Illinois, Department of Natural Resources and Environmental Sciences, Urbana, IL 61801.

Drew Sovilla, Montana Land Steward, The Nature Conservancy, Choteau, MT 59601.

John Stanovick, Mathematical Statistician, U.S. Department of Agriculture Forest Service, Northern Research Station, Long Pond, PA 18334.

Brytten E. Steed, Entomologist, U.S. Department of Agriculture Forest Service, Forest Health Protection, Missoula, MT 59807.

Michael Ulyshen, Research Entomologist, U.S. Department of Agriculture Forest Service, Southern Research Station, Athens, GA 30602.

Matt Voigt, Forestry Technician, U.S. Department of Agriculture Forest Service, National Forest System, Region 1, Great Falls, MT 59405.

G. Geoff Wang, Professor, Clemson University, Department of Forestry and Environmental Conservation, Clemson, SC 29634.

Jen Weimer, Forest Health Specialist, New Hampshire Division of Forests and Lands, Concord, NH 03001.

Potter, Kevin M.; Conkling, Barbara L., eds. 2022. Forest health monitoring: national status, trends, and analysis 2021. Gen. Tech. Rep. SRS-266. Asheville, NC: U.S. Department of Agriculture Forest Service, Southern Research Station. 193 p. https://doi.org/10.2737/SRS-GTR-266.

The annual national report of the Forest Health Monitoring (FHM) program of the Forest Service, U.S. Department of Agriculture, presents forest health status and trends from a national or multistate regional perspective using a variety of sources, introduces new techniques for analyzing forest health data, and summarizes results of recently completed Evaluation Monitoring projects funded through the FHM national program. In this 21st edition in a series of annual reports, national survey data are used to identify recent geographic patterns of insect and disease activity. Satellite data are employed to detect geographic patterns of forest fire occurrence. Recent drought and moisture surplus conditions are compared across the conterminous United States. Data collected by the Forest Inventory and Analysis (FIA) program are employed to detect regional differences in tree mortality. Fine-scale change in Normalized Difference Vegetation Index (NDVI) was used to detect broad patterns of forest disturbance across the conterminous United States. Seven recently completed Evaluation Monitoring projects are summarized, addressing forest health concerns at smaller scales.

Keywords—Change detection, disturbance, drought, fire, forest health, forest insects and disease, tree canopy, tree mortality.

Southern Research Station
200 W.T. Weaver Blvd.
Asheville, NC 28804
www.srs.fs.usda.gov

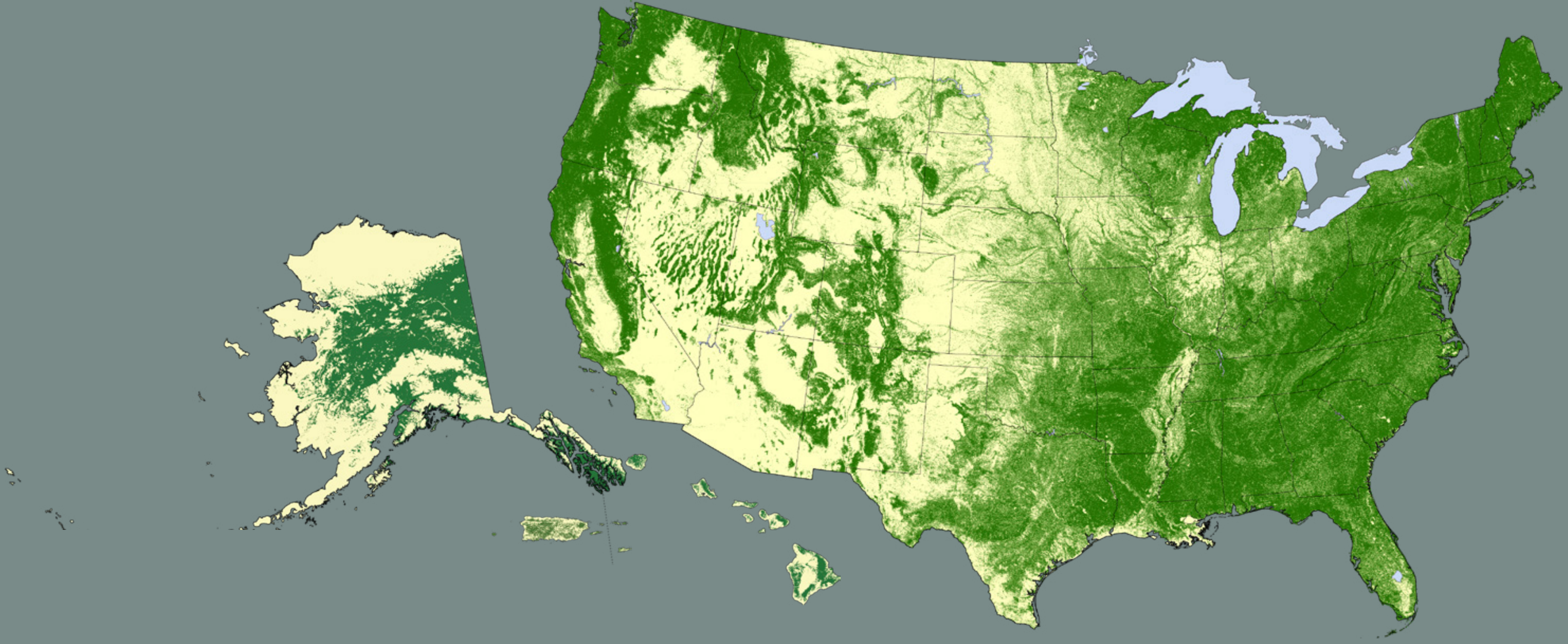

In accordance with Federal civil rights law and U.S. Department of Agriculture (USDA) civil rights regulations and policies, the USDA, its Agencies, offices, and employees, and institutions participating in or administering USDA programs are prohibited from discriminating based on race, color, national origin, religion, sex, gender identity (including gender expression), sexual orientation, disability, age, marital status, family/parental status, income derived from a public assistance program, political beliefs, or reprisal or retaliation for prior civil rights activity, in any program or activity conducted or funded by USDA (not all bases apply to all programs). Remedies and complaint filing deadlines vary by program or incident.

Persons with disabilities who require alternative means of communication for program information (e.g., Braille, large print, audiotape, American Sign Language, etc.) should contact the responsible Agency or USDA's TARGET Center at (202) 720-2600 (voice and TTY) or contact USDA through the Federal Relay Service at (800) 877-8339. Additionally, program information may be made available in languages other than English.

To file a program discrimination complaint, complete the USDA Program Discrimination Complaint Form, AD-3027, found online at http://www. ascr.usda.gov/complaint_filing_cust.html and at any USDA office or write a letter addressed to USDA and provide in the letter all of the information requested in the form. To request a copy of the complaint form, call (866) 632-9992. Submit your completed form or letter to USDA by: (1) mail: U.S. Department of Agriculture, Office of the Assistant Secretary for Civil Rights, 1400 Independence Avenue, SW, Washington, D.C. 20250-9410; (2) fax: (202) 690-7442; or (3) email: program.intake@usda.gov.

USDA is an equal opportunity provider, employer, and lender.